CALIFORNIA INSTITUTE OF TECHNOLOGY

EARTHQUAKE ENGINEERING RESEARCH LABORATORY

IMPACT OF SEISMIC RISK ON LIFETIME PROPERTY VALUES

BY

J.L. BECK, K.A. PORTER, R.V. SHAIKHUTDINOV, S.K. AU,
K. MIZUKOSHI, M. MIYAMURA, H. ISHIDA, T. MOROI,
Y. TSUKADA, AND M. MASUDA

REPORT NO. EERL 2002-04

A REPORT ON RESEARCH SUPPORTED BY THE
CUREE-KAJIMA JOINT RESEARCH PROGRAM, PHASE IV

PASADENA, CALIFORNIA

DECEMBER, 2002

A REPORT ON RESEARCH SUPPORTED BY THE CUREE-KAJIMA JOINT RESEARCH PROGRAM PHASE IV UNDER THE SUPERVISION OF J.L. BECK

Impact of Seismic Risk on Lifetime Property Values

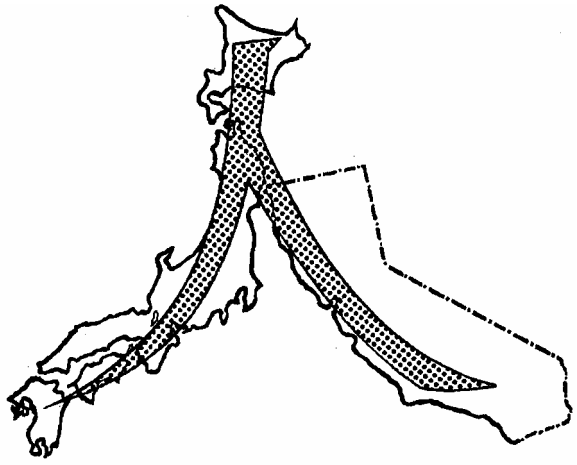

Final Report
CUREE-Kajima Joint Research Program
Phase IV

December, 2002

Final Report for CUREE-Kajima Phase IV Project

IMPACT OF SEISMIC RISK ON LIFETIME PROPERTY VALUES

CUREE	KAJIMA
J. L. Beck	K. Mizukoshi
K. A. Porter	M. Miyamura
R. Shaikhutdinov	H. Ishida
S. K. Au	T. Moroi
	Y. Tsukada
	M. Masuda

December 31, 2002

Impact of Seismic Risk on Lifetime Property Values

J. L. Beck, K. A. Porter, R. Shaikhutdinov and S. K. Au
California Institute of Technology, Pasadena, CA

K. Mizukoshi, M. Miyamura, H. Ishida, T. Moroi, Y. Tsukada, and M. Masuda
Kajima Corporation, Tokyo, Japan

Abstract

This report presents a methodology for establishing the uncertain net asset value, NAV, of a real-estate investment opportunity considering both market risk and seismic risk for the property. It also presents a decision-making procedure to assist in making real-estate investment choices under conditions of uncertainty and risk-aversion. It is shown that that market risk, as measured by the coefficient of variation of NAV, is at least 0.2 and may exceed 1.0. In a situation of such high uncertainty, where potential gains and losses are large relative to a decision-maker's risk tolerance, it is appropriate to adopt a decision-analysis approach to real-estate investment decision-making. A simple equation for doing so is presented. The decision-analysis approach uses the certainty equivalent, CE, as opposed to NAV as the basis for investment decision-making. That is, when faced with multiple investment alternatives, one should choose the alternative that maximizes CE. It is shown that CE is less than the expected value of NAV by an amount proportional to the variance of NAV and the inverse of the decision-maker's risk tolerance, ρ.

The procedure for establishing NAV and CE is illustrated in parallel demonstrations by CUREE and Kajima research teams. The CUREE demonstration is performed using a real 1960s-era hotel building in Van Nuys, California. The building, a 7-story non-ductile reinforced-concrete moment-frame building, is analyzed using the assembly-based vulnerability (ABV) method, developed in Phase III of the CUREE-Kajima Joint Research Program. The building is analyzed three ways: in its condition prior to the 1994 Northridge Earthquake, with a hypothetical shearwall upgrade, and with earthquake insurance. This is the first application of ABV to a real building, and the first time ABV has incorporated stochastic structural analyses that consider uncertainties in the mass, damping, and force-deformation behavior of the structure, along with uncertainties in ground motion, component damageability, and repair costs. New fragility functions are developed for the reinforced concrete flexural members using published laboratory test data, and new unit repair costs for these components are developed by a professional construction cost estimator. Four investment alternatives are considered: do not buy; buy; buy and retrofit; and buy and insure. It is found that the best alternative for most reasonable values of discount rate, risk tolerance, and market risk is to buy and leave the building as-is. However, risk tolerance and market risk (variability of income) both materially affect the decision. That is, for certain ranges of each parameter, the best investment alternative changes. This indicates that expected-value decision-making is inappropriate for some decision-makers and investment opportunities. It is also found that the majority of the economic seismic risk results from shaking of $S_a < 0.3g$, i.e., shaking with return periods on the order of 50 to 100 yr that cause primarily

architectural damage, rather than from the strong, rare events of which common probable maximum loss (PML) measurements are indicative.

The Kajima demonstration is performed using three Tokyo buildings. A nine-story, steel-reinforced-concrete building built in 1961 is analyzed as two designs: as-is, and with a steel-braced-frame structural upgrade. The third building is 29-story, 1999 steel-frame structure. The three buildings are intended to meet collapse-prevention, life-safety, and operational performance levels, respectively, in shaking with 10%exceedance probability in 50 years. The buildings are assessed using levels 2 and 3 of Kajima's three-level analysis methodology. These are semi-assembly based approaches, which subdivide a building into categories of components, estimate the loss of these component categories for given ground motions, and combine the losses for the entire building. The two methods are used to estimate annualized losses and to create curves that relate loss to exceedance probability. The results are incorporated in the input to a sophisticated program developed by the Kajima Corporation, called Kajima D, which forecasts cash flows for office, retail, and residential projects for purposes of property screening, due diligence, negotiation, financial structuring, and strategic planning. The result is an estimate of NAV for each building. A parametric study of CE for each building is presented, along with a simplified model for calculating CE as a function of mean NAV and coefficient of variation of NAV. The equation agrees with that developed in parallel by the CUREE team.

Both the CUREE and Kajima teams collaborated with a number of real-estate investors to understand their seismic risk-management practices, and to formulate and to assess the viability of the proposed decision-making methodologies. Investors were interviewed to elicit their risk-tolerance, ρ, using scripts developed and presented here in English and Japanese. Results of 10 such interviews are presented, which show that a strong relationship exists between a decision-maker's annual revenue, R, and his or her risk tolerance, $\rho \approx 0.0075R^{1.34}$. The interviews show that earthquake risk is a marginal consideration in current investment practice. Probable maximum loss (PML) is the only earthquake risk parameter these investors consider, and they typically do not use seismic risk at all in their financial analysis of an investment opportunity. For competitive reasons, a public investor interviewed here would not wish to account for seismic risk in his financial analysis unless rating agencies required him to do so or such consideration otherwise became standard practice. However, in cases where seismic risk is high enough to significantly reduce return, a private investor expressed the desire to account for seismic risk via expected annualized loss (EAL) if it were inexpensive to do so, i.e., if the cost of calculating the EAL were not substantially greater than that of PML alone.

The study results point to a number of interesting opportunities for future research, namely: improve the market-risk stochastic model, including comparison of actual long-term income with initial income projections; improve the risk-attitude interview; account for uncertainties in repair method and in the relationship between repair cost and loss; relate the damage state of structural elements with points on the force-deformation relationship; examine simpler dynamic analysis as a means to estimate vulnerability; examine the relationship between simplified engineering demand parameters and performance; enhance category-based vulnerability functions by compiling a library of building-specific ones; and work with lenders and real-estate industry analysts to determine the conditions under which seismic risk should be reflected in investors' financial analyses.

CONTENTS

FIGURES

TABLES

Chapter 1. Introduction

1.1 OVERVIEW OF SEISMIC RISK AND REAL-ESTATE INVESTMENT DECISIONS

This report documents a joint research project by the California Institute of Technology and the Kajima Corporation of Japan, under Phase IV of the CUREE-Kajima Joint Research Program. It addresses how a real estate investor should deal with seismic risk when making an investment decision, and seeks to answer several questions:

- Should an investor be concerned with seismic risk at all, or does risk associated with market volatility swamp seismic risk?
- How can one estimate seismic risk on a building-specific basis?
- How can seismic risk be accounted for using current business practices?
- How should the decision-maker's risk attitude influence a purchasing decision?

Current practice among real-estate investors to deal with seismic risk is to commission a study of earthquake probable maximum loss (PML) during the due-diligence phase of a purchase, i.e., during the bidding and negotiation period before a purchase is finalized. If the PML exceeds a certain fraction of the building replacement cost, lenders either decline to underwrite a mortgage, or require earthquake insurance. If the loan is unavailable or the insurance too expensive, the investor might pass on the purchase.

The problem with this approach is that PML does not represent a business expense that can be used in a financial analysis of the investment opportunity. Consequently, the analysis ignores a potentially significant expense, thus possibly overestimating return. Because the earthquake expense varies between properties, the investor cannot reasonably consider it a constant error that can be neglected in a choice between competing opportunities. Since PML is a worst-case expense at an unknown future time, it cannot be amortized for use in risk-management cost-benefit analysis.

This study proposes that seismic risk be treated in financial analyses as an uncertain discounted present value of operating expenses related to repairs and loss of

use from future earthquakes affecting the building. The study compares seismic risk with market risk (represented by uncertain future net income neglecting seismic risk) to determine whether earthquake risk is significant enough to be worth considering. The study then examines various methods to quantify seismic risk for particular investment opportunities on a building-specific basis. A methodology to quantify net asset value (including both seismic risk and market risk) is then presented.

The study also treats the effects of uncertainty and risk attitude on the investment decision. Whenever a financial decision involves substantial uncertainty and large sums relative to the investor's wealth, risk-neutral decision-making based on expected property value becomes inappropriate. A decision-analysis approach to real estate investment decision-making is therefore developed, using the concept of certainty equivalent of the property value as the central decision parameter.

1.2 OBJECTIVES OF THE PROJECT

The principal objectives of this project were: (1) to develop a methodology for establishing real estate risk-return profiles that not only consider market risk (the uncertain lifetime net income stream), but also seismic risk (the uncertain lifetime earthquake losses for a property); and (2) to show how these profiles may be used in decision-making related to real estate risk management and property investment and development choices.

A comprehensive methodology that includes the financial risks from all sources, including seismic risk, allows better decision-making in the allocation of resources when purchasing or constructing property, retrofitting property to mitigate seismic risk, assessing the total risk for a property and managing risk through insurance or other financial instruments.

This research builds on results of the project *Decision Support Tools for Earthquake Recovery of Businesses* funded under Phase III of the CUREE-Kajima Joint Research Program (Beck *et al.*, 1999). The product of this Phase-IV research project is a methodology for establishing real-estate risk-return profiles that not only considers market risk but also the seismic risk for the property; and a decision-making procedure

to assist in making real estate investment choices. These products are built up from the following fundamental results of the research:

- A methodology for establishing the risk-return profile of investment real estate accounting for important financial variables as well as earthquakes or other hazards.

- A new methodology for establishing the full statistical properties (not just the mean) of the present value of the lifetime earthquake losses for a property based on a building-specific loss estimation methodology that integrates a probabilistic seismic hazard analysis with a building-specific seismic-vulnerability analysis.

- A risk-averse decision-making procedure to assist in making real estate investment choices that is based on the project methodologies and principles of decision analysis applied to the net asset value that is affected by an uncertain future. This procedure incorporates the decision makers' attitude to risk, e.g., whether they put more emphasis on avoiding large losses or more on making large profits.

- A preliminary comparison of seismic risk with other major sources of property-damage risk such as fire.

- Demonstration of the methodology for establishing risk-return profiles and for risk-averse decision-making using example buildings in the U.S. and Japan.

1.3 ORGANIZATION OF REPORT

Chapter 2 presents a literature review of real-estate investment risk, methods to evaluate earthquake risk, and theory for real-estate investment decision-making. Chapter 3 develops a methodology creating a risk-return profile considering building-specific earthquake losses. A decision-making methodology that considers market risk, seismic risk, and the decision-maker's risk attitude is presented in Chapter 4. Chapter 5 illustrates the methodology using a California demonstration building examined by the CUREE research team. Chapter 6 offers a parallel demonstration by Kajima researchers, using three Japanese buildings. Chapter 7 examines real estate investment practice in

the U.S. and Japan, and presents case studies of several investors, in order to understand how the proposed procedures might be used in practice. Conclusions and future work are presented in Chapter 8. References are shown in Chapter 9.

A number of appendices include detailed supporting analyses and data-gathering techniques. Appendix A provides a detailed script of an interview and analytical technique to estimate a decision-maker's risk attitude. Appendix B presents this script translated into Japanese. Appendix C presents our analysis of the fragility, repair techniques, and repair costs of reinforced concrete beam-columns. Appendix D presents a mathematical formulation of the discrete-time present value of a property with uncertain future returns that can vary from year to year. Appendix E presents a continuous-time equivalent to Appendix D, i.e., a stochastic model of net income, considering a random, continuously varying after-tax yield. The moment-generating function for the moments of future (lifetime) earthquake loss is derived in Appendix F. Appendix G presents details of the structural model created for the of CUREE demonstration building. Appendix H contains a professional cost estimate of the seismic retrofit designed here for the CUREE demonstration building. Finally, Appendix I shows the output of the Kajima-D program for cash-flow analysis.

Chapter 2. Literature Review

2.1 INTRODUCTION

Before addressing the calculation of the lifetime effects of earthquakes on property value and how this may be used in real-estate investment and risk-management decisions, it is important first to understand the relative significance of the various sources of risk that are involved. Section 2.2 presents a literature review regarding how real-estate investment return is ordinarily calculated in practice and the relative magnitude of risk on return from market forces, earthquake and fire. It shows that in California, earthquake risk may be of the same order of magnitude as market risk in terms of effect on real-estate investment return, and that risk from fire is on average probably an order of magnitude less than earthquake.

Given that earthquake risk appears to have a potentially significant effect on overall return and therefore on property value, it is important to understand how potential earthquake losses can be quantified. Section 2.3 therefore presents a literature review of available means to calculate potential costs to the property owner if an earthquake occurs. The typical approach to this loss estimation is to combine a probabilistic seismic hazard analysis with a building vulnerability analysis that can be category-based, prescriptive or building-specific. Each of these procedures is briefly reviewed, with a final focus on a building-specific vulnerability approach, called assembly-based vulnerability, or ABV, which is selected for the present study of the CUREE demonstration building. A three-tiered vulnerability approach developed by the Kajima Corporation is selected for the present study of the Kajima demonstration building, and is described later in Chapter 6.

In this work, uncertainty in market valuation based on net income is dealt with but the emphasis here is on earthquake risk. It is important to understand how earthquake risk might appropriately be considered in an investment analysis. Section 2.4 therefore presents a literature review of real-estate valuation and investment theory, including discussion of the criteria typically used to make a real estate investment decision. It is concluded that an approach based on decision analysis (also known as

decision theory) provides the best approach to decision-making under risk. Therefore, the decision-analysis approach, including the decision-maker's attitude toward risk, is also reviewed.

2.2 RISK IN REAL ESTATE INVESTMENT

2.2.1 Sources and magnitude of market risk

The intrinsic value of commercial real estate comes from the net operating income stream that it generates. Since future income is uncertain because of changes in the real estate market, property value is subject to market risk.

In the case of purchasing an existing property, the net operating income during ownership and the liquidation value of the property are the major uncertainties affecting the establishment of the property value. The liquidation value will depend on the future net operating income that is perceived by a purchaser at the time the property is liquidated. The basic source of uncertainty in property value is therefore the net operating income stream over a specified property lifetime, which depends on future rental rates, vacancy rates and operating expenses. Taxation plays a significant role in return on investment and so an investor should consider after-tax return. Another source of uncertainty is therefore future tax rates. Figure 2-1 summarizes a procedure that is adapted from Case (1988) for the calculation of the income stream resulting from the purchase of an existing building.

Byrne and Cadman (1984) present a framework for real estate valuation from the point of view of a property developer. The authors include a typical investment value calculation, identify important and lesser uncertain variables, and identify likely sources for information on those variables. Figure 2-2 presents a flowchart for calculation of investment value, based on the procedures presented by Byrne and Cadman (1984). The figure shows the variables, data sources, and calculation procedures to determine investment value. These authors find that the most significant sources of uncertainty on the developer's return for a new development project (as opposed to an investment in an existing building) are short-term borrowing cost, building costs and property value upon completion. The latter depends on the future net operating income and investors'

expectation on yield (e.g., market gross income multipliers) and so is subject to the same market risk as in the purchase of existing properties.

Neither Figure 2-1 nor Figure 2-2 explicitly shows non-market-related costs such as repair of earthquake damage, but such costs could be readily included. Earthquake repair costs could be represented by an additional uncertain variable, denoted by y, that would be added to the operating expense, g in Figure 2-1, or deducted from capital value, u in Figure 2-2.

Given the procedure by which property value is calculated, it is important to quantify the overall uncertainty on value. Such knowledge is crucial to understanding the conditions under which seismic risk significantly contributes to overall investment risk. Some research has recently been performed to quantify overall uncertainty in market value. Holland *et al.* (2000) estimate the volatility of real estate return as part of a larger study of how uncertainty affects the rate of investment. Using this implied volatility of return, the authors specify a model in which property returns follow a standard Brownian-motion process with drift. By estimating the capitalization rate (i.e., return on the purchase price) for U.S. office and retail real estate investments from 1979 to 1993, they find the implied volatility of the capitalization rate for commercial real estate (i.e., the standard deviation of the difference between return in two successive years) to be on the order of 0.15 to 0.30.

It can be shown (see Appendix C for the derivation) that such a model of value implies a coefficient of variation on the property value equal to several times the ratio of volatility to initial capitalization rate, i.e., if σ represents volatility of return, x_0 represents the initial return and r is the discount rate, then the coefficient of variation on the present value of the net operating income stream, denoted by δ_V, is given by

$$\delta_V = \frac{\sigma}{\sqrt{2r}x_0} \tag{2-1}$$

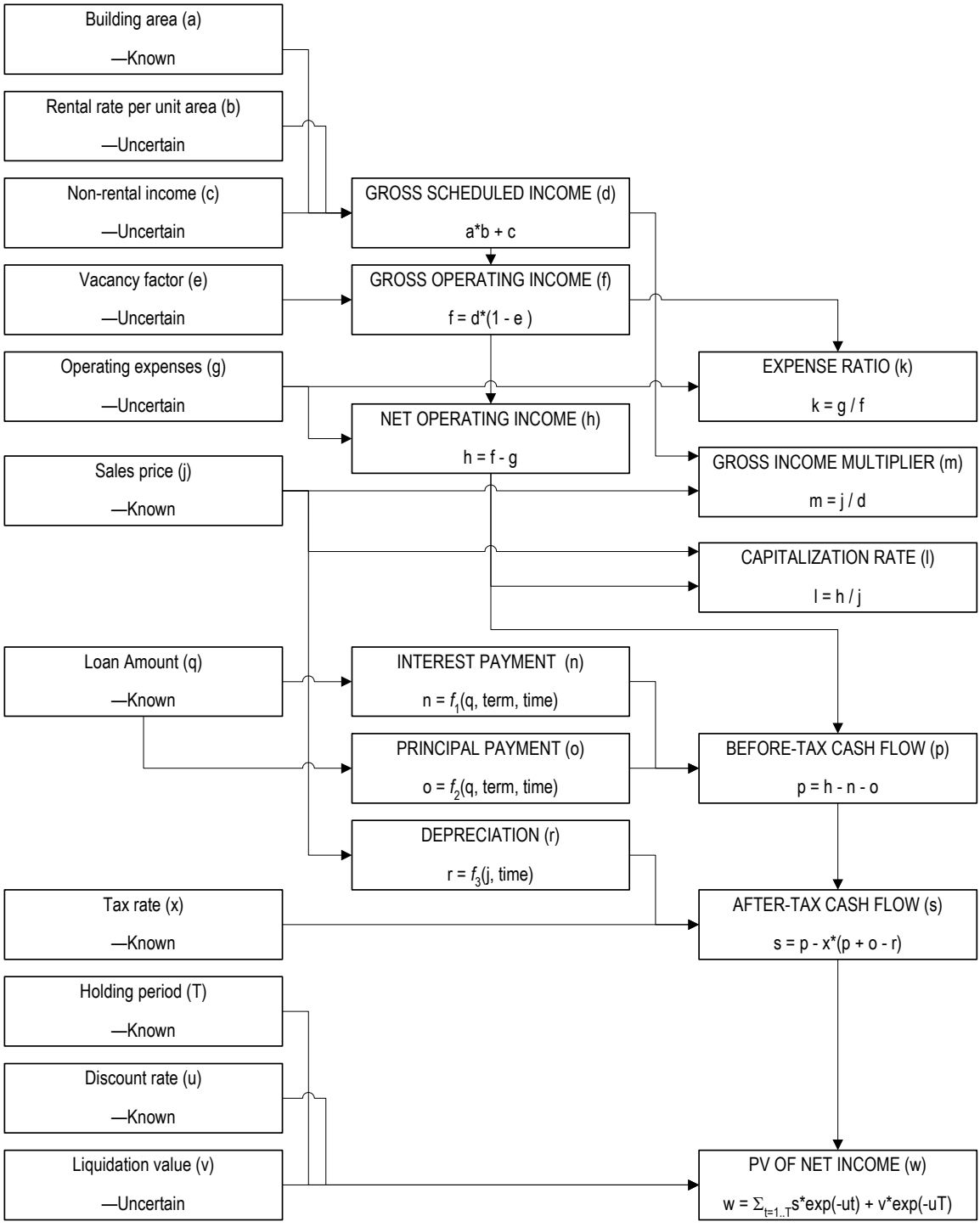

Figure 2-1. Calculation of the present value of an existing income property.

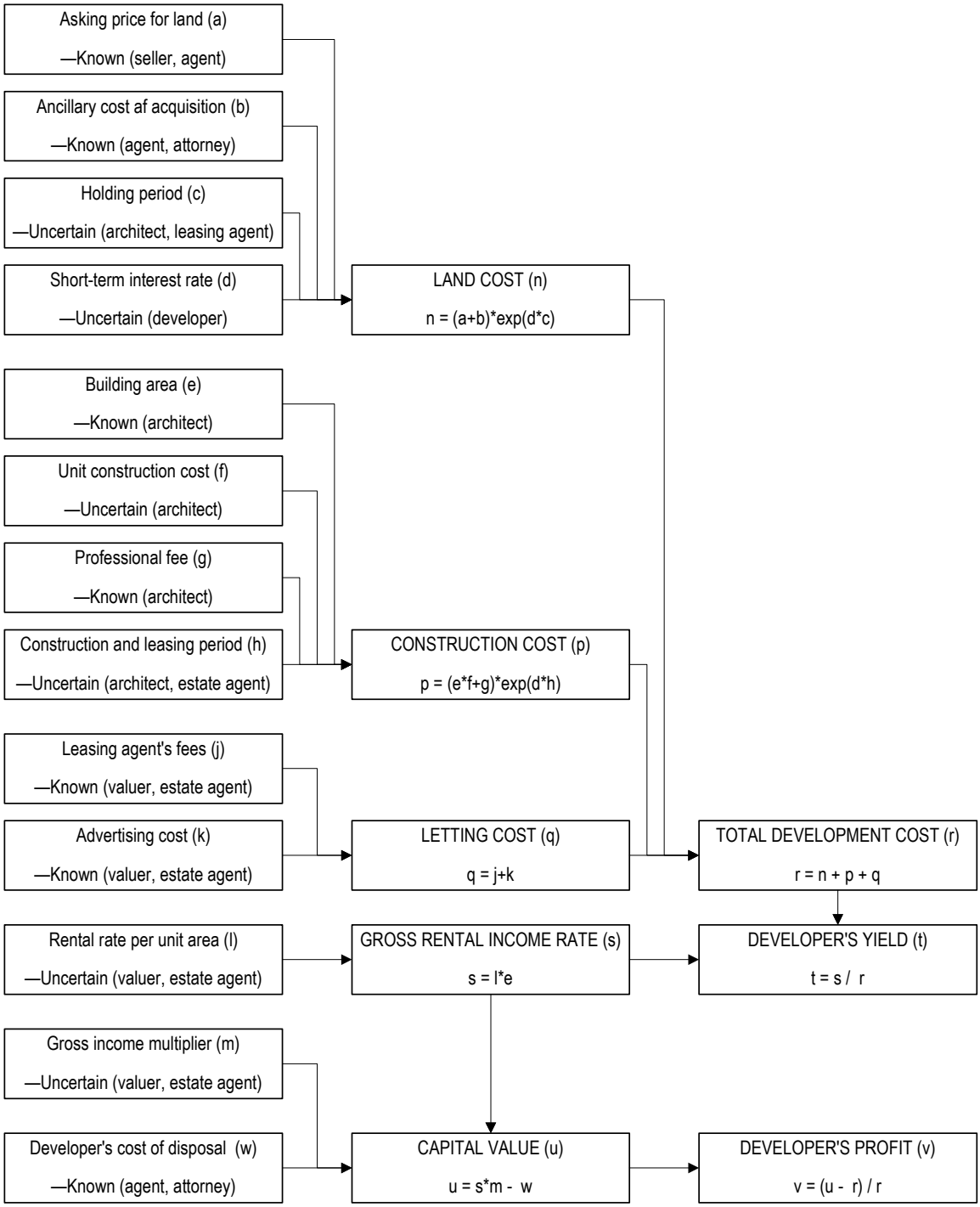

Figure 2-2. Variables and data sources for valuing a development project.

This coefficient of variation probably substantially overstates the investor's uncertainty on property value based on the discounted long-term net income stream, because the investor has some advance knowledge of, and control over, future returns. Equation 2-1 therefore indicates an upper-bound uncertainty in value. For an initial capitalization rate of 0.1, a volatility of 0.2 and a discount rate of 5%, the coefficient of variation on property value is in excess of 6, a very high value! It depends, of course, on the acceptance of the Brownian-motion ("random walk") model of capitalization rate and the empirical value for σ estimated by Holland *et al.* (2000). It does suggest, however, that the effect of market risk on property value can be substantial.

This coefficient of variation on value can be contrasted with the judgment of a real estate investor interviewed for an earlier phase of the present study. Flynn (1998) expressed the belief that when skilled investors independently estimate the market value of an individual commercial property, they generally agree within 20 percent or so. This figure represents the investor's uncertainty on mean value, akin to standard error, and is not the same as the investor's uncertainty on value, which might be akin to standard deviation. It does represent a reasonable lower bound: if the investor's estimate of mean value is uncertain by ±20%, then his or her overall uncertainty on value must be at least 20%, probably more.

Taken together, these two sources imply that market risk, as measured by the coefficient of variation on long-term property value, is at least 0.2 and may exceed 1.0. A reasonable value to assume is a coefficient of variation of 1.0, keeping in mind that the investor's advance knowledge of, and control over, future returns should reduce the value below the upper bound given in Equation 2-1.

2.2.2 Market risk compared with earthquake risk

It is important to understand how earthquake risk compares with the effect of market volatility on property value. In cases where earthquake risk is small compared with market risk, there is no point in considering it when making real-estate investment decisions. If earthquake risk is of the same order of magnitude or larger than market risk, then the ability to quantify earthquake risk would be of great value to real estate investors.

In current practice, when earthquake risk is considered in real estate investment decisions, analysis is typically limited to an evaluation of probable maximum loss (PML), as noted by Maffei (2000). Though there is no commonly accepted quantitative definition of earthquake PML (Zadeh, 2000; ASTM, 1999), most working definitions involve the level of loss associated with a large, rare event (Rubin, 1991). Commercial lenders often use PML to help decide whether to underwrite a mortgage, but otherwise PML is not used in estimating the value of a property. PML represents a scenario loss estimate, and is therefore not directly comparable with the term typically associated with financial risk, namely, the standard deviation of annual return.

Thus, the principal parameter used by investors to examine earthquake risk provides little information about the degree to which earthquake risk contributes to overall risk. The subject of the present study is, of course, how better to include earthquake risk in real estate valuation, but an initial order-of-magnitude comparison of earthquake risk with market risk is of interest.

No published data on the effect of earthquake risk on real estate return is readily available, but Porter (2000) presents a risk study involving the purchase of a hypothetical commercial property in Los Angeles. The property in question is a 3-story pre-Northridge welded steel moment-frame (WSMF) office building. It has an estimated mean present value of the long-term net income stream of $3.1 million, ignoring earthquake costs. If the market risk were associated with a coefficient of variation of 1.0 for the net present value, this would be equivalent to an uncertainty in value (as measured by the standard deviation of market value) of $3.1 million. In comparison, the present value of earthquake loss to the building over a 100-year lifetime has a mean value of $2.2 million and a standard deviation of $1.1 million, using a similar loss-estimation approach as in Porter (2000) and a discount rate of 5%.

For this example building then, the mean present value of earthquake loss is about 70% of the mean net present value ignoring earthquakes while the uncertainty on earthquake loss is about 35% of the market value uncertainty ($1.1 million versus $3.1 million). The total uncertainty in value for this building (assuming market risk and earthquake risk are independent) is $3.3 million. Thus, for this building, the uncertainty

from market risk swamps that from earthquake risk. That is not to say that earthquake loss is unimportant. In this example, the mean earthquake loss reduces the present value of the building by 70%. However, unless the standard deviation of earthquake loss reaches about ½ of the standard deviation of the market value, uncertainty in earthquake loss need not be considered in a probabilistic analysis of investment value.

2.2.3 Fire risk compared with earthquake risk

Fire risk is typically transferred from the building owner via insurance, so the owner ends up bearing only the risk associated with the deductible. For US residential properties, the deductible is typically on the order of $250 to $1,000, so the expected annual value of fire loss for a homeowner or renter is on the order of $1,000 times the annual probability of the occurrence of fire.

Karter (1999) reports summary statistics about US fire losses that are informative about probability of the occurrence of fire. As shown in Table 2-1, in 1998, the total US structure damage due to fire was approximately $6.7 billion, of which $4.4 billion in damage was to residential structures (381,500 fires); the remaining $2.3 billion occurred in non-residential (commercial, industrial, institutional, and government) structures (136,000 fires). Civilian casualties numbered 3,220 deaths and 17,200 injuries in residential structures, and approximately 800 deaths and 2,200 injuries in non-residential structures. There is a slight but continuous downward annual trend in total number of fires, dollar losses and casualties. However, inflation-adjusted property loss per structure fire has been approximately constant since 1977, with the 1998 average property loss being approximately $12,980 per structure fire. The figure for residential fires alone is $11,500, while non-residential structure fires resulted on average in a loss of $17,100.

There are approximately 88 million residential structures in the US (US Census Bureau, 1999), so the number of residential fires reported by Karter (1999) implies an annual probability of the occurrence of a fire in a residential building of approximately 0.4%. Hence the mean loss borne by an insured owner or tenant is on the order of $4 per year ($1,000 deductible times 0.4% per year). An uninsured owner is exposed to a mean annual loss on the order of $50 per year ($11,500 times 0.4%).

The number of non-residential buildings in the US is not readily available. However, it is likely to be on the order of 10 to 30 million buildings. Deductibles for non-residential buildings vary more widely than residential deductibles, and are sometimes accompanied by coinsurance (a fraction of loss above the deductible paid for by the insured). So before considering the effect of insurance, it is worthwhile evaluating expected fire damage prior to risk transfer. If the number of non-residential properties is 20 million, and 136,000 fires occurred in non-residential buildings in 1998, then the average annual probability of fire in such a property is on the order of 0.7% (136,000/20 million). The corresponding expected annual cost of fire damage to a non-residential property is on the order of $100 per year (0.0068 * $17,100).

California represents approximately 12.2% of the US population (US Census Bureau, 2000a), and per-capita fire-related property losses in the western US are approximately 71% of the national average (Karter, 1999), so it can be estimated that in 1998, California structure fire losses were approximately $580 million ($6.7 billion * 0.71 * 0.122). This annual figure of fire losses can be compared on an order-of-magnitude basis with annual earthquake losses in California over the last 30 years.

Since 1971, California earthquake losses have totaled approximately $49 billion in year-2000 dollars, for an average amount of $1.6 billion per year. Thus, total annual California earthquake losses exceed fire by a factor of 3, with a far greater proportion of the fire loss being transferred from building owners via insurance. If earthquake losses were adjusted for rising population, the factor would be greater.

The conclusion from this very approximate analysis is that fire loss borne by building owners is probably an order of magnitude less than earthquake loss, suggesting that fire hazard can be ignored in a probabilistic analysis of property value.

Table 2-1. 1998 US fire risk

	Residential	Nonresidential	Total
Fire totals			
Structures (est.)	88,000,000	25,000,000	113,000,000
Structure fires	381,500	136,000	517,500
Structure damage ($M)	4,391	2,326	6,717
Civilian injuries	17,200	2,200	19,400
Civilian deaths	3,220	800	4,020
Civilian casualties/fire	0.05	0.02	0.05
Fire, per building			
Annual probability of fire	0.43%	0.54%	0.46%
Average cost given a fire	$ 11,510	$ 17,103	$ 12,980

2.3 METHODS TO EVALUATE EARTHQUAKE LOSSES

2.3.1 Probabilistic seismic risk analysis

How can a probabilistic description of earthquake loss be developed? This requires a site-specific, probabilistic seismic risk analysis involving loss estimation. A recent compilation of loss-estimation research efforts is presented in a special issue of Earthquake Spectra (EERI, 1997). Virtually all such analyses employ a common framework that combines a probabilistic seismic hazard analysis for the site with a building vulnerability analysis as follows:

1. Characterize the seismic sources in the region around the site: their probabilistic magnitude-frequency relationship, faulting mechanism, and the probability distribution of potential rupture initiating within each fault segment.

2. For an event of given magnitude on a given fault segment, determine a probabilistic description of ground motion at the site (and possibly other site effects such as liquefaction, landslides, etc.), considering the fault mechanism, regional geology, fault distance, and site soil conditions. For example, the shaking intensity at a site is often described by peak ground acceleration or

response spectral acceleration using a probabilistic attenuation relationship involving distance from the source. Such relationships for shaking intensity in terms of magnitude, distance, and soil conditions are provided, for example, by Boore *et al.* (1997).

3. Use the Theorem of Total Probability to combine the probabilistic descriptions of the seismicity in Step 1 and the attenuation in Step 2 to get a probabilistic description of the ground motion at the site. This is typically described by a frequency form of the hazard function for the site, denoted by $g(S)$, where the parameter S describes the shaking intensity at the site. The hazard function is defined so that $g(S)dS$ is the expected rate of occurrence of events at the site (e.g. mean annual frequency) with shaking intensity S in the range $(S, S+dS)$.

4. For the probabilistic description of the ground motion at the site in Step 3, derive a probability distribution on the total loss for the building at the site, considering its value, use, occupancy, and its seismic vulnerability function, that is, a probability distribution on total loss conditioned on the ground shaking.

5. For the total loss estimated in Step 4, quantify the loss borne by the interested party, e.g., an insured property owner.

While the details may vary from study to study, the general methodology for loss estimation that considers as individual components of the analysis, seismic hazard, seismic vulnerability and loss, is consistent. Sometimes hazard is expressed in more detail in terms of seismic sources (characteristics, distances, and attenuation) or the hazard is expressed in time-dependent terms. Sometimes an uncertainty is ignored, or only particular earthquake scenarios are considered, or site hazard is quantified in a separate step, but these variations do not significantly change the theoretical framework.

The present study focuses primarily on the development of the building vulnerability function for Step 4, as opposed to improved modeling of seismicity and ground motion attenuation. There are several approaches used to create seismic

vulnerability functions: category-based, prescriptive and building-specific approaches are briefly described here.

2.3.2 Category-based seismic vulnerability

Most familiar is the category-based approach, which characterizes the seismic vulnerability of an individual building based on a limited number of parameters. These can number as few as one, but typically three or four are considered, usually construction material, lateral-force-resisting system, height range, and era of construction. Methods to develop category-based vulnerability functions have included empirical methods, expert opinion, and a combination of engineering and expert opinion approaches.

Scholl (1981) sought to gather from available literature enough data on past earthquake loss to quantify seismic vulnerability functions on an entirely empirical basis. He found that the available data were either inadequately descriptive of the loss, inconsistent, or otherwise too unreliable to create a significant set of seismic vulnerability functions.

The Applied Technology Council (1985), recognizing the deficiencies in available data, used expert opinion to create several dozen seismic vulnerability functions, through a modified Delphi process involving 58 self-described experts in earthquake engineering. The results of this study have been widely used by a variety of studies.

The Federal Emergency Management Agency (FEMA), through the National Institute of Building Sciences (NIBS), sponsored the development of the latest version of category-based seismic vulnerability functions, which are documented in NIBS (1995) and embodied in the HAZUS software. This approach uses engineering methods to characterize the load-displacement behavior of categories of buildings, to relate displacement and acceleration to damage for large categories of building components, and then to relate damage to loss.

This approach grew in part from a methodology discussed by Scholl (1981), as a complement to his empirical approach, which was developed by Kustu *et al.* (1982), Scholl and Kustu (1984), and Kustu (1986). This approach employs structural analysis to

determine building response. Laboratory test data are used to relate structural response to component damage. Components are defined at a moderate level of aggregation, as shown in Table 2-2. Component damage is then related to repair cost through standard construction contracting principles. The method is illustrated in Figure 2-3. As employed for developing category-based vulnerability functions, the method requires a significant amount of engineering judgment to characterize the fragility of aggregated components and to quantify the relative values of various components within a building category. The seismic vulnerability functions developed for HAZUS are in the end category-based, and the vulnerability for any building is typically defined by the four parameters described above.

A consequence of category-based approaches is that one cannot evaluate the effect of vulnerability on a choice between buildings of the same category, nor can one evaluate the effect of design or construction details on the vulnerability of an individual building. Finally, while the use of engineering judgment is not theoretically inseparable from category-based approaches, in practice, category-based approaches have relied heavily on judgment, which often results in skepticism about the validity of the results.

2.3.3 Prescriptive seismic vulnerability

Often, seismic vulnerability is assessed in terms of whether a building meets the seismic evaluation criteria of various building codes. New and existing structures in the U.S. are often evaluated in terms of code requirements, that is, the requirements of various editions of the Uniform Building Code (e.g., International Conference of Building Officials, 1997), the Uniform Code for Building Conservation (International Conference of Building Officials, 1991), FEMA 273 (Federal Emergency Management Agency, 1997), and other guidelines. These codes have the advantage of addressing vulnerability on a building-specific basis, and employ structural analysis techniques that do not depend heavily on engineering judgment. However, they are designed only to determine whether a building meets minimum safety and serviceability criteria, not to produce loss estimates or quantify the probability of exceeding any particular limit state.

2.3.4 Building-specific seismic vulnerability

The approach discussed by Scholl (1981) and Kustu *et al.* (1982) can be used to develop a motion-damage relationship based on detailed structural analysis of an individual building, followed by an assessment of damage to a variety of components based on structural response. In this approach, one uses dynamic analysis (either via response spectrum, linear, or nonlinear dynamic time-history analysis) to estimate structural response on a floor-by-floor basis, and then applies these structural response parameters to appropriate component vulnerability functions. Again, the term *component* refers to a category of building elements; see Table 2-2 for components considered in this approach. Using the component vulnerability function, a damage ratio for each component is evaluated for each floor and multiplied by the value of each component. Damage to the whole building is obtained by adding the damage to its modules or pieces. Figure 2-3 summarizes this approach.

Table 2-2. Building components considered by Scholl (1981) and Kustu *et al.* (1982).

Damage component	**Motion parameter**
Structural	
Steel frame	Maximum interstory drift
Concrete frame	Maximum interstory drift
Masonry shear wall	Maximum interstory drift
Braced frames	Maximum interstory drift
Foundations	
Nonstructural	
Drywall partitions	Maximum interstory drift
Brick infill walls	Maximum interstory drift
Concrete block infill walls	Maximum interstory drift
Glazing	Maximum interstory drift
Cladding	Max. floor acceleration or velocity
Other (ceilings, mechanical, and electrical equipment)	Max. floor acceleration or velocity
Contents	Max. floor acceleration

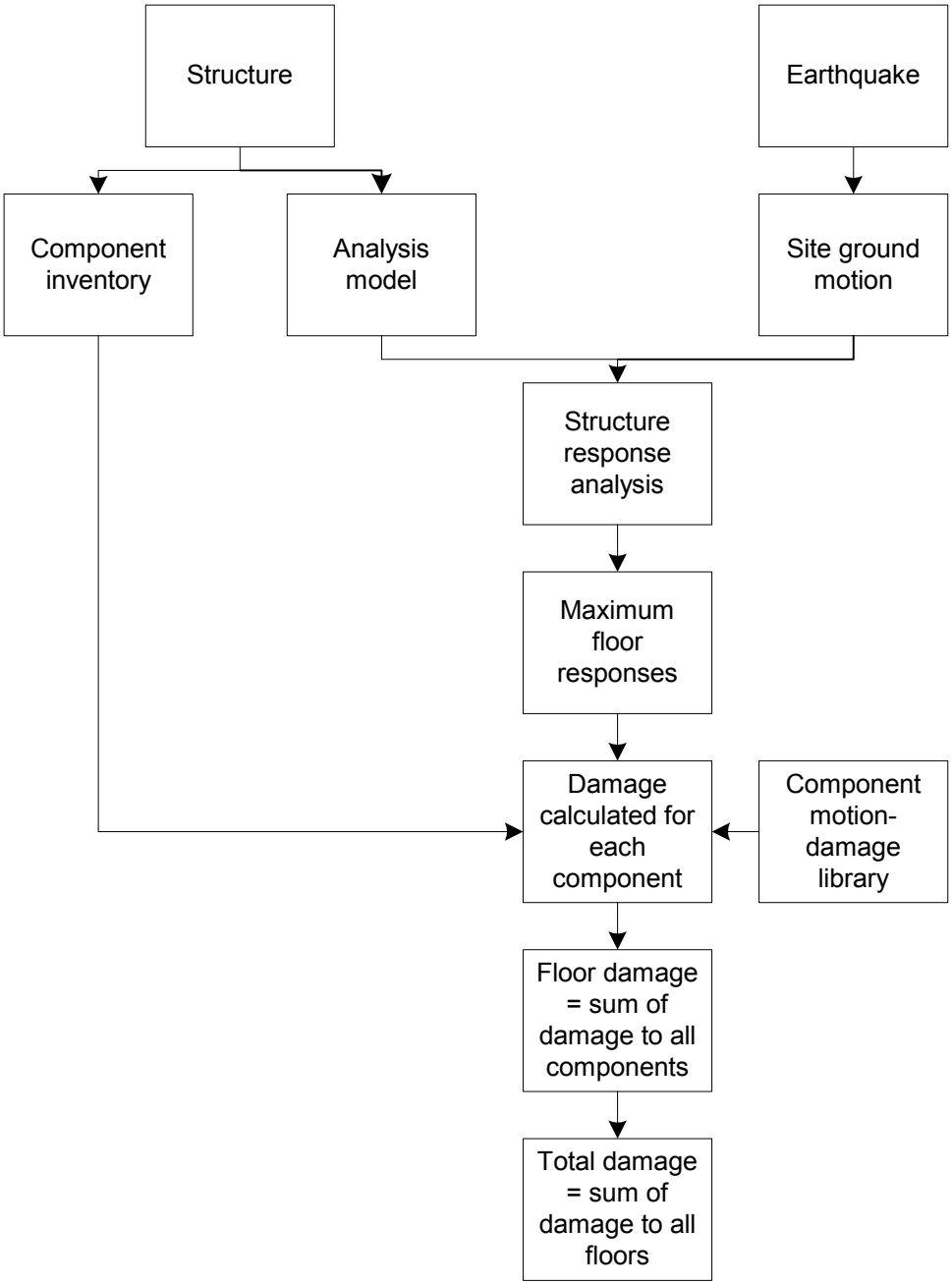

Figure 2-3. Component-based damage prediction (after Scholl, 1981).

A similar analysis methodology called assembly-based vulnerability (ABV) is documented in early form during Phase III of the CUREE-Kajima Joint Research Program (Beck *et al.*, 1999). It produces a probabilistic relationship between economic loss (in the present case, repair cost) and shaking severity (measured in the present study in terms of the spectral acceleration at the building's small-amplitude fundamental period). ABV builds on Kustu and Scholl's approach in several ways. It

models components at the more-detailed level of individual building assemblies. An assembly, as used here, is a set of basic elements assembled to construct a distinct, recognizable part of a facility such as a window installed and in place, a segment of installed gypsum wallboard partition, or a reinforced concrete column. Thus, an assembly can comprise structural elements, nonstructural elements, or contents in a building or other facility. A formal taxonomy of assemblies is employed to provide unambiguous reference to assembly types and to their possible damage states, repair methods and repair costs.

By modeling building behavior at this level of detail, one can explicitly model the behavior of detailed components whose damageability, repair methods, and repair costs substantially differ within an aggregated component type such as shown in Table 2-2. For example, one can distinguish the behavior of ductile and nonductile concrete-frame members; between drywall partitions on metal versus wood studs, or between various types of cladding, such as stucco versus aluminum panels. This ability is an important requirement if one wants to assess the economic desirability of seismic retrofit alternatives, a goal in the present study.

A more-detailed approach is also necessary to avoid heavy reliance on judgment. One reason is that one can reasonably perform a laboratory test of the mechanical characteristics of a detailed assembly. By contrast, it is problematic to create a practical laboratory test of all ceilings, mechanical, and electrical equipment. One can compile test results of various subcategories of these components, but then one must rely on judgment to create weighted-average component damageability relationships. Finally, a detailed approach is necessary to assess performance at the level used by performance-based earthquake engineering methods such as FEMA-273 (1997) and FEMA-356 (2000).

For these reasons, ABV is used in the present study. The methodology is recapitulated in Chapter 5 (along with the enhancements introduced since CUREE-Kajima Phase III). It is described in greater detail in Porter (2000), Porter *et al.* (2001), and Porter *et al.* (2002a).

2.4 THEORY FOR REAL-ESTATE INVESTMENT DECISION-MAKING

2.4.1 Theoretical framework for investment decisions

Given that risk from market changes and earthquake losses should be considered when making a real-estate investment decision, how are such decisions to be made? There is widespread agreement that present value of net after-tax cash-flow over some period should be used as the basic parameter in evaluating a real-estate investment opportunity. However, this valuation of property is uncertain because of market risk and seismic risk, and this uncertainty should be treated explicitly when ranking real estate investments.

It is reasonable to use as the decision criterion maximizing the expected value of the investor's wealth. Suppose, however, that for two possible investments, an investor predicts for one property a higher expected gain in wealth but with more uncertainty than that predicted for the other property. How should this extra risk influence the ranking of the two investment alternatives? There is a well-developed theory for decision making under risk that can be applied to real-estate investment decision-making. The fundamental principles are presented in the seminal work of Von Neumann and Morgenstern (1944). See also Howard and Matheson (1989). The objective in this approach is to maximize the expected value of the utility of cash-flow. Utility is used to reflect the investor's attitude toward risk. It is discussed in more detail below.

Ratcliff and Schwab (1970) propose the use of decision theory in real-estate investment decision-making. The financial parameters treated in their model are the same as for maximizing investor's wealth, but Ratcliff and Schwab (1970) additionally require probability distributions on cash-flow and on net proceeds from liquidation at the end of the period of ownership. They also require the selection of a discount rate, which represents the investor's time-preference for money, as opposed to alternative opportunity rate, i.e., the rate that might be earned from alternative investments. Finally, they require an expression of the investor's utility curve.

Byrne and Cadman (1984) expand on the notion of using decision theory in real estate investment, and present a complete analytical methodology. Note that the decision-theory approach is identical to traditional approaches when the decision-maker is risk neutral and point estimates are employed in the place of uncertain variables. Because decision theory explicitly accounts for the risk attitude and uncertain parameters, it can be considered more robust, and will therefore be used in the present study.

2.4.2 Use of decision analysis and risk attitude

Decision analysis is a powerful tool for the rational and systematic assessment of decision situations involving significant uncertainty. It allows a decision-maker (DM) to select an optimal alternative considering all the alternatives and information relevant to the decision situation, and to account for the DM's personal subjective attitude toward risk. Most people are risk-averse to some extent, in that they feel more pain in the potential loss of a monetary value x than pleasure in a potential gain of x. The larger the stakes involved, the greater the divergence between a risk-averse DM's actions and the actions of someone who is risk neutral. Thus, when the stakes are large and there is significant uncertainty involved, such as in earthquake risk, benefit-cost analysis (which assumes risk-neutral decision-making) may be an inappropriate decision-making tool. In such cases, a proper decision-making tool should account for the DM's attitude toward risk.

Risk attitude has been quantified in an abstract quantity referred to as *utility* which is a measure of a DM's preference or desire for different financial outcomes (see, for example, Howard, 1970). A relationship between utility and financial outcome is referred to as a *utility function*. A utility function is typically continuous and monotonically increases with financial outcome, indicating that a larger amount has greater utility (greater desirability). According to the theory of Von Neumann and Morgenstern (1944), in the presence of uncertainty in future outcomes, a DM should select that action or alternative among a set of possible actions that maximizes the expected utility.

Since preferences are subjective, DM's have their own utility function that reflects their attitude toward risk. Various idealized utility functions have been developed. One idealized function of interest is a utility function with exponential form:

$$u(x) = a + b\exp(-x/\rho) \tag{2-2}$$

In this equation, $u(x)$ represents the utility of a monetary amount x, a and b are arbitrary constants ($b < 0$), and ρ is the measure of risk attitude, referred to as the *risk tolerance parameter*. The equation thus defines risk attitude with this single parameter. Two points of the utility function, and hence the parameters a and b, can be arbitrarily chosen without affecting the resulting decision (as long as the two points indicate that the DM prefers more wealth to less).

Howard (1970) sketches a methodology for determining a DM's risk attitude under the assumption of an exponential utility curve. The DM is presented with the two hypothetical deals shown in Figure 2-4. In the first deal, the DM must invest an amount R. There is a 50-50 chance of either doubling the investment or losing half of it. The maximum amount the DM would invest is approximately equal to his or her risk tolerance, ρ. (That is, a DM's risk-tolerance parameter ρ can be estimated by judging the maximum amount the DM would be willing to bet on a coin toss if the winnings were ρ and the losses were $\rho/2$.) In the second deal, there is again an initial investment of R, and in this case a 75% probability of doubling the investment, and a 25% probability of losing it. Again, the maximum amount the DM would invest is approximately equal to his or her risk tolerance, ρ.

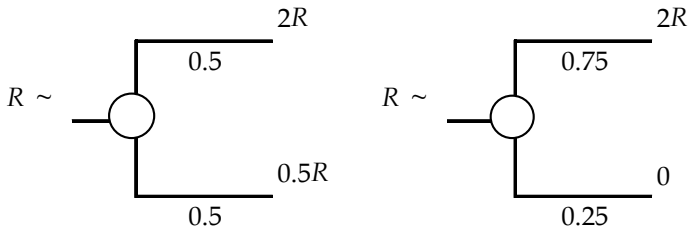

Figure 2-4. Two deals that estimate risk tolerance, per Howard (1970).

Spetzler (1968) describes in greater detail a methodology for creating a logarithmic utility function based on a series of 40 questions in which the DM is asked to

judge whether he or she should accept or reject a hypothetical financial deal. Each deal relates to an initial investment of $\$x_o$, yielding two possible financial outcomes, a positive outcome $\$x_1$ with probability *p*, and a negative outcome $\$x_2$ with probability $1-p$. In addition, to make the question as intuitive as possible, each deal is described in terms of equivalent uniform annual cashflow and of rate of return. In each deal, the interviewer finds the probability *p* such that the DM is just indifferent between accepting the deal and rejecting it, as shown in Figure 2-5. That is, the independent variables are x_o, x_1, and x_2, and the dependent variable, determined from the interview, is the indifference probability *p*.

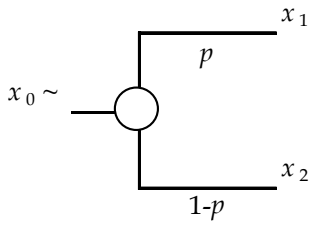

Figure 2-5. Form of deal used in Spetzler (1968) approach to determining risk attitude.

After the interview, the expected utility of each deal is calculated from

$$E\left[u_{deal}\right] = pu\left(x_1\right) + \left(1-p\right)u\left(x_2\right) \tag{2-3}$$

Since the DM is indifferent between accepting and rejecting the final deal, it is inferred that $u\left(x_0\right) = E\left[u_{deal}\right]$. The non-arbitrary parameters of the assumed utility function (e.g. risk tolerance, ρ) are found by regression analysis that effectively produces a best fit to this equation over all deals.

A modified version of this approach was developed by Porter (2000), and found to be effective in producing an exponential utility function of the form of Equation 2-2. After a few interviews of different DMs, an interesting trend appeared that relates risk attitude to size of business. The trend may be useful in estimating the risk attitude of DMs who are unavailable for an interview, for example, DMs of competing bidders on a project. Appendix A contains a more-detailed explanation of risk attitude, discusses

Porter's (2000) modifications to the Spetzler (1968) approach, and presents a detailed script for interviewing a DM to assess his or her risk attitude.

Porter (2000) also presents a decision-analysis approach to making seismic risk-management decisions for individual buildings, using the ABV methodology. The decision analysis accounts for the decision-maker's business practices and risk attitude, and produces a recommendation of the best alternative on an expected-utility basis. The methodology is illustrated using a realistic example of decision-making. It is found that risk attitude can make a material difference in the selection of the optimal risk-management alternative, thus calling into question techniques that assume risk neutrality and rely on cost-effectiveness as the key measure of desirability.

Chapter 3. Methodology for Lifetime Loss Estimation

3.1 BUILDING-SPECIFIC LOSS ESTIMATION PER EVENT AND PER ANNUM

The approach used here for loss estimation for a building is to combine a probabilistic seismic hazard analysis (PSHA) for the building site with an assembly-based vulnerability (ABV) analysis for the building, as described in Section 2.3.

Let $p(C|S)$ denote the building vulnerability function; that is, the PDF (probability density function) for the total earthquake losses C (arising from the after-tax costs of repairs and loss-of-use), given ground shaking of intensity S at the site. The PDF $p(C|S)$ is derived by the ABV method discussed in Chapters 2 and 5. Let $p(S|EQ)dS$ denote the probability that the shaking intensity lies in the interval $(S, S+dS)$, given that an earthquake has occurred somewhere in the region that produces shaking intensity exceeding a specified threshold S_0 at the site. The PDF $p(S|EQ)$ comes from the probabilistic seismic hazard analysis and is related to the hazard function for the site, as described below. From the Theorem of Total Probability, the PDF for the earthquake loss given an event in the region is:

$$p(C|EQ) = \int_{S_o}^{\infty} p(C|S)\,p(S|EQ)\,dS \tag{3-1}$$

The nth moment of the loss given that an earthquake has occurred is then given by:

$$\begin{aligned} E[C^n|EQ] &= \int_0^{\infty} C^n\,p(C|EQ)dC \\ &= \int_{S_0}^{\infty} E[C^n|S]\,p(S|EQ)dS \end{aligned} \tag{3-2}$$

where $E[C^n|S] = \int_0^{\infty} C^n\,p(C|S)dC$ is the nth moment of the loss given shaking of intensity S.

If the temporal occurrence of shaking at the site with intensity $S>S_0$ is modeled by a Poisson process with the mean rate of occurrence denoted by ν, then the mean rate of occurrence of events at the site with shaking intensity in the range $(S, S+dS)$ is given by:

$$\nu p(S \mid EQ)\,dS = g(S)\,dS \tag{3-3}$$

where $g(S)$ is the frequency form of the site hazard function. But $\int_{S_o}^{\infty} p(S \mid EQ)dS = 1$, so:

$$\nu = \int_{S_o}^{\infty} g(S)\,dS \tag{3-4}$$

$$p(S \mid EQ) = \frac{g(S)}{\int_{S_0}^{\infty} g(S)\,dS}, \text{ if } S > S_0$$
$$= 0, \qquad \text{otherwise} \tag{3-5}$$

Using these results, one can calculate the mean loss over time period t, denoted by $\overline{C}(t)$, in terms of the mean loss given that an event has occurred, $E[C]$:

$$\begin{aligned} \overline{C}(t) &= \nu t E[C] \\ &= t\int_{S_o}^{\infty} E[C \mid S]\,\nu p(S \mid EQ)\,dS \\ &= t\int_{S_o}^{\infty} E[C \mid S]\,g(S)\,dS \end{aligned} \tag{3-6}$$

where Equations 3-4 and 3-5 have been used. For example, the mean annual loss would be given by $\overline{C}(t = 1\ \text{yr})$. Similarly, the mean-square loss over time period t is given by:

$$\begin{aligned} \overline{C^2}(t) &= \nu t E\left[C^2\right] \\ &= t\int_{S_0}^{\infty} E\left[C^2 \mid S\right] g(S)\,dS \end{aligned} \tag{3-7}$$

3.2 BUILDING-SPECIFIC LOSS ESTIMATION OVER LIFETIME

In Section 3.1, the probability distribution and moments of the earthquake losses for a building, given that an event has occurred, were investigated. It is necessary for this study to investigate the present value of the losses (i.e., discounted future losses) over some time period t, such as the designated lifetime of the building.

During some time period t, suppose there are $N(t)$ earthquakes occurring at successive times T_1, …, $T_{N(t)}$ in the region around the site of a structure of interest, which lead to losses C_1, …, $C_{N(t)}$, respectively, in the structure. The present value of the total earthquake losses, $L(t)$, can be formulated as:

$$L(t) = \sum_{k=1}^{N(t)} C_k e^{-rT_k} \tag{3-8}$$

where r is the specified discount rate. The factor $\exp(-rT_k)$ discounts the future loss C_k at time T_k so that $L(t)$ is formulated in present value (reference time at present is taken to be zero). Also, since the earthquake losses are tax-deductible expenses, the C_k and $L(t)$ are after-tax costs. The total earthquake loss $L(t)$ is an important quantity in seismic risk-management decision-making for real estate.

The uncertainties in the earthquake occurrences, that is, the number of earthquakes N(t) and the arrival times T_1, T_2, … , as well as the uncertainties in the earthquake losses C_1, C_2, …, render the total earthquake loss $L(t)$ uncertain. If a probability model is specified for the temporal occurrence of earthquakes affecting the building site and the probability model in Equation 3-1 for $p(C_k \mid EQ)$ is used to describe the uncertain loss C_k caused by an earthquake at time T_k, there is an implied probability distribution for $L(t)$. It is not an easy task, however, to determine this probability density function. Instead, we investigate statistical properties of $L(t)$ that are important, such as its moments and moment generating function.

To study the statistical properties of the total earthquake loss $L(t)$, several simplifying assumptions that are often made are adopted here:

(1) The number of earthquake events of interest during the lifetime t, $N(t)$, is modeled by a Poisson process with mean occurrence rate v.

(2) The earthquake losses $\{C_1, C_2, \ldots\}$ are assumed to be independent and identically distributed (i.i.d.) with probability density function $p(C \mid EQ)$ given by Equation 3-1.

(3) These losses are also assumed to be independent of the time of occurrence of the earthquakes, that is, the arrival times $\{T_1, T_2, \ldots\}$.

These assumptions would be reasonable, for example, if the seismic hazard were stationary (time-independent) and the building were always restored to its original state

before the next damaging event so that the building vulnerability $p(C|S)$ remained the same.

The distribution of the arrival times is implied by the probability model for $N(t)$. Obviously, each $T_k \left(k \le N(t)\right)$ assumes values between 0 and t. From the theory of Poisson processes, they are dependent (e.g., $T_1 < \ldots < T_{N(t)}$) and each T_k follows a Gamma distribution with parameters k and v. The dependent nature of the arrival times $\{T_1, T_2, \ldots\}$ unfortunately renders $L(t)$ difficult to analyze.

To date, expressions that are of a computationally manageable form have only been obtained for the first moment (i.e., mean) of $L(t)$. By directly conditioning on the number of earthquakes occurring during the lifetime t, Ang *et al.* (1996) adopted an expression for the expected value of $L(t)$ which involves a double sum over all possible number of earthquakes during the lifetime:

$$E[L(t)] = E[C]\sum_{n=1}^{\infty}\sum_{k=1}^{n}\frac{(vt)^n}{n!}e^{-vt}\int_0^t e^{-r\tau}p_k(\tau|\tau \le t)\,d\tau \tag{3-9}$$

where $E[C]$ denotes the expected value of the loss C given that an earthquake affecting the site has occurred, and

$$p_k(\tau|\tau \le t) = \frac{v(v\tau)^{k-1}}{\Gamma(k, vt)}e^{-v\tau} \tag{3-10}$$

is the conditional (gamma) probability density function for T_k given that $T_k \le t$. It was shown in Beck *at al.* (1999) and Irfanoglu (2000) that the expression for $E[L(t)]$ in Equation 3-9 reduces to the following simple form:

$$E[L(t)] = E[C]\frac{\nu}{r}\left(1 - e^{-rt}\right) = \frac{\bar{C}(1)}{r}\left(1 - e^{-rt}\right) \tag{3-11}$$

where $\bar{C}(1)$ is the annual mean loss when discounting is ignored (see Equation 3-6).

It is of interest to compute $E[e^{xL(t)}]$, the moment generating function for L(t) since this gives the higher moments of $L(t)$, that is, $E[L(t)^m]\,(m \ge 2)$ (Papoulis, 1991). Also, it is shown in Chapter 4 that the moment generating function plays an important role in the

risk-averse decision-making procedure. However, the approach leading to Equations 3-9 and 3-11 does not seem to provide an expression that is conducive to computation. In particular, the resulting expression for the m^{th} moment of $L(t)$ involves an $(m + 1)$-fold sum which is not trivial to simplify. In Appendix D, we develop a more elegant approach to obtain the statistical properties of $L(t)$ that leads to the following expression for the logarithm of its moment generating function:

$$\ln M_{L(t)}(x) = \frac{\nu}{r} \sum_{n=1}^{\infty} \frac{x^n}{n!n} E[C^n](1 - e^{-nrt}) \tag{3-12}$$

The mean and variance of $L(t)$ can be readily derived from the first and second derivatives of Equation 3-12 with respect to x when evaluated at x=0 (these correspond to the first and second cumulants—see Papoulis, 1991). This leads directly to Equation 3-11 for E[$L(t)$] and the following expression for the variance:

$$\mathrm{Var}[L(t)] = \frac{\nu}{2r} E[C^2](1 - e^{-2rt}) \tag{3-13}$$

It is interesting to note that Var[$L(t)$] depends on $E[C^2]$ rather than on Var[C]. This means that even in the case when C_k are fixed to a common value (Var[C_k]=0), there will still be variability in $L(t)$. Such variability comes from the variability in the arrival times of the events.

3.3 FORMULATION OF RISK-RETURN PROFILE

The basic measure of value for the purchase (or construction) of income-producing property that is used in this study is its *lifetime net asset value*:

$$V(t_L) = I(t_L) - C_o - L(t_L) \tag{3-14}$$

where

$I(t_L)$ = Present value of net income stream over the property lifetime t_L, ignoring earthquakes

C_0 = Initial investment, i.e., property equity

$L(t_L)$ = Present value of losses from future earthquakes over lifetime t_L

Only C_0 is known with certainty. The uncertainty in the value of $I(t_L)$ creates a market risk while the uncertainty in $L(t_L)$ creates seismic risk. The resulting uncertainty in net asset value V can be described by a risk-return profile:

$$P(v) = \text{Prob}\{V > v | \text{Seismic \& market risks}\}$$

based on the probability models for $I(t_L)$ and $L(t_L)$, that is, for a specified property, $P(v)$ gives the probability that the lifetime net asset value V exceeds a value v.

It is not an easy task to derive $P(v)$ from the models for the seismic and market risk, although the mean and variance of V are readily derived:

$$E[V(t_L)] = E[I(t_L)] - C_o - E[L(t_L)] \tag{3-15}$$

$$\text{Var}[V(t_L)] = \text{Var}[I(t_L)] + \text{Var}[L(t_L)] \tag{3-16}$$

where $E[L(t_L)]$ and $\text{Var}[L(t_L)]$ are given by Equations 3-11 and 3-13, respectively. Equation 3-16 is based on stochastic independence of $I(t_L)$ and $L(t_L)$. The mean and variance of $I(t_L)$ depend on the probability model for the market risk, that is, the variability in the net income stream over the lifetime t_L.

A stochastic process model for the net income stream is developed in Appendix E. It is based on modeling the after-tax income per period as a Wiener process (Papoulis, 1991), which is a continuous-time version of the random walk model used in Appendix D. In this model, the after-tax income per period at time t is a Gaussian stochastic process with mean $E[r_e(t)]P$, variance $(\text{Var}[r_e(0)]+\lambda^2 t)P^2$ and autocovariance $(\text{Var}[r_e(0)]+\lambda^2 \min(t, \tau))P^2$ at times t and τ. Here, $r_e(t)$ is the after-tax yield at time t, λ^2 is the volatility (the rate of increase per unit time in the variance of the after-tax yield) and P is the purchase price for the property. For fixed-interest-rate loans and a constant tax rate, the uncertainty in the after-tax yield is dominated by the uncertainty in the capitalization rate, that is, the ratio of the net operating income per period to the purchase price. In turn, the uncertainty in the capitalization rate depends primarily on the unknown variations in future rental rates, vacancy rates and operating expenses. The effect of these uncertainties is captured in the stochastic model for $r_e(t)$ by the linearly increasing variance, $\text{Var}[r_e(t)] = \text{Var}[r_e(0)]+\lambda^2 t$.

In Appendix E, it is shown that the stochastic model for $r_e(t)$ implies that $I(t_L)$, the discounted after-tax net income stream over the lifetime t_L, has a Gaussian distribution with mean and variance:

$$E[I(t_L)] = P\int_0^{t_L} e^{-rt} E[r_e(t)]dt \tag{3-17}$$

$$\begin{aligned}\mathrm{Var}\left[I(t_L)\right] = \frac{\lambda^2 P^2}{2r^3}\left[1 - 4e^{-rt_L} + 3e^{-2rt_L} + 2rt_L e^{-2rt_L}\right] \\ + \mathrm{Var}[r_e(0)]\frac{P^2}{r^2}[1 - e^{-rt_L}]^2\end{aligned} \tag{3-18}$$

If the mean after-tax yield $E[r_e(t)]$ is taken as constant and $\mathrm{Var}[r_e(0)]=0$, then as $t_L \to \infty$:

$$E[I(t_L)] \to \frac{P}{r} E[r_e(1)] \tag{3-19}$$

$$\mathrm{Var}\,[I(t_L)] \to \frac{P^2}{2r^3}\ \mathrm{Var}\,[r_e(1)] \tag{3-20}$$

This implies that as $t_L \to \infty$, the coefficient of variation on $I(t_L)$ is given by:

$$\delta_I = \frac{1}{\sqrt{2r}}\delta_{r_e} \tag{3-21}$$

where δ_{r_e} is the coefficient of variation in the after-tax yield over one period. Equation 3-21 is the continuous-time analog of the discrete-time result given in Equation 2-1 and derived in Appendix D.

Although $I(t_L)$ has a Gaussian distribution, this is not true for the discounted lifetime earthquake losses $L(t_L)$ under the seismic risk model described in Section 3.2 and Appendix D. Therefore, the net asset value $V(t_L)$ in Equation 3-14 does not have a Gaussian distribution. In principle, the probability distribution for V is determined (through an inverse Laplace transform) by its moment generating function. Although this inversion is not an easy task, the moment generating function for V is readily derived:

$$\ln M_{V(t_L)}(\xi) = \ln M_{I(t_L)}(\xi) - C_o + \ln M_{L(t_L)}(-\xi) \tag{3-22}$$

where $\ln M_{L(t_L)}(-\xi)$ is given by Equation 3-12 and:

$$\ln M_{I(t_L)}(\xi) = E[I(t_L)]\xi + \tfrac{1}{2}\ \text{Var}\ [I(t_L)]\xi^2 \tag{3-23}$$

because $I(t_L)$ has Gaussian distribution. As shown in Chapter 4, Equation 3-22 is all that is needed for risk-averse decision making when using an exponential utility function on the net asset value V.

Chapter 4. Formulation of Decision-Making Methodology

4.1 THE INVESTMENT DECISION

Suppose that an investor wishes to purchase income-producing real estate and has a list of properties of interest. As part of the decision-making procedure, the investor may want to rank the properties as investments and also to consider risk-management alternatives for each property rather than simply buying the property and doing nothing to reduce its seismic risk; for example, such alternatives may include:

1. Buy the property and do nothing more
2. Buy the property and perform seismic retrofit
3. Buy and insure the property
4. Buy, seismically retrofit and insure.

One strategy that the investor could adopt is to rank the list of properties according to the best risk-management alternative for each property. This property ranking should also include the option of no purchase since it is possible that some properties may rank below this option, which therefore serves as a cut-off point on the ranked property list.

4.1.1 Expected utility of uncertain property value

The decision-analysis approach used in this work for real-estate investment decision-making ranks alternatives on the basis of the expected value of utility of the lifetime net asset value V defined by Equation 3-14. The preferred choice between any two alternatives is the one that has higher expected value of utility (Von Neumann and Morgenstern, 1944; Howard and Matheson, 1989). The decision-maker's utility function is modeled by:

$$u(x) = 1 - \exp(-x/\rho) \tag{4-1}$$

where x is the amount of economic gain and ρ is the decision-maker's risk tolerance parameter. (It is assumed that the decision-maker's risk-tolerance parameter ρ is

known. Appendix A presents an interview methodology for determining ρ.) This utility function is illustrated in Figure 4-1.

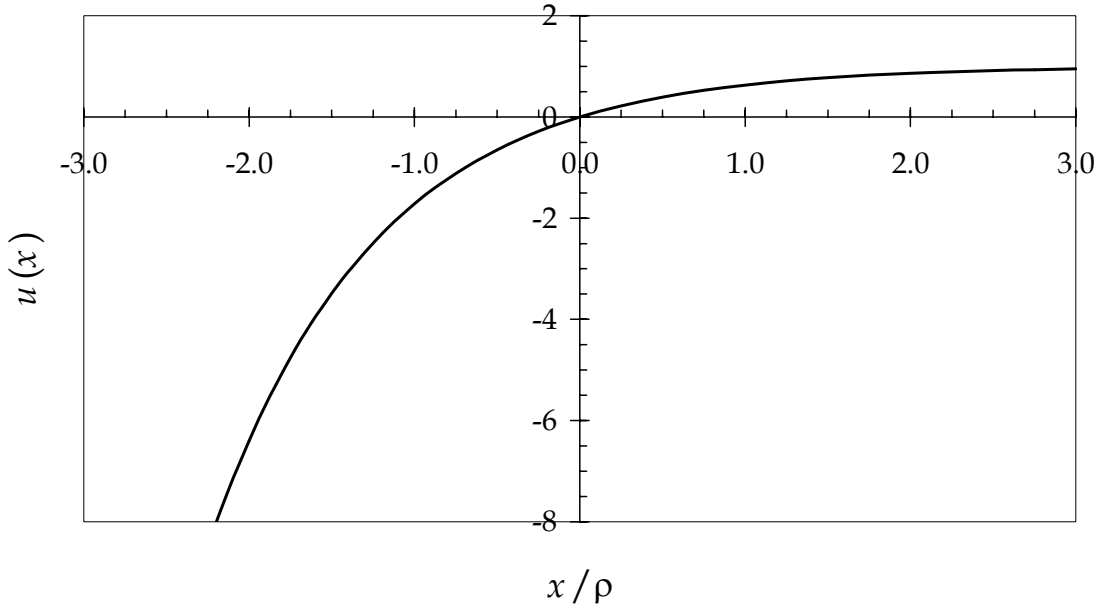

Figure 4-1. Exponential utility function.

The expected utility of buying a property is the expected utility of its lifetime net asset value V:

$$E[u(V)] = 1 - E[\exp(-V/\rho)] = 1 - M_V(-1/\rho) \tag{4-2}$$

where the moment generating function for V is given by Equation 3-22. For example, suppose the decision is between buying property A or property B, given a known purchase price, an uncertain market value, and uncertain lifetime earthquake loss for each property. Then, according to decision theory, property A should be preferred over property B if $E[u(V_A)]$ is greater than $E[u(V_B)]$.

For illustrative purposes, suppose that V is distributed according to a Gaussian distribution with a mean value denoted by μ_V and standard deviation denoted by σ_V, then:

$$E\left[u(V)\right] = 1 - \exp\left(-\frac{\mu_V}{\rho} + \frac{\sigma_V^2}{2\rho^2}\right) \tag{4-3}$$

Expected utility can then be plotted as contours in an (x, y)-plane where the x-axis is the normalized mean net asset value, denoted by μ_V/ρ, and the y-axis shows the normalized standard deviation of the net asset value, denoted by σ_V/ρ. Each property under consideration can be depicted as a point in this plane. The preferred property is the one with the greatest expected utility as given by Equation 4-3. Such a plot can help to clarify the relationship between mean value, standard deviation, and utility.

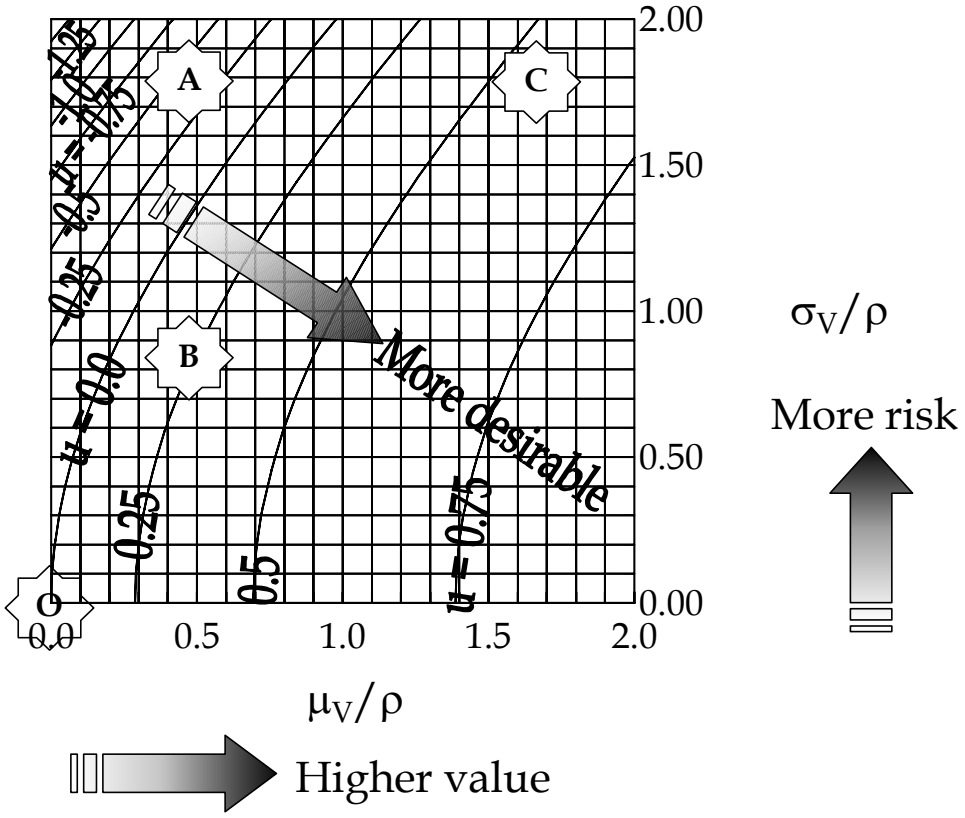

Figure 4-2. Investment utility diagram.

Figure 4-2 illustrates such a plot, referred to here as an investment utility diagram. In the figure, mean net asset value is plotted on the horizontal axis, increasing to the right. Standard deviation of net asset value risk is depicted on the vertical axis, increasing to the top. Expected utility is numbered on the contours. Thus, the best properties—those with high value and low risk—are in the lower right-hand corner of the plot, while the worst ones—those with low value and high risk—are in the upper left-hand corner of the plot.

Four illustrative cases are shown Figure 4-2: they are labeled O, A, B, and C. Several aspects of the relationship between risk, return, and utility can be seen. First, note that O corresponds to making no purchase and so has mean value, standard deviation and utility all equal to zero. Points A, B, and C correspond to three properties with net asset values of varying means and standard deviations that the decision-maker could purchase.

Consider property A. The mean net asset value is positive (equal in value to half the risk tolerance parameter), but because of the uncertainty on net asset value, its expected utility is less than zero, the utility of not buying the property. Thus, even though the expected value of owning property A is substantial, the uncertainty on value makes the purchase undesirable, and so the decision-maker should not buy it.

Property B has a mean net asset value the same as property A but its standard deviation is substantially less than that of A. Consequently, the expected utility of property B is 0.25, which is greater than that of A. Therefore, the decision-maker should prefer property B over property A, and should also prefer to buy property B than not to buy it. Property C has the same uncertainty as property A, but much greater mean value. As a consequence, property C lies on a higher contour than either A or B, so the decision-maker should choose to buy property C rather than A or B.

Thus, an investment utility diagram, as shown in Figure 4-2, succinctly depicts the relationship between risk, return, and expected utility of competing investment alternatives. The best alternative among a competing set is the one that lies on the highest contour, closest to the lower right-hand corner of the diagram.

4.1.2 Certainty equivalent of uncertain property value

The expected utility scale is arbitrary to within a linear (affine) transformation. Also, the expected utility of value is not expressed in terms of a monetary value. This motivates the introduction of the *certainty equivalent* of an uncertain property value V which is defined to be the single monetary amount that has the same utility value as the expected utility of V and is denoted here by CE. Since utility is a monotonically increasing function of property value, a property has higher expected utility if, and only

if, it has higher certainty equivalent. For decision-making purposes, properties can therefore be ranked by the size of the certainty equivalent of their net asset value. For a property whose uncertainty in value is small compared with the decision-maker's risk tolerance ρ, the certainty equivalent equals the expected net asset value. For deals with larger uncertainty relative to the decision-maker's risk tolerance, the certainty equivalent is less than the expected utility of the property value, with the decrease in CE being larger for higher uncertainty.

As a consequence of its definition, the certainty equivalent of a property value may be evaluated from the inverse of the utility function evaluated at the expected utility of the uncertain value *V*:

$$CE = u^{-1}(E[u(V)]) \tag{4-4}$$

If the decision-maker's utility function is described by Equation 4-1, then the certainty equivalent of property value V is given by:

$$CE = -\rho \ln(1 - E[u(V)]) \tag{4-5}$$

For example, consider a coin toss, where with probability 0.5, the decision-maker either wins an amount of $100 or wins nothing. Suppose the decision-maker has a risk tolerance parameter of $50, then the expected utility of the uncertain deal is 0.5*0 + 0.5*u($100) = 0.432. By Equation 4-5, this deal has certainty equivalent *CE* = -50*ln(1 – 0.432), or $28.31, that is, the decision-maker should be indifferent between having a gain of $28.31 for certain and having the coin tossed for a gain of $100 or nothing, because the two alternatives have the same certainty equivalent. Thus, if the decision-maker could choose between having either $35.00 for certain or the uncertain coin toss for $100 or nothing, the preferable alternative is taking the $35.00.

Consider a property with uncertain net asset value *V* that has a Gaussian distribution with mean value denoted by μ_V and coefficient of variation denoted by δ_V. (Thus, the standard deviation $\sigma_V = \mu_V \delta_V$). The certainty equivalent of the uncertain value *V* is then given by substituting Equation 4-3 into Equation 4-5:

$$CE = \rho\left[\frac{\mu_V}{\rho} - \frac{1}{2}\delta_V^2\left(\frac{\mu_V}{\rho}\right)^2\right] \tag{4-6}$$

This certainty equivalent is appropriate for property value considering only market risk where μ_V and σ_V are given by Equations 3-17 and 3-18 because, as described in Appendix E, the discounted after-tax net income stream over the lifetime t_L, $I(t_L)$, may then be modeled as Gaussian.

One can depict various property alternatives on a plot of contours of certainty equivalent in an investment diagram similar to Figure 4-2. Figure 4-3 is an example of such a plot, referred to here as an investment certainty-equivalent diagram, which is based on Equation 4-6. The *x*-axis gives the expected value of *V* normalized by the risk tolerance, the *y*-axis gives the coefficient of variation, and the contours give certainty equivalent normalized by the risk tolerance, i.e., CE/ρ. Note that *CE* decreases with increasing μ_V/ρ for high values of δ_V. The reason is that the property net asset value is assumed to be unbounded above, and more importantly, unbounded below, which allows for negative value outcomes (losses). For high δ_V, probabilities increase for losses. As the mean value increases, so does the magnitude of possible losses. The aversion to possible large losses outstrips the desire for increasing mean gain, giving a decreasing *CE* in this region of the investment decision space.

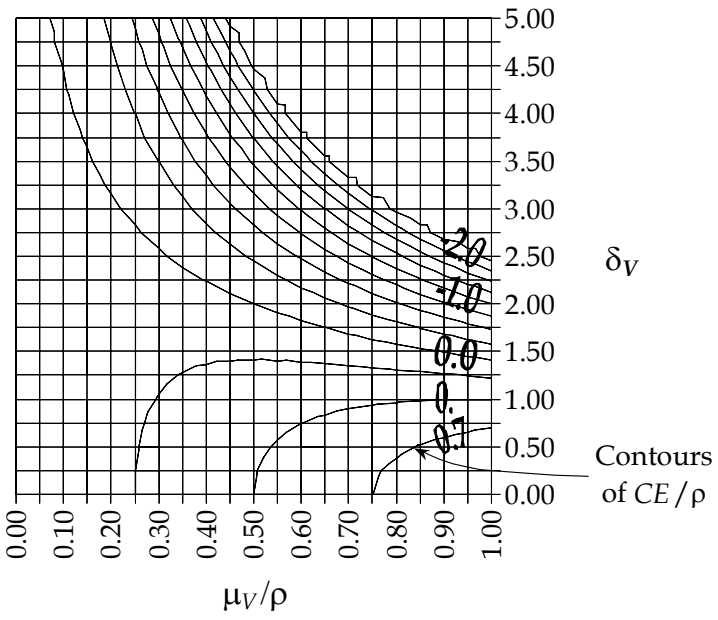

Figure 4-3. Investment certainty-equivalent diagram.

Figure 4-3 shows when decision-making can be evaluated solely based on mean value. If the certainty equivalent of a property value V is approximately equal to its mean value μ_V, then one need not consider uncertainty. This region corresponds to the lower left-hand portion of Figure 4-3. Figure 4-4 more clearly illustrates the effect of uncertainty and risk aversion on the value of a property for decision-making purposes: the contours in this figure show the ratio of the certainty equivalent to the mean value of the investment, CE/μ_V. Where this ratio is greater than 0.90, there is little difference between the expected value of the investment and its certainty equivalent. In this region, risk-neutral decision-making using expected net asset value is appropriate.

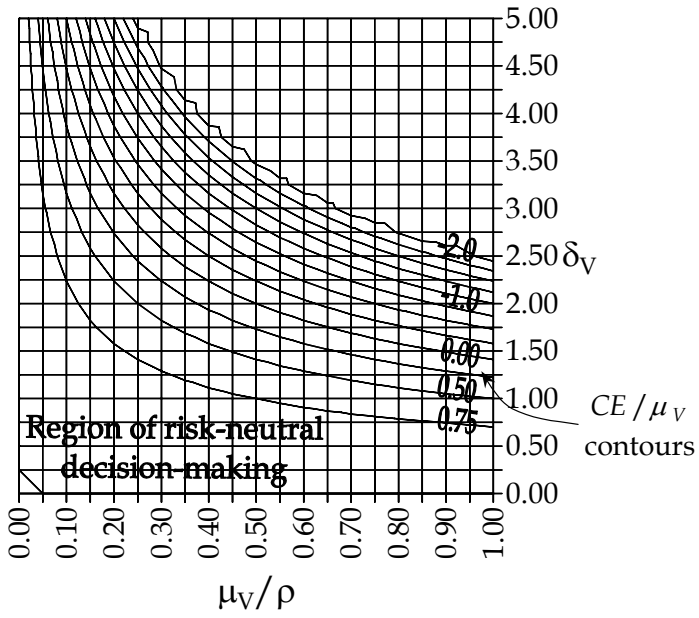

Figure 4-4. Effect of risk aversion on deal value.

Where do typical real estate investment opportunities lie in the (μ_V/ρ, δ_V) investment space? It has been found (see Chapter 7) that for six decision-makers interviewed prior to and during this study, the value of μ_V/ρ for an individual investment is typically on the order of 0.02 to 0.50. In Chapter 2, it was concluded based on market risk alone that δ_V is the order of 1.0 but that it could be as low as 0.2 or as high as 5 or more. Thus, these investors tend to operate in the left-hand half of the investment space in Figure 4-4. A large, highly uncertain deal lies in the top left-hand side of the figure. Thus, for these cases, the figure shows that the uncertainty on property value has an important effect on the certainty equivalent of the deal; risk attitude does matter and the perceived value of the deal will be much less than the expected value of the property. A deal with small uncertainty would lie in the lower left-hand area of the investment space. For these deals, a risk-neutral approach is appropriate.

4.1.3 Certainty equivalent under seismic risk and market risk

We have emphasized the importance of valuing real estate investments using the certainty equivalent *CE* of the uncertain lifetime net asset value *V* of the income-

producing property. The new theory developed in Appendix F allows an explicit expression for *CE* to be derived based on the seismic risk model. By using Equations 3-22 and 4-2 in Equation 4-6, *CE* can be expressed in terms of moment generating functions:

$$\begin{aligned} CE &= -\rho \ln M_{\nu}\left(-\frac{1}{\rho}\right) \\ &= -\rho \ln M_{I(t_L)}\left(-\frac{1}{\rho}\right) - C_0 - \rho M_{L(t_L)}\left(\frac{1}{\rho}\right) \end{aligned} \tag{4-7}$$

The moment generating functions of the present value of the lifetime net income stream $I(t_L)$ and the present value of the lifetime earthquake loss $L(t_L)$ can be replaced by Equations 3-23 and 3-12 respectively, to give:

$$CE = E[I(t_L)] - C_o - E[L(t_L)] - \frac{1}{2\rho}\ \text{Var}\,[I(t_L)] - \frac{1}{2\rho}\ \text{Var}\,[L(t_L)] - \rho R \tag{4-8}$$

The first three terms in this expression for the certainty equivalent are the risk-neutral part (the value of CE if the risk tolerance $\rho \to \infty$). The other terms correspond to the risk-averse part with *R* corresponding to the terms for $n \geq 3$ in the series expansion for $\ln M_{L(t_L)}\left(\frac{1}{\rho}\right)$ in Equation 3-12.

It is shown in Appendix F that an upper bound can be derived for *R* (Equation F-34 where $\xi = \frac{1}{\rho}$ for Equation 4-8). The factor $(\exp(P/\rho) - 1 - P/\rho)/9$ in this bound is less than 0.02 because interviews with real estate investors show that the value *P* of their property deals is less than one-half of their risk tolerance ρ i.e. $P/\rho < 0.5$. Thus, ρR in Equation 4-8 has an upper bound equal to about 2% of the mean lifetime earthquake loss, $E[L(t_L)]$ for $t_L \to \infty$, and so it can be neglected in Equation 4-8. Furthermore, it is shown in Chapter 5 that for the demonstration building, the variance on lifetime earthquake loss is small compared with the variance on income, and so it too can be neglected:

$$CE = E\left[I\left(t_L\right)\right] - C_0 - E\left[L\left(t_L\right)\right] - \frac{1}{2\rho} Var\left[I\left(t_L\right)\right] \tag{4-9}$$

where

CE = certainty equivalent—the basis on which the investment decision is made

$E[I(t_L)]$ = expected present value of net income, $I(t_L)$

C_0 = initial investment, i.e., property equity

$E[L(t_L)]$ = expected present value of lifetime losses from future earthquakes over lifetime t_L.

ρ = decision-maker risk tolerance, e.g., from Appendix A or B

$\text{Var}[I(t_L)]$ = variance of $I(t_L)$ = $(E[I(t_L)]\delta_I)^2$

δ_I = coefficient of variation on $I(t_L)$

With these approximations, the expression for CE is equivalent to the certainty equivalent for the net asset value having a Gaussian distribution. Equation 4-6 and the discussion in the previous section regarding the investment diagrams are therefore applicable even though V is not exactly Gaussian distributed.

4.2 POST-INVESTMENT DECISIONS

Risk-management decisions during ownership of real estate can be performed similarly to investment decisions. While the property is held, generic risk-management alternatives include:

1. Do nothing
2. Liquidate the property
3. Perform seismic retrofit
4. Insure the property
5. Seismically retrofit and insure

As with the purchase decision, the best alternative for risk-management is the one with the greatest expected value of utility.

4.3 PROPOSED INVESTMENT DECISION-MAKING PROCEDURE

This report so far has discussed methodologies for evaluating seismic vulnerability, evaluating lifetime property values, and accounting for decision-maker risk attitude in the investment decision. These elements can now be combined to present a decision-making procedure for real estate investments with seismic risk, as shown in Figure 4-5.

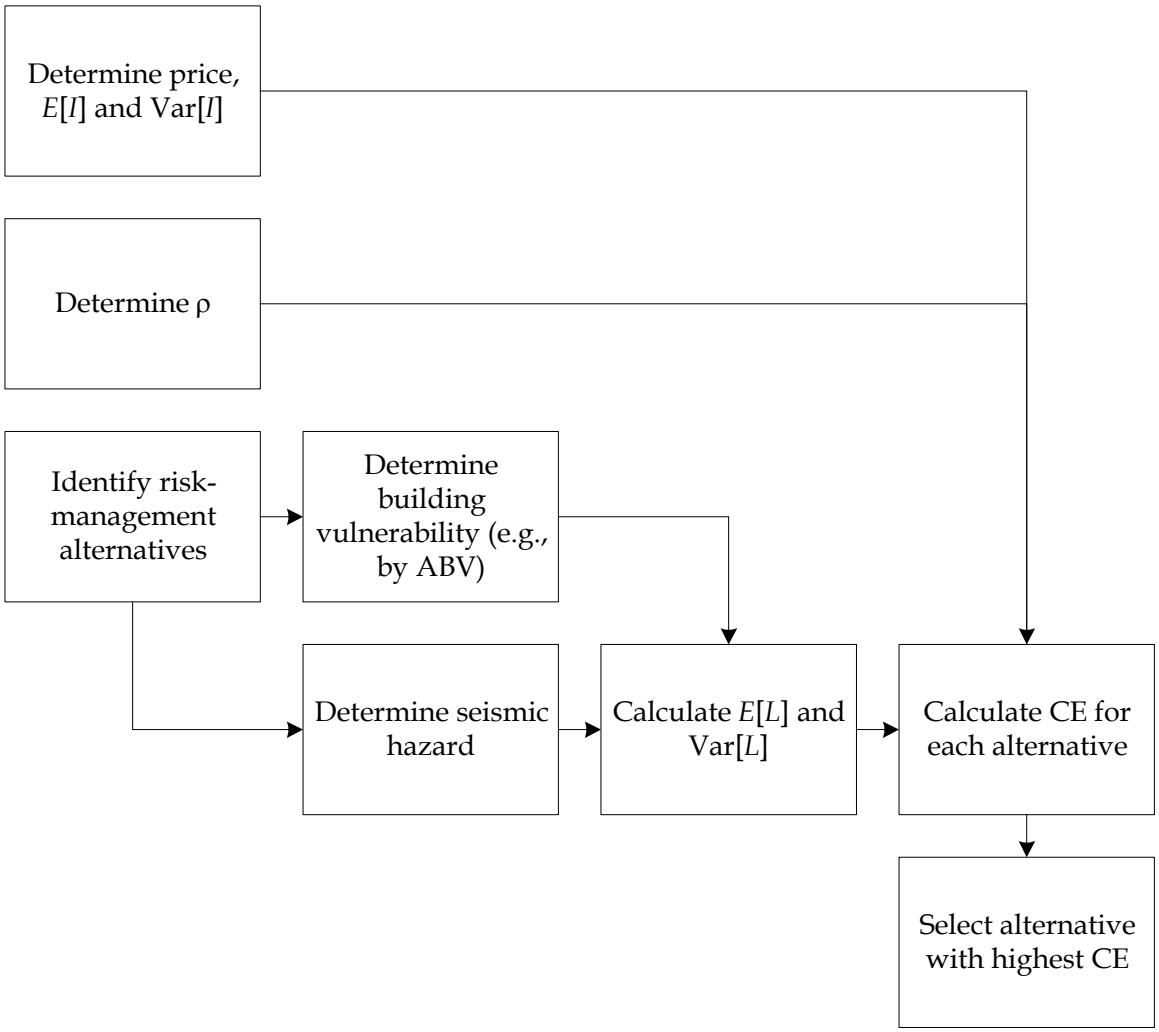

Figure 4-5. Proposed investment decision procedure.

The first step is mostly familiar to investors. It requires a financial analysis to determine price and the net present value of income (mean and variance), after tax and ignoring seismic risk. Step 2 is to determine the investor's risk tolerance parameter, ρ. Next, one evaluates the present value of earthquake loss (mean and variance), under

various risk-management alternatives. This requires evaluating the hazard and creating a seismic vulnerability function for each alternative, and combining these to determine earthquake loss as in Chapter 3. Finally, one calculates the certainty equivalent for each alternative using Equation 4-8 and selects the alternative with the highest *CE*. The two major differences between this decision procedure and common practice are how it accounts for risk attitude and seismic risk.

By explicitly accounting for the investor's risk attitude, various analysts within the investor's organization can use a single consistent risk tolerance parameter that is established and approved by the chief decision-makers. In common practice, risk is dealt with either using a discount rate that is increased to account for perceived risk, or by performing deterministic sensitivity studies on income parameters, and judging worst-case scenarios.

The proposed procedure explicitly accounts for the effect of seismic risk on net asset value by reducing income by mean annualized earthquake loss. In common practice, seismic risk is evaluated only in terms of probable maximum loss (PML) and the effect of seismic risk on net asset value is ignored, thus significantly overestimating return. Furthermore, by evaluating seismic risk for various risk-management alternatives, the investor can quantitatively and consistently determine the appropriate alternative.

Chapter 5. CUREE Demonstration Building

5.1 RECAP OF ASSEMBLY-BASED VULNERABILITY METHODOLOGY

It is worthwhile before presenting the real-estate decision-making analysis of the CUREE demonstration building to recap the assembly-based vulnerability (ABV) approach, both for the convenience of the reader and because the present study includes some enhancements to ABV that have not been previously published.

ABV is a framework developed in Phase III of the CUREE-Kajima Joint Research Program to assess the probabilistic relationship between shaking severity, damage and loss on a building-specific basis (or conceivably for a bridge or other facility). ABV ahs been implemented using Monte Carlo simulation, and it is this approach that is summarized here. It may be practical to implement it using reliability approaches or other simulation techniques (e.g., Au and Beck, 2000), but we have not yet done so. For more technical detail about ABV, see also Beck *et al.* (1999), Porter (2000), and Porter *et al.* (2001).

5.1.1 Define the facility as a collection of assemblies

The methodology is illustrated in Figure 5-1. The analyst begins by determining the facility's location and by describing the facility as a collection of discrete, standard assemblies. An assembly is a set of components assembled to construct a distinct, recognizable part of a facility such as a window installed and in place, a reinforced concrete column, an air-handling unit, or a desktop computer. Thus, assemblies can consist of structural and nonstructural components or contents. A formal taxonomy of assemblies is employed to provide unambiguous reference to assembly types and to their possible damage states, repair methods and repair costs. Table 5-1 presents the portion of the taxonomy that is used in the present study. It is based on the assembly numbering system of RS Means Co., Inc. (2001), with the addition of a fifth set of digits to indicate seismic installation conditions.

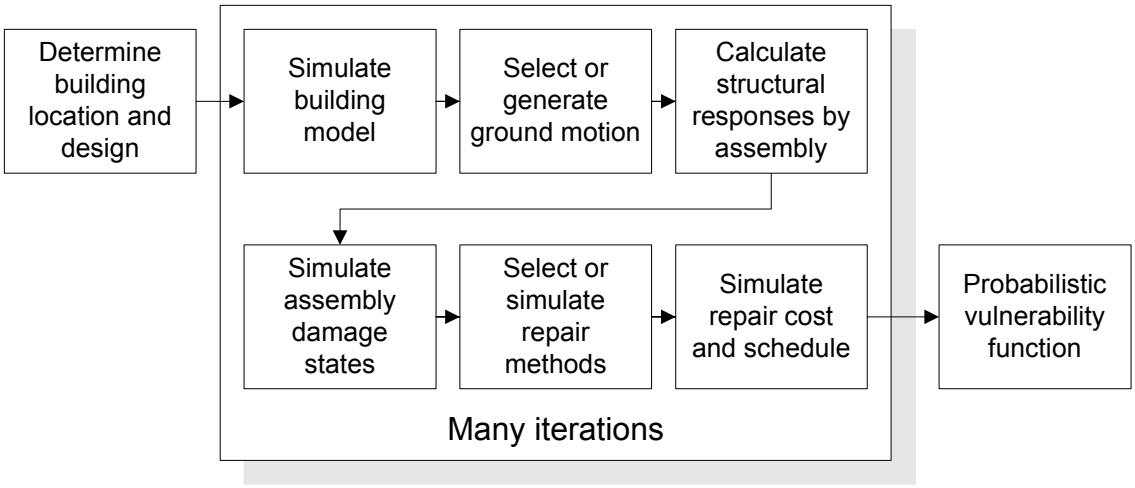

Figure 5-1. ABV methodology.

Table 5-1. Sample of assembly taxonomy.

Assembly	Description	Unit
3.5.180.1101.01	Nonductile CIP RC column A_g in [250,500) in^2, L in [100,200) in	ea
3.5.190.1102.01	Nonductile CIP RC beam A_g in [100, 250) in^2, L in [200, 300) in	ea
4.7.110.6700.02	Window, Al frame, sliding, heavy sheet glass, 4'-0x2'-6"x3/16"	ea
6.1.500.0001.01	Drywall partition, 5/8-in., 1 side, on metal stud, screws	64 sf
6.1.500.0002.01	Drywall finish, 5/8-in., 1 side, on metal stud, screws	64 sf
6.1.510.1202.02	Stucco finish, 7/8 in, on 3-5/8-in mtl stud, 16"OC, typ quality	64 sf

Once the facility is defined in this way, the subsequent analysis has four steps: hazard analysis, structural analysis, damage analysis, and loss analysis. Each of these steps is described in the succeeding sections.

5.1.2 Hazard analysis

The hazard analysis produces ground motions characteristic of the site soils, seismic setting (types, sizes, and distances to local faults), and shaking severities of interest. In this and previous ABV analyses, shaking severity has been measured in terms of damped elastic spectral acceleration at the small-amplitude fundamental period of the building, denoted by S_a, although other measures of severity could be used. To account for uncertainty in ground motion, we have selected a set of N_S x N_I ground

motion time histories, where N_S refers to the number of ground motions per level of shaking severity, and N_I refers to the number of levels of shaking severity of interest. To date, we have used $N_S = N_I = 20$, although different ground-motion selection schemes can be used.

5.1.3 Structural analysis

The structural analysis begins with the creation of a structural model, i.e., a model of the facility's mass, damping, and force-deformation characteristics. Unlike our previous analysis for CUREE-Kajima (Beck *et al.*, 1999), we have explicitly modeled uncertainty in each feature. (In Porter *et al.* 2002a, we model uncertainty in mass and damping; in the present study we account for uncertainty in force-deformation behavior as well.)

In the structural analysis, one estimates the structural deformations and internal member forces resulting from the ground motion. Structural deformations are parameterized in whatever terms are most relevant to the damageability of the facility assemblies, typically meaning peak transient interstory drift ratios at each story and column line, peak floor accelerations, and peak ductility demands in structural members, although other structural response could be of interest in other situations.

Uncertain mass. Uncertainty in mass is accounted for by multiplying nominal masses by a random factor ε_M. The mean value of ε_M accounts for the ratio of the mean mass (denoted by $\overline{M}$) to the nominal mass (denoted by M_n) that an engineer would calculate based on a quantity takeoff from the drawings. We have used a mean factor of $\mu_M = \overline{M}/M_n = 1.05$, which indicates that actual building mass is on average 5% greater than that assumed based on quantity takeoffs from the design drawings. (We generically denote an error factor here with ε. Its expected value is denoted by μ, and its coefficient of variation by δ, with a subscript to indicate the particular variable of interest.) The coefficient of variation of mass, denoted by δ_M, is taken as $\delta_M = 0.10$. Both μ_M and δ_M are taken from Ellingwood *et al.* (1980). All masses in a particular simulation of the building model are multiplied by the same ε_M, i.e., masses are assumed to be

perfectly correlated, which would tend to result in a slightly conservative estimate of loss uncertainty.

Uncertain damping. Uncertainty in damping is accounted for by multiplying the nominal Rayleigh damping by a random factor ε_β, whose mean value is taken to be μ_β = 1.0, with coefficient of variation of δ_β = 0.4. The estimation of δ_β is based on two sources of uncertainty: variability of the damping coefficient given a system-identification model of damping, and variability associated with model selection. Details of these two sources of uncertainty are detailed in Porter *et al.* (2002b), but a summary can be given here. For a given system-identification model, and considering many different reinforced concrete moment-frame buildings, there appears to be a coefficient of variation of viscous damping of $\delta_{\beta 1}$ = 0.3. In addition, different system-identification models of the same buildings yield a coefficient of variation of $\delta_{\beta 2} = 0.3$. Treating the two sources of uncertainty as independent, one can estimate overall uncertainty as $\delta_\beta = (\delta^2_{\beta 1} + \delta^2_{\beta 2})^{0.5} \approx 0.4$.

Uncertain force-deformation behavior. The present project introduces for the first time in an ABV model uncertainty in force-deformation behavior. Each member has associated hysteretic behavior, idealized with a force-deformation relationship constructed from several control points, e.g., yield, ultimate, and collapse. Let each uncertain control point i be denoted by a point in the force-deformation space, $(D, F)_i$. (We observe the convention of referring to the space as force-deformation, but plot it with deformation on the x-axis and force on the y-axis.) We model each random control point as the product of a mean correction term, an error term, and the nominal (calculated) control point:

$$[D, F]^T = \mu_K \varepsilon_K [D_n, F_n]^T \tag{5-1}$$

We estimated the effect of modeling error—the difference between observed force-deformation behavior and that modeled using all known material properties and member dimensions—by comparing the observed ultimate strengths of 20 reinforced concrete beam-columns drawn from Eberhard *et al.* (2001), with that calculated using UCFyber (ZEvent, 2000), using the measured material properties and dimensions of the

members in question. The ratio of the observed ultimate strength to the calculated strength had a mean value of 1.15 and a coefficient of variation of 0.08. One must also account for uncertainty in material properties and member dimensions. Ellingwood *et al.* (1980) recommend a coefficient of variation in member strength 0.08 to account for uncertain material properties and dimensions of reinforced concrete flexural members.

In estimating overall uncertainty in strength, we assume no correlation between modeling error and uncertainty in material properties, and calculate the overall coefficient of variation of strength as $\delta_K = (0.08^2 + 0.08^2)^{0.5} = 0.11$. Thus, we take μ_K as 1.15, and ε_K as a normally distributed random variable with unit mean and standard deviation of 0.11.

We have used nonlinear time-history structural analysis to estimate structural deformation and internal member forces. We deal with uncertainty in all of the structural characteristics by generating a number of simulated structural models whose mass, damping, and force-deformation characteristics are consistent with their probability distributions, and then randomly paired a structural model with ground motion time histories when performing structural analyses. In particular, we have generated N_S structural models. At each level of the N_I shaking severity levels, we randomly pair a structural model with a ground motion time history without replacement, but for convenience allow re-use of the structural models for each of the N_I severity levels. That is, we choose from the same N_S models for each of the N_I levels.

5.1.4 Damage analysis

The structural response is used as input to an analysis of physical damage to the building. Recall that the building is described as a collection of damageable assemblies such as windows, wall segments, reinforced concrete beam-columns, etc. Each damageable assembly can have one or more possible damage states. In general, damage states are defined in terms of the repair efforts required to restore the assembly to its undamaged state.

The analysis is performed as follows. For each damageable assembly, let N_D denote the number of possible damage states, which along with the undamaged state

form a mutually exclusive and collectively exhaustive set. Damage states may or may not have an order to them, i.e., one may or may not have the ability to arrange the damage states so that each successive state requires more effort than the previous one to repair. In the present analysis, such an ordering is possible, so only this case will be treated here.

Let each damage state be denoted by an integer that increases with increasing severity of damage. Thus, each assembly must be in one damage state $d \in \{0, 1, \ldots N_D\}$, where $d = 0$ denotes a state of no damage, and $d = i + 1$ involves greater repair effort than does $d = i$. The probability that a particular assembly will reach or exceed a particular damage state d, conditioned on the structural response z to which it is subjected, is calculated from a previously developed fragility function as

$$P_f(d) = P[D \geq d \mid Z = z] = \Phi\left(\frac{ln(z/x_m(d))}{\beta(d)}\right) \tag{5-2}$$

in which D is the uncertain damage state of a particular assembly, d is a possible particular damage state of that assembly, Z is the uncertain structural response to which the assembly is subjected, z is the calculated, particular value of the structural response from a particular simulation, and x_m and β are parameters of the fragility function, defined for each assembly type and damage state d.

Damage is simulated for each assembly and each ground motion as follows. The structural analysis produces the structural response z to which the assembly is subjected. Equation 5-2 is evaluated for each possible damage state. A random sample u is then drawn from a uniform probability distribution over [0, 1]; this value is compared with each failure probability $P_f(d)$ for $d = 1, 2, \ldots N_D$. The assembly is said to have reached or exceeded damage state d if $u \leq P_f(d)$. The maximum damage state reached or exceeded is the final simulated damage state of the assembly. That is,

$$d = max\, d : u \leq P_f(d) \tag{5-3}$$

Note that the probability that an assembly is in damage state d, denoted by $P[D=d \mid Z=z]$, is equal to $1 - P_f(1)$ for $d = 0$ (the undamaged state), or $P_f(d) - P_f(d+1)$ for $1 \le d < N_D$, or $P_f(d)$ for $d = N_D$ (the most severe damage state).

5.1.5 Loss analysis

In the damage analysis, the damage state of every assembly in the building was simulated for each paired ground motion and structural model. This means that in each simulation, there is a snapshot of damage, and one knows how many windows are broken, how many beams have suffered minor damage repairable by epoxy injection, and so on. The loss analysis involves the calculation of the cost to repair these damages.

There may be several possible repair measures for a given assembly damage state. For example, a nonductile reinforced concrete beam-column with spalled cover might repaired by jacketing with concrete, steel or advanced fiber material. The decision depends in part on the preferences of the owner, structural engineer, building department officials, and possibly others. A probabilistic one-to-many relationship between damage state and repair effort could be created and employed in future ABV analyses. In the present analysis, we have associated a particular repair effort with each damage state, on a one-to-one basis.

Given a repair approach for each assembly type and assembly damage state, one multiplies the number of damaged assemblies by the cost to repair each unit of damage (the unit repair cost) and sums to calculate total direct repair cost. Unit repair costs are uncertain, however, and so simulation is used. In the present analysis, these costs are assumed to be distributed according to a lognormal distribution, and so are simulated using the inverse method as:

$$C_{j,d} = \exp\left(\beta \Phi^{-1}(u) + \ln(x_m)\right) \tag{5-4}$$

where

$C_{j,d}$ = cost to restore one unit of assembly type j from damage state d

u = sample of a Uniform(0,1) random variate

x_m = the median value of the unit repair cost

β = logarithmic standard deviation of the unit repair cost

$\Phi^{-1}(u)$ = inverse of the standard normal cumulative distribution at u

For each simulation of structural model, ground motion, structural response, assembly damage, and assembly repair cost, one value of the total repair cost is then calculated as:

$$C_R = (1 + C_P)\left(\sum_{j=1}^{N_J}\sum_{d=1}^{N_{D,j}} C_{j,d} N_{j,d}\right) \tag{5-5}$$

where

C_p = contractor overhead and profit

$N_{D,j}$ = number of possible damage states for assembly type j

N_J = number of damageable assembly types present in the building

$N_{j,d}$ = number of assemblies of type j in damage state d

The total repair cost is then divided by the replacement cost new (RCN) to arrive at the damage factor. Repair costs are capped at RCN, and collapses are assumed to represent a damage factor of 1.0.

A professional construction cost estimator contracted for this project informs us that C_P is typically 0.15 to 0.20 (Machin, 2001). The use of a separate factor for overhead and profit is also introduced with this study. In addition, this study accounts for line-of-site costs, that is, painting an entire room, hallway, etc., if any portion of it needs repainting. This is standard practice because of the difficulty of matching paint.

5.2 DESCRIPTION OF CUREE DEMONSTRATION BUILDING

To demonstrate the calculation of the risk-return profile and to illustrate the investment decision procedures discussed in Chapters 3 and 4, a real commercial property in the United States was selected for analysis by the CUREE team, and several investment alternatives were considered. Chapter 4 listed five alternatives, of which four are examined here: do not buy, buy and leave the building as-is, buy and retrofit, and buy and insure. Note that the alternative to buy, retrofit and insure is neglected for

simplicity. Note also that, literally speaking, the as-is alternative should be called "as-was," since it reflects the demonstration building just prior to the 1994 Northridge Earthquake, not as it exists today. However, the term *as-is* is used here because of its familiarity.

The CUREE demonstration building was selected with several criteria in mind. First, it is desirable to examine a building of investment quality, to ensure applicability to the present study. Second, it should be an engineered building amenable to structural analysis, a prerequisite of the ABV approach. It should be constructed of an interesting and commonly used material, preferably reinforced concrete, as this will involve the development of useful new assembly fragility functions, repair-cost distributions, etc., that add to the library of available ABV tools. Lastly, it should be accessible to the researchers, and preferably be the subject of prior research by other investigators. There are two reasons for this: first, to reduce the effort required to acquire construction data, and second because a building that has already been examined provides a degree of interest and accessibility to other researchers.

With these criteria in mind, the selected CUREE demonstration building is a 7-story, 66,000 sf (6,200 m^2) hotel located at 8244 Orion Ave, Van Nuys, CA, at 34.221° north latitude, 118.471° west longitude, in the San Fernando Valley of Los Angeles County. The location is shown in Figure 5-2. It was built in 1966 according to the 1964 Los Angeles City Building Code. The lateral force-resisting system is a reinforced concrete moment frame in both directions. The building was lightly damaged by the M6.6 1971 San Fernando event, approximately 20 km to the northeast, and severely damaged by the M6.7 1994 Northridge Earthquake, whose epicenter was approximately 4.5 km to the southwest. The building location relative to these events is shown in Figure 5-3. The building has been studied extensively, e.g., by Jennings (1971), Scholl *et al.* (1982), Islam (1996a, 1996b), Islam *et al.* (1998), and Li and Jirsa (1998). In 2001, it was also selected as a testbed for the development of a performance-based earthquake engineering (PBEE) methodology by the Pacific Earthquake Engineering Research Center (2001).

Figure 5-2. Location of CUREE demonstration building, at the "+" symbol near "405."

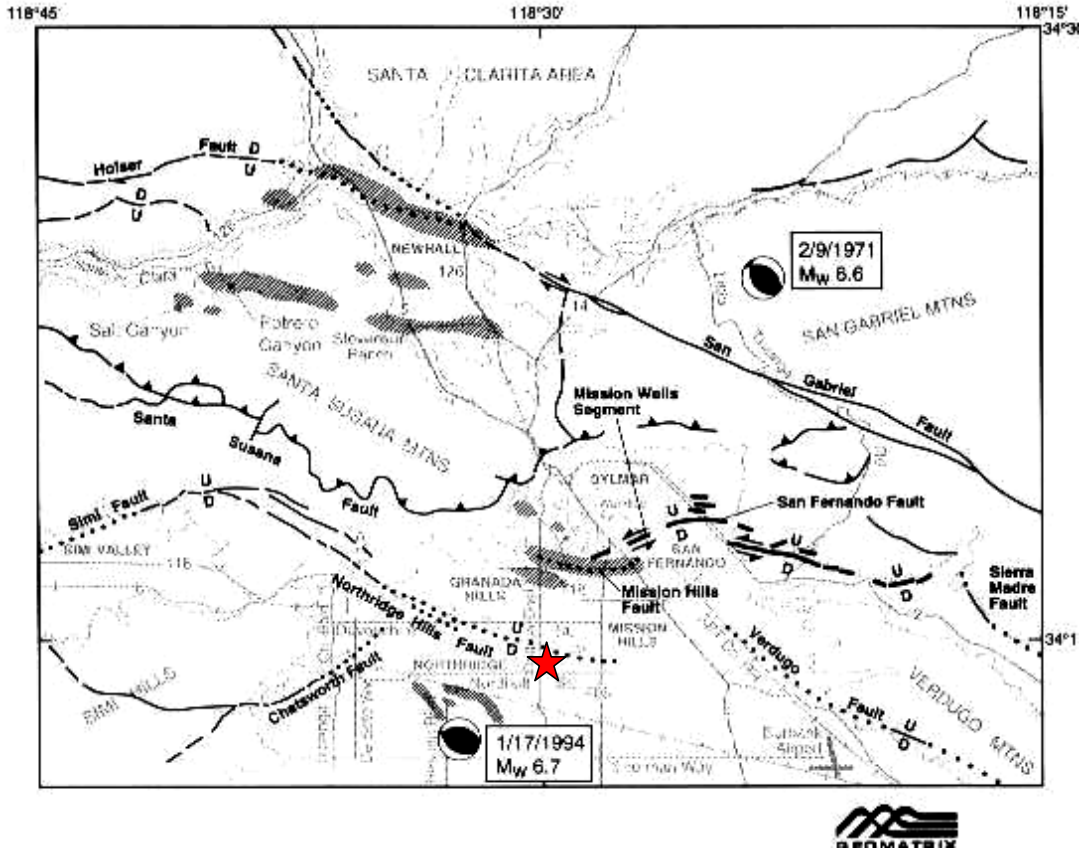

Figure 5-3. Demonstration building (star) relative to earthquakes (EERI, 1994b).

Soil conditions at the site are found in Tinsley and Fumal (1985), who map surficial soil deposits in the Los Angeles region using a variety of sources. They describe the site soil as Holocene fine-gained sediment (silt and clay) with a mean shear-wave velocity of 200 m/sec (and a standard deviation of 20 m/sec), corresponding to site class D, stiff soil, as defined by the International Code Council (2000), and soil profile type S_D according to the Structural Engineers Association of California (1999). In his study of the same building, Islam (1996b) reaches the same conclusion, that site soils are "primarily fine sandy silts and silty fine sands. This suggests a site coefficient factor of S2 or greater."

The site hazard is calculated as follows. Frankel and Leyendecker (2001) provide the seismic hazard—defined in terms of $G(S_a)$, the annual expected frequency of exceedance versus spectral acceleration response—for any latitude and longitude in the United States. The site hazard is presented for soil at the boundary between NEHRP soil classes B and C, and for the fundamental periods 0.3, 0.5, 1.0, and 2.0 sec.

The site of interest stands on soil class D, so it is first necessary to adjust shaking severity to account for soil class. Figure 5-5 (left) shows the soil adjustment factor used here. The figure shows the ratio of the site coefficient F_V for soil class D to that of the average of soil classes B and C, according to International Code Council (2000). Dots in the figure give tabulated values. They are plotted as a function of the spectral acceleration response on B-C soil for a fundamental period of 1 sec. The (x,y) coordinates of the two points at the edges of the plateaus are shown for convenience. The solid curve between the upper and lower plateaus is a polynomial fit to the data; its equation is shown on the chart. Figure 5-5 (right) shows the site hazard for the fundamental periods 0.5, 1.0, and 2.0 sec, before adjusting for soil (B-C soil class, dashed lines) and after (D soil class, solid lines). The ratio of the x-value of the solid line to that of the dashed line at a given y-value is $F_{V,D/B\text{-}C}$.

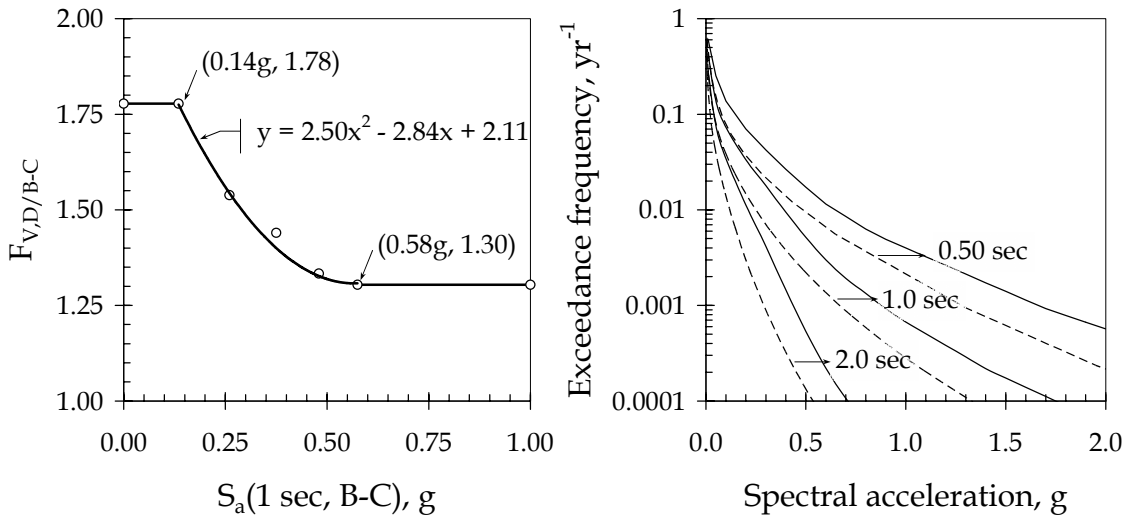

Figure 5-4. Adjusting site hazard to account for soil.

As will be shown later, the fundamental periods of interest are 0.75 sec and 1.5 sec. The site hazard for these fundamental periods is calculated by linear interpolation in the log-frequency domain, as shown in Figure 5-5 (left). The (light solid) hazard curves for 1.0 sec and 2.0 sec fundamental periods are interpolated to arrive at the (heavy solid) 1.5-sec curve. Likewise, the 0.5-sec and 1.0-sec curves are used to calculate the 0.75-sec hazard curve.

Finally, it is desirable to express site hazard in terms of a discrete occurrence-frequency relationship, i.e., number of events per year as a discrete function of spectral acceleration response. Let $n(S_a)$ denote the annual number of events of severity $S_a \pm \Delta S_a/2$. This discrete relationship can be simply evaluated as

$$n(S_a) = G(S_a - \Delta S_a/2) - G(S_a + \Delta S_a/2) \tag{5-6}$$

The values of $n(S_a)$ calculated for the CUREE demonstration building are shown in Figure 5-5 (right). As is evident from Figure 5-5 (left), the expected exceedance frequency can be locally approximated as a log-linear function of spectral acceleration, so

$$G(x) \approx \exp(ax + b) \tag{5-7}$$

and thus from a first-order Taylor series approximation of G in Equation 5-6,

$$n(x) \approx -dG/dx^*\Delta x = -aG(x)\Delta x \qquad (5\text{-}8)$$

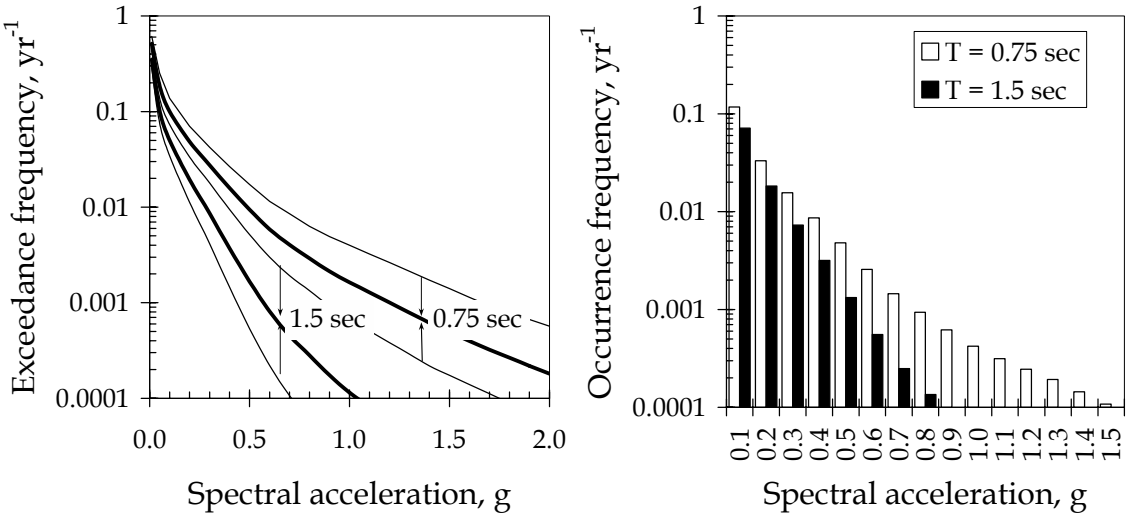

Figure 5-5. Site hazard for fundamental periods of interest.

After establishing the site hazard conditions, we turn to the structural and architectural conditions of the CUREE demonstration building. The building's design information is drawn from the architectural and structural drawings on file with the Los Angeles Building Department. As noted above, the building was built in 1966. In plan, the building is 63 ft by 150 ft, 3 bays by 8 bays, 7 stories tall. The long direction is oriented east-west. The building is approximately 65 ft tall: the first story is 13 ft, 6 in; stories 2 through 6 are 8 ft, 6-½ in; the 7th story is 8 ft, 6 in. Floors 2 through 7 have 22 hotel suites each, for a total of 132 suites. The ground floor contains the reception area, the hotel office, a banquet room, tavern, dining room, kitchen, linen room, and other hotel services.

The structural designer is Rissman and Rissman Associates (1965). The structural system is a 7-story cast-in-place reinforced-concrete moment-frame building with nonductile column detailing. Lateral force resistance is provided primarily by the perimeter moment frames, although the interior columns and slabs also contribute to lateral stiffness. The gravity system comprises 2-way reinforced-concrete flat slabs

supported by square columns at the interior and the rectangular columns of the perimeter frame. Slabs are 10-in deep at the 2nd floor, 8½ in at the 3rd through 7th floors, and 8 in at the roof. The roof also has lightweight concrete topping varying in thickness between 3-1/4 in and 8 in. The building is founded on 24-in diameter drilled piers in groups of two, three, and four piers per pilecap, and columns centered on the pilecap. The three-pier configuration on a triangular arrangement is used for most of the perimeter columns. Interior columns are supported on 4-pier pilecaps.

The column plan (with the designer's column numbers) is shown Figure 5-6. In this analysis, the south frame is analyzed, and the structural response is assumed to be symmetrical, i.e., the same peak response is assumed to apply to the north frame as well. The arrangement of column reinforcement is shown in Figure 5-7; Table 5-2 provides the reinforcement schedule. The frame is regular in elevation, as shown in Figure 5-8. The figure shows the designer's notation for beam and column numbering. Columns in the south frame are 14 in wide by 20 in deep, i.e., oriented to bend in their weak direction when resisting lateral forces in the plane of the frame. Spandrel beams in the south frame are generally 16 in wide by 30 in deep at the 2nd floor, 16 in wide by 22-½ in deep at the 3rd to 7th floors, and 16 in wide by 22 in deep at the roof. Spandrel beam reinforcement is shown in Table 5-3 and Table 5-4.

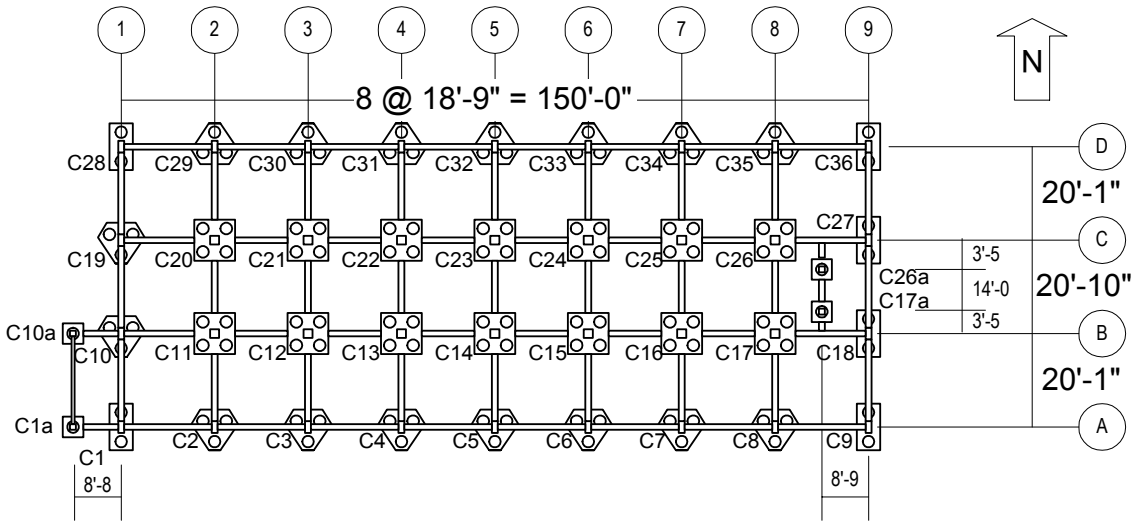

Figure 5-6. Column plan.

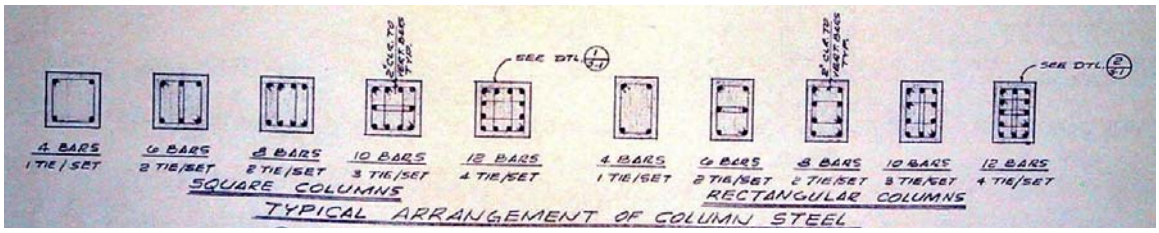

Figure 5-7. Arrangement of column steel (Rissman and Rissman Associates, 1965).

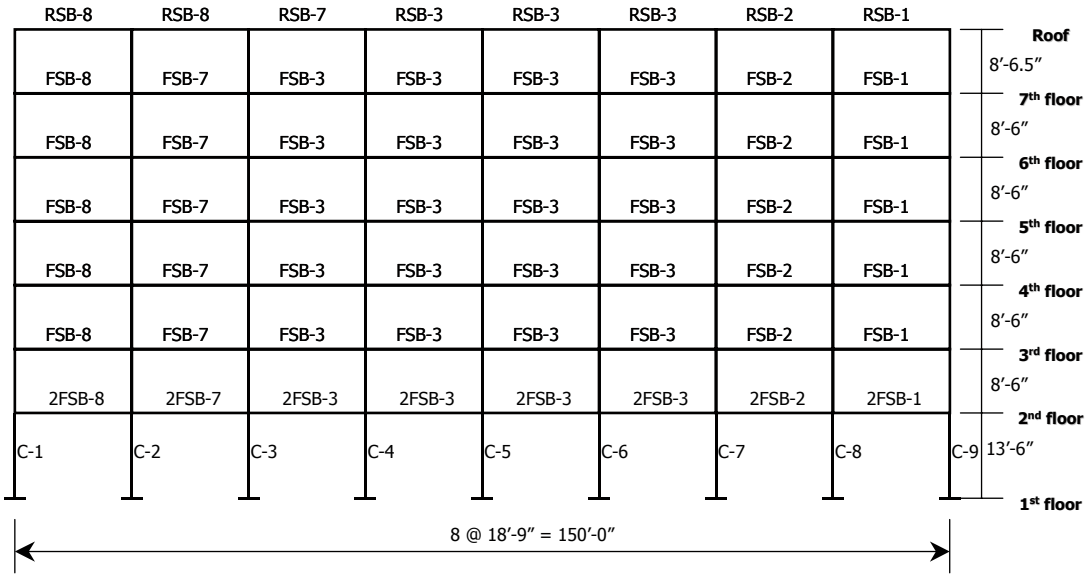

Figure 5-8. South frame elevation with element numbers.

Column concrete has nominal strength of f'_c = 5 ksi for the first story, 4 ksi for the second story, and 3 ksi from the third story to the seventh. Beam and slab concrete is nominally f'_c = 4 ksi at the second floor and 3 ksi from the third floor to the roof. Column reinforcement steel is scheduled as A432-62T (Grade 60) for billet bars. Beam and slab reinforcement is scheduled as ASTM A15-62T and A305-56T (Grade 40) for intermediate grade, deformed billet bars.

The building is clad on the north and south facades with aluminum window wall, comprising 3/16-in heavy sheet glass in sliding frames, and ¼-in cement asbestos board panels with an ornamental site-obscuring mesh of baked enamel or colored vinyl. Interior partitions are constructed of 5/8-in gypsum wallboard on 3-5/8 in metal studs at 16-in centers. Ceilings at the 2nd through 7th floors are a textured coating applied to the soffit of the concrete slab above; at the first floor, ceilings are suspended wallboard

or lath and plaster. The east and west endwalls are finished on the inside with gypsum wallboard and on the outside with stucco. Room air conditioning is provided by through-wall air-conditioning units mounted in the waist panels below the windows. The ground floor architectural plan is duplicated in Figure 5-9. The 2nd floor architectural plan, which is typical of floors 2 through 7, is shown in Figure 5-10. The plan of a typical hotel suite is shown in Figure 5-11.

Table 5-2. Column reinforcement schedule.

		Column mark							
		C-13 to C-17, C-21 to C-26	C-11, C-12, C-20	C-30 to C-34	C-10, C-18, C-19, C-27	C-2, C-3, C-8, C-29, C-35	C-1, C-9, C-28, C-36	C-1A, C-10A	C-17A, C-26A
Level	Col size	18"x18"	18"x18"	14"x20"	14"x20"	14"x20"	14"x20"	10"x12"	10"x12"
7th floor	Vert. bars	6-#7	6-#7	6-#7	6-#7	6-#7	6-#7	4-#5	
	Ties	#2@12"	#2@12"	#2@12"	#2@12"	#2@12"	#2@12"	#2@10"	
6th floor	Vert. bars	6-#7	6-#7	6-#7	6-#7	6-#7	6-#7	4-#5	4-#5
	Ties	#2@12"	#2@12"	#2@12"	#2@12"	#2@12"	#2@12"	#2@10"	#2@10"
5th floor	Vert. bars	6-#7	6-#8	6-#7	6-#7	6-#7	6-#7	4-#5	4-#5
	Ties	#2@12"	#3@12"	#2@12"	#2@12"	#2@12"	#2@12"	#2@10"	#2@10"
4th floor	Vert. bars	6-#8	8-#9	6-#7	6-#9	6-#7	6-#7	4-#5	4-#5
	Ties	#3@12"	#3@12"	#2@12"	#3@12"	#2@12"	#2@12"	#2@10"	#2@10"
3rd floor	Vert. bars	8-#9	12-#9	6-#9	8-#9	8-#9	6-#7	4-#6	4-#5
	Ties	#3@12"	#3@12"	#3@12"	#3@12"	#3@12"	#2@12"	#2@10"	#2@10"
2nd floor	Vert. bars	10-#9	12-#9	6-#9	8-#9	8-#9	6-#7	4-#6	4-#5
	Ties	#3@12"	#3@12"	#3@12"	#3@12"	#3@12"	#2@12"	#2@10"	#2@10"
1st floor	Col size	20"x20"	20"x20"						
	Vert. bars	10-#9	12-#9	10-#9	12-#9	10-#9	8-#9	4-#8	4-#6
	Ties	#3@12"	#3@12"	#3@12"	#3@12"	#3@12"	#3@12"	#3@10"	#2@10"

Table 5-3. Spandrel beam reinforcement schedule, floors 3 through 7.

Beam mark	Width	Height	Top bars					Bottom bars	#3 ties
			7F	6F	5F	4F	3F		
FSB-1	16″	22-½″	①⑨ 2#7	2#9	2#9	3#8	3#8	2#7 (2#8 @ 3F, 4F)	①⑨ 3@5″, 5@6″, rest @10″, 3F- 5F
			②⑧ FSB-2 top bars						②⑧ 6@4″, 5@6″, 3F-5F
FSB-2	16″	22-½″	②⑧ 2#9	3#8	3#8	3#8	3#9	2#6	8@5″, 5@6″ ea end
			③⑦ FSB-3 top bars						Rest @ 10″ 3F-5F
FSB-3	16″	22-½″	2#8	2#9	3#8	3#8	3#9	2#6	3@5″, 5@6″ ea end
									Rest @ 10″ 3F-5F
FSB-7	16″	22-½″	③ FSB-3 top bars					2#7	3@5″, 5@6″ ea end
			② FSB-8 top bars						Rest @ 10″ 3F-5F
FSB-8	16″	22-½″	② 2#8	2#9	2#9	3#8	3#8	2#7 (2#8 @ 5F, 2#9 @ 3F, 4F)	① 3@5″, 5@6″, rest@10″ 3F-5F
			① 2#7	2#8	2#9	2#9	3#8		② 6@4″, 5@6″ 3F-5F

①, ②, etc.: column lines
3F, 4F, etc: floor levels

Table 5-4. Roof and second-floor spandrel beam reinforcement schedule.

Beam mark	Width	Height	Top bars	Bottom bars	#3 ties
RSB-1	16″	22″	①⑨ 2#6 ②⑧ 2#8	2#7	#3@10″
RSB-2	16″	22″	②⑧ RSB-1 top bars ③⑦ RSB-3 top bars	2#6	Same
RSB-3	16″	22″	2#8	2#6	Same
RSB-7	16″	22″	④ RSB-3 top bars ③ 2#9	2#6	Same
RSB-8	16″	22″	③ 2#9 ② 3#9	2#9	Same
2FSB-1	16″	30″	①⑨ 2#9 ②⑧ 2FSB-2 top bars	2#8	4 @ 6″, 2 @ 8″, ea end, rest @ 13″
2FSB-2	16″	30″	②⑧ 3#8 ③⑦ 2FSB-3 top bars	2#6	Same
2FSB-3	16″	30″	2#9	2#6	Same
2FSB-7	16″	30″	③ 2FSB-3 top bars ② 2FSB-8 top bars	2#7	Same
2FSB-8	16″	30″	② 2#9 ① 2#9	2#8	Same

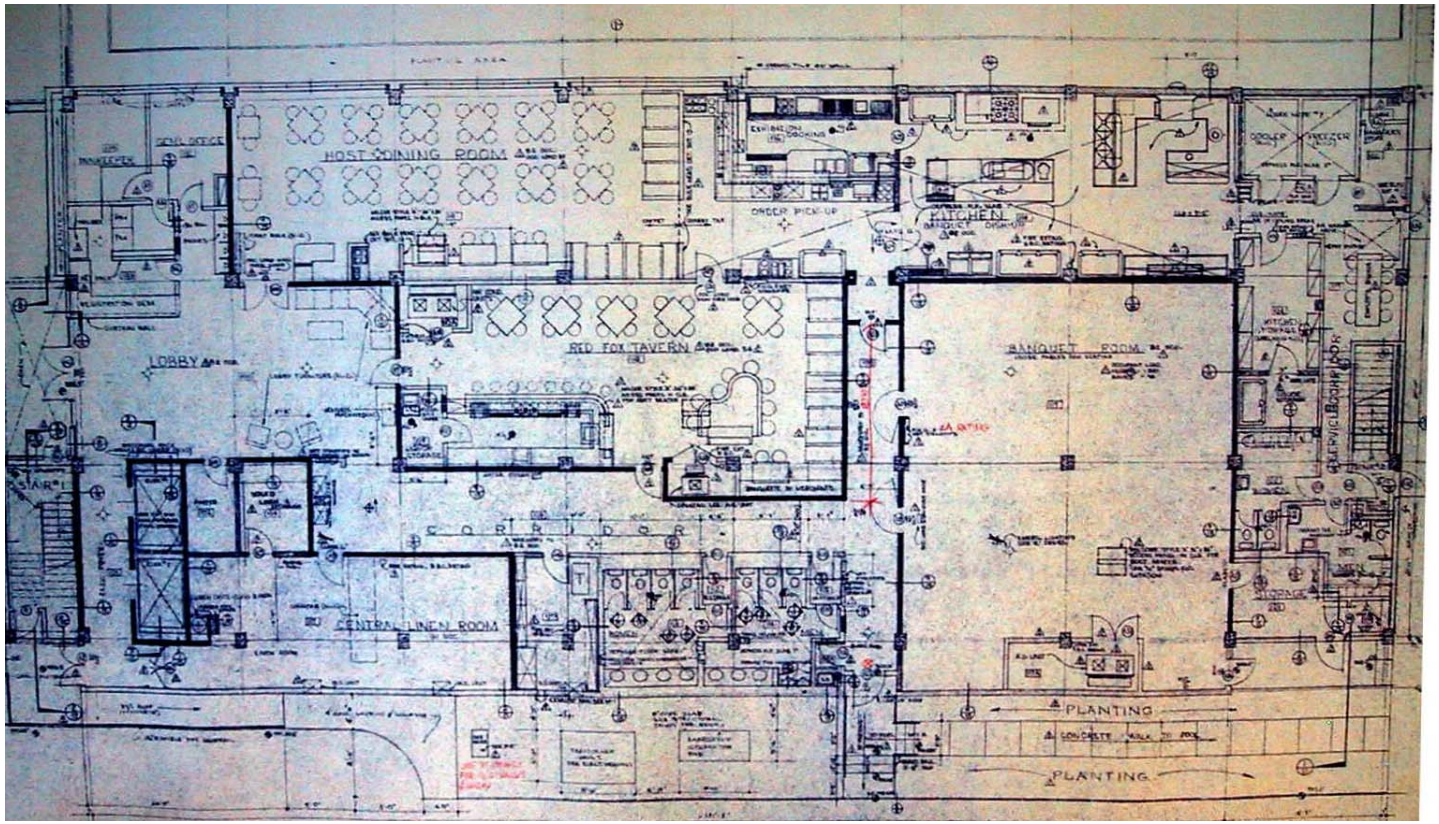

Figure 5-9. First floor architectural plan (Rissman and Rissman Associates, 1965).

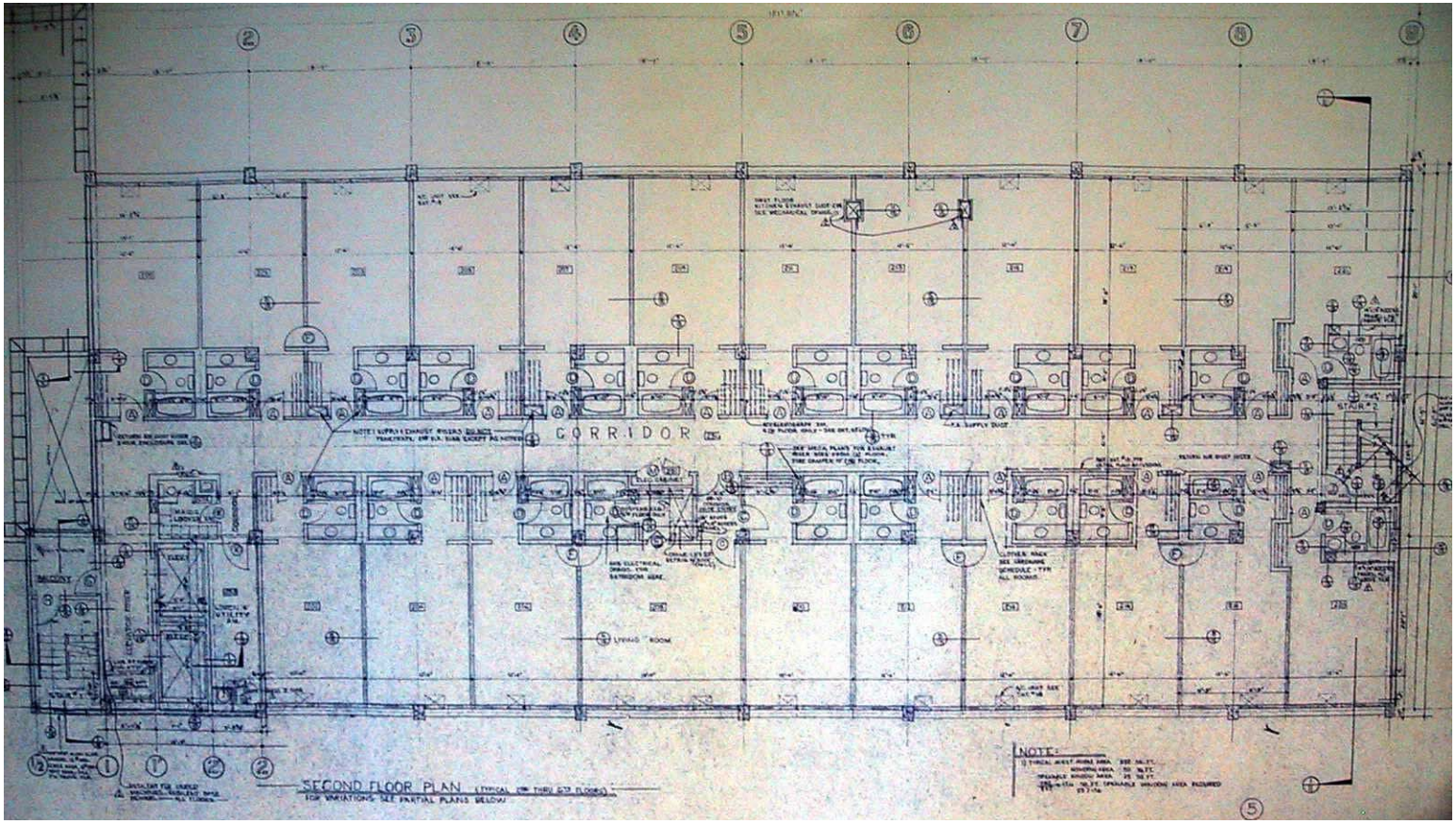

Figure 5-10. Second floor architectural plan (Rissman and Rissman Associates, 1965).

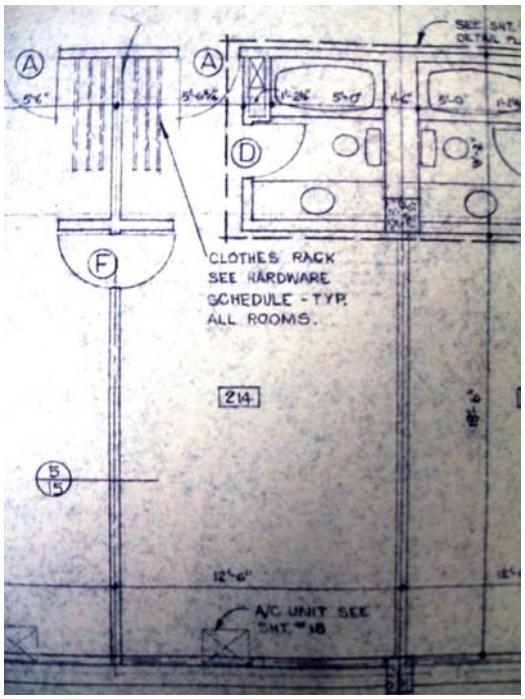

Figure 5-11. Typical hotel suite floor plan (Rissman and Rissman Associates, 1965).

Based on the structural and architectural drawings, an inventory was created for the damageable assemblies on the south half of the building, excluding the spandrel beams along column lines 1 and 9 (the east and west end walls), and the columns along line B. The inventory is summarized in Table 5-5. Note that it includes only structural and architectural elements, and excludes all contents, and any potentially damageable mechanical, electrical, and plumbing components. Detailed information on these assemblies and their installation conditions was unavailable.

Assembly fragility functions and repair costs have been developed for all of the damageable assemblies in the inventory (see Porter, 2000, Beck *et al.*, 1999, and Porter *et al.*, 2001), with the exception of reinforced-concrete columns and beams. The fragility of the reinforced-concrete assemblies is developed in Appendix B.

Table 5-5. Summary of damageable assemblies (south half of demonstration building).

AssyType	Description	Floor	Unit	Qty
3.5.180.1101.01	Nonductile CIP RC beam-column (column)	1	ea	9
3.5.180.1101.01	Nonductile CIP RC beam-column (column)	2	ea	9
3.5.180.1101.01	Nonductile CIP RC beam-column (column)	3	ea	9
3.5.180.1101.01	Nonductile CIP RC beam-column (column)	4	ea	9
3.5.180.1101.01	Nonductile CIP RC beam-column (column)	5	ea	9
3.5.180.1101.01	Nonductile CIP RC beam-column (column)	6	ea	9
3.5.180.1101.01	Nonductile CIP RC beam-column (column)	7	ea	9
3.5.190.1101.01	Nonductile CIP RC beam-column (beam)	2	ea	8
3.5.190.1101.01	Nonductile CIP RC beam-column (beam)	3	ea	8
3.5.190.1101.01	Nonductile CIP RC beam-column (beam)	4	ea	8
3.5.190.1101.01	Nonductile CIP RC beam-column (beam)	5	ea	8
3.5.190.1101.01	Nonductile CIP RC beam-column (beam)	6	ea	8
3.5.190.1101.01	Nonductile CIP RC beam-column (beam)	7	ea	8
3.5.190.1101.01	Nonductile CIP RC beam-column (beam)	8	ea	8
4.7.110.6700.02	Window, Al frame, sliding, heavy sheet glass, 4'-0x2'-6"x3/16"	2	ea	42
4.7.110.6700.02	Window, Al frame, sliding, heavy sheet glass, 4'-0x2'-6"x3/16"	3	ea	42
4.7.110.6700.02	Window, Al frame, sliding, heavy sheet glass, 4'-0x2'-6"x3/16"	4	ea	42
4.7.110.6700.02	Window, Al frame, sliding, heavy sheet glass, 4'-0x2'-6"x3/16"	5	ea	42
4.7.110.6700.02	Window, Al frame, sliding, heavy sheet glass, 4'-0x2'-6"x3/16"	6	ea	42
4.7.110.6700.02	Window, Al frame, sliding, heavy sheet glass, 4'-0x2'-6"x3/16"	7	ea	42
6.1.500.0001.01	Drywall partition, 5/8-in., 1 side, on metal stud, screws	1	sf	3520
6.1.500.0001.01	Drywall partition, 5/8-in., 1 side, on metal stud, screws	2	sf	3696
6.1.500.0001.01	Drywall partition, 5/8-in., 1 side, on metal stud, screws	3	sf	3696
6.1.500.0001.01	Drywall partition, 5/8-in., 1 side, on metal stud, screws	4	sf	3696
6.1.500.0001.01	Drywall partition, 5/8-in., 1 side, on metal stud, screws	5	sf	3696
6.1.500.0001.01	Drywall partition, 5/8-in., 1 side, on metal stud, screws	6	sf	3696
6.1.500.0001.01	Drywall partition, 5/8-in., 1 side, on metal stud, screws	7	sf	3696
6.1.500.0002.01	Drywall finish, 5/8-in., 1 side, on metal stud, screws	1	sf	3520
6.1.500.0002.01	Drywall finish, 5/8-in., 1 side, on metal stud, screws	2	sf	3976
6.1.500.0002.01	Drywall finish, 5/8-in., 1 side, on metal stud, screws	3	sf	3976
6.1.500.0002.01	Drywall finish, 5/8-in., 1 side, on metal stud, screws	4	sf	3976
6.1.500.0002.01	Drywall finish, 5/8-in., 1 side, on metal stud, screws	5	sf	3976
6.1.500.0002.01	Drywall finish, 5/8-in., 1 side, on metal stud, screws	6	sf	3976
6.1.500.0002.01	Drywall finish, 5/8-in., 1 side, on metal stud, screws	7	sf	3976
6.1.510.1202.02	Stucco finish, 7/8", on 3-5/8" mtl stud, 16"OC, typ quality	1	sf	512
6.1.510.1202.02	Stucco finish, 7/8", on 3-5/8" mtl stud, 16"OC, typ quality	2	sf	512
6.1.510.1202.02	Stucco finish, 7/8", on 3-5/8" mtl stud, 16"OC, typ quality	3	sf	512
6.1.510.1202.02	Stucco finish, 7/8", on 3-5/8" mtl stud, 16"OC, typ quality	4	sf	512
6.1.510.1202.02	Stucco finish, 7/8", on 3-5/8" mtl stud, 16"OC, typ quality	5	sf	512
6.1.510.1202.02	Stucco finish, 7/8", on 3-5/8" mtl stud, 16"OC, typ quality	6	sf	512
6.1.510.1202.02	Stucco finish, 7/8", on 3-5/8" mtl stud, 16"OC, typ quality	7	sf	512

5.3 VULNERABILITY ANALYSIS OF AS-IS BUILDING

5.3.1 Structural model

The design information presented above is used to create a model for structural analysis, detailed in Appendix F. In summary, the south frame, which was heavily damaged in the 1994 Northridge Earthquake, is selected for modeling in a 2-D nonlinear time-history structural analysis. Material nonlinearities are considered, and geometric nonlinearities ignored. The moment-curvature and P-M interaction characteristics of the reinforced concrete members are assessed using UCFyber (ZEvent, 2000). The cylinder strength of reinforced concrete is taken as the 28-day nominal value, plus 1.5 standard deviations (σ = 600 psi for $f'_c \geq 4$ ksi) to account for initial overstrength, plus an additional 30% to account for concrete maturity.

The flexural behavior of the beams and columns is represented by a one-component Giberson beam with plastic hinges at the ends (Sharpe, 1974). The shear deformation for the beams is assumed to be elastic and is incorporated in the flexural elements. The shear deformation for the columns is modeled by inelastic springs attached to the ends of the flexural elements. Centerline dimensions are used with rigid block offsets to account for joint stiffness.

Two types of inelastic hysteretic rules are used to model the nonlinear behavior of the reinforced-concrete members: the SINA tri-linear hysteresis rule (Saiidi and Sozen, 1979) is used to model stiffness degradation of reinforced concrete members in flexure. The Q-HYST bi-linear hysteresis (Saiidi and Sozen, 1979) is used to model the stiffness degradation of reinforced concrete members in shear. Strength degradation similar to that introduced by Pincheira *et al.* (1999) is applied to both hysteretic rules.

The interior frames are assumed to provide 35% of the overall lateral force resistance, as suggested by Islam (1996a). Consequently, their stiffness is accounted for by attributing 65% of the building mass to the two perimeter moment frames in the longitudinal direction. The resulting structural model has a small-amplitude fundamental period of 1.5 seconds, similar to that exhibited by the demonstration building at the beginning of the 1994 Northridge Earthquake.

Uncertainty in mass, damping, and member force-deformation behavior are accounted for as described in Section 5.1.3, using a set of N_S = 20 sample structural models simulated to be consistent with the probability distributions of the structural characteristics.

5.3.2 Selection of ground motions

Ground motions are drawn from the records presented by Somerville *et al.* (1997), who collected them for use in the SAC Steel Project (1999). These records include real and simulated acceleration time histories from earthquakes in the U.S., Japan, and Turkey. They reflect earthquakes of magnitude 5.7 to 7.7, recorded at distances ranging from 1.1 km to 107 km. They are intended to reflect firm-soil site conditions, similar to those of the demonstration building. It is desired to select from among these recordings and scale the selected motions to specified spectral accelerations in the range of 0.1g and 2.0g at increments of 0.1 g. Recording are selected and scaled according to the following rules:

1. To minimize errors associated with soil nonlinearity, uniformly scale the acceleration amplitudes at most by a factor of 2 (i.e., x2 or ÷2).

2. Prefer real recordings to simulated recordings.

3. Prefer recordings made near the site of interest, in this case, from California.

Ground motions that meet all three rules are denoted "category 3." If more than 20 records are available at any level of spectral acceleration, then 20 are selected at random. If at any level of spectral acceleration an inadequate number of records are available, rule 3 is relaxed, and records that met rules 1 and 2 but not 3 are added. These are denoted "category-2" records. For cases where still too few records are available, rule 2 is relaxed; the resulting records are denoted "category 1." Finally, rule 1 is incrementally relaxed until an adequate number of records (20) is available at each level of S_a. These are called "category 0." In the present analysis, category-0 records mostly include records with small-amplitude scaled S_a.

Of the 100 SAC records considered, 75 are used for 400 structural analyses of the as-is building, each record being used on average 5 to 6 times, and typically scaled by a factor of 1.34 ± 0.49 (mean scaling factor ± 1 standard deviation, considering all records).

Table 5-6 shows the scaling factors used, listed by SAC record ID (row headings) and spectral acceleration desired for the analysis (column headings). Consider the row labeled "LA01". As shown in the column labeled "0.5", record LA01 was scaled by a factor of 0.70 to analyze the as-is building at S_a = 0.5g. Other records used for the 0.5g analyses include LA03 (scaled by 1.00), LA04 (scaled by 1.02), LA05 (scaled by 1.30), etc.

Note that at each level of S_a, a new set of 20 records were drawn at random from among the available category-3 records, supplemented as necessary with category-2, category-1, or category-0 records. This approach differs from incremental dynamic analysis (IDA) in two ways: first, a new sample of ground motions is drawn at random at each level of spectral acceleration; second, the scaling factor was limited, which was practical for all $S_a \geq 0.5$g.

Table 5-6. Records used and their associated scaling factors, for the as-is building.

Record	Real	U.S.	Desired spectral acceleration, T_1 = 1.5 sec, β = 5%																		
			0.1	0.2	0.3	0.4	0.5	0.6	0.7	0.8	0.9	1.0	1.1	1.2	1.3	1.4	1.5	1.6	1.7	1.8	1.9	2.0
LA01	True	True			0.77		1.28	1.53														
LA02	True	True					1.35	1.62														
LA03	True	True			0.75	1.00	1.25	1.50	1.75													
LA04	True	True	0.55																			
LA05	True	True			0.87	1.16	1.45	1.74														
LA06	True	True	0.48	0.97		1.94																
LA07	True	True				1.23	1.54															
LA08	True	True			0.87	1.15		1.73														
LA09	True	True							0.78	0.89	1.00	1.11	1.22	1.33	1.44	1.55	1.66	1.78	1.89	2.00	2.11	2.22
LA10	True	True					0.82			1.32	1.48	1.65	1.81	1.98								
LA11	True	True					0.78	0.93	1.09	1.24	1.40	1.55	1.71	1.87								
LA12	True	True		0.72																		
LA13	True	True						1.00	1.17	1.33		1.67	1.83									
LA14	True	True					0.71	0.85	0.99	1.13	1.28	1.42	1.56	1.70	1.84	1.99						
LA15	True	True				0.71		1.06	1.24		1.59	1.77	1.95									
LA16	True	True					0.74		1.04	1.19	1.33	1.48	1.63	1.78	1.93							
LA17	True	True				0.85		1.28	1.49	1.71	1.92											
LA18	True	True							0.88	1.00		1.25	1.38	1.51	1.63	1.76	1.88	2.01	2.13	2.26	2.38	2.51
LA19	True	True		0.68		1.36	1.70															
LA20	True	True						0.85	0.99	1.13	1.27	1.41	1.55	1.70	1.84	1.98						
LA21	True	False												0.76	0.83	0.89	0.95	1.02	1.08	1.14	1.21	1.27
LA22	True	False													1.91							
LA23	True	True					0.72			1.15	1.30		1.59	1.73	1.87							
LA24	True	True									0.70	0.78		0.93	1.01	1.09	1.17	1.25	1.32	1.40	1.48	1.56
LA25	True	True							0.76		0.98	1.09	1.20	1.31	1.41	1.52	1.63	1.74	1.85	1.96	2.07	2.18
LA26	True	True								0.73	0.82	0.91	1.00	1.09	1.18	1.28	1.37	1.46	1.55	1.64	1.73	1.82
LA27	True	True							0.92	1.05	1.18	1.31	1.44	1.57	1.70	1.84	1.97	2.10	2.23	2.36		
LA28	True	True									0.69	0.77	0.85	0.93	1.00	1.08	1.16	1.23	1.31	1.39	1.47	1.54

Table 5-6 (continued). Records used and their associated scaling factors, for the as-is building.

Record	Real	U.S.	Desired spectral acceleration, T_1 = 1.5 sec, β = 5%																		
			0.1	0.2	0.3	0.4	0.5	0.6	0.7	0.8	0.9	1.0	1.1	1.2	1.3	1.4	1.5	1.6	1.7	1.8	1.9	2.0
LA29	True	True					1.15			1.83												
LA30	True	True				0.70	0.88		1.23	1.41	1.58		1.94									
LA33	False	True																			2.08	2.19
LA37	False	True																			2.02	2.13
LA39	False	True															2.04	2.18	2.32	2.45		
LA41	True	True			0.73	0.97		1.46	1.70	1.95												
LA42	True	True	0.37	0.73		1.47																
LA43	True	True	0.61	1.22	1.83																	
LA44	True	True	1.02																			
LA45	True	True	0.41	0.81	1.22																	
LA46	True	True	0.51	1.03																		
LA47	True	True	0.44	0.87	1.31																	
LA48	True	True	0.96	1.92																		
LA49	True	True	0.46	0.92	1.39																	
LA50	True	True	0.47	0.94																		
LA51	True	True	0.60	1.21	1.81																	
LA52	True	True	1.05																			
LA53	True	True	0.57	1.13	1.70																	
LA54	True	True	0.46	0.93	1.39	1.85																
LA55	True	True	0.43	0.87	1.30	1.73																
LA56	True	True	0.54	1.09	1.63																	
LA57	True	True	0.78	1.57																		
LA58	True	True	0.37	0.74		1.48	1.84															
LA59	True	True			0.78		1.30															
LA60	True	True		0.71	1.07	1.42	1.78															
NF01	True	True				0.71	0.89	1.06	1.24		1.59		1.95									
NF02	True	True			0.69	0.91	1.14	1.37		1.83												
NF03	True	True										0.67	0.74	0.80	0.87	0.94	1.01	1.07	1.14	1.21	1.27	1.34

Table 5-6 (continued). Records used and their associated scaling factors, for the as-is building.

Record	Real	U.S.	Desired spectral acceleration, T_1 = 1.5 sec, β = 5%																		
			0.1	0.2	0.3	0.4	0.5	0.6	0.7	0.8	0.9	1.0	1.1	1.2	1.3	1.4	1.5	1.6	1.7	1.8	1.9	2.0
NF04	True	True										0.87		1.05	1.14	1.22	1.31	1.40	1.49	1.57	1.66	1.75
NF05	True	True									0.68	0.76	0.84	0.91	0.99	1.06	1.14	1.22	1.29	1.37	1.44	1.52
NF06	True	True						1.76														
NF07	True	True							0.88	1.01		1.26		1.51	1.64	1.76	1.89	2.01	2.14	2.27	2.39	2.52
NF08	True	True				0.83	1.04	1.24	1.45		1.86											
NF09	True	False													1.79	1.93	2.06					
NF11	True	True			0.67		1.12	1.34	1.56													
NF12	True	True	0.37	0.75	1.12	1.49																
	True	True								0.74	0.84	0.93	1.02	1.12	1.21	1.30	1.40	1.49	1.58	1.67	1.77	1.86
NF14	True	True			0.94			1.88														
NF15	True	True						0.72	0.84	0.96		1.19	1.31	1.43	1.55	1.67	1.79	1.91	2.03	2.15	2.27	2.39
NF16	True	True				0.76		1.14	1.33	1.53	1.72											
NF17	True	False														1.01	1.08	1.16	1.23	1.30	1.37	1.44
NF19	True	False														0.87	0.93	0.99	1.05	1.11	1.18	1.24
NF23	False	True																0.48	0.51	0.54	0.57	0.60
NF24	False	True																2.01	2.13	2.26	2.38	2.51
NF26	False	True																2.01	2.14	2.27	2.39	2.52
NF29	False	True														0.61	0.65					
NF40	False	True															2.06					

5.3.3 Structural analyses

In the present analyses, nonlinear time-history structural analyses are performed using Ruaumoko 2-D (Carr, 2001). Material nonlinearities are considered but geometric nonlinearities (including P-Δ effects) are ignored. The total computational time for 400 analyses on a Pentium III, 900 MHz computer, is approximately seven hours. Of the 400 analyses of the as-is building, none failed to converge at a displacement solution.

Structural response parameters extracted from these analyses include peak floor displacements, peak transient drifts, and the maximum beam-end and column-end curvatures. In addition, peak spring deformations of the column-end shear elements are captured.

The peak structural response of the north frame is assumed to be the same as the south frame. We did not analyze the structural response in the transverse (north-south) direction. However, in an attempt to capture at least some aspect of damage and loss to architectural features aligned in the transverse direction (wallboard partitions and stucco endwalls), we assumed that peak transient drifts in that direction were 30%of those due to motion in the longitudinal direction. We neglected the estimation of deformation and damage to structural members running in the transverse direction, ias well as to the interior gravity-frame elements.

Figure 5-12 shows the envelope of peak floor relative displacements by floor and S_a level for the as-is building. The curves in the figure show average values for 20 analyses per S_a value. The figure also shows an estimated value of peak roof displacement, for an equivalent single-degree-of-freedom, linear elastic oscillator, i.e., one with a period of T = 1.5 sec and 5% damping. These elastic displacements are denoted by $D_{e,Sa}$ and are calculated as $1.3S_a/\omega^2$, where $\omega = 2\pi/T$. The equivalent roof displacement is calculated as $1.3S_d$ to account for the fundamental mode participation factor. The figure shows that peak displacements are significantly less than the value that would be predicted by linear elastic spectral methods at high values of S_a. This suggests that linear elastic modeling of the building would overestimate structural response, and that material nonlinearities and hysteretic damping substantially decrease the response. Variability in peak transient drifts is significant, typically having

logarithmic standard deviation on the order of 0.2 to 0.5, with a modest trend to greater variability at higher levels of spectral acceleration.

Table 5-7 presents the floor displacements relative to the ground, recorded in the 1994 Northridge Earthquake, and those estimated in the present study for S_a = 0.5g. (Recorded displacements are taken from Li and Jirsa, 1998.) Agreement is only fair, with recorded displacements falling generally 0.8 to 1.0 standard deviations of the estimated mean for an earthquake with S_a = 0.5g, i.e., near the 15th to 20th percentiles of displacements from the suite of ground motions. There is of course no reason to expect a particular realization of S_a = 0.5g such as the Northridge Earthquake to produce displacements that fall precisely at the mean value. The fact that the actual responses lie within perhaps the $\mu \pm 1\sigma$ bounds indicates general agreement. It would be valuable to compare the recorded responses with those modeled using the Northridge Earthquake base excitation, in order better to check the model; however, this was not done in the present study.

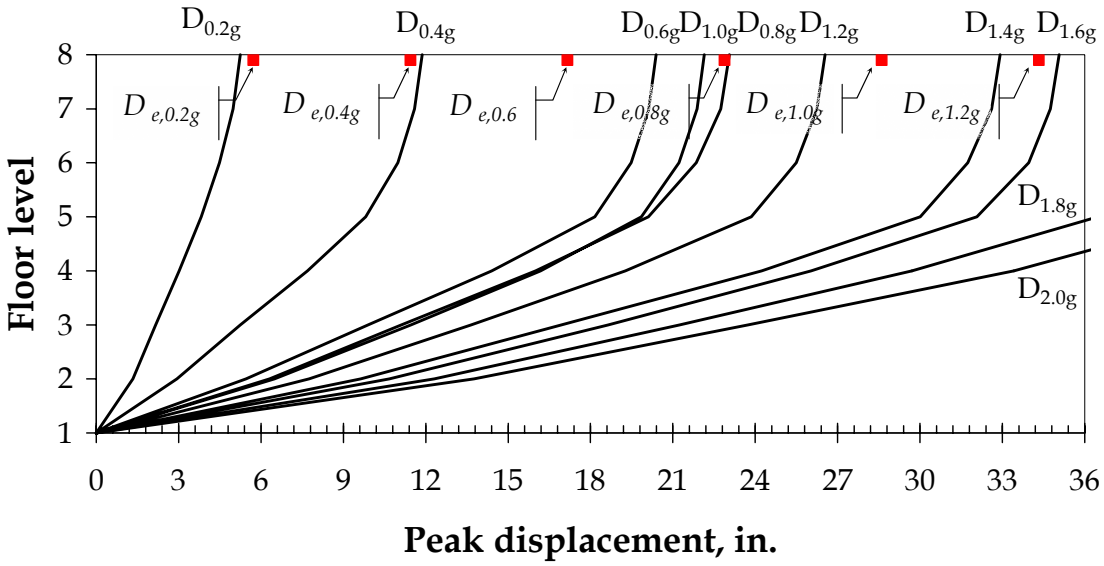

Figure 5-12. Mean peak floor displacements (relative to ground) of as-is building.

Table 5-7. Displacements recorded in Northridge 1994 and estimated for S_a=0.5g.

Level	Recorded, in.	Estimated mean ± stdev, in.	Estimated, excluding near-fault motions
Roof	9	16.5 ± 7.6	15.6 ± 8.1
6th Fl	8	15.5 ± 7.7	14.6 ± 8.1
3rd Fl	3.5	7.5 ± 3.7	7.0 ± 3.9
2nd Fl	1.5	4.2 ± 1.9	3.9 ± 2.0

Table 5-8 presents peak transient drift ratios recorded in the 1994 Northridge Earthquake, and those estimated in the present study for S_a = 0.5g. Only the first- and second-story drift ratios are available because of the location of the instruments in the building. (Recorded values again taken from Li and Jirsa, 1998.) Agreement again is only fair, with recorded displacements in Northridge falling 0.9 to 1.25 standard deviations below the estimated mean for a similar-sized event, i.e., near the 10th to 20th percentiles of the suite of simulations.

Table 5-8. Peak drift ratios recorded in Northridge 1994 and estimated for S_a=0.5g.

Level	Recorded	Estimated mean ± stdev
2nd story	1.8%	3.4% ± 1.8%
1st story	1.1%	2.6% ± 1.2%

Figure 5-13 shows estimated peak interstory drift ratios by floor and S_a level for the as-is building. The curves in the figure show average values for 20 analyses per S_a value. The figure shows that the third story (between the third and fourth floor) experiences the greatest interstory drift ratios, greater than the 2nd or 1st story. This can be explained by considering that the nominal concrete strength of the columns at the third story and above have nominal strength of f'_c = 3 ksi, versus 4 ksi at the second-

story columns and 5 ksi at the first-story columns. This reduction in concrete cylinder strength would reduce the modulus of elasticity *E*, which would in turn reduce the column bending stiffness *EI* and increase the consequent story drift. Note that the damage to the south frame in the 1994 Northridge Earthquake was primarily to the beam-column joints at the top of the fourth-story level, not the third, as shown in Figure 5-14.

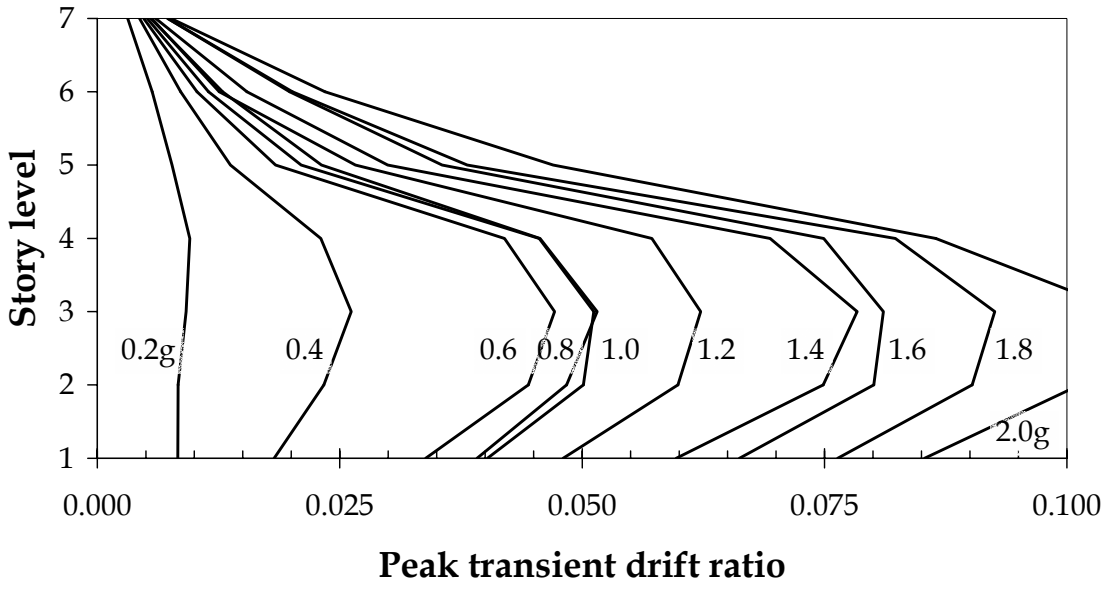

Figure 5-13. Peak transient drift ratios for as-is building.

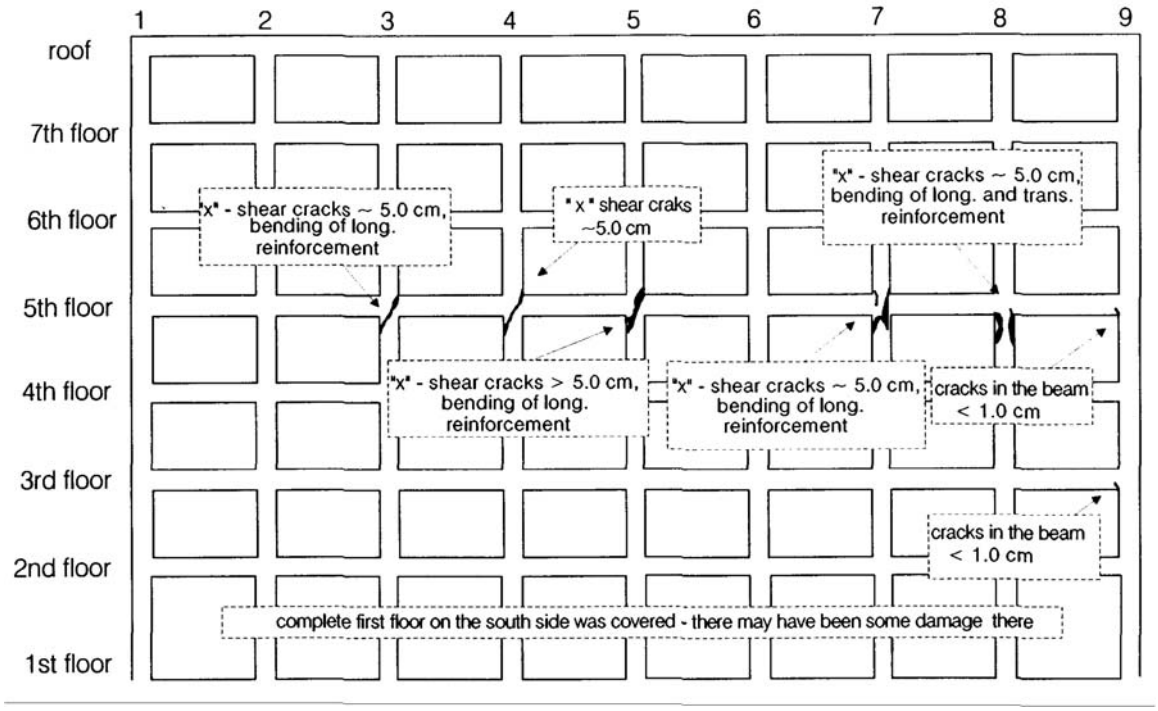

Figure 5-14. Structural damage in 1994 Northridge Earthquake, south frame (Trifunac *et al.*, 1999)

The present analysis offers an opportunity to gather some evidence about the statistical distribution of structural response. It is of interest to know whether the probability distribution of peak transient drift ratio closely matches some idealized probability distribution such as the Gaussian or lognormal distributions. If it does, this would suggest that in the future, one could simplify analysis by estimating the mean value of drift at a floor and its standard deviation, and assume that the drift is distributed according to the ideal.

Figure 5-15 shows the distribution of peak floor displacements (left-hand figure) and peak transient drift ratio (right-hand figure) over all stories, along with the cumulative Gaussian distribution. The jagged line in the left-hand figure shows the "observed" (i.e., the simulated) cumulative distribution of z, defined as $z = (\ln(x) - \mu_{\ln X})/\sigma_{\ln X}$, where x is a sample of the peak floor displacement, $\mu_{\ln X}$ is the mean value of the natural logarithm of x considering all the samples at that floor level and shaking

severity; and $\sigma_{\ln X}$ is the standard deviation of the natural logarithm of x. The smooth line in the left-hand figure is the Gaussian distribution.

One can test how well the idealized distribution matches observation using the Kolmogorov-Smirnov goodness-of-fit test. The agreement between the observed and idealized curves for both displacement and drift suggest that peak transient drift is approximately lognormally distributed. The figures, reflecting a sample size of 2,786, both pass the Kolmogorov-Smirnov goodness-of-fit test at the 1% significance level. These observations imply that the lognormal distribution is a reasonable approximation for both peak relative floor displacement and peak transient interstory drift, for this building.

It is also of interest to see how the dispersion (or uncertainty) of peak transient drift, measured by $\sigma_{\ln(PTD)}$, varies with shaking severity and with mean peak transient drift. Figure 5-16 illustrates the value of $\sigma_{\ln(PTD)}$ plotted against spectral acceleration (left) and against mean peak transient drift (right). In the figure, each dot represents one story level. Both figures show that $\sigma_{\ln(PTD)} \approx 0.37 \pm 0.11$ ($\pm$ 1 standard deviation of $\sigma_{\ln(PTD)}$) for the as-is building; a modest positive correlation (approximately 0.4) appears to exist relating dispersion of drift and both and shaking severity and mean drift. Story level does not seem to be strongly related to the dispersion on drift: the coefficient of correlation between story level and $\sigma_{\ln(PTD)}$ for these data is -0.2.

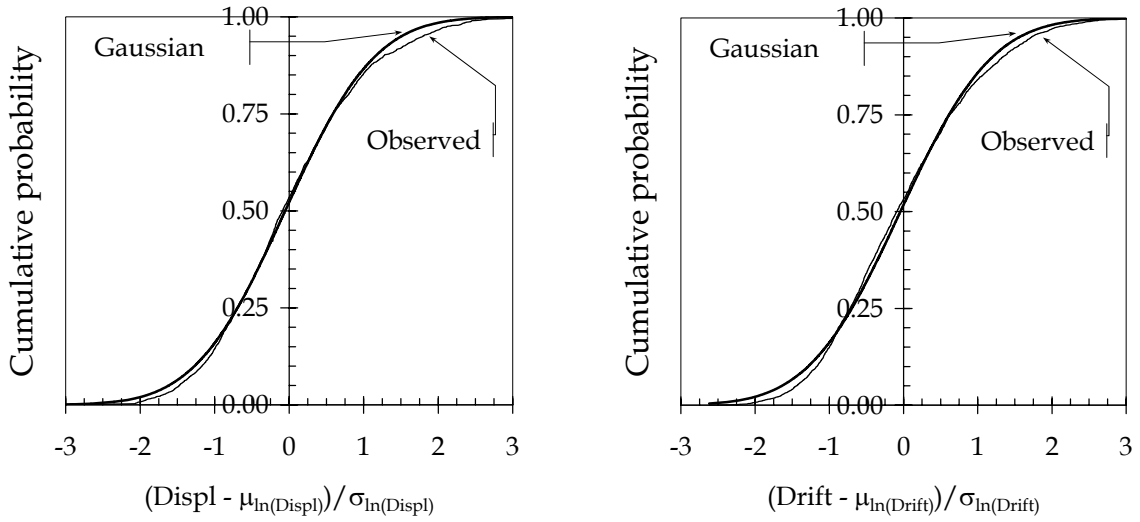

Figure 5-15. Distribution of peak transient displacement (left) and drift ratio (right).

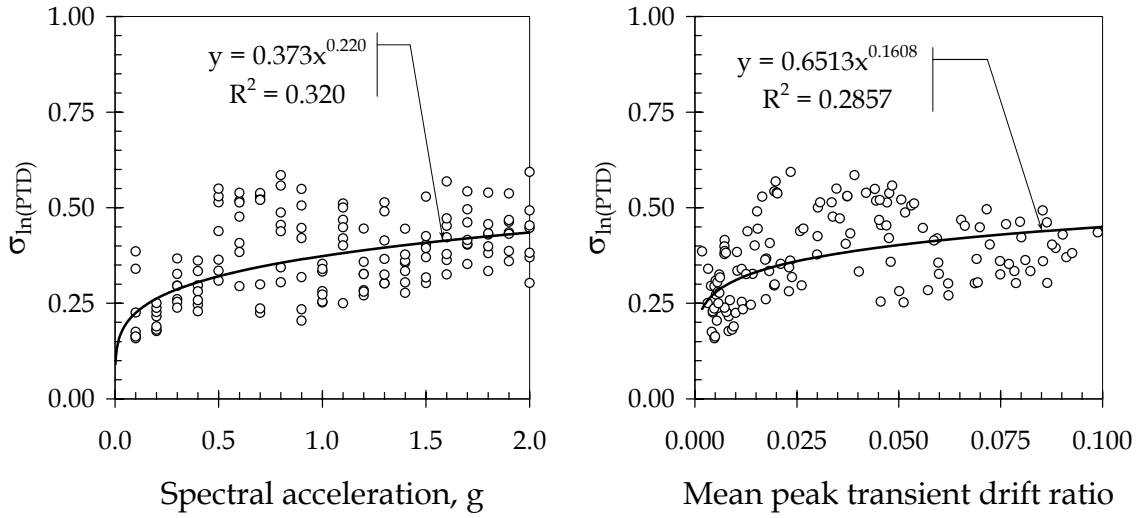

Figure 5-16. Dispersion of peak transient drift ratio.

5.3.4 Damage simulation

Table 5-8 summarizes the assembly fragility functions used in the present study. Details of the fragility functions for reinforced concrete members is presented in Appendix B. Fragilities for gypsum wallboard partitions and windows are developed in Porter (2000). The as-is building is modeled using 2,466 distinct damageable structural

and nonstructural assemblies. Damage is simulated separately for each assembly in each structural analysis.

Note that several of the damage states have fairly ambiguous, qualitative names. For example, damage state 1 for drywall is called visible damage, and damage state 2 for reinforced concrete beam-columns is called moderate damage. These damage states are nonetheless defined and the associated fragility functions are created so that each damage state is associated with particular repair efforts, as will be shown during the discussion of the loss analysis.

Table 5-8. Summary of assembly fragility parameters.

Assembly type	Description	d	Damage State	Resp	x_m	β
6.1.510.1202.02	Stucco finish, 7/8", on 3-5/8" mtl stud, 16"OC, typ quality	1	Cracking	PTD	0.012	0.5
6.1.500.0002.01	Drywall finish, 5/8-in., 1 side, on metal stud, screws	1	Visible dmg	PTD	0.0039	0.17
6.1.500.0002.01	Drywall finish, 5/8-in., 1 side, on metal stud, screws	2	Signif. Dmg	PTD	0.0085	0.23
6.1.500.0001.01	Drywall partition, 5/8-in., 1 side, on metal stud, screws	1	Visible dmg	PTD	0.0039	0.17
6.1.500.0001.01	Drywall partition, 5/8-in., 1 side, on metal stud, screws	2	Signif. Dmg	PTD	0.0085	0.23
3.5.180.1101.01	Nonductile CIP RC beam-column	1	Light	PADI	0.080	1.36
3.5.180.1101.01	Nonductile CIP RC beam-column	2	Moderate	PADI	0.31	0.89
3.5.180.1101.01	Nonductile CIP RC beam-column	3	Severe	PADI	0.71	0.8
3.5.180.1101.01	Nonductile CIP RC beam-column	4	Collapse	PADI	1.28	0.74
4.7.110.6700.02	Window, Al frame, sliding, heavy sheet glass, 4'-0x2'-6"x3/16"	1	Cracking	PTD	0.023	0.28

"Resp" = type of structural response to which the assembly is sensitive
PTD = peak transient drift ratio; PADI = Park-Ang damage index (displacement portion)
x_m = median capacity; β = logarithmic standard deviation of capacity

Some meaningful summary statistics on physical damage from the damage analysis can be presented. Figure 5-17 shows the average damage ratios (fraction of elements damaged) by assembly type and by spectral acceleration. Consider first the structural elements (beams and columns) that comprise the lateral force resisting system and represent the highest-cost elements to repair. There are a total of 63 columns in the south frame, so five columns with shear failure as in the 1994 Northridge Earthquake (S_a = 0.50g) would represent 8% in the "collapsed" damage state. The simulation matches observation, i.e., 4.5 columns on average were in the collapsed damage state at S_a = 0.5g. There are a total of 56 beams in the south frame. At S_a = 0.5g, as in the 1994 Northridge Earthquake, the model estimates an average of 40% of beams (22 beams) would be in the

light, moderate, or severe damage states, and that on average one or two would collapse. Comparison with Figure 5-14 shows that far fewer beams failed than the model predicts, from which one can infer that the beam-columns in the demonstration building are either less fragile or experienced lower seismic demand than modeled here. The model also estimates that on average three beams in the south frame would collapse at S_a = 0.5g. None actually did collapse, which reinforces the idea that the beams are less fragile than modeled.

The damage ratios for window breakage (lower left) and estimated drywall partition damage ratios (lower right) indicate widespread nonstructural damage under strong ground motion. Note that window breakage assumes that all windows are latched shut at the time of the earthquake. The significance of this assumption is that windows that are free to slide are less likely to be cracked by in-plane deformation of the frame caused by transient drift. The fragility function for the window glazing in the present study assumes panes are not free to slide.

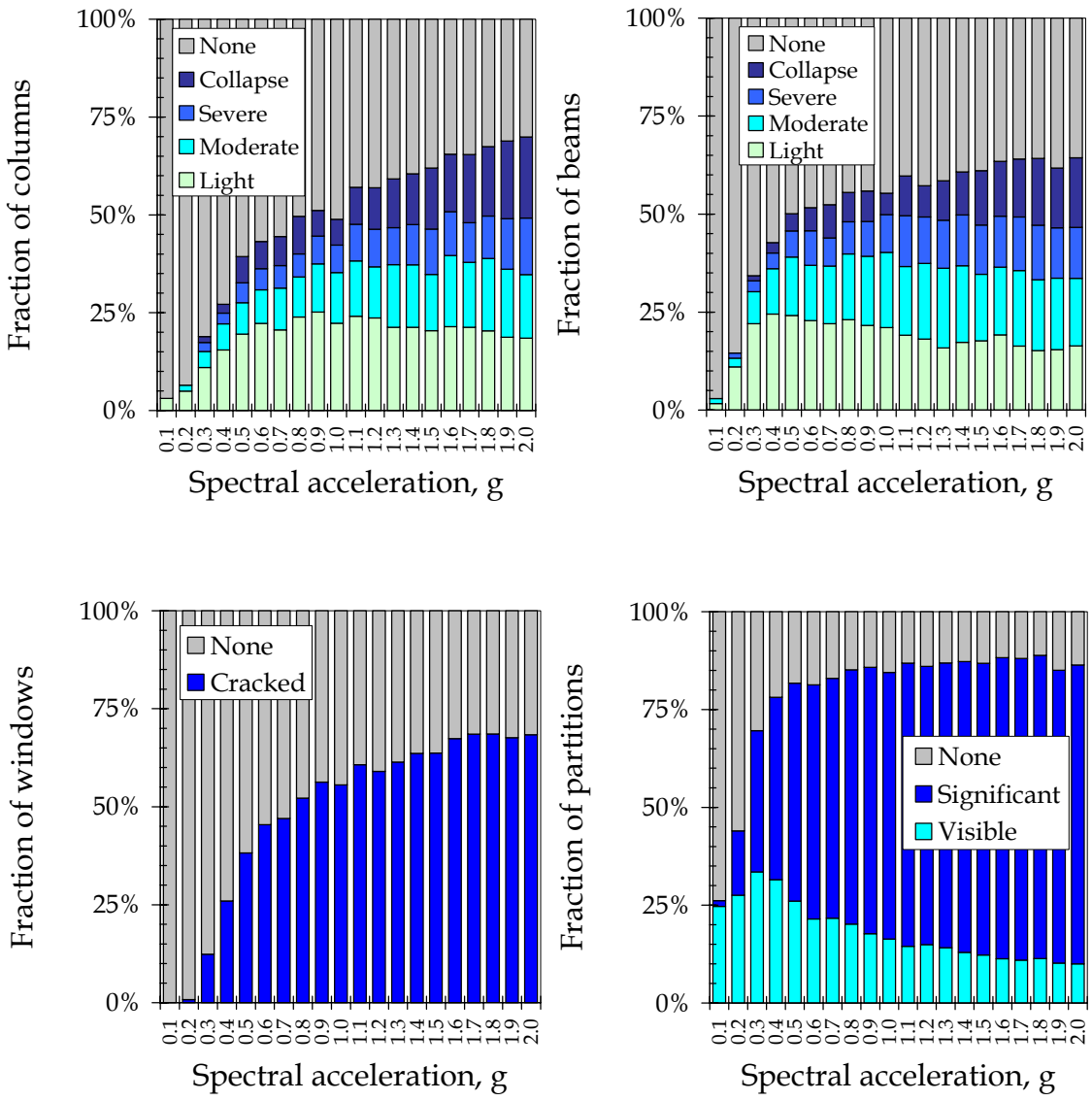

Figure 5-17. Assembly damage under as-is conditions.

5.3.5 Repair costs and vulnerability functions

The development of the unit repair-cost distributions (the median cost, x_m, and the logarithmic standard deviation, β) is detailed in Appendix C and summarized in Table 5-9.

Table 5-9. Summary of unit repair costs.

Assembly Type	Description	d	Repair	Unit	x_m	β
6.1.510.1202.02	Stucco finish, 7/8", on 3-5/8" mtl stud, 16"OC, typ quality	1	Patch	64 sf	125	0.2
6.1.500.0002.01	Drywall finish, 5/8-in., 1 side, on metal stud, screws	1	Patch	64 sf	88	0.2
6.1.500.0002.01	Drywall finish, 5/8-in., 1 side, on metal stud, screws	2	Replace	64 sf	253	0.2
6.1.500.0001.01	Drywall partition, 5/8-in., 1 side, on metal stud, screws	1	Patch	64 sf	88	0.2
6.1.500.0001.01	Drywall partition, 5/8-in., 1 side, on metal stud, screws	2	Replace	64 sf	525	0.2
3.5.180.1101.01	Nonductile CIP RC beam-column	1	Epoxy injection	ea	8,000	0.42
3.5.180.1101.01	Nonductile CIP RC beam-column	2	Jacketed repair	ea	20500	0.4
3.5.180.1101.01	Nonductile CIP RC beam-column	3,4	Replace	ea	34300	0.37
4.7.110.6700.02	Window, Al frame, sliding, hvy sheet glass, 4'-0x2'-6"x3/16"	1	Replace	ea	180	0.2
09910.700.1400	Paint on exterior stucco or concrete	1	Paint	sf	1.45	0.2
09910.920.0840	Paint on interior concrete, drywall, or plaster	1	Paint	sf	1.52	0.2

In the present study, 20 simulations are performed for each level of spectral acceleration S_a = 0.1, 0.2, … 2.0g, for a total of 400 simulations. Again, each simulation involves one ground motion, one simulation of the structural model, one simulation of the damage state for each assembly, and one simulation of repair costs. The repair cost divided by the replacement cost gives the damage factor.

The damage factor for each simulation is plotted against the spectral acceleration of the ground motion used in the simulation. Figure 5-18 presents the results for the building, along with a second-order polynomial regression curve based on a least-squares fit to the simulated damage-factor data. (If the regression curve were used in practice, the negative portion below $S_a < 0.04$g would be ignored.) The regression curve is referred to in the discussion below as the as-is ABV curve, since it is based on the assembly-based vulnerability method described in this report.

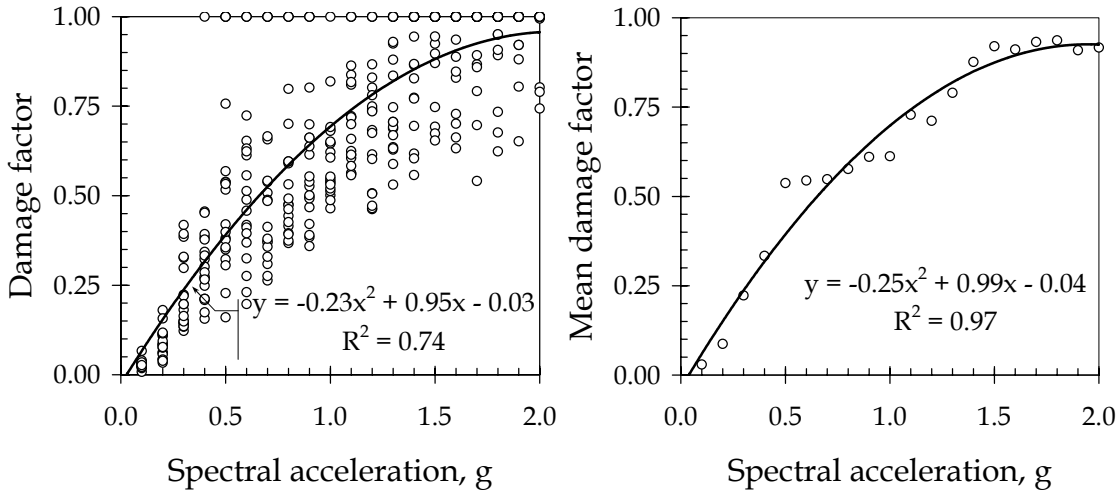

Figure 5-18. As-is building damage-factor simulations (left) and mean values (right).

Some validation is possible. Figure 5-19 shows the ABV curve compared with repair costs from the 1971 San Fernando earthquake, in which repairs cost 11% of the initial construction cost, and with the ATC-13 (Applied Technology Council, 1985) expert opinion on the vulnerability of similar construction, viz., highrise reinforced-concrete nonductile moment-frame construction. The ATC-13 experts express the building vulnerability as a function of Modified Mercalli Intensity (MMI). To make the comparison here, MMI is converted to peak horizontal acceleration (PHA) using Trifunac and Brady (1975). PHA is then converted to S_a for the period T = 1.5 sec and 5% damping using the design spectrum employed by the 2000 International Building Code (International Code Council, 2000). The ATC-13 (Applied Technology Council, 1985) curve shown is the mean best estimate after the third round of polling of the experts.

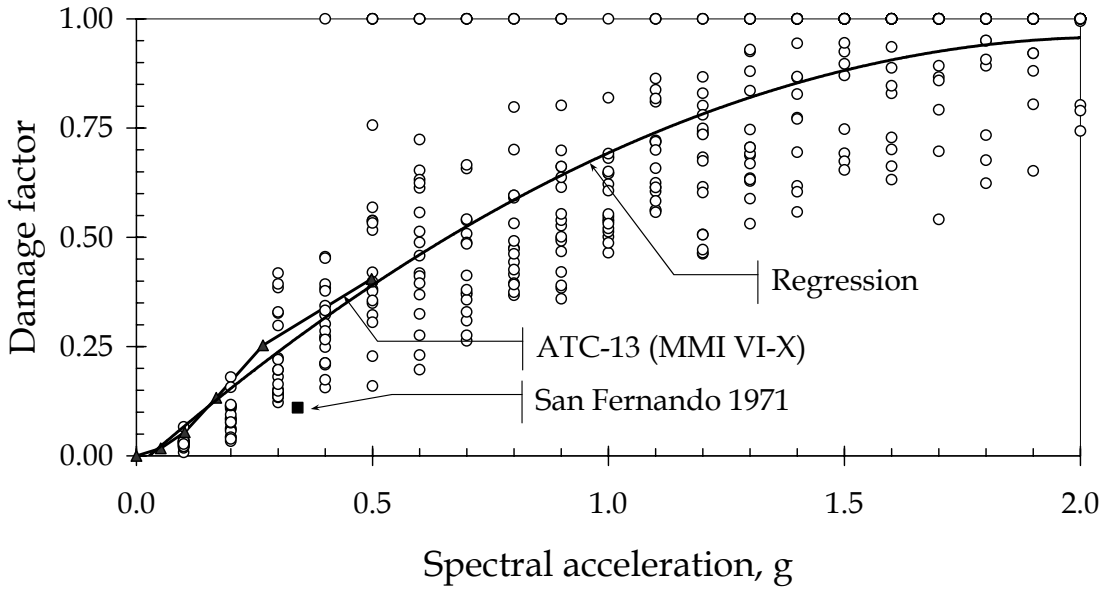

Figure 5-19. Validation of as-is vulnerability function.

No data are readily available on 1994 losses. Figure 5-19 shows that agreement of the simulation with ATC-13 (Applied Technology Council, 1985) is very good, but poor compared with the experience of this building in the 1971 San Fernando Earthquake, which lies below the 5th percentile of simulated losses. This is something of an apples-to-oranges comparison, and actually understates the discrepancy between the simulated and observed losses for two reasons. First, the present analysis assumes that the concrete has aged 35 years, and is consequently substantially stronger than it would have been in 1971. Furthermore, most of the actual losses in San Fernando were associated with bathroom finishes (tilework, etc.), which are not modeled here. Thus, had 1971 conditions been assumed here, and had bathroom finishes been modeled, the simulated losses would have been higher, and thus the observed loss would have been an even lower percentile of the simulated loss.

Figure 5-20 shows the average contribution to total repair costs from the various building components. (Exterior paint and stucco finish are omitted. They contribute only a negligible amount that would not be discernable on the diagram.) The figure shows that nonstructural damage is estimated to contribute the majority of costs at low

levels of shaking ($S_a \leq 0.2$g). At moderate to strong shaking, structural damage dominates, contributing 75% to 85% of the total repair cost.

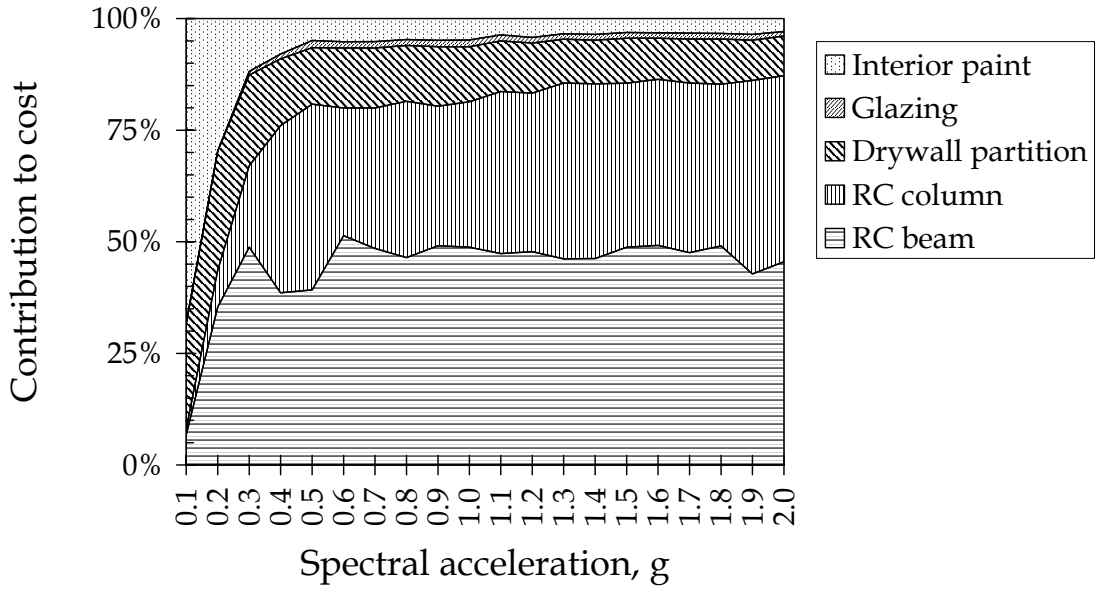

Figure 5-20. Relative contribution of building components to total repair cost.

Thus, if one were considering seismic retrofit for the purpose of reducing economic losses in frequent earthquakes, the retrofit design should focus on reducing nonstructural damage, either by stiffening the structural system, or by changing the connections between drywall partition and intersecting walls, and between the partition and the floor above, to allow more drift without inducing damage to the partitions. To mitigate damage to the structural system in less frequent, stronger events, one could strengthen the structural system, change its stiffness to reduce resonance with site ground motions, or both. The retrofit performed on the building following the 1994 Northridge Earthquake strengthened and stiffened the structural system by adding new shearwall elements along both the north and south frame. This would tend to reduce interstory drift and so reduce expected nonstructural costs. This retrofit is discussed in a later section of this chapter.

5.3.6 Distribution of repair cost conditioned on shaking intensity

It has been shown that peak transient drift ratios are distributed approximately lognormally. Here, we examine possible Gaussian and lognormal distributions for the damage factor. Let the as-is repair-cost statistics be binned by S_a = 0.1, 0.2, … 2.0g. Let the uncertain earthquake loss be denoted by C and the loss in any simulation be denoted by c. For a Gaussian distribution for C, let the mean value of loss at any level of spectral acceleration be denoted by $\mu_{C|Sa}$ and the standard deviation be denoted by $\sigma_{C|Sa}$. Similarly, for the lognormal distribution for C, define $\mu_{\ln C|Sa}$ and $\sigma_{\ln C|Sa}$ as the mean value and standard deviation of ln(C) at a given level of S_a. All moment parameters are estimated by corresponding sample moments.

Let $s_1 = (C - \mu_{C|Sa})/\sigma_{C|Sa}$ and let $s_2 = (\ln(C) - \mu_{\ln C|Sa})/\sigma_{\ln C|Sa}$. Figure 5-21 shows the cumulative distributions of s_1 and s_2 (the jagged lines), considering only the 300 simulations up to $S_a \le 1.5$g. Also plotted is the standard Gaussian distribution (the smooth curve). Both distributions pass the Kolmogorov-Smirnov (K-S) goodness-of-fit test at the 5% significance level. (Both fail when one considers all 400 simulations up to $S_a \le 2.0$g). Thus, when the data are limited to all but very rare, strong shaking, either the Gaussian or lognormal distributions can be used with this building to model residual variance about the mean vulnerability function.

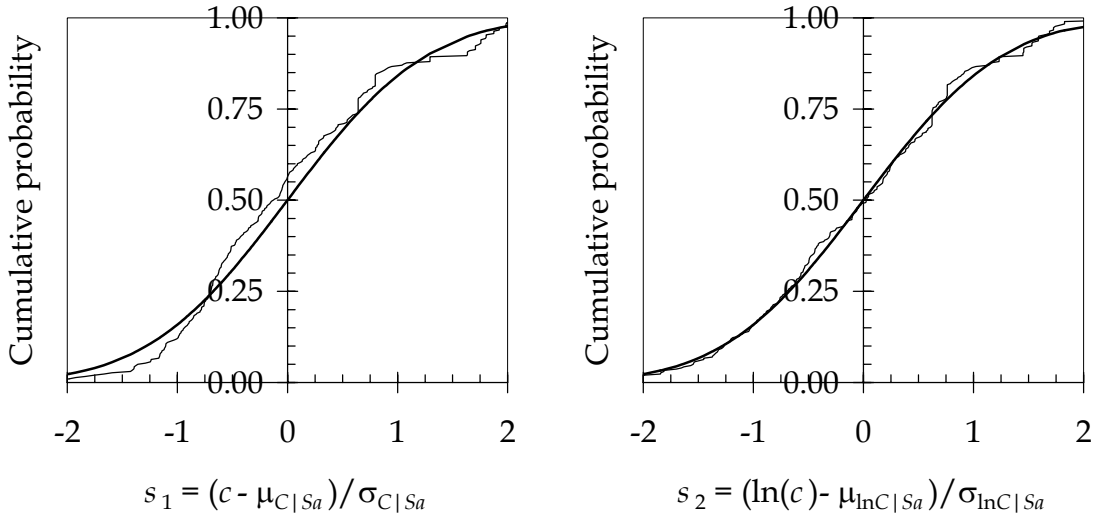

Figure 5-21. Gaussian and lognormal distributions fit to cost given S_a for $S_a \le 1.5$g.

5.3.7 Uncertainty on loss conditioned on spectral acceleration

Let the coefficient of variation on repair cost conditioned on spectral acceleration be denoted by $\delta_{c|Sa}$. It is calculated as the sample standard deviation of repair cost at a given level of S_a, for the N_S samples of loss at that S_a (here, N_S = 20), divided by the sample mean value at that S_a level. Figure 5-22 presents $\delta_{c|Sa}$ for the as-is building. Also shown is a regression curve given by least-squares fit to the damage factor coefficient of variation (COV). Figure 5-22 shows that uncertainty on loss given S_a decreases rapidly over the intensity range of interest, possibly because of loss saturation (only so much loss is possible). Another possibility has to do with the fact that the expected number of damaged elements increases as the shaking intensity increases: since the damage of different elements is taken to be independent conditioned on structural response, the standard deviation of loss increases more slowly than the mean value, hence producing a decreasing COV.

Figure 5-22 also compares the building-specific uncertainty derived here with the category-based uncertainty expressed by the experts who contributed to ATC-13 (Applied Technology Council, 1985). The figure shows the coefficient of variation on damage factor derived from the ATC-13 data. The ATC experts were asked to express the 90% upper and lower bounds of damage factor, i.e., the 5th and 95th percentiles. The difference between these two figures represents 3.3 standard deviations based on the Gaussian distribution. The standard deviation is divided by the mean value (the experts' weighted-average best estimate is taken here as the mean), and the resulting coefficients of variation are plotted in Figure 5-22. The experts appear to be approximately equally confident about their estimates of the vulnerability of an entire class of buildings as is the present study, which examines a single building of known detailed design.

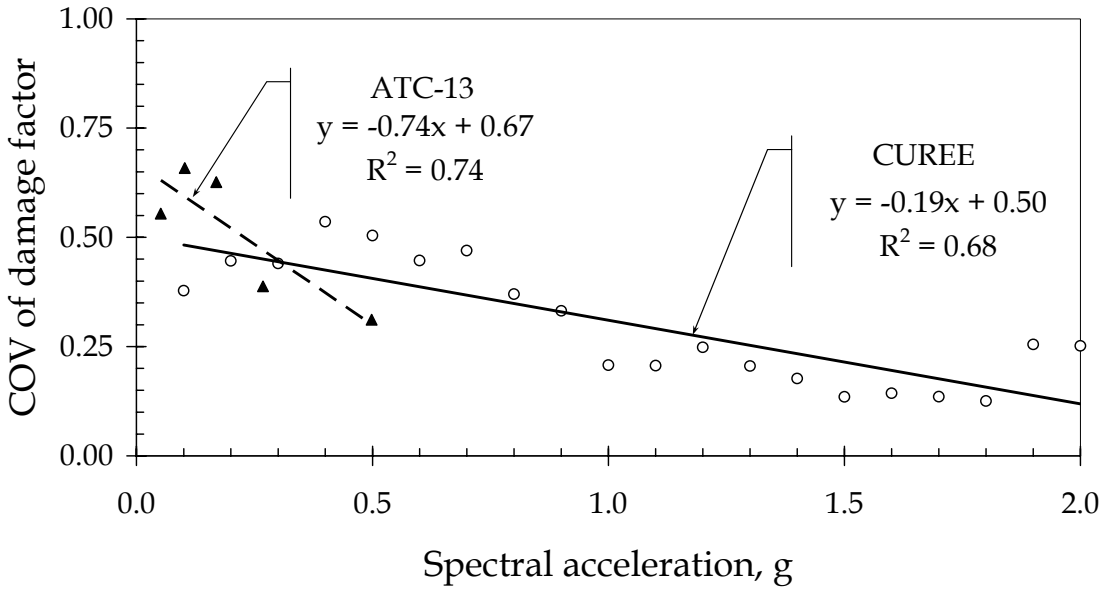

Figure 5-22. Uncertainty on damage factor as a function of spectral acceleration.

One of three possible inferences can be drawn from this comparison. First, the present study might substantially overestimate uncertainty for this particular building, which seems unlikely given the care taken in identifying and quantifying major sources of uncertainty, and the fact that several other uncertainties can be identified that we have omitted. Second, the example building could be highly atypical of this category of buildings in that uncertainty in damage is much greater for it than for the typical highrise nonductile concrete frame building. We can think of nothing particularly unusual about this structure that would support this second hypothesis. Finally, it could be that the experts substantially underestimated uncertainty for the class of buildings. This seems to be the most reasonable interpretation. Overly narrow confidence intervals, which reflect excessive confidence, are a common peril in the gathering of expert opinion. This is particularly true when the experts are asked to state values corresponding to given probability levels, as was the case with ATC-13. Tversky and Kahneman (1974) discuss this subject in detail.

5.4 VULNERABILITY ANALYSIS OF RETROFITTED BUILDING

Limited information is available on the seismic retrofit performed on the demonstration building following the 1994 Northridge Earthquake. Exterior

photographs and a limited interior examination of the building between column lines A1 and A2 at an upper floor indicate a seismic retrofit was performed by adding shearwalls at three columns of the south frame (3, 7, and 8) and four columns of the north frame (3, 5, 7, and 8). Figure 5-23 shows the building as it appeared in March 2001.

Figure 5-23. New shearwalls added to the south frame (left) and north frame (right).

Structural details such as reinforcement schedules, concrete strength, etc., are unavailable. Therefore, the retrofit considered here is hypothetical, and is not intended to reflect the retrofit measure actually constructed after the 1994 Northridge Earthquake. It is nonetheless useful for illustrating the investment decision-making procedure, which is after all the focus of the present study. (Since performing this analysis, we have learned from the engineer who designed the actual post-Northridge retrofit that the work included the addition of shearwalls at the interior as well as perimeter frames, and the addition of new grade beams to provide fixity at the base of the shearwalls [Rocha, 2002].)

The shearwalls are 108 in wide, with a panel somewhat thinner than the attached column. They are modeled using a rectangular shearwall element 15.6 in. thick, constructed of 5 ksi (nominal) concrete, with 5.9 ksi actual mean cylinder strength. The steel ratio is taken as the same as that at the ground floor (3.6%), and constant through the height of the shearwall. Boundary elements are 14 in wide, with #4 hoops at 3 in. centers. The cost of the retrofit is estimated to be $2.4 million, or $37/sf. See Appendix F for details of the cost estimate.

The south frame (column line A) of the retrofitted building is modeled by modifying the as-is structural model to account for the new shearwalls, as shown in Figure 5-24. (The pinned-based model for the new shearwall elements does not reflect the actual retrofit. It might not reflect professional practice. However, it is adequate for present purposes of illustration.)

The moment-curvature and axial-moment interaction behavior of the new structural elements is modeled using UCFyber (ZEvent, 2000). The results are used to modify the Ruaumoko (Carr, 2001) model of the as-is building. This retrofitted model has a small-amplitude fundamental period of approximately 0.75 sec.

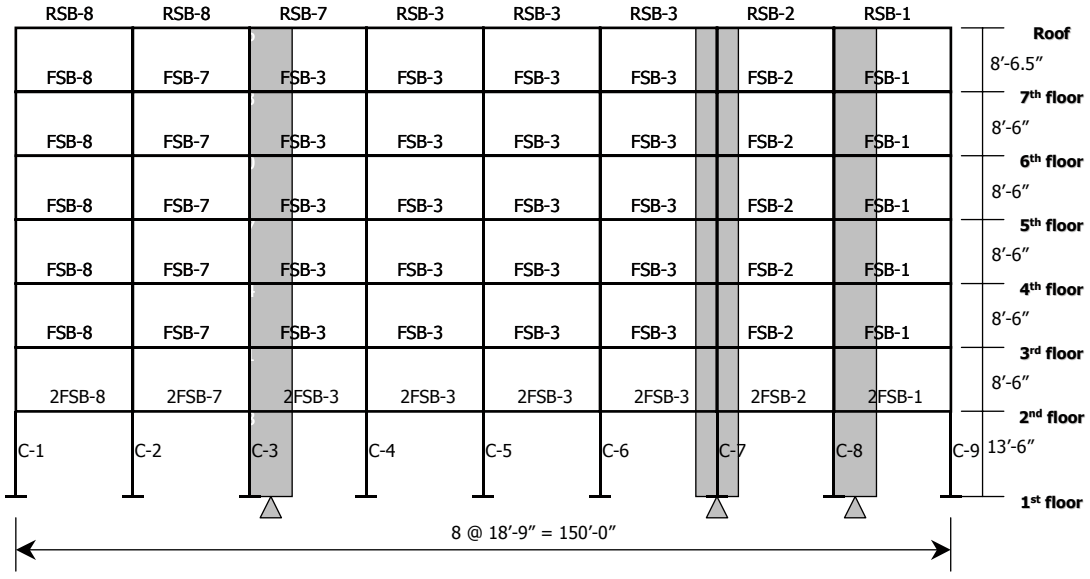

Figure 5-24. Structural model of retrofitted south frame.

An ABV analysis of the retrofitted building produces the mean structural responses plotted in Figure 5-25. (The contours are average values considering all samples at the S_a of interest.) Note that peak transient drift ratios are approximately constant through the building height, largely because of the pinned-base assumption for the new shearwalls. Comparison with Figure 5-13 shows that drift ratios at upper stories are actually greater in this retrofitted building than in the as-is structure.

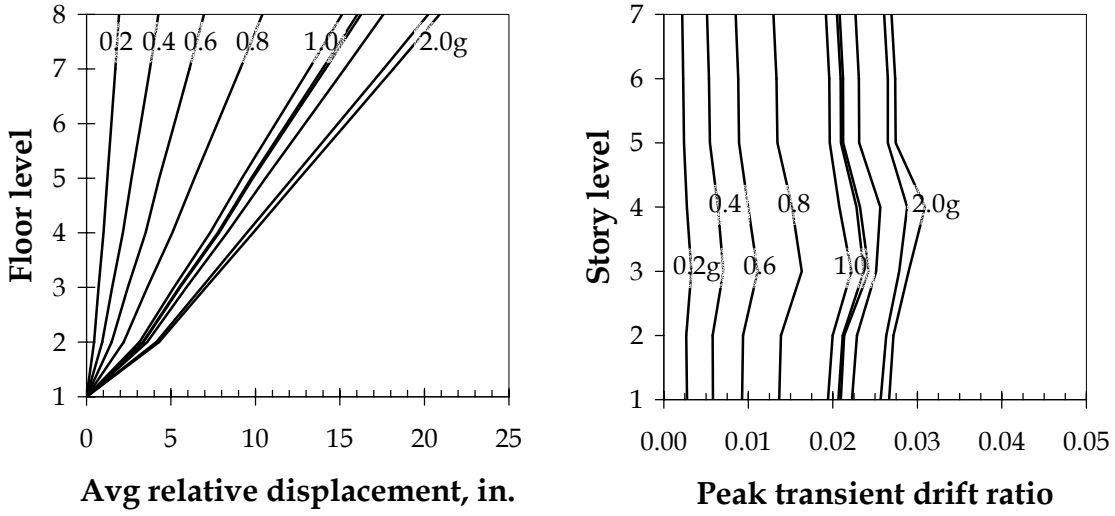

Figure 5-25. Structural response of retrofitted building.

The ABV damage analysis produces the damage ratios (fraction of assemblies damaged) shown in Figure 5-26. Comparison with Figure 5-17 indicates that column damage is reduced by 2/3 relative to the as-is case, while beam damage is modestly aggravated, owing to the greater demand placed on them by the pinned-base columns. (Of course, it is generally desirable to force damage into beams from columns, because of the implications for collapse mitigation.) Window damage is modestly reduced, by 1/3 to ½, and partition damage is likewise modestly reduced. In terms of physical damage then, the retrofit produces mixed results.

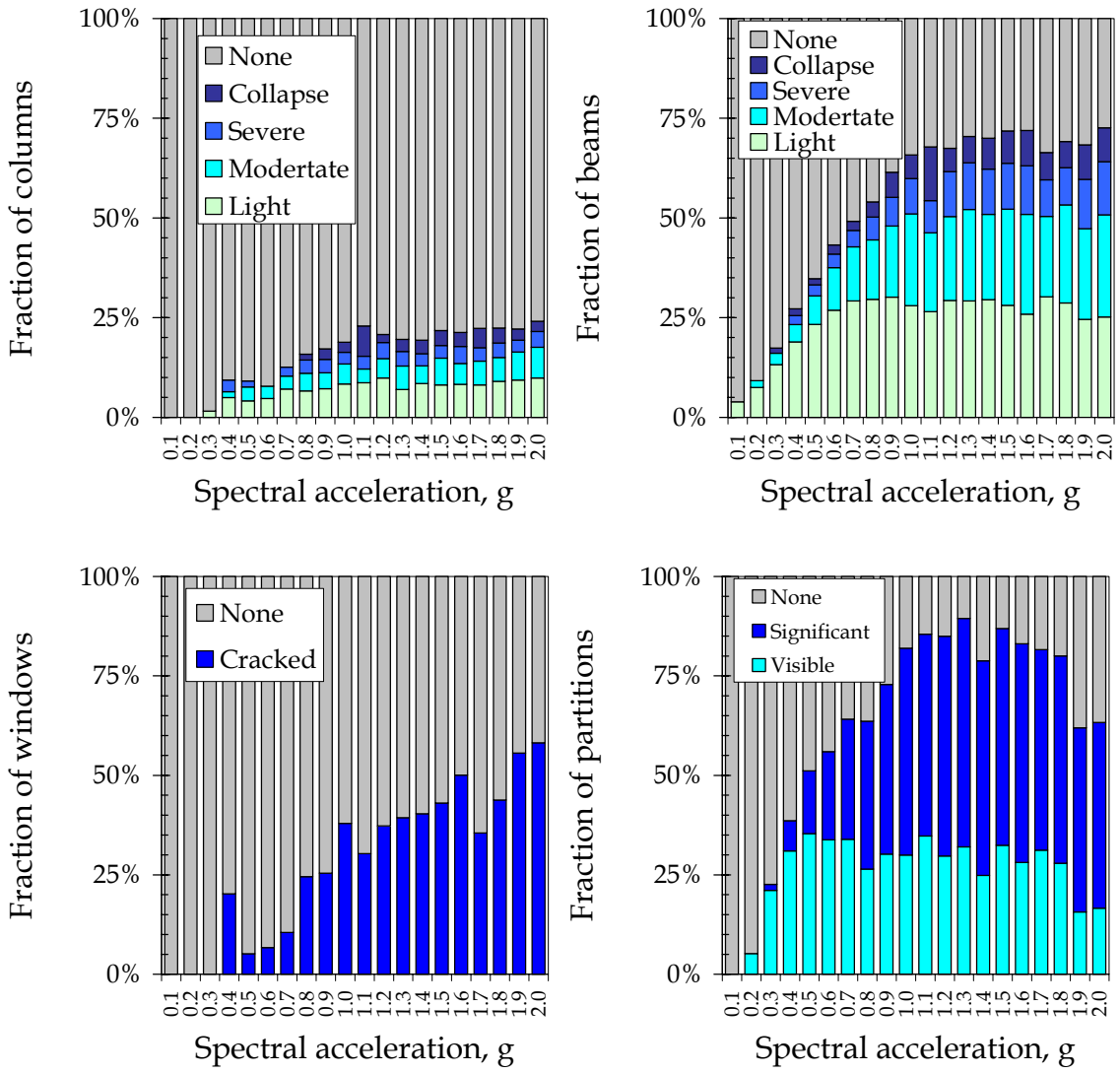

Figure 5-26. Mean damage ratios for assembly types in retrofitted building.

The loss analysis produces the repair-cost samples and mean vulnerability function shown in Figure 5-27. The losses are generally 1/3 to ½ less than the as-is case.

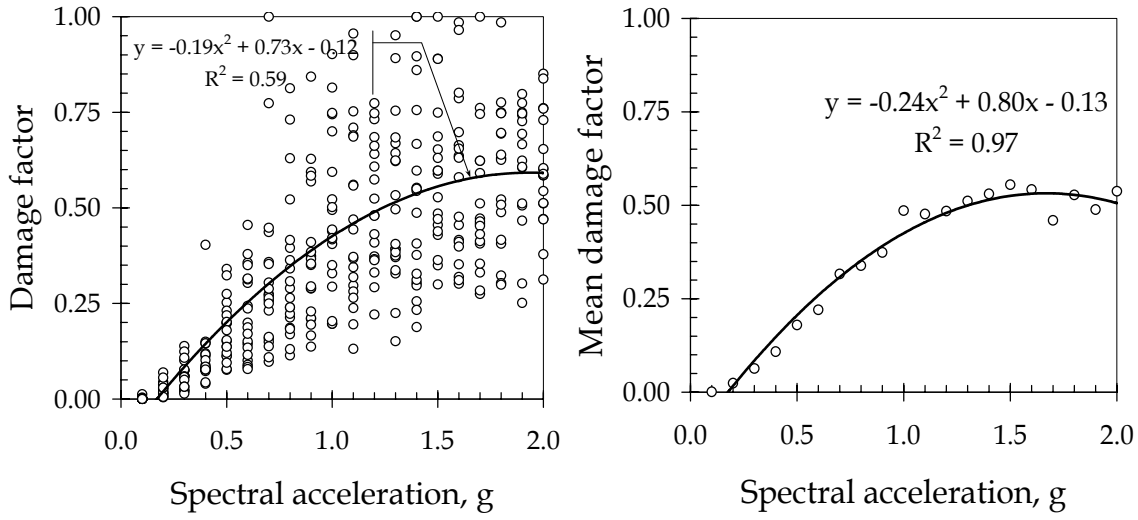

Figure 5-27. Retrofitted building damage-factor simulations and mean values.

Figure 5-28 shows the contribution to overall cost from the various assembly types. The figure shows that beams account for a greater portion of the overall repair costs, consistent with the observation that beam damage is greater in the retrofitted case than in the as-is case. Note that stucco repair and exterior painting contribute a very small portion to the overall repair costs, and so are omitted from the figure.

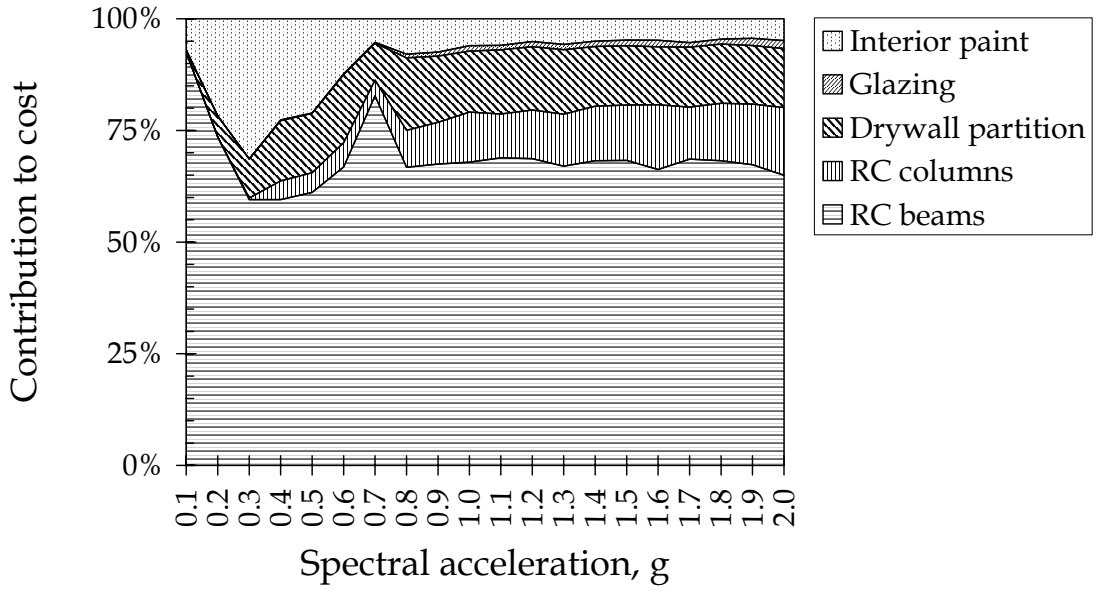

Figure 5-28. Contribution of building components to total repair cost in retrofitted case.

5.5 RISK-RETURN PROFILE AND CERTAINTY EQUIVALENT

The mean and variance of the net asset value are calculated for the CUREE demonstration building using Equations 3-15 and 3-16, repeated here for convenience. These require the evaluation of Equations 3-6, 3-11, and 3-13, which deal with the seismic-risk portion of V.

$$E[V] = E[I(t_L)] - C_o - E[L(t_L)] \tag{3-15}$$

$$\mathrm{Var}[V] = \mathrm{Var}[I(t_L)] + \mathrm{Var}[L(t_L)] \tag{3-16}$$

where

$$\begin{aligned} \overline{C}(t) &= \nu t E[C] \\ &= t\int_{S_o}^{\infty} E[C \mid S]\nu p(S \mid EQ)\,dS \\ &= t\int_{S_o}^{\infty} E[C \mid S]\,g(S)\,dS \end{aligned} \tag{3-6}$$

$$E[L(t)] = E[C]\frac{\nu}{r}\left(1 - e^{-rt}\right) = \frac{\overline{C}(1)}{r}\left(1 - e^{-rt}\right) \tag{3-10}$$

$$\mathrm{Var}[L(t)] = \frac{\nu}{2r}E[C^2](1 - e^{-2rt}) \tag{3-13}$$

$\overline{C}(t)$ = mean loss over time period t

C = earthquake repair cost given occurrence of an earthquake with intensity $S > S_0$

$I(t_L)$ = Present value of net income stream over the property lifetime t_L, ignoring earthquakes but including operating expenses such as earthquake insurance

$L(t_L)$ = present value of the total earthquake losses over time period t_L

r = risk-free discount rate

V = net asset value of the building

ν = Poisson rate of occurrence of shaking at the site with intensity $S \geq S_0$ (S_0 is a specified threshold, taken here to be 0.05g)

For the present example, t_L is taken as 30 yr, $I(t_L)$ is estimated using a purchase price of \$10M, a capitalization rate of 0.13 (a figure published recently for a similar hotel for sale in the Los Angeles area), a combined (federal and state) tax rate of 0.40, and a risk-free discount rate of 2%. Earthquake insurance is assumed to cost \$250,000 per year (approximately 3.5% rate on line, a reasonable figure for a Southern California commercial property) with a deductible of \$250,000 and a limit equal to the replacement cost of the building. This results in

$$\begin{aligned} E[I(t_L)] &= \frac{PE[r_e(t)]}{r}\left(1 - e^{-rt_L}\right) \\ &= \frac{\$10M \cdot 0.13 yr^{-1} \cdot (1 - 0.4)}{0.02 yr^{-1}}\left(1 - e^{-0.02 yr^{-1} \cdot 30 yr}\right) \\ &= \$18M \end{aligned} \tag{5-9}$$

for the case of no earthquake insurance, or \$14M for the case of earthquake insurance.

Using the discrete approximation for site hazard presented in Figure 5-5, the expected annualized loss is calculated as

$$\overline{C}(1) \approx \sum_{S_0}^{\infty} E[C \mid S] n(S) \tag{5-10}$$

where $n(S)$ represents the expected annual number of earthquakes of $S_a = S \pm \Delta S/2$.

The variance on the present value of the net income stream is calculated assuming a coefficient of variation of 1.0 (an intermediate value between an interviewee's estimate of 0.2 and the value of 6.0 implied by Holland *et al.*, 2000, as described in Chapter 2).

Using these figures, one arrives at mean and variance of net asset value for three of the four alternatives as shown in Table 5-10. (The fourth alternative, do not buy, has $E[V]$ = Var[V] = 0.) All figures are in units millions of dollars after tax, with the exception of expected annualized loss, $\overline{C}(1)$, which is in before-tax millions of dollars.

Variance figures are in units of after-tax ($M)^2. Earthquake insurance premiums are deducted from $E[I]$, and retrofit costs are added to C_0.

Table 5-10. Net asset value and certainty equivalent of CUREE demonstration building

	Alternative		
	As-is	**Insure**	**Retrofit**
$E[I]$	$39.0	$31.5	$39.0
C_0	10.0	10.0	12.4
$\overline{C}(1)$	0.055	0.033	0.043
$E[L]$	1.64	0.99	1.29
$E[V]$	27.4	20.5	25.3
Var[I]	1521.0	1521.0	1521.0
Var[L]	0.908	0.717	0.701
Var[V]	1521.9	1521.7	1521.7
COV[V]	1.4	1.9	1.5
CE	19.8	12.9	17.7

All figures in $M

First, consider the risk-return profile implied by these results. Observe from Table 5-10 that variance on earthquake loss, Var[L], is small compared with the variance on income, Var[I], which shows that the uncertainty on lifetime earthquake losses is unimportant in the decision-making here. Thus, the distribution on net asset value has very nearly the same form as that of net income. As the present value of net income is the sum of many random variables (albeit correlated ones), it is reasonable to approximate the distribution of income, and therefore net asset value, as Gaussian. With this assumption and the results shown in Table 5-10, one can readily plot the risk-return profile of the property as the probability of exceeding V, given the seismic risk and market risk, as shown in Figure 5-29.

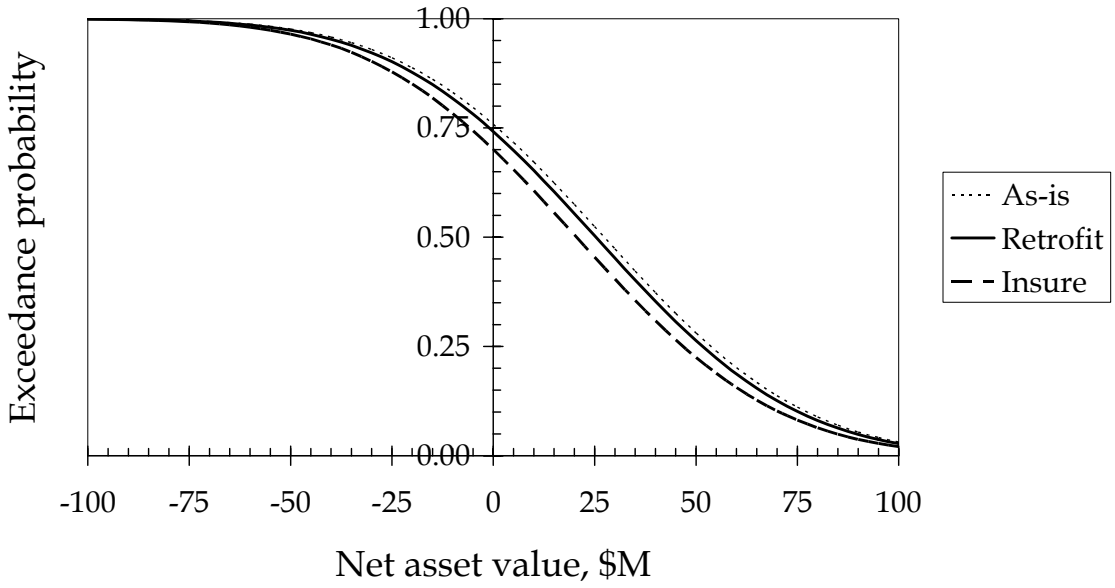

Figure 5-29. Risk-return profile of CUREE demonstration building.

The figure shows that the as-is and retrofit alternatives are nearly indistinguishable. The cost of the retrofit alternative is $2.4 million, and it reduces the present after-tax value of earthquake loss by $350,000, resulting in an after-tax net cost of $2.0M, a small difference on the scale of the figure. (Note that the retrofit, in contrast with repairs, would be deemed a capital improvement by the Internal Revenue Service, and so would not be tax-deductible.) The figure also shows that the property is more than likely to be a profitable investment: the net asset value is positive with at least 70% probability.

Table 5-10 also shows the certainty equivalent (CE) for the CUREE demonstration building and a decision-maker with a risk tolerance of $100M. The derivation of CE is discussed in Chapter 4. As shown in Chapter 4, if one assumes a Gaussian distribution on the net asset value, the CE is given by Equation 4-8, which is simplified as

$$CE = E[V] - \frac{1}{2\rho} Var[V] \tag{5-11}$$

The table shows that the CE of all three alternatives is positive, meaning that all three alternatives are preferable to the do-not-buy alternative. Also, the CE is substantially less than the expected net asset value E[V], showing that risk aversion should play an important role in the decision-making process.

Notice that earthquake insurance is significantly less desirable than either the as-is or retrofit alternative. The as-is alternative has the highest CE, and is therefore the preferable choice for the conditions examined here. (This study neglects the value of human life, which if considered would reduce the difference between as-is and retrofit, and could make the retrofit alternative preferable.) The table shows that average annual earthquake losses are $33,000 to $55,000, a significant amount as an operating expense.

Observe from Table 5-10 that earthquake loss $E[L]$ of the as-is case is a modest fraction (4%) of the expected present value of income, $E[I]$. This is equivalent to a reduction in the capitalization rate from the nominal level of 13%, to an earthquake-risk-adjusted value of 12.5%. Thus, earthquake risk can cause a significant reduction in the true capitalization rate, and might therefore be considered in a prudent financial analysis.

To reiterate: in this example, uncertainty on earthquake loss is irrelevant to a prudent real-estate investment decision. However, mean annualized loss is relevant: it materially reduces the capitalization rate, from 13% to 12.5%. Looked at another way, earthquake loss represents an average annual operating expense of $33,000 to $55,000, figures that would be noticeable—and in fact could be readily used—in the financial analysis of an investment opportunity.

5.6 SENSITIVITY STUDIES

The CE is affected by several important uncertain parameters, four of which are examined here. In the foregoing analysis, the after-inflation risk-free discount rate was assumed to be 2%. In practice, it could reasonably vary between 1% and 7%. The risk tolerance of the decision-maker was assumed to be $100M, a reasonable middle figure for an investor who deals with properties costing $10M. However, it is reasonable for an investor to pursue a deal valued anywhere between 2% and 50% of his or her risk

tolerance, meaning that ρ could reasonably range between $20M and $500M. The coefficient of variation on income (indicating market risk) was taken as 1.0, but interviews with investors and examination of Holland *et al.* (2000) indicate that value could be almost an order of magnitude lower or higher. Finally, the insurance premium was taken as $250,000 per year, approximately 3.5% rate on line (percent of insurance limit). In practice, it might be anywhere from 2% to 5%.

Figure 5-30 shows how CE is affected by each uncertain variable. The figures show that the preferred decision is materially affected by risk tolerance and variability of income, but not discount rate or insurance rate on line. Consider first the sensitivity of the certainty equivalent to discount rate (upper left chart in Figure 5-30). The CE is highest for the as-is case for all reasonable values of discount rate, meaning that the preferable alternative is to buy and leave the property as-is for all reasonable values of discount rate.

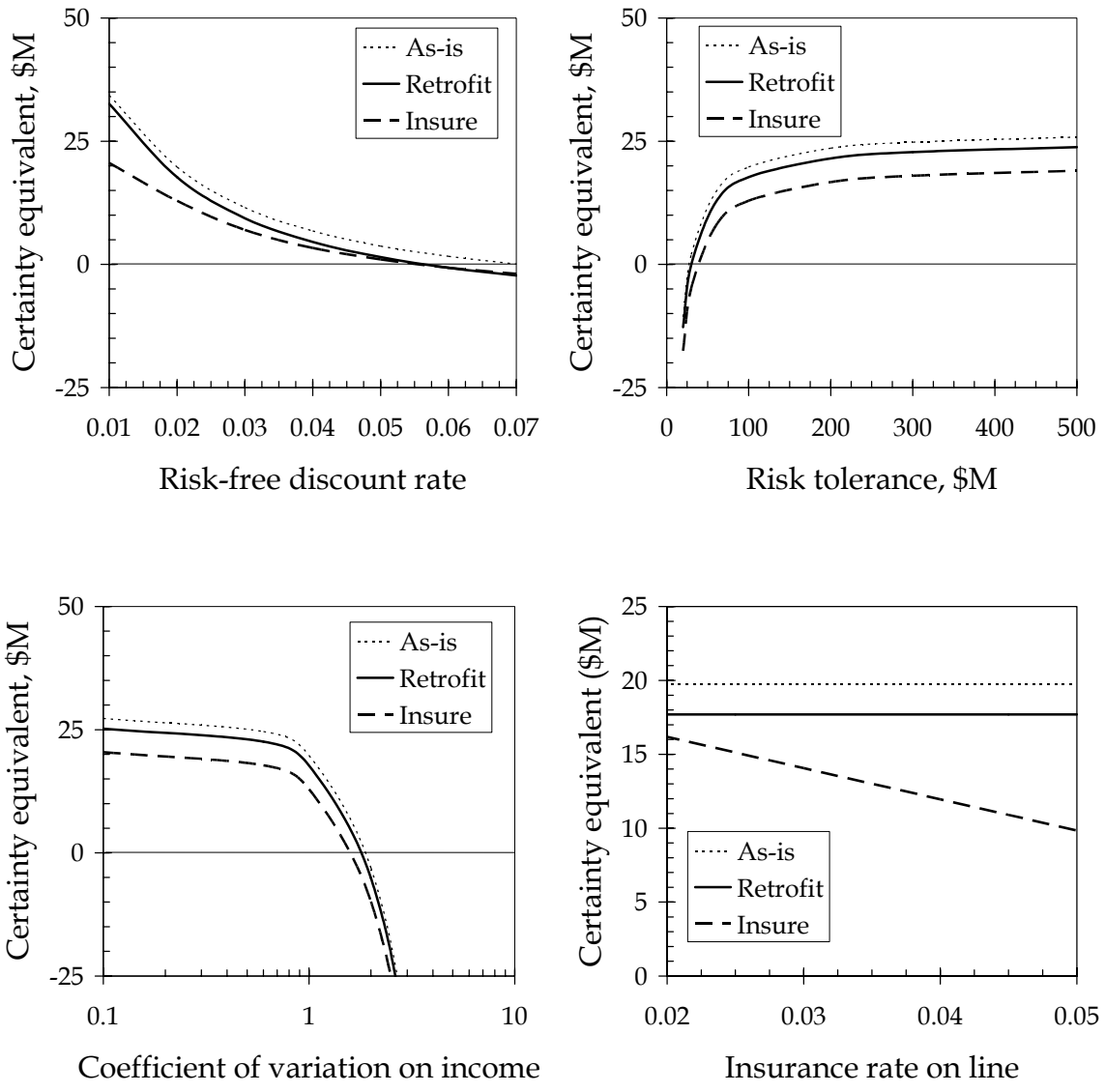

Figure 5-30. Sensitivity of CE to discount rate, risk tolerance.

Likewise, as shown in the upper right-hand chart of Figure 5-30, CE is highest for the as-is case for all except the lowest values of risk tolerance. For decision-makers whose risk tolerance is less than about $30M, the preferred alternative is not to buy (the CE for the do-not-buy alternative is zero, which exceeds that of as-is). This is important: the risk tolerance is a property of the buyer, not of the building or the site hazard. This means that the preferred decision can depend on who is making the decision. The most risk-averse decision-maker who might reasonably consider this property should pass on

it. Similarly, if the decision-maker believes the coefficient of variability of income is less than 2.0, he or she should buy and leave as-is; in excess of that value, the market risk is too great and the preferred alternative is not to buy.

Finally, the lower-right chart of Figure 5-30 shows that the preferred decision is not sensitive to insurance premium: under all values of rate on line, the preferred alternative is to buy and leave as-is. The reason is indirectly related to risk tolerance. Insurers must price insurance so that they make a profit on average, so insurance is desirable only where the insurance-buyer faces a significant probability of losses that are large compared with the buyer's risk tolerance. In the present situation, the earthquake risk is dwarfed by market risk. No decision-maker who can accept this level of market risk is going to be risk-averse enough to find earthquake insurance desirable, unless the earthquake insurance is actually priced less than the mean annualized earthquake loss, which will not happen if the insurance is properly priced.

Finally, it is interesting to examine the contribution to mean annual earthquake loss, $\overline{C}(1)$, from various levels of shaking intensity. That is, let $\overline{C}_{S_1}(1)$ denotes the mean earthquake loss over one year from earthquakes with $S_0 \le S \le S_1$, where S_0 = 0.1g. It is given by

$$\overline{C}_{S_1}(1) = \int_{S_0}^{S_1} E[C \mid S] g(S) dS \tag{5-12}$$

Comparing this equation and Equation 11, it is clear that $\overline{C}_{S_1}(1) \to \overline{C}_S(1)$ as $S_1 \to \infty$. Figure 5-31 shows the ratio $\overline{C}_{S_1}(1) / \overline{C}(1)$ as a function of spectral acceleration for the as-is, retrofitted, and insured buildings. The figure shows that approximately 50% of as-is loss is attributable to ground motion with $S_a \le 0.2$g, more than 75% of annualized as-is loss is attributable to ground motion with $S_a \le 0.3$g, and 90% is attributable to ground motion with $S_a \le 0.5$g.

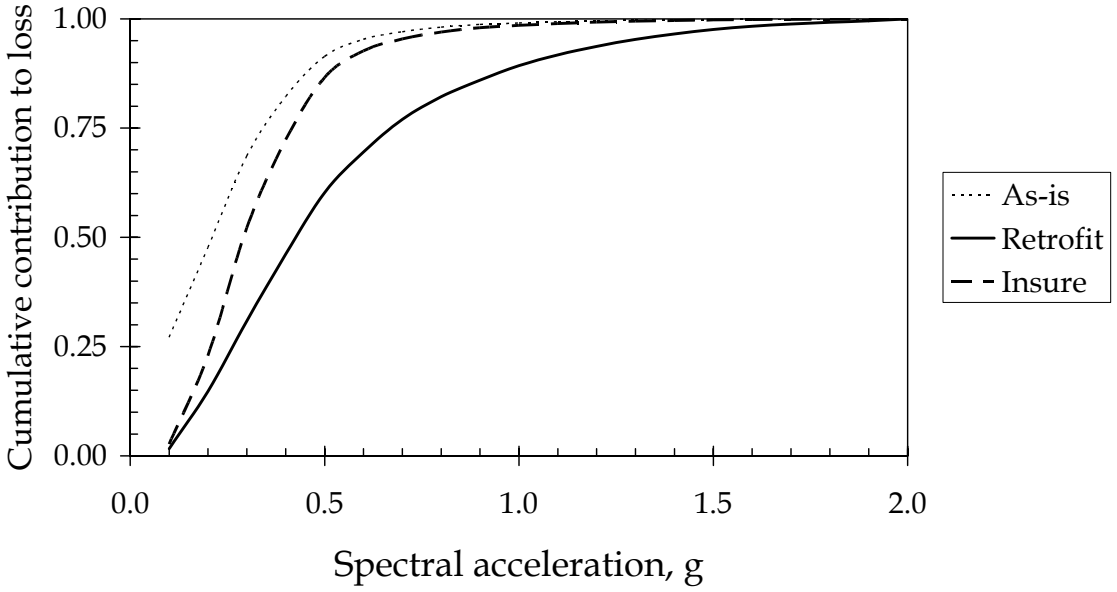

Figure 5-31. Contribution to mean annual loss from increasing S_a.

Two important conclusions can be drawn from this observation. First, note from Figure 5-18 that the mean damage factor of the as-is building evaluated at S_a = 0.1g is 3% and at S_a = 0.2g is 9%. Note also from Figure 5-5 that events with S_a = 0.1g have a mean annual occurrence frequency of 0.07, and the S_a = 0.2g event has a mean annual occurrence frequency of 0.02. This means that at least half of annualized loss for the as-is building is attributable to relatively frequent, modest shaking that produces light to moderate nonstructural damage, and very little structural damage. The loss in a large, rare event, which the probable maximum loss (PML) is intended to reflect, is irrelevant to the annualized loss (except as an ambiguous reflection of the general damageability of the building). As has been shown, only the annualized earthquake loss materially affects the CE of building. Since the PML is irrelevant to CE, it should not affect the investment decision. This agrees with practice: real-estate investors do not care about PML except insofar as it affects their ability to secure a commercial mortgage without earthquake insurance. Real-estate investors cannot use the PML in a typical financial analysis, *nor should they*.

The second conclusion is that there may be a scalar loss parameter that is more relevant to the investment decision than the PML. Again, half the annualized loss is

associated with shaking of S_a of 0.2g or less. (To be more precise, considering the discrete numerical integration performed here, half the annualized loss is associated with shaking severities of $0.05g \leq S_a \leq 0.25g$.). Referring to Figure 5-5, the mean frequency of this level of shaking is approximately 0.02 per year. So if earthquake risk for investment decisions is to be characterized by a single value of loss, that loss would be better expressed as the mean value associated with a more-frequent event, something like the shaking that is estimated to be exceeded once every 50 years, rather than the mean loss associated with 500-year shaking. Perhaps this more-useful level of loss could be referred to as the *probable frequent loss*, or PFL.

Let the PFL be defined as the mean loss conditioned on the occurrence of an earthquake whose shaking severity has 10% exceedance probability in 5 years. (For earthquakes modeled as Poisson arrivals, the PFL event would have a mean recurrence period of approximately 47 years, but "50-year shaking" is reasonable shorthand.) One definition of the PML is the mean loss conditioned on the occurrence of an earthquake whose shaking severity has 10% exceedance probability in 50 years. (The PML event thus has a mean recurrence period of approximately 500 years.) Thus, the PFL is identical to one definition of PML, except that it is associated with an earthquake that occurs ten times as often.

This definition of PFL appeals in four ways. First, it is a scalar value of loss associated with a scenario event, rather than some probabilistic average annualized value. Second, it closely resembles the familiar PML, which should make it readily understood by real-estate investors and readily assessed by engineering practitioners. Third, it uses a planning period (5 years) common to most real-estate investment decisions, and therefore again should resonate with real-estate investors. Lastly, if PFL can be used to estimate expected annualized loss, it could be directly employed in real-estate investment decision-making. This last topic is being explored in a companion study currently in development.

Chapter 6. Kajima Demonstration Buildings

6.1 SUMMARY OF KAJIMA DEMONSTRATION BUILDINGS

Three Japanese buildings, with different levels of earthquake resistance, were selected to demonstrate how the seismic performance of the buildings impacts property values. Building #1 is a nine-story, 388,000-sf, steel-reinforced-concrete building constructed in 1961, which was designed according to the 1950 building code. Building #2 is the same building as Building #1, but with structural upgrade to comply with the Seismic Rehabilitation Standard. Building #3 is a premier-class 29-story high-rise, 958,000-sf building. Buildings #1, #2 and #3 are presumed to have different seismic performance levels of low, medium, and very high, respectively. Table 6-1 and Table 6-2 show a summary of the demonstration buildings and their seismic performance levels. All three demonstration buildings are assumed to be located at the same site, in order to compare their property values including seismic risk.

Table 6-1. Summary of exposure data

	Building #1	**Building #2**	**Building #3**
Class	B	A	Premier
Seismic performance	Low	Medium	Very high
Year built	1961	1961	1999
Retrofit		1999	
Stories	9F/B3/P2	9F/B3/P2	29F/B4/P2
Use	Office	Office	Office
Floor area	388,000sf	388,000sf	958,000sf
Site area	38,000sf	38,000sf	81,000sf
Rentable area	269,000sf	269,000sf	667,000sf
Parking spaces	50	50	150
Construction	SRC	SRC	S
Replacement cost	US$73.0M	US$73.0M	US$254.0M
Retrofit cost		US$7.2M	

The semi-assembly based approach developed by Kajima is applied to construct customized vulnerability curves for three buildings based on design/construction details. The Kajima methodology consists of subdividing the building into components

and estimating the vulnerability of each component separately. The overall vulnerability of the structure is obtained by combining the vulnerability of all the components into a single weighted-average building vulnerability.

Table 6-2. Seismic performance levels of demonstration buildings

		Seismic Performance Level			
		Operational	Immediate Occupancy	Life Safety	Collapse Prevention
Earthquake Hazard Level	50%/50Year				
	20%/50Year				
	10%/50Year	Building #3		Building #2	Building #1
	2%/50Year				

6.1.1 Building site

Figure 6-1. Building site

The selected site is located in front of JR Tokyo railway station, one of the most prominent commercial areas in Japan. The site is situated at latitude 35° 40′ 29.93′′ N and longitude 139° 46′ 16.51′′ E (see Figure 6-1).

6.1.2 Building #1

Building #1 is a nine-story office building whose main structure is a steel-concrete composite structure, with encased truss frames comprising angles and steel plates, which was a common structural type for buildings of this size in the time period when it was built. The building is 56.4 m by 40.2 m in plan, which is essentially rectangular, and there are six bays in the longitudinal direction and five bays in the transverse direction (Figure 6-3).

The lateral load-carrying systems consist of moment-resisting frames with shear walls, both in the longitudinal and transverse directions. The building's foundations consist of cast-in-place reinforced concrete piles. Ninety-four benoto piles with diameters of 1,000mm are placed beneath perimeter columns, and twenty enlarged bottom bored piles, with shaft diameters of 2,000mm to 2,500mm and bell diameters of 4,000mm to 4,900mm, are placed beneath other columns. The bearing stratum is a sandy gravel layer that has 50-plus N-value (Standard Penetration Test), 25 m below the ground level. There is almost no configuration irregularity either in plan or elevation, and shear walls and braces are well-balanced at the center core without significant discontinuity in their vertical alignment.

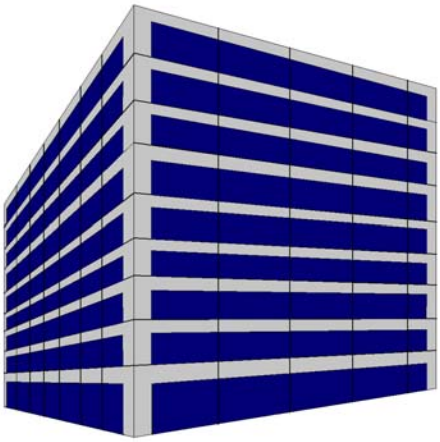

Figure 6-2. Building #1 façade

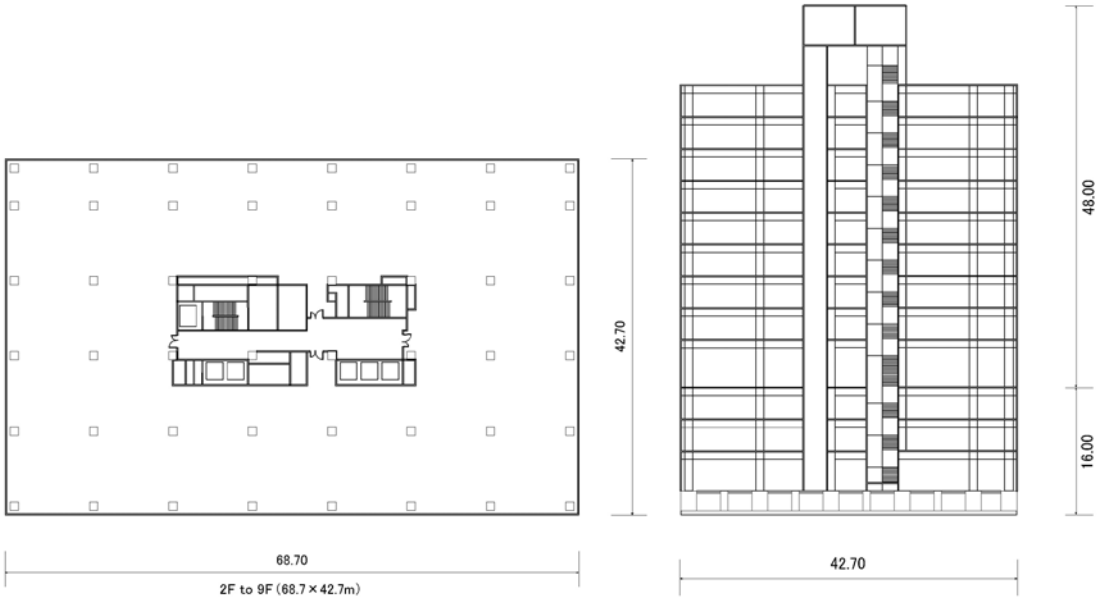

Figure 6-3. Building #1 typical floorplan (left) and elevation (right)

6.1.3 Building #2

Building #2 is the same building as the Building #1. However, it is structurally upgraded using a proposed steel-braced frame in order to reduce the potential loss to an acceptable range by improving the seismic performance without adversely impacting or losing the functions of the building as an office (see Figure 6-5). The conceptual retrofit is

also designed to meet the requirements of the Seismic Retrofit Promotion Law in Japan, which took effect in 1995.

It should be noted that, according to the Seismic Evaluation Standard, the earthquake-resisting performance of the structure should be such that:

- The occupancy functions of the building are maintained (Immediate-Occupancy Performance Level) in the event of small to medium-scale earthquakes that are frequently encountered during the life of the building, and

- Life safety from collapse of the building (Life-Safety Performance Level) is ensured in the event of a large-scale earthquake that could occur once in the life of the building, even if damage such as local cracking occurs in the structural and non-structural elements of the building.

The location of the reinforcement steel braces is shown in Figure 6-4 and Figure 6-5. The reinforcement steel braces are located at the openings in the perimeter walls in order not to adversely affect the functions or interfere with the floor layout as an office building. Figure 6-4 and Figure 6-5 show the building appearances with the steel braced frames added. The reinforcement steel braced frames would be installed at almost all the openings on the perimeter at levels 1 through 3, and at two bays from the 4th to the 7th and the 9th floor levels in the longitudinal direction, and at four bays at from the 4th to the 6th and two bays from the 7th to the 9th levels. The total number of the locations of the steel braced frame is 106.

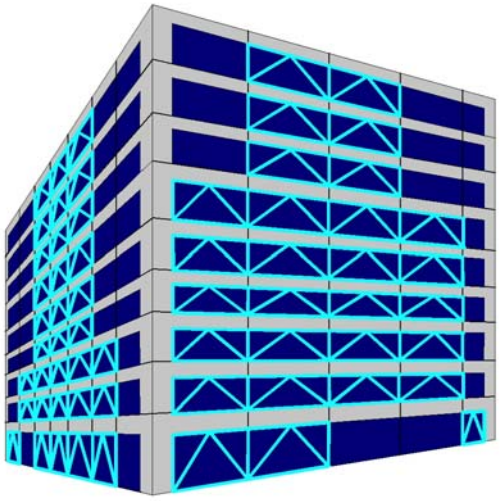

Figure 6-4. Building #2 facade

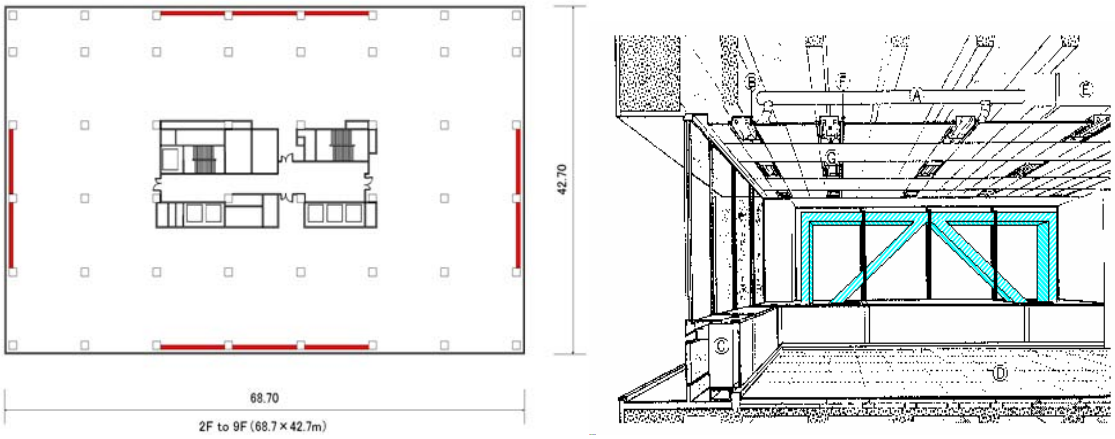

Figure 6-5. Building #2 brace layout (left) and interior view (right)

The estimated construction cost of the upgrade by adding steel braces is approximately US$7.2 million. It should be noted that there can be significant variations between the estimated cost and an actual construction cost, according to bids of individual contractors.

6.1.4 Building #3

Building #3 is a 29-story high-rise commercial complex with a four-level basement and a two-story penthouse (Figure 6-6). The superstructure consists of

moment-resisting steel frames with braces and concrete-filled steel tubes, while the substructure consists of moment-resisting reinforced-concrete/steel-encased reinforced-concrete frames with shear walls. The structural height of the building prescribed in the Building Standard Law of Japan is 147.0m, and the story heights on the ground and typical floors are 8.8m and 4.2m, respectively. The foundation system is mainly a monolithic mat foundation, borne by the bearing stratum 24.3 m below the ground level, which is made of fine sands/silts, whose N-value exceeds 50.

Since the structural height exceeds 60m and special structural materials/systems are employed, the structural design of the building has been conducted according to "the Methodology Approved by the Ministry of Construction," which includes non-linear dynamic response analyses using three different recorded ground motions (El Centro 1940NS, Taft 1952EW, and Hachinohe 1968NS) and an artificially-developed engineering ground motion (Art Wave 456) as a site-specific earthquake. The design criteria for the dynamic analyses are: the inter-story drift shall be less than 1/200 and the ductility factor shall be less than 1.0 for a Level 1 seismic input (earthquake with the maximum peak ground velocity of 30 cm/sec that may occur once or twice during the lifetime of the building); the inter-story drift shall be less than 1/100 and the ductility factor shall be less than 2.0 for a Level 2 seismic input (earthquake with the maximum peak ground velocity of 60 cm/sec that occurs with a very low probability during the lifetime of the building). Since those criteria are more severe than the common requirements by the High Rise Building Appraisal Committee, the seismic performance of the building appears to be higher than that of average high-rise buildings in Japan.

In plan, the building has a 47.2m-by-53.7m rectangular shape from the ground floor to the top floor (Figure 6-7). In spite of a slightly off-centered core, consisting of elevator shafts and staircases of each floor (Figure 6-7), adequate arrangement of lateral-load resisting elements prevents severe torsional response in a major seismic event. Furthermore, viscous-coupling seismic response control devices are installed in the core walls from the ground floor to the 22nd floor to reduce the seismic response.

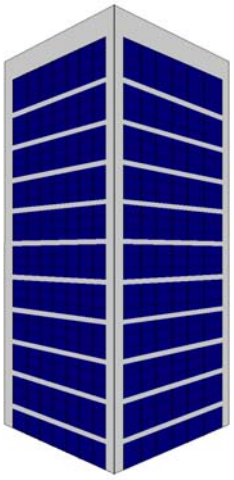

Figure 6-6. Building #3 facade

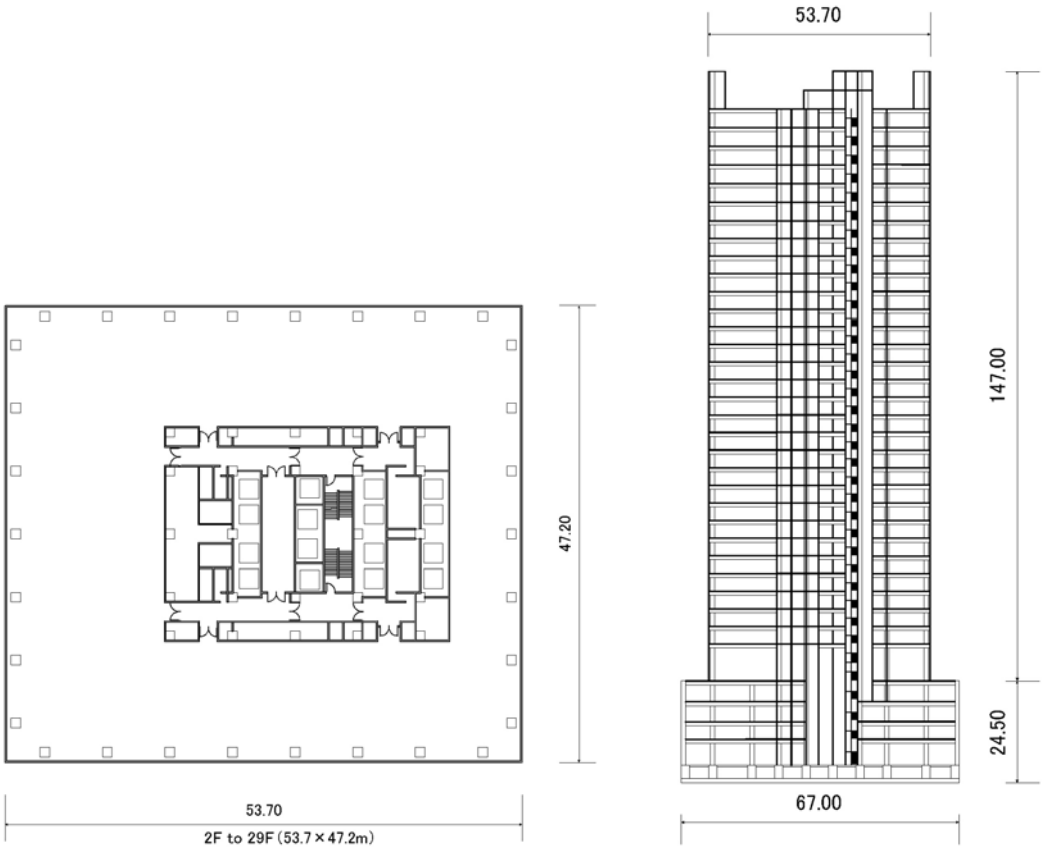

Figure 6-7. Building #3 typical floorplan (left) and elevation (right)

6.2 SEISMIC HAZARD ESTIMATION

6.2.1 Hazard model

There are no active faults with a high earthquake occurrence frequency around the center of Tokyo. The Kanto earthquake and the seismogenic zone for the background seismicity were considered as seismic sources for the seismic hazard analysis. The point of interest and the seismic sources are shown in Figure 6-8. The seismogenic zone model for the background seismicity is one of the seismogenic zones used for the seismic hazard estimation for Akasaka, Tokyo in the CUREE-Kajima project in 1994, as is shown in Figure 6-9. The 1994 model consists of 13 seismogenic zones, but it was found that the zone just beneath Tokyo used in this analysis determined the whole hazard. The zone modeled the interplate area between the North America plate and the Philippine Sea plate. The parameters of the two seismic sources are shown in Table 6-3 and Table 6-4. The attenuation equation by Takahashi et al. (1998) was used, and the logarithmic standard deviation was assumed to be 0.5.

Table 6-3. Parameters of the Kanto earthquake

Parameter	Used value	Note
Mean event interval	250years	seismological surveys
COV of event interval	0.23	average value in Japan
Elapsed time	77years	previous event in 1923
Magnitude of previous event	7.9	previous event in 1923
Mean slip rate	2.0cm/year	seismological surveys

Table 6-4. Parameters of the background seismicity

Parameter	Used value	Note
Size	80km×70km	
Depth	20km – 40km	interplate area
b value	0.968	data of 1885-1993
Upper-bound magnitude	7.5	
Annual frequency (M≧5)	1.19	data of 1885-1993

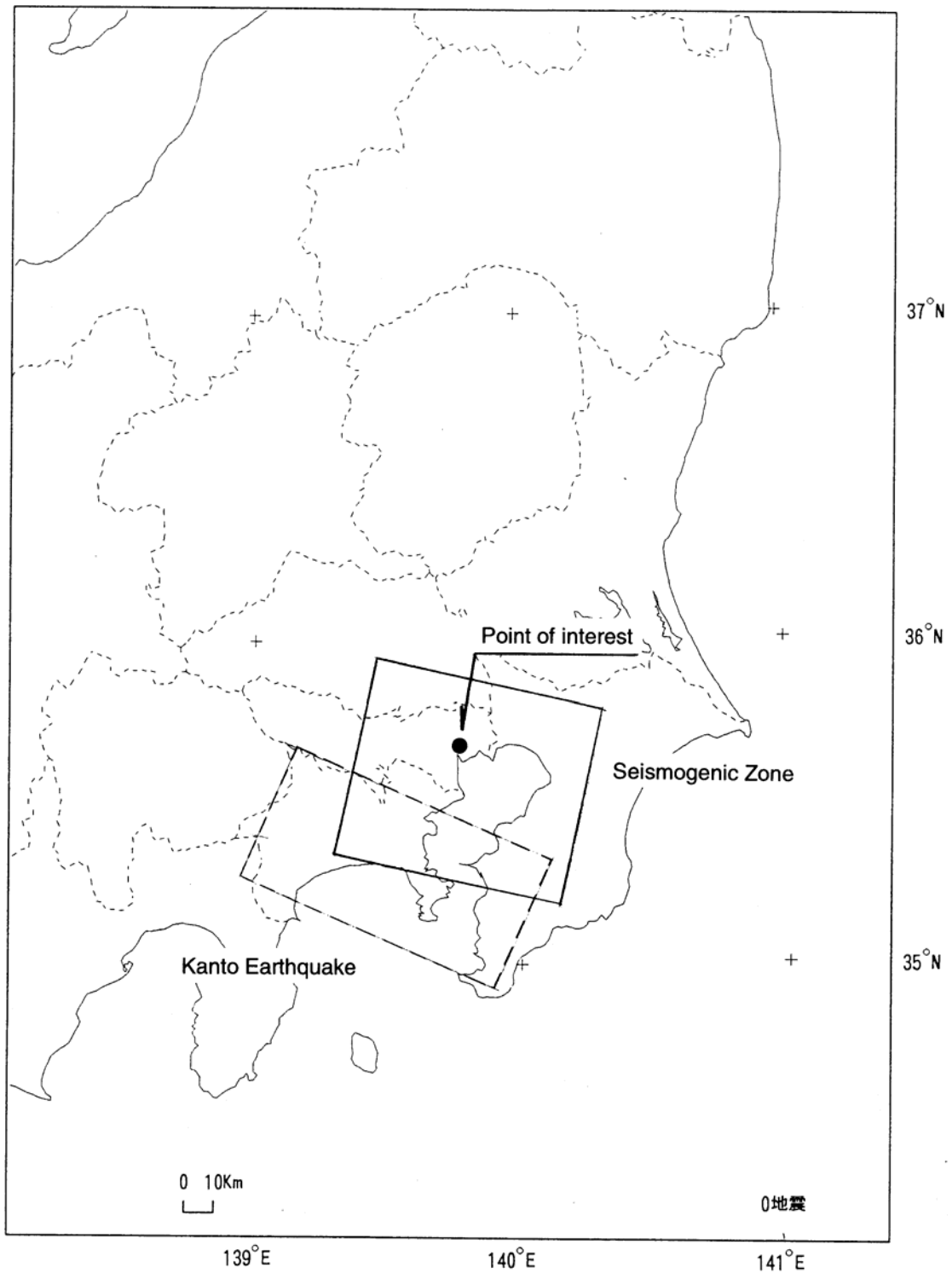

Figure 6-8. Seismic sources

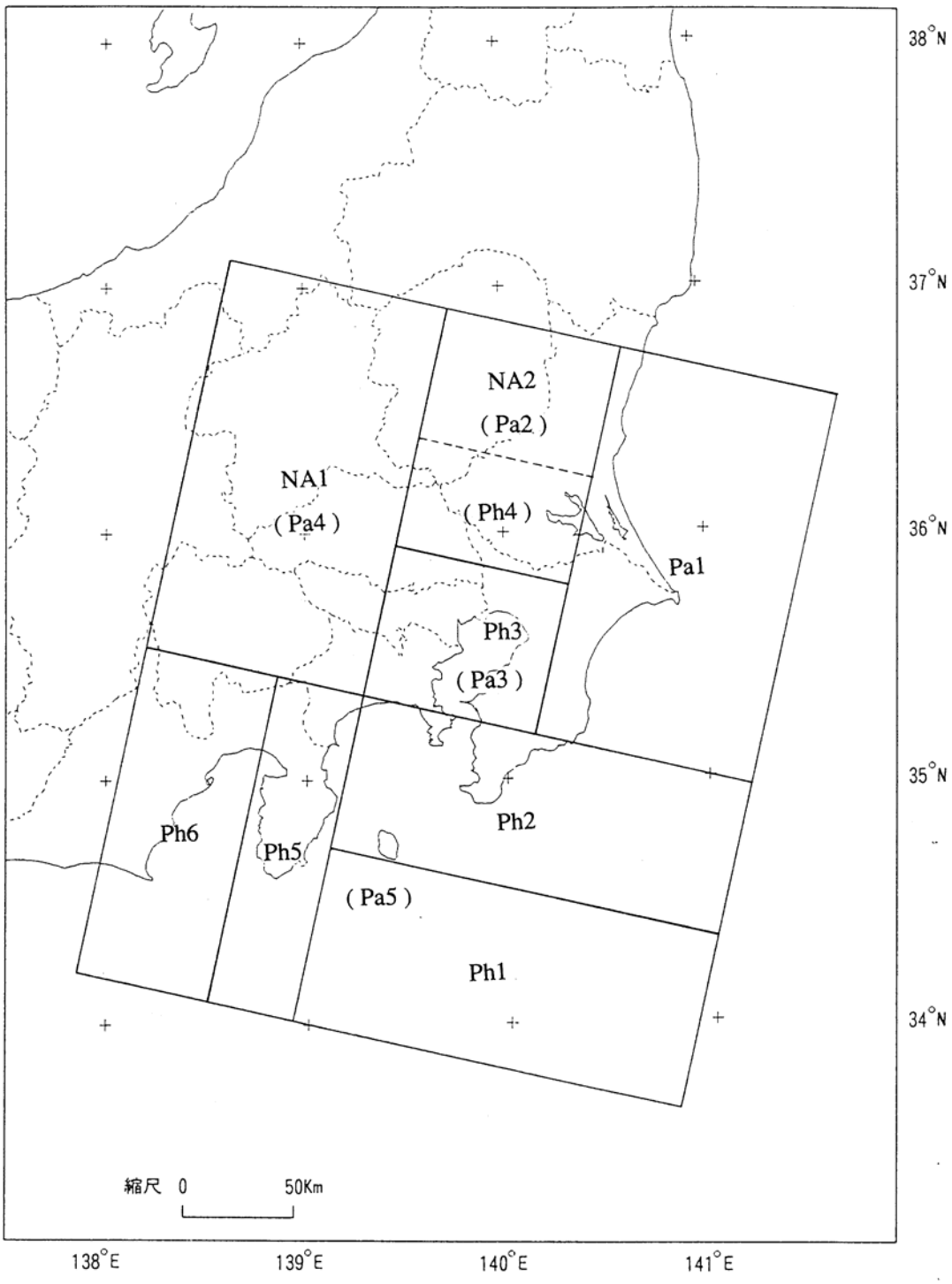

Figure 6-9. Seismogenic zone model for the CUREE-Kajima project in 1994

6.2.2 Seismic hazard curve at the subject site

Earthquake occurrence probabilities at elapsed times from the present are shown in Figure 6-10. It appears that the earthquake occurrence probability is very small in the next 50 years. The exceedance probabilities at the peak basement rock accelerations (PGAs) within the next 100 and 30 years are shown in Figure 6-11 and Figure 6-12. In these figures, the exceedance probabilities due to only the Kanto earthquake and only the background seismicity are also shown. Figure 6-11 shows that the exceedance probabilities at the PGAs lower than about 700 Gal are determined by the background seismicity, but those at other PGAs are determined by the Kanto Earthquake. However, it is seen from Figure 6-12 that the effect of the Kanto earthquake to the exceedance probability in the next 30 years is negligible.

Considering the above, the seismic hazard in the next 30 years is determined only by the background seismicity, which is assumed stationary. Therefore, the annual probability of exceedance for the peak ground acceleration shown in Figure 6-13 is constant, at least in the next 30 years.

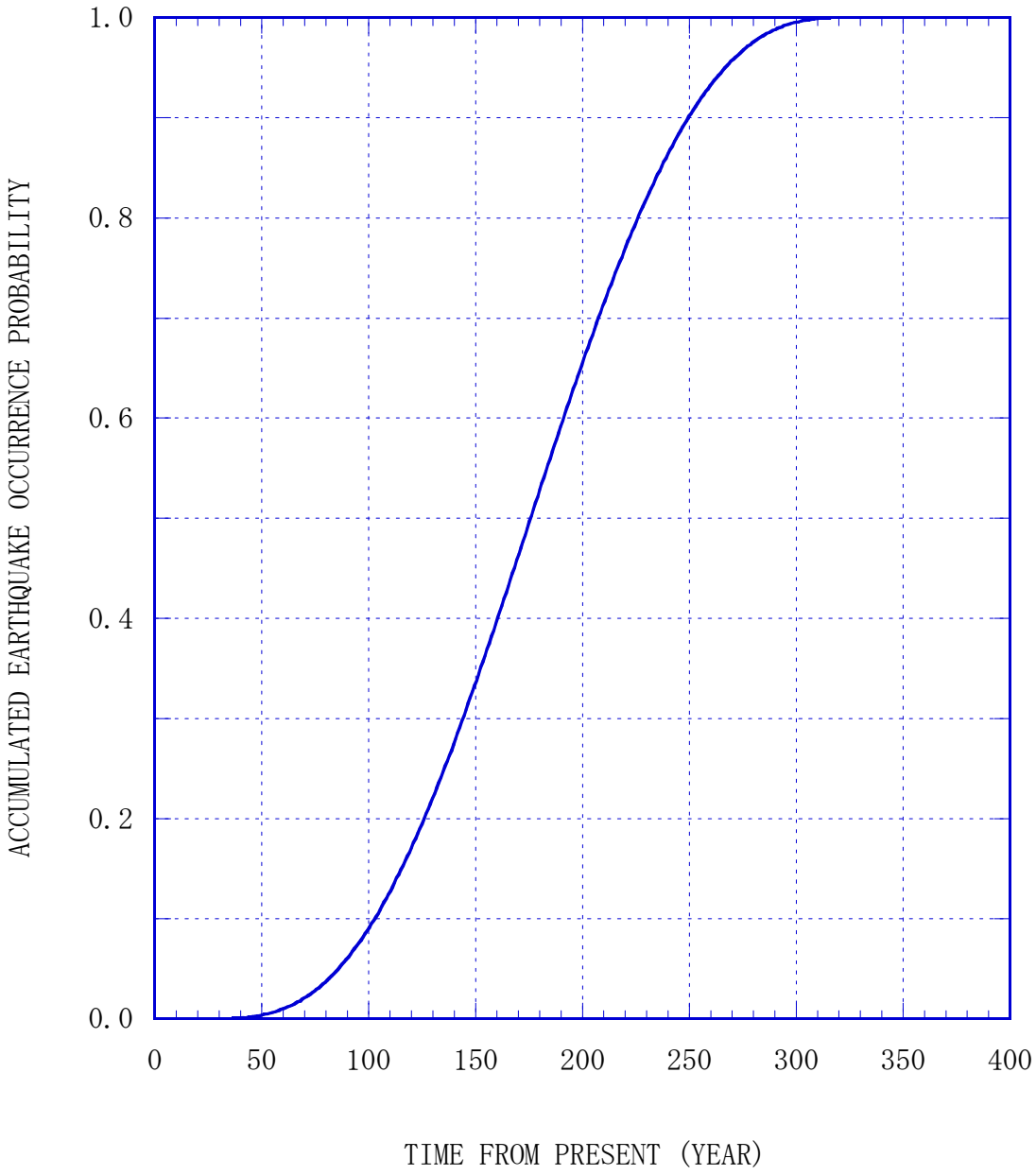

Figure 6-10. Accumulated earthquake occurrence probability of the Kanto earthquake

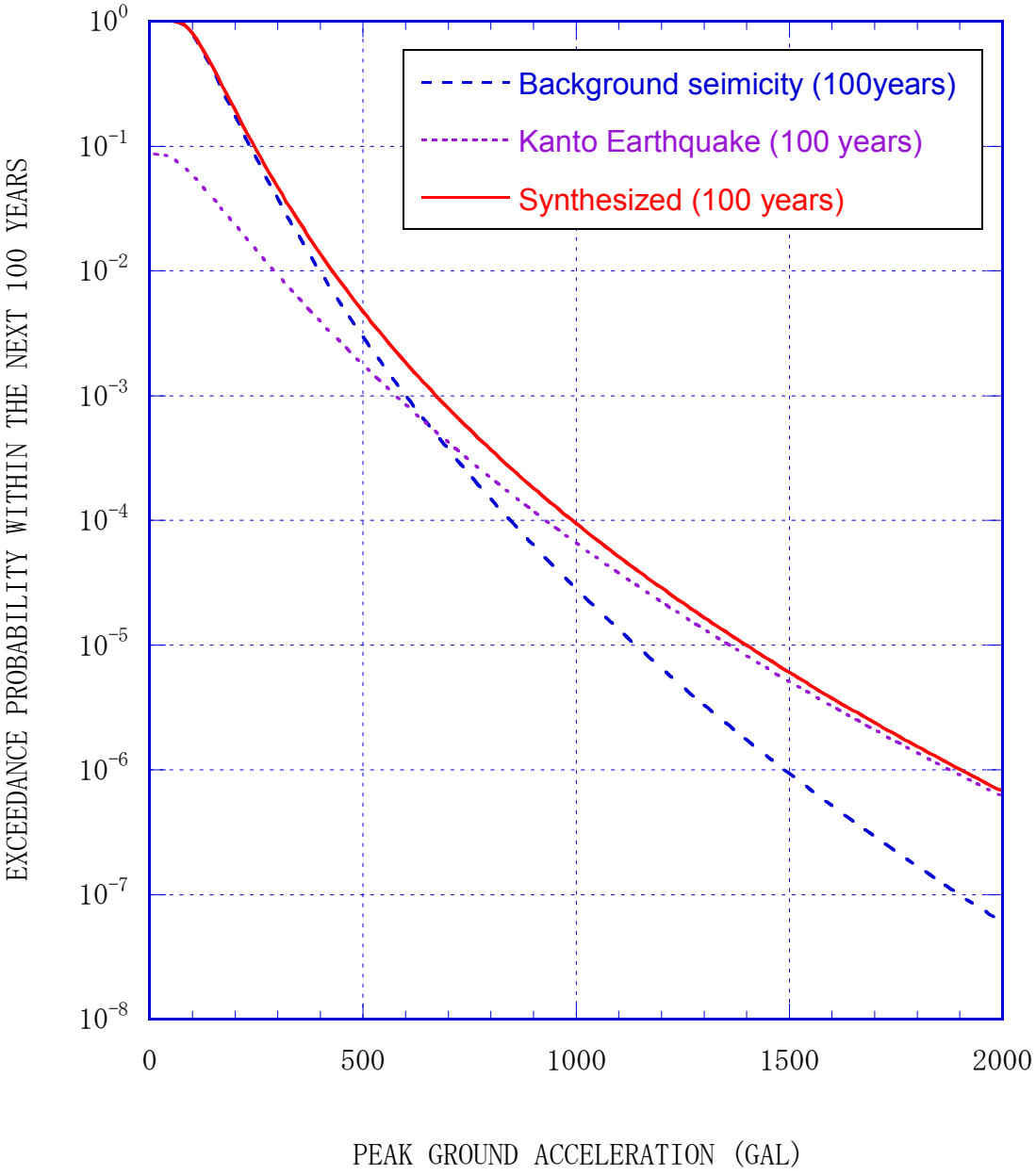

Figure 6-11. Seismic hazard curves for Tokyo within the next 100 years

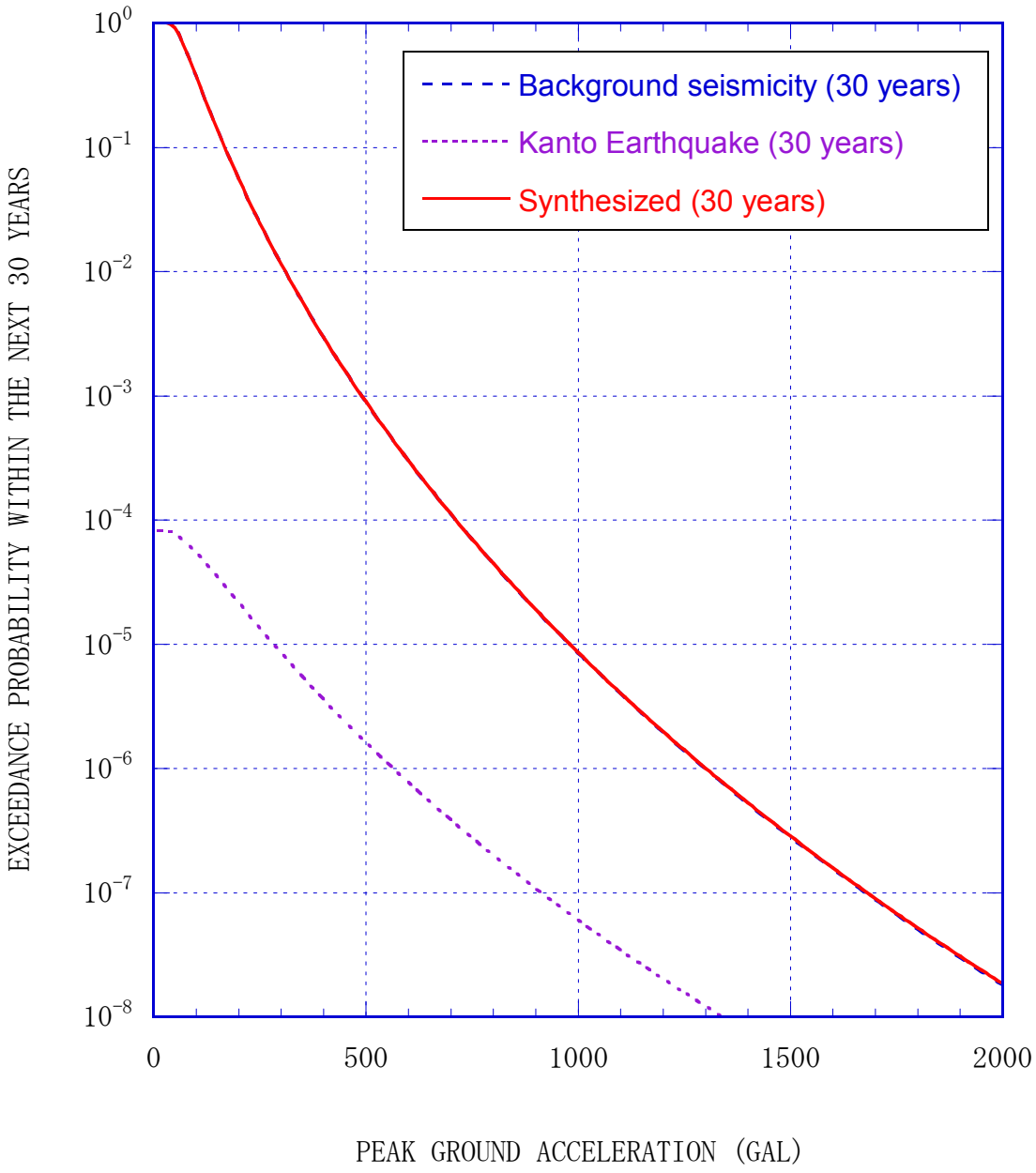

Figure 6-12. Seismic hazard curves for Tokyo within the next 30 years

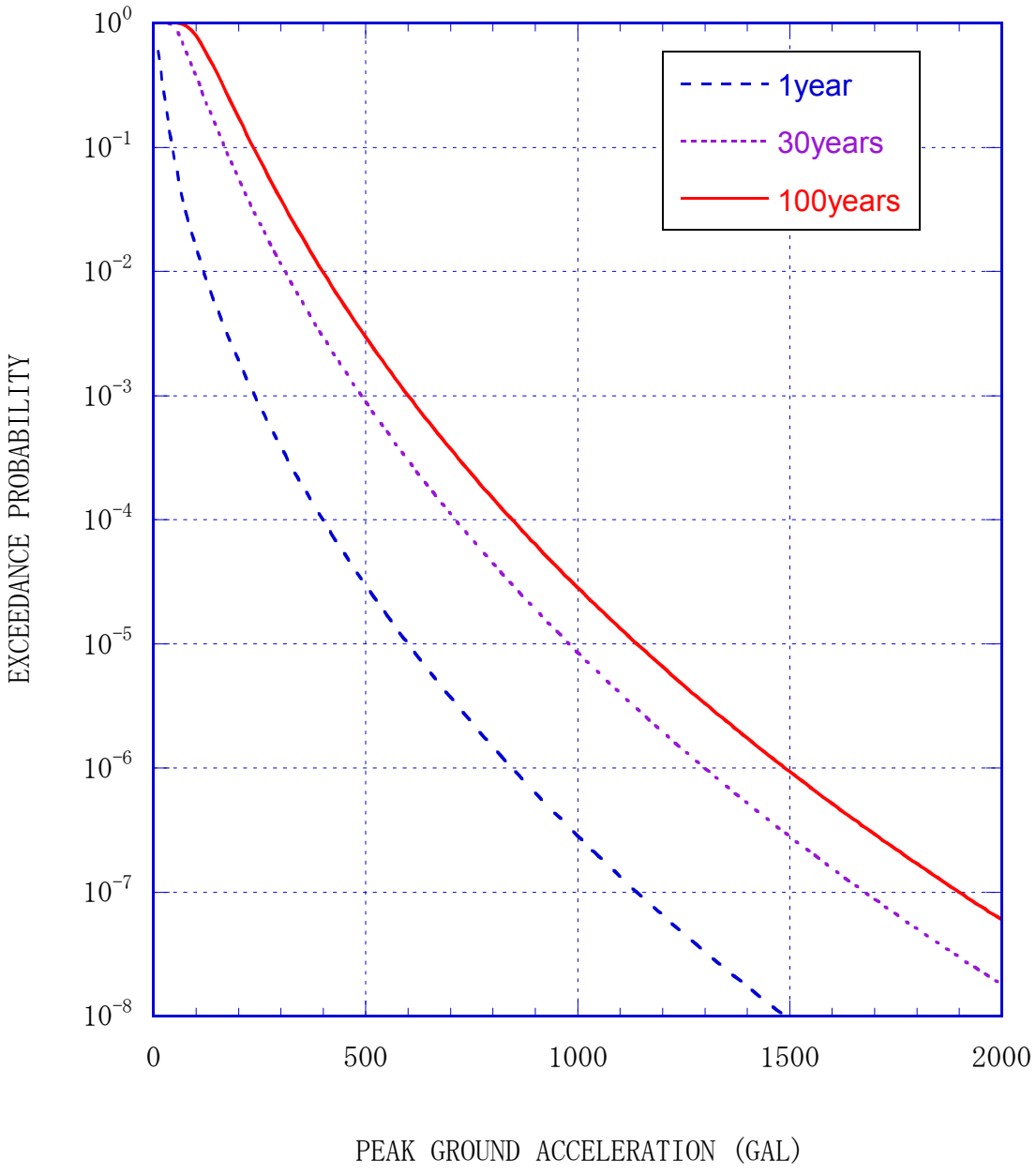

Figure 6-13. Seismic hazard curves for Tokyo due to the ground seismicity within the next 1, 30, and 100 years

6.3 KAJIMA SEISMIC-VULNERABILITY METHODOLOGIES

6.3.1 Overview of Kajima methodologies

There are three methodologies, Levels 1 to 3, for the Kajima vulnerability evaluation (Figure 6-14). The Level-1 method is similar to those found in ATC-13, ATC-21 or FEMA-178, in which damage matrices and a scoring system are used based on the building information such as construction type, the year designed, geologic conditions, structural characteristics, and building conditions. However, Level 1 is a preliminary screening procedure and it is not discussed in this report.

The Level-2 and Level-3 methodologies are semi-assembly based approaches, which consist of subdividing a building into components, estimating the response of these components for given ground motions, and estimating the vulnerability of each component separately. The overall vulnerability of the structure is obtained by combining the vulnerability of all the components into a single-value weighted building vulnerability.

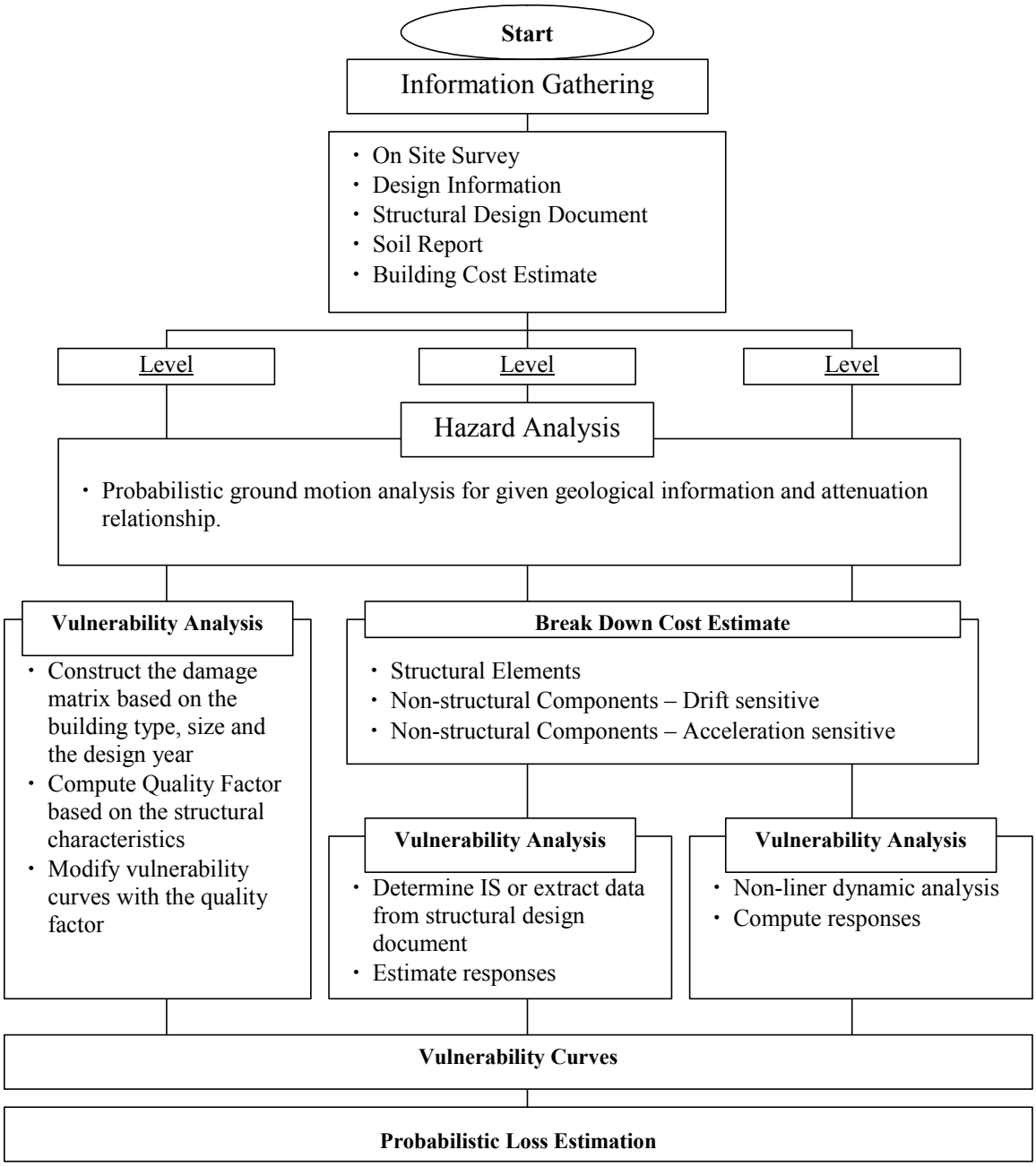

Figure 6-14. Kajima loss estimation overview

6.3.2 Level-2 method

The Level-2 method involves detailed seismic evaluation procedures in which the Is value (structural seismic index) is determined to represent the expected seismic performance of the buildings, which has been commonly used in Japan for years. The seismic evaluation concept was presented by Nakano and Okada (1989) based on

damage records of school buildings due to the Miyagikenoki and Tokachioki earthquakes. The Is concept was also studied based on damage records of the Hyogoken-Nanbu (Kobe) Earthquake by Fujiwara (1996). It should be noted that the seismic evaluation procedure discussed above was developed based on studies for reinforced-concrete buildings. In the methodology, the following parameters apply:

Is: Structural seismic index
Ct: Strength index
F: Ductility index
Sd: Shape index
T: Time index

They are calculated for a building, and then these indices are used to estimate the variation of the building response with respect to the ground motion.

6.3.2.1 Loss estimation for structural components

Based on a review of the work of Nakano and Okada (1989) and Fujiwara (1996), along with Kajima's study of the damage records of the Great Hanshin Earthquake, several structural components curves were derived based on construction materials (steel and reinforced concrete) and building age (construction time before and after 1981, when a major code amendment took place in Japan). The final base fragility curves were developed as shown in Figure 6-15, by using a weighted average of all the different curves.

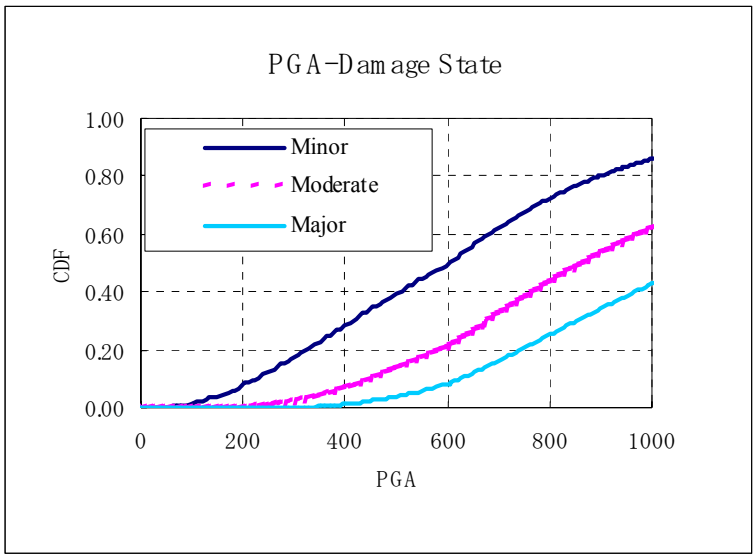

Figure 6-15. Kajima base fragility curves

Kajima also developed the base Is damage distribution functions with damage states according to a review of the study of Fujiwara (1996). In Figure 6-16, the Is distribution of the building stock is plotted according to Eq. 6-1 from Nakano and Okada (1989):

$$P_{IS}(x) = \frac{1}{\sqrt{2\pi\sigma}_y x} \exp\left\{-\frac{1}{2}\left(\frac{(y-\bar{y})}{\sigma_y}\right)^2\right\} \qquad (6\text{-}1)$$

where y = ln(x), $\bar{y}$ = –0.281, and σ_y = 0.499. The other three curves in Figure 6-16 are damage distribution functions with respect to each damage state in terms of Is value for given PGA of 600cm/sec^2, assuming the average peak ground acceleration in the areas studied after the Great Hanshin Earthquake is approximately 600cm/sec^2. All damage distribution functions are assumed to have a lognormal probability distribution.

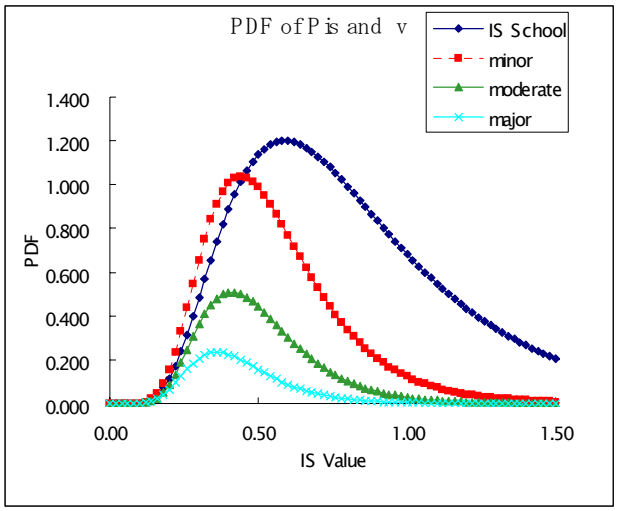

Figure 6-16. Damage distribution curves for given PGA of 600 cm/sec^2

Table 6-5. Base damage distributions in terms of Is index

	Damage State		
	Minor	**Moderate**	**Major**
$\bar{y}$	-0.64	-0.73	-0.87
σ_y	0.390	0.366	0.354

For reference, Figure 6-17 and Figure 6-18 show scatter plots of the Great Hanshin Earthquake damage data for four failure damage states. The parameters above were obtained by fitting lognormal distribution functions supplemented by engineering judgment.

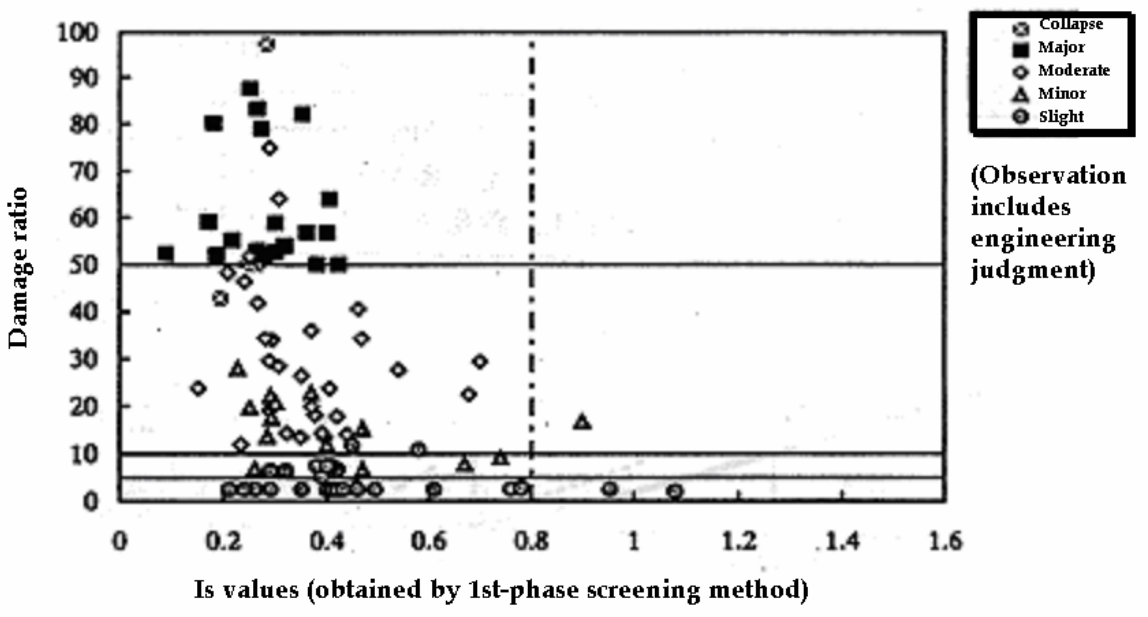

Figure 6-17. Damage ratio D vs Is (by the 1st-phase screening method)

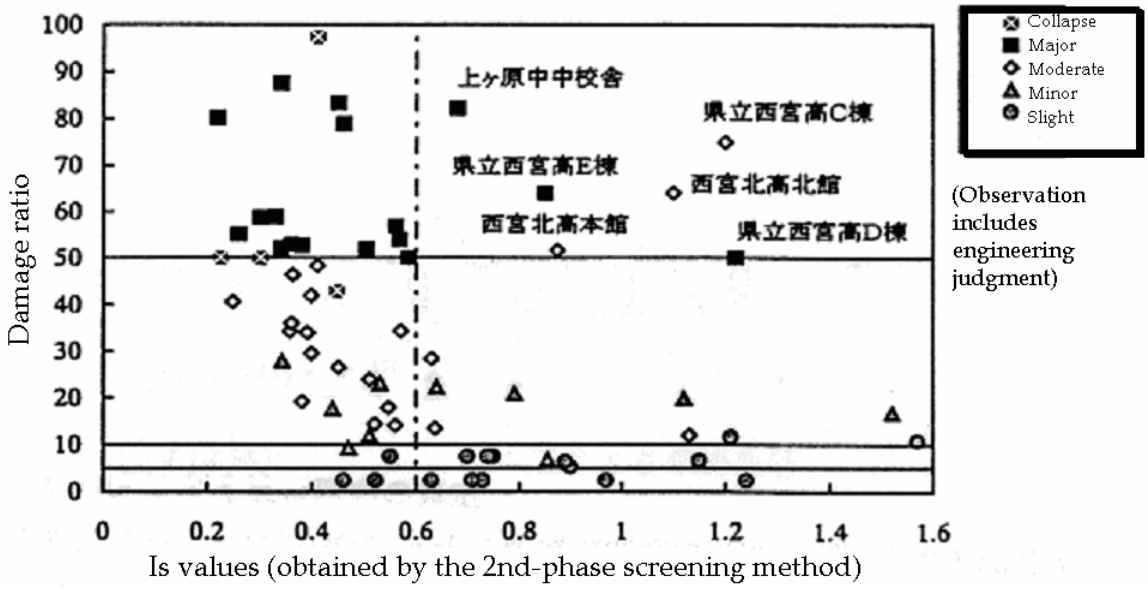

Figure 6-18. Damage ratio D vs Is (by the 2nd-phase screening method)

After obtaining the base fragility curves and base damage distribution functions with respect to damage states, a damage distribution function based on a given Is value and PGA, can be determined as follows. A probability that the damage of a building with Is=x would exceed the damage state F when a earthquake with PGA = a occurs is:

$$P(F \mid Is = x, A = a) = P(F \mid x, a) = \frac{P(x \mid F, a) \cdot P(F \mid a)}{P_{IS}(x)} \tag{6-2}$$

where

$P_{Is}(x)$: Is distribution function of the building stock

$P(x \mid F,a)$: Is distribution function with the damage exceeding the damage state F for given PGA of a.

$P(F \mid a)$: The probability that the building damage exceeds the damage state F for given PGA of a.

For an earthquake of PGA = 600 cm/sec^2, $P(x \mid F,a)$ is given using the parameters in Table 6-5. As PGA approaches a_u (the PGA of an ultimate earthquake), the Is distribution and damage distribution functions become identical. Thus, for $a=a_u$:

$$\begin{aligned} &P(F \mid a_u) = 1 \\ &P(x \mid x, a_u) = P_{IS}(x) \end{aligned} \tag{6-3}$$

In order to estimate Is damage distributions, linear interpolation is applied to determine the mean and standard deviation of $P(F \mid a)$. Accordingly, for the moderate damage distribution function, as the PGA changes from 600 cm/sec^2 to a_u, $P(F \mid a)$ changes from 0.210 to 1, the lognormal mean $\bar{y}(a)$ changes from -0.73 to –0.281 and the standard deviation σ_y changes from 0.366 to 0.499 :

$$\begin{aligned} \bar{y}(a) &= \bar{y}(600) + \frac{\bar{y}(a_u) - \bar{y}(600)}{1 - P(F \mid 600)} \{(P(F \mid a) - P(F \mid 600)\} \\ \sigma_y(a) &= \sigma_y(600) + \frac{\sigma_y(a_u) - \sigma_y(600)}{1 - P(F \mid 600)} \{(P(F \mid a) - P(F \mid 600)\} \end{aligned} \tag{6-4}$$

where $P(F \mid a)$ is the value obtained from Figure 6-15 and :

$$P(F \mid 600) = 0.210$$
$$\bar{y}(600) = -0.73, \bar{y}(a_u) = -0.281$$
$$\sigma_y(600) = 0.366, \sigma_y(a_u) = 0.499$$

Based on the damage distribution functions that are obtained, a mean damage factor can be determined with damage ratios for each damage state. Kajima assigned the damage ratios of 5%, 15%, and 45%, to the minor, moderate, and major damages, respectively, based on a literature review and expert opinion:

$$\begin{aligned} MDF(x) = &\{P_{IS}(x) - P(F_1 \mid x, A)\} \cdot D_0 + \{P(F_1 \mid x, A) - P(F_2 \mid x, A)\} \cdot D_1 \\ &- \{P(F_2 \mid x, A) - P(F_3 \mid x, A)\} \cdot D_2 - \{P(F_3 \mid X, A)\} \cdot D_3 \end{aligned} \quad (6\text{-}5)$$

F_1, F_2, F_3: Damage States (Minor, Moderate, Major)

D_0=2.5%, D_1=10%, D_3=30%, D_4=75%

Figure 6-19 shows an illustration of the development of the mean damage functions. Using the base fragility curves at the top, the damage distribution functions can be obtained using Eq. 6-4 for PGAs of 200cm/sec^2, 400 cm/sec^2, and 600 cm/sec^2, as shown in the middle three diagrams. Then, looking at the point of Is=0.7, the three points of the damage ratios for each PGA are determined using Eq. 6-5. Similarly, we can derive the mean damage factors for any Is value.

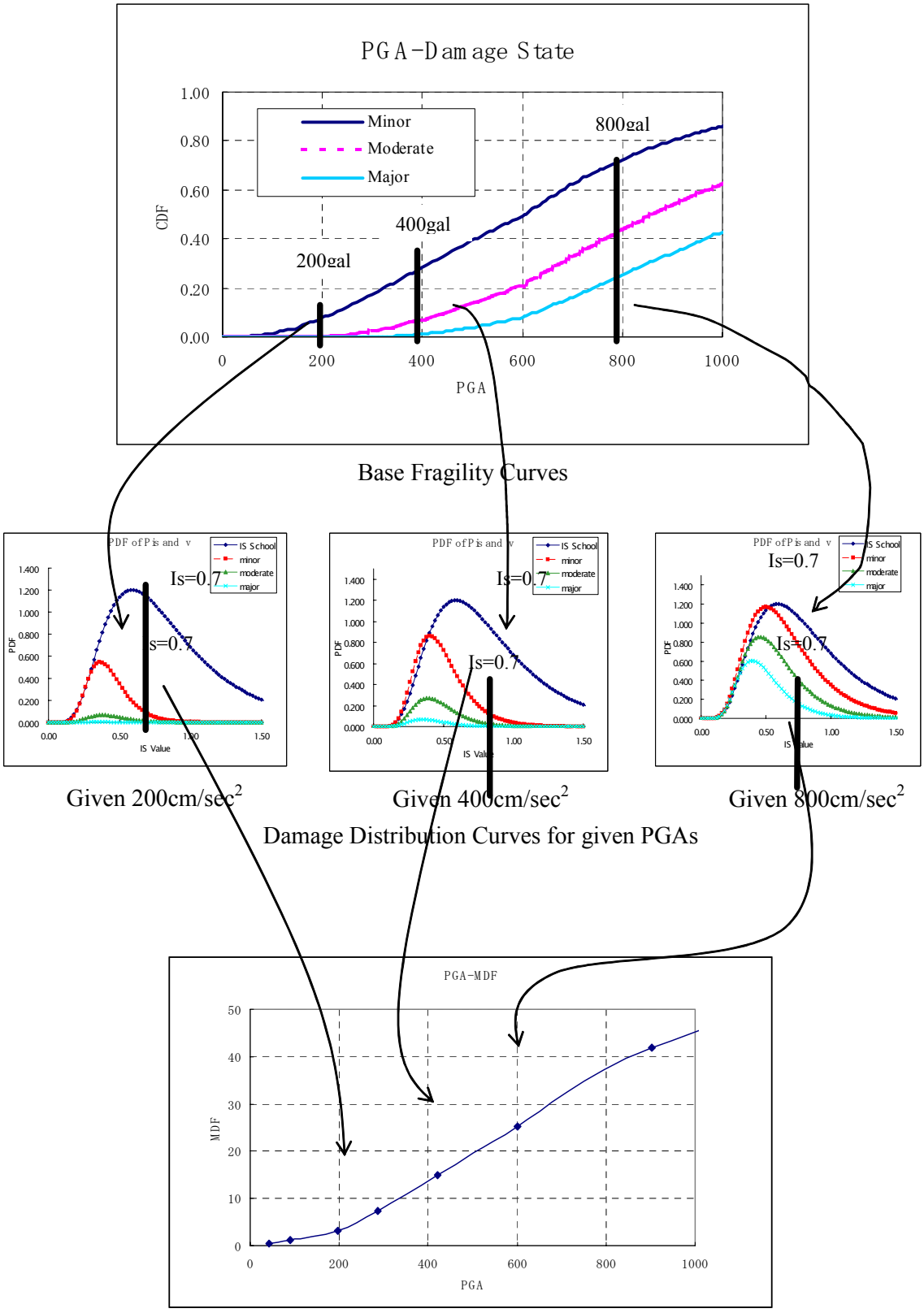

Figure 6-19. Illustration of procedure to develop mean damage functions

6.3.2.2 Loss estimation for non-structural components

Based on the various indices that are determined in the process to derive the seismic index Is of the building, inter-story drifts and the peak accelerations at each floor level may be estimated.

The inter-story drift at each floor of the building is estimated by following the seismic evaluation guideline procedure. Conceptually, the seismic performance of the building, or its Is index, is expressed as a product of the strength index Ct and the ductility index F as illustrated in Figure 6-20. Even if two buildings have the same value of Is, one building could have high strength and low ductility, and the other could have low strength and high ductility. Then, a parameter F' is computed as a function of Is, Is_{req}, and F by using Eqs. 6-6 and 6-7, where Is_{req} refers to Is=0.6 with a PGA of 230 cm/sec^2 in the guideline procedure (see Figure 6-19); it is the Is value necessary to have a 97% chance of not exceeding moderate damage (approximately 15%) for given earthquakes.

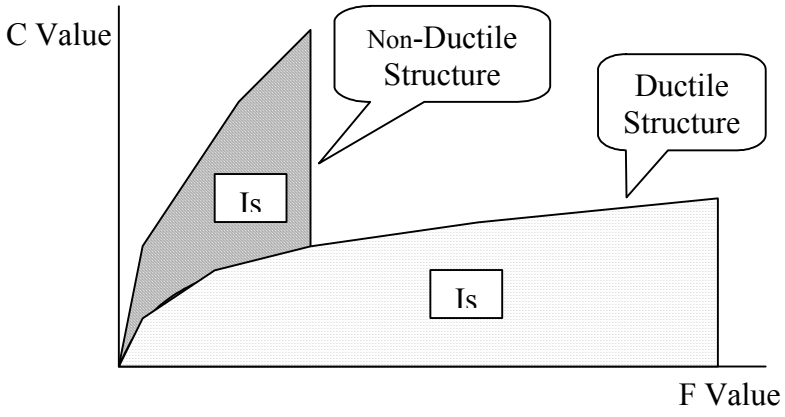

Figure 6-20. Is index associated with C and F

$$Is_{req} = LognormalInverse(97\%, y, \sigma_y)$$
$$y = 0.399 \times \frac{PGA}{230}, \sigma_y = 0.2107 \quad (6\text{-}6)$$

$$F' = \begin{cases} F \times \left(\dfrac{Is_{req}}{Is} \right)^{\sqrt{F}} & for \quad Is \geq Is_{req} \\ F + \left(\dfrac{Is_{req} - Is}{CtSdT} \right) & for \quad Is \leq Is_{req} \end{cases} \tag{6-7}$$

The inter-story drift can then be obtained by using the drift vs. F′ relation shown in Figure 6-21, which is given by the guideline procedure.

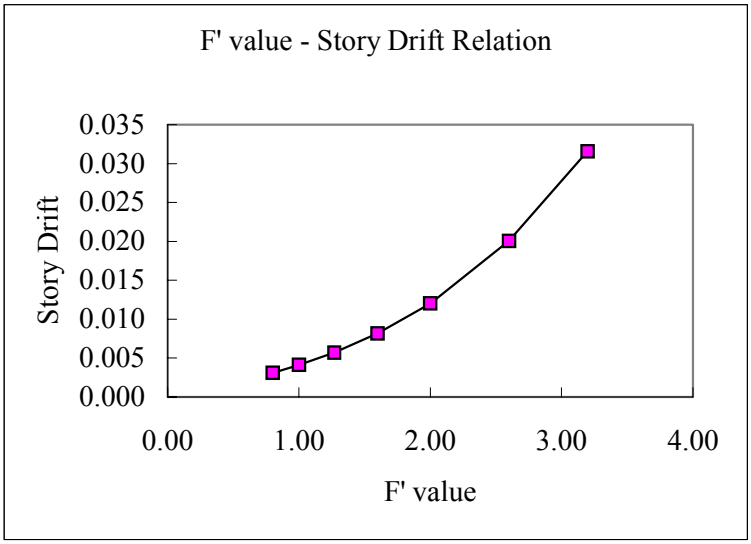

Figure 6-21. Inter-story drift vs. F′ value

It is assumed that the value provided by the guideline procedure represents 90% of the response and that the median response can be derived by assuming a log normal distribution with given coefficient of variation.

The acceleration at each floor of the building is estimated following the modified building code procedure for floor amplifications. The floor amplification factor AiRt is

$$AiRt = \left\{ 1 + 0.5 \times \left(\frac{1}{\sqrt{a_i}} - a_i \right) \times \frac{2T}{1 + 3T'} \right\} \times Rt \tag{6-8}$$

where

$$T' = T \times \left(\frac{Ctave}{0.6} \right)^{0.25}$$ T: the fundamental natural period by the building code.

a_i: ratio of the weight above the i^{th} story to the weight of the building above ground.

Rt: the design spectral coefficient, which is determined by the type of soil profile Tc (0.4 for hard soil, 0.6 for medium soil, and 0.8 for soft soil) as follows:

$$Rt = \begin{cases} 1 & for \quad T' < Tc \\ 1 - 0.2\left(\frac{T'}{Tc} - 1 \right)^2 & for \quad Tc < T \le 2Tc \\ \frac{1.6Tc}{T'} & for \quad 2Tc \le T' \end{cases} \qquad (6\text{-}9)$$

It is assumed that the value provided by the modified code procedure represents the median response and that the 90% response can be derived assuming a log normal distribution with given coefficient of variation. An additional amplification factor of 1.25 is introduced to reflect the amplification of the component itself. Vulnerability curves of acceleration sensitive components have been developed based on the damage records from the Great Hanshin Earthquake, and they are discussed later in section 6.3.2.

The damage ratios for both drift-sensitive and acceleration-sensitive components are estimated by floor and by component type. The total damage ratio for all the components of the building is obtained by calculating a weighted-average of all the component values.

6.3.3 Level-3 method

The Level-2 method using the Is index was developed for low-rise to medium-rise reinforced-concrete buildings. The Level-3 method is preferable for steel buildings and for high-rise buildings including steel and RC. The Level-3 method uses the results

of a non-linear dynamic analysis with several recorded and artificial earthquakes that is commonly used in the structural design procedure for high-rise buildings in Japan, known as the Methodology Approved by the Minister of Construction.

In this method, rather than estimating structural responses by running a large number of dynamic analyses, a linear interpolation is adopted to estimate responses based on the response results for two levels of earthquakes that usually correspond to peak ground velocities of 25 cm/sec and 50 cm/sec. Also, tables of coefficients of variation are developed to treat response uncertainty based on literature reviews and empirical data.

In the analysis, the assumption is made that the response quantities are 100 percent correlated. The uncertainty associated with the component vulnerability curves is ignored and only the mean vulnerability curves are used to estimate component damage. This reduces the uncertainty associated with damage by ignoring extreme occurrences while leaving the mean value unchanged.

6.3.3.1 Loss estimation for structural components

The assumption is made that at the ultimate limit, the mean damage ratio (MDR) is 15%, while MDR is 0% at the elastic limit for steel buildings and at the one third of the elastic limit for RC buildings. Linear interpolation and extrapolation are used to obtain the value of MDR at other levels of ground motion.

6.3.3.2 Loss estimation for non-structural components

The inter-story drift and the peak acceleration at each floor level are estimated by using linear interpolation and extrapolation of the results of the response analyses. The estimated acceleration and story drift are assumed to be the median values, and the 90% responses are derived as in the Level-2 method. A component amplification factor of 1.25 is also introduced.

6.3.3.3 Development of vulnerability functions for non-structural components

The Kajima method estimates damage to structural and non-structural components separately. Actually, buildings are subdivided into three types of components: structural components, drift-sensitive components, and acceleration–sensitive components, as shown in Table 6-6. The total building value is broken down into each component type on a floor-by-floor basis and the vulnerability is determined for each floor and each type of component. The overall vulnerability of the building is obtained by a weighted accumulated value of the component vulnerability calculated at each floor.

Table 6-6. Classes of building component

Structural	Drift-Sensitive	Acceleration–Sensitive
Columns Beams Shear walls	Exterior wall panels Cladding Piping Glass Ornamentation	Mechanical and electrical equipment Suspended ceiling Elevators

Vulnerability functions for non-structural elements are developed based on a literature review and on damage records from the Great Hanshin Earthquake. Most of the information is from published papers, journals, specifications or design guidelines of mechanical societies or equipment suppliers, and also from Kajima's records of repair work carried out after the Great Hanshin Earthquake. However, it should be noted that the development of the vulnerability functions for the non-structural components relies heavily on expert opinions and code requirements because of the following reasons:

- Since damage of non-structural elements was repaired or removed immediately after the earthquake by building owners, it was difficult to obtain reliable data.
- There are many failure types, such as overturning, sliding, failure of anchorage, cracks, deformation, loss of function of equipment itself and damage due to other structural or non-structural elements.

- Repair costs vary according to repair techniques and availability of contractors or materials.

- The definitions of damage state vary depending on the types of equipment and individuals making the judgments.

The non-structural components were classified into 53 subclasses according to the types of equipment, construction methods, and sometimes the sequences used to construct mechanical systems. For example, ALC boards are classified into 5 classes based on the types of anchorage, such as slide method, cover plate method, rocking method, bolt method, or conventional re-bar anchorage. However, because it is not practical to breakdown components into 53 subclasses all of the time, it was decided that architectural components should be grouped into eleven classes, and mechanical components should be re-grouped into five classes, as shown in Table 6-7.

Table 6-7. Classes of nonstructural component

Architectural	Mechanical, electrical, and plumbing
Drift-Sensitive	Acceleration-Sensitive
1. Glass with putty	1. General equipment (electric transformer, HVAC, pump, tank etc.)
2. Concrete/plaster/stone/ceramic tile	2. Control panel
3. Concrete brick/glass brick	3. Suspended equipment (lighting, sprinkler, AC, etc.)
4. ALC/PC (inflexible)	4. Piping/lighting
5. Gypsum board/partition wall	5. Elevator/mechanical parking
6. Partition wall/door/shutter	
7. ALC/PC (flexible)	
8. Curtain walls (PC, metal)	
Acceleration-Sensitive	
9. Suspended ceiling /signboard/emergency staircase	
10.Raised floor	
11.Roof and floor finishing	

The 41 subclasses were re-grouped into five classes according to the equipment types associated with various failure types. Five damage states represented the level of damage from 0% to 100%. Since the specific location of the equipment was not known in

the damage database, the most probable locations of the equipment were guessed in order to estimate the acceleration amplification.

In addition, the specific PGA at the buildings was not known, so the range of the possible PGA values was determined based on the JMA intensity of the area in which each building existed. This resulted in giving a range of equipment acceleration for each damage state. The lower and upper limits of the range were assumed to be the 10% and 90% of the acceleration distribution felt by the equipment. Figure 6-22 and Figure 6-23 show plotted data and fitted curves of general equipment and control panels respectively.

The five subclasses of mechanical components were then broken down and re-composed into four groups of mechanical systems using a weighted average; these groups are electrical, piping, HVAC equipment and elevator. Figure 6-24 shows vulnerability functions for the four mechanical systems.

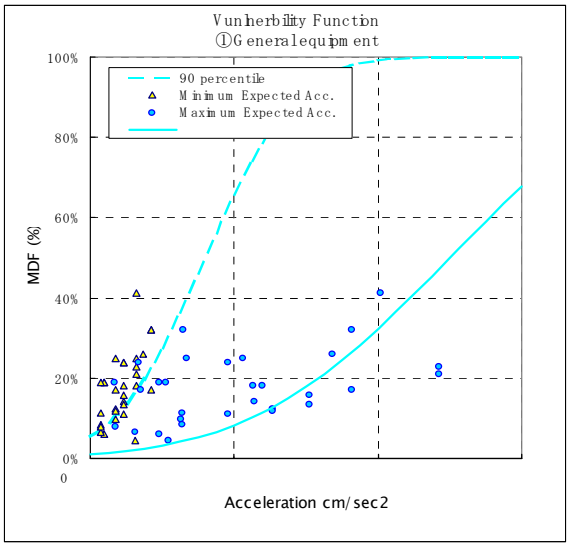

Figure 6-22. General equipment vulnerability function

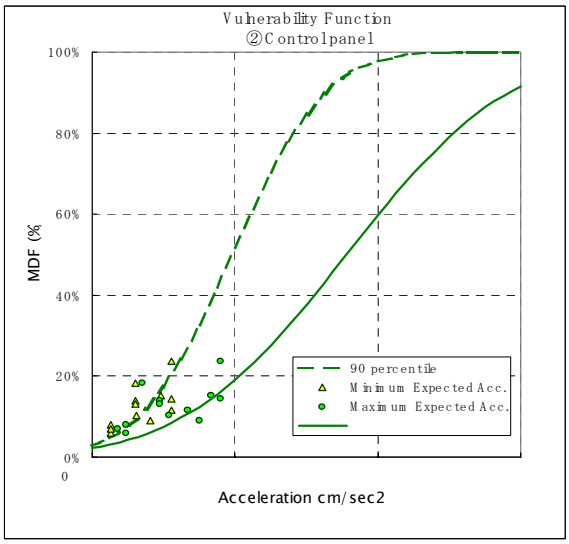

Figure 6-23. Vulnerability function of control panels

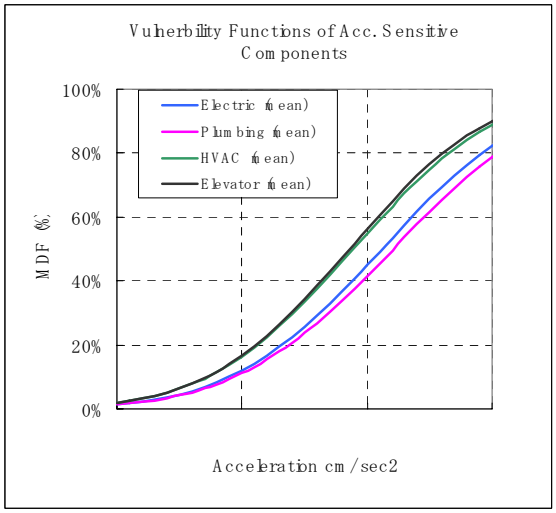

Figure 6-24. Vulnerability functions of mechanical systems

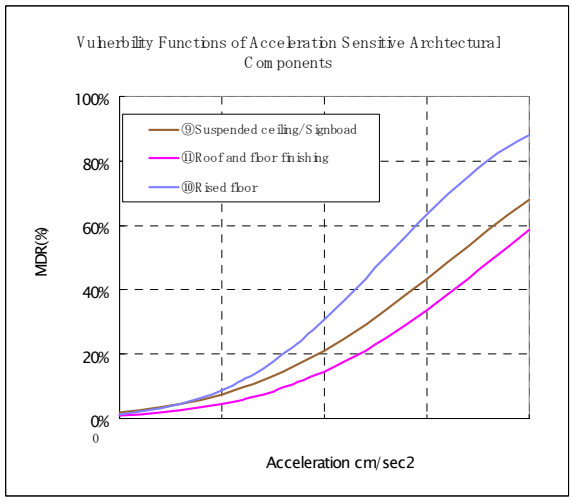

Figure 6-25. Vulnerability functions of acceleration-sensitive architectural components

The vulnerability curves for drift-sensitive components were developed based on experimental data and code design requirements. Figure 6-26 and Figure 6-27 show plots of the data and the 10th percentile and 90th percentile vulnerability functions for concrete walls and curtain walls, respectively. Mean damage functions of eight subclasses are shown in Figure 6-28.

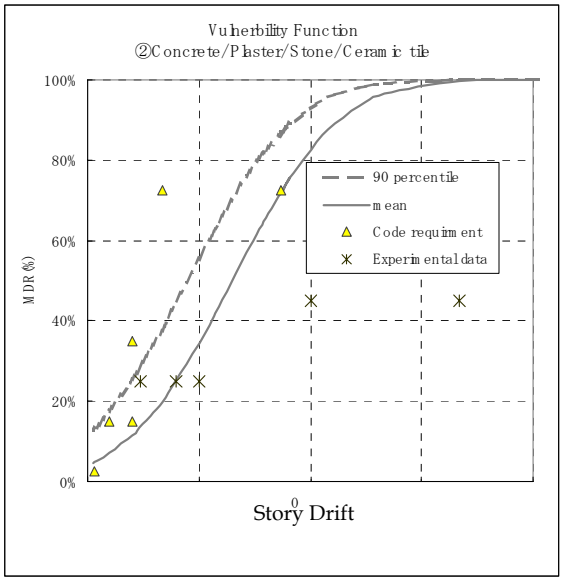

Figure 6-26. Vulnerability functions of concrete/plaster/stone/ceramic tile

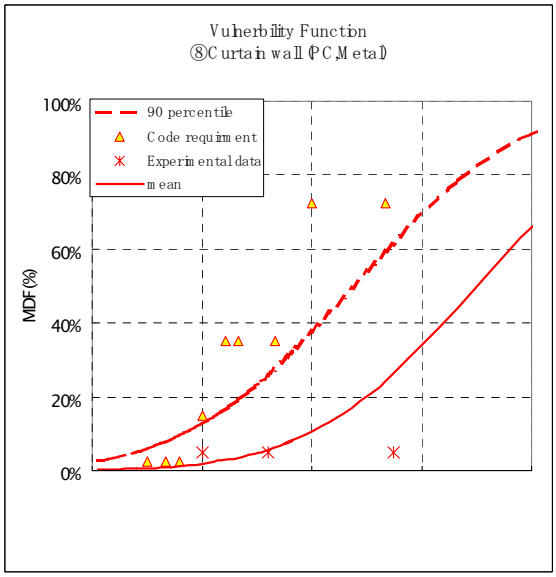

Figure 6-27. Vulnerability functions of curtain wall (PC, metal)

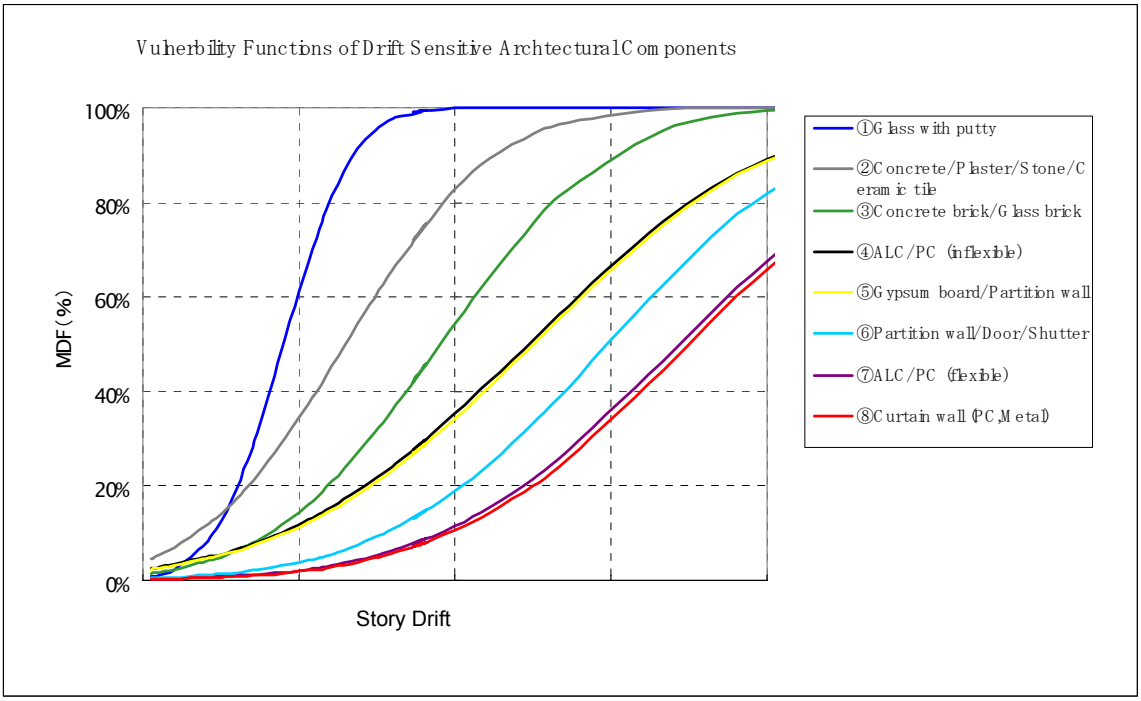

Figure 6-28. Vulnerability functions of drift sensitive architectural components

Then, eight subclasses were re-grouped into four classes (Interior flexible, interior rigid, exterior flexible and exterior rigid), as shown in Figure 6-29.

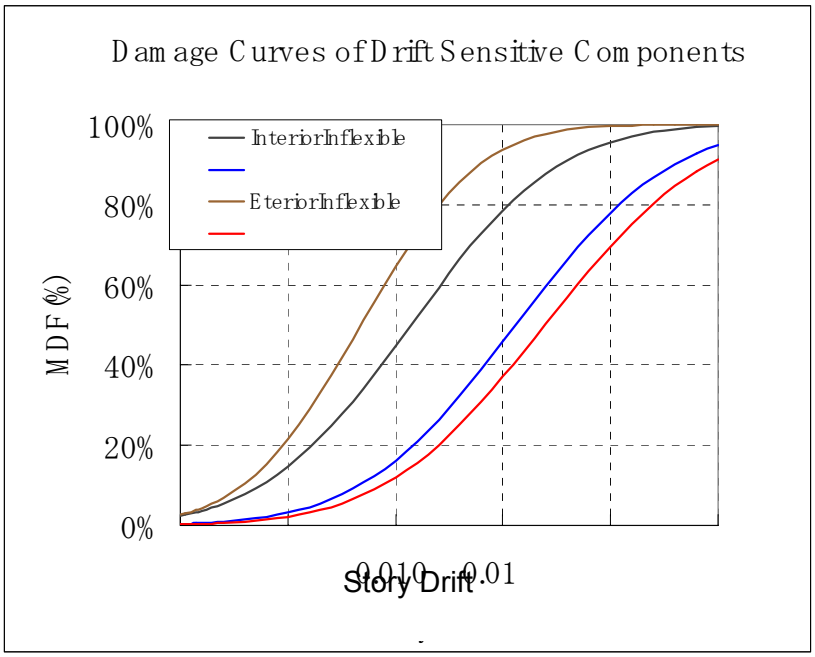

Figure 6-29. Vulnerability functions of re-grouped drift sensitive components

6.4 SEISMIC VULNERABILITY FUNCTIONS

6.4.1 Buildings #1 and #2

Building #1 is a nine story, 38,800 sf, steel reinforced-concrete building constructed in 1961, which was designed according to the 1950 building code. Building #2 is the same building as the Building #1, but it is structurally upgraded to comply with the Seismic Rehabilitation Standard.

Since the subject building is a mid-rise steel reinforced composite structure, the Level-2 method is used for its seismic assessment. First of all, the building is broken down into types of construction work as shown in Table 6-8. Then, these values are associated with component vulnerability functions on a floor-by-floor basis, as shown in Table 6-9.

Table 6-8. Cost breakdown of Buildings #1 and #2

Item	US $	Value/sf	%
Temporary Work	6,216,286	16.0	8.5%
Excavation	5,790,837	14.9	7.9%
Piles	0	0.0	0.0%
Structure	16,663,429	42.9	22.8%
Exterior	6,854,460	17.7	9.4%
Interior	9,572,608	24.7	13.1%
Landscaping	437,267	1.1	0.6%
Other		0.0	0.0%
Sub Subtotal	45,534,887	117	62.4%
Electrical	11,380,767	29.3	15.6%
Sanitary	3,557,228	9.2	4.9%
HVAC	11,321,677	29.2	15.5%
Elevator	1,205,440	3.1	1.7%
Machine Parking		0.0	0.0%
Other Equipment		0.0	0.0%
Sub Subtotal	27,465,113	71	37.6%
Total	73,000,000	188	100.0%

Table 6-9. Value of above-ground components in percent

		Acceleration-sensitive				Displacement- sensitive	
Story	Structural	Electric	Plumbing	HVAC	Ceiling	Exterior	Interior
9	1.98	2.6	0.74	3.34	0.26	1.12	0.43
8	1.98	1.3	0.74	1.67	0.26	1.12	0.43
7	1.98	1.3	0.74	1.67	0.26	1.12	0.43
6	1.98	1.3	0.74	1.67	0.26	1.12	0.43
5	1.98	1.3	0.74	1.67	0.26	1.12	0.43
4	1.98	1.3	0.74	1.67	0.26	1.12	0.43
3	1.98	1.3	0.74	1.67	0.26	1.12	0.43
2	1.98	1.3	0.74	1.67	0.26	1.12	0.43
1	1.98	1.3	0.74	1.67	0.26	1.12	0.43

Secondly, structural responses are estimated based on Is indices. The Is indices of the buildings that are obtained are shown in Figure 6-30. As a reference, the required Is values at PGAs of 200, 400, and 600 cm/sec^2 are plotted in the same diagram. The Is

values are improved by the structural upgrade, as shown in Tables 6-10 and 6-11 with the related indices.

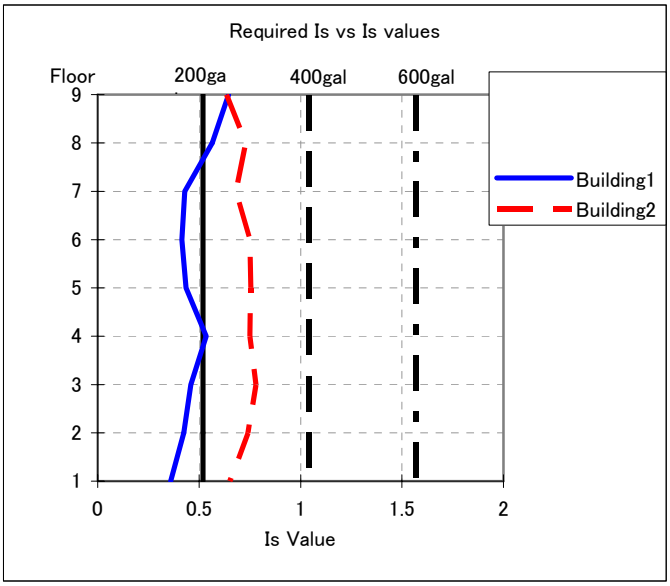

Figure 6-30. Is values of buildings #1 and #2

Table 6-10. Seismic indices of Building #1

Floor	Seismic Index IS		Strength Index Ct		Ductility Index F	
	X	Y	X	Y	X	Y
9	0.81	0.48	0.83	0.49	1.00	1.00
8	0.71	0.42	0.73	0.43	1.00	1.00
7	0.52	0.34	0.54	0.35	1.00	1.00
6	0.49	0.34	0.50	0.35	1.00	1.00
5	0.49	0.38	0.42	0.39	1.20	1.00
4	0.58	0.49	0.42	0.42	1.41	1.19
3	0.52	0.40	0.38	0.38	1.41	1.08
2	0.45	0.40	0.38	0.38	1.23	1.07
1	0.41	0.31	0.42	0.42	1.00	0.75

Shape Index Sd=1.08
Time Index T=1.00

Table 6-11. Seismic indices of Building #2

Floor	Seismic Index IS		Strength Index Ct		Ductility Index F	
	X	Y	X	Y	X	Y
9	0.81	0.48	0.83	0.49	1.00	1.00
8	0.78	0.68	0.80	0.70	1.00	1.00
7	0.75	0.61	0.77	0.62	1.00	1.02
6	0.69	0.81	0.71	0.75	1.00	1.11
5	0.78	0.73	0.73	0.62	1.20	1.21
4	0.77	0.73	0.68	0.57	1.41	1.32
3	0.83	0.73	0.71	0.60	1.41	1.25
2	0.78	0.70	0.69	0.58	1.23	1.24
1	0.69	0.61	0.71	0.57	1.00	1.11

Shape Index Sd=1.08
Time Index T=1.00

Using Eqs. 6-7 to 6-8, story-drifts and floor accelerations responses for various peak ground acceleration are estimated on a floor-by-floor basis. The 50th-percentile responses are shown in Figure 6-31 and Figure 6-32.

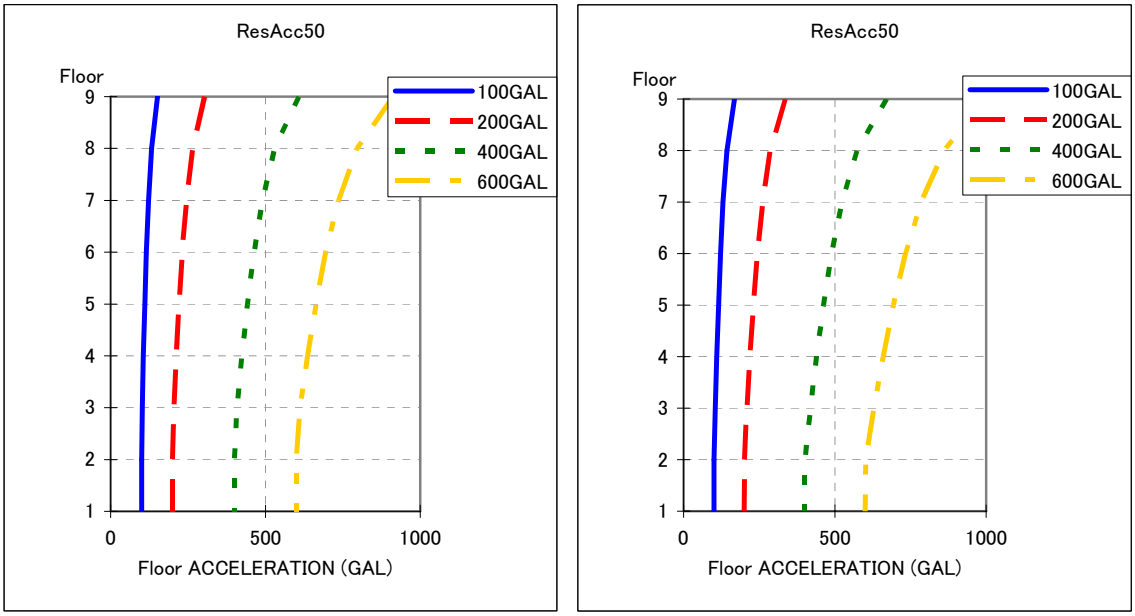

Figure 6-31. Estimated floor responses for Buildings #1 (left) and #2 (right)

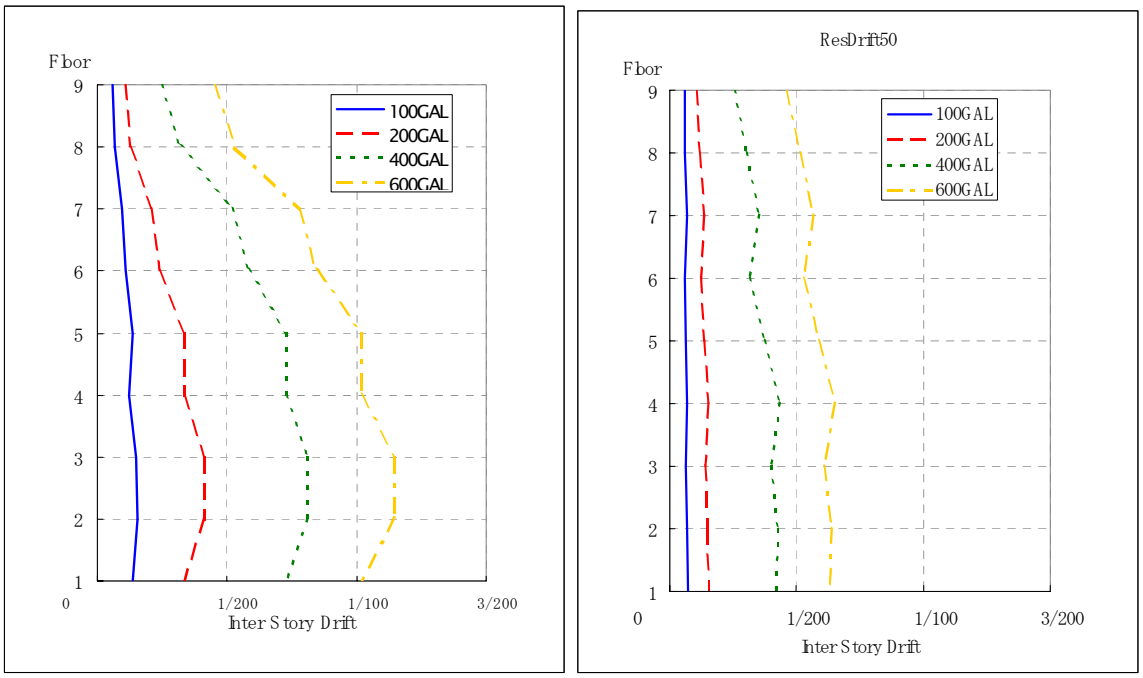

Figure 6-32. Estimated interstory drift responses for buildings #1 (left) and #2 (right)

Finally, overall vulnerability is obtained by combining the vulnerability of all the components into a weighed single-value building vulnerability. Figure 6-33 and Figure 6-34 show the mean (lower curve) and 90% (upper curve) vulnerability cures and damage distribution functions at PGA of 300 cm/sec^2 for Buildings #1 and #2, respectively.

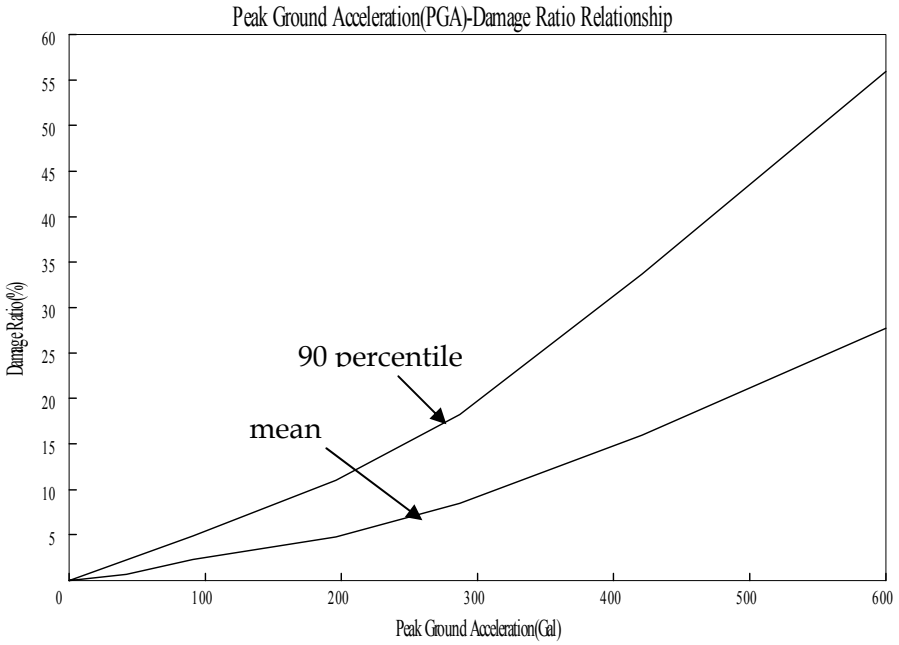

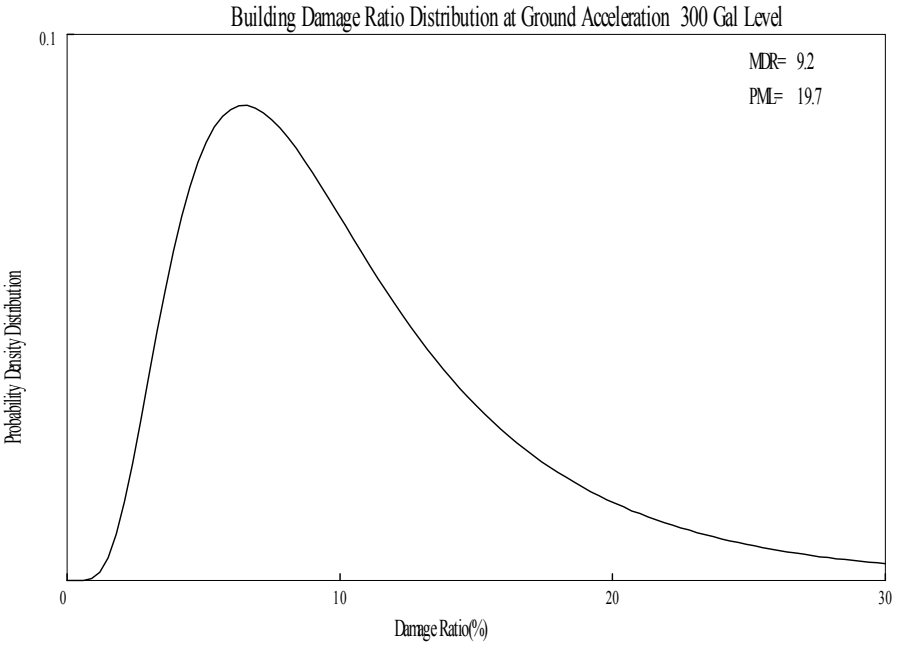

Figure 6-33. Vulnerability function of Building #1

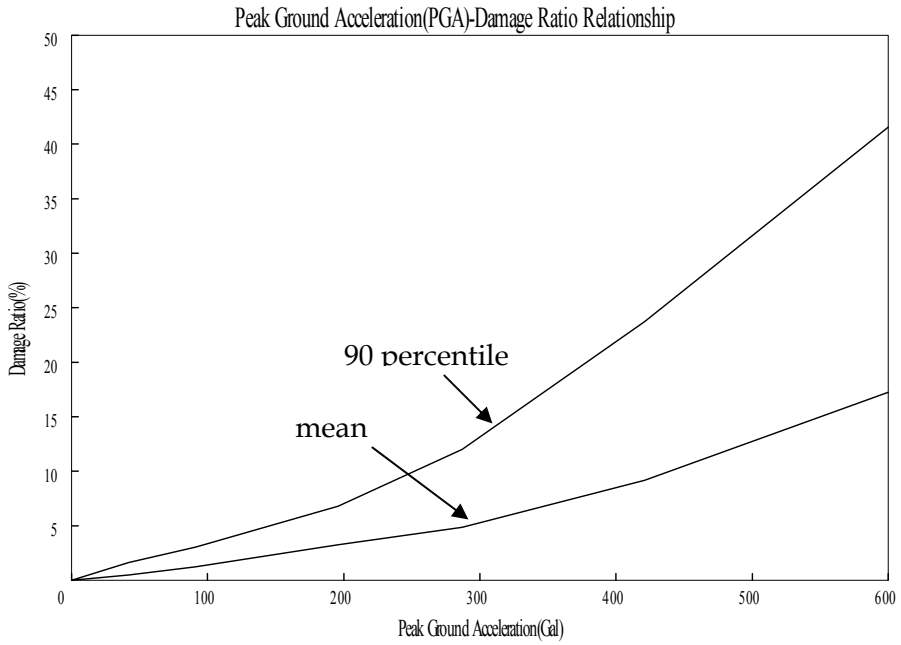

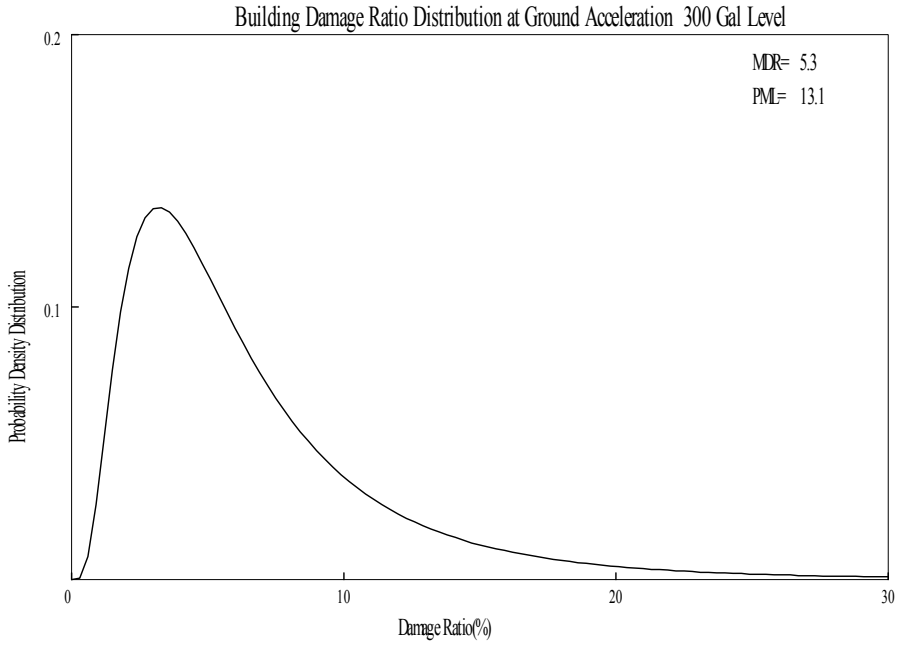

Figure 6-34. Vulnerability function of Building #2

6.4.2 Building #3

Building #3 is a 29-story high-rise commercial complex with a four-level basement and a two-story penthouse. The superstructure consists of moment-resisting steel frames with braces and concrete-filled steel tubes, while the substructure consists of moment-resisting reinforced-concrete/steel-encased reinforced-concrete frames with shear walls. The structural height of the building prescribed in the Building Standard Law of Japan is 147.0 m. Since Building #3 is a high-rise building, the Level-3 method is used for its seismic assessment. In contrast to the Level-2 method, the structural responses at a PGV of 30 cm/sec and 60 cm/sec are given by performing non-linear three-dimensional dynamic analyses. Such analyses are required as part of the design for high-rise buildings taller than 60 m in Japan. Design criteria are that all structural elements should be in the elastic range and the story drifts should be less than 0.5% for a given PGV of 30 cm/sec. Story drifts should be less than 1.0% for a given PGV of 60 cm/sec.

Building components are broken down into vulnerability classes floor by floor using the same procedure in the Level-2 method. The structural responses, story shears, story drifts and accelerations are then estimated by interpolating and extrapolating the results of the analyses. Figure 6-35 shows estimated story shear responses for various intensities of ground motions with the elastic limits and ultimate strength limits of the buildings. Floor acceleration and story drift responses are shown in Figure 6-36. Following the Level-3 procedure, the building vulnerability curves are composed and are shown in Figure 6-37 and Figure 6-38.

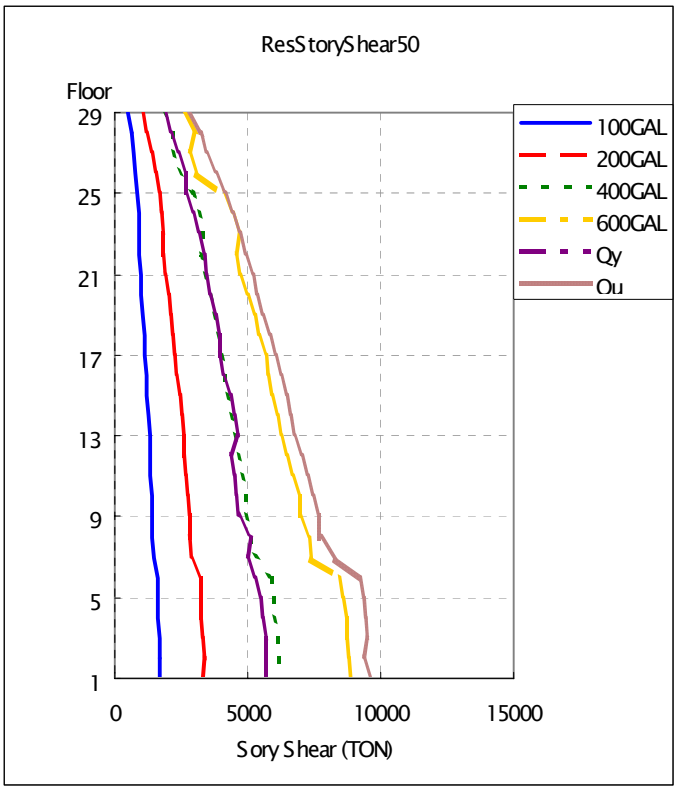

Figure 6-35. Story shear responses of Building #3

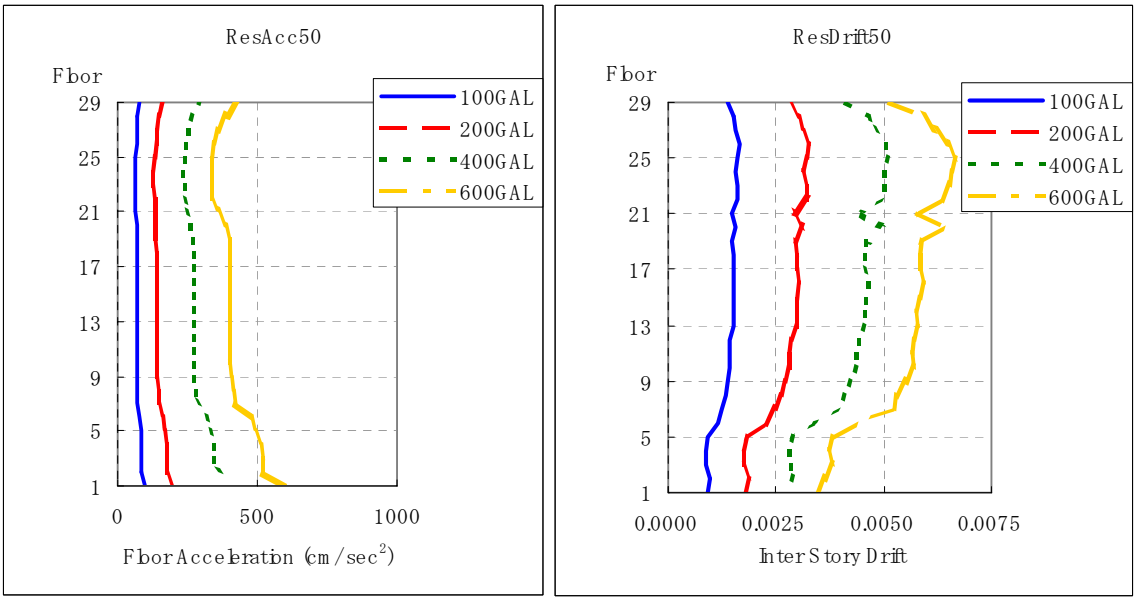

Figure 6-36. Response of Building #3: floor acceleration (left), interstory drift (right)

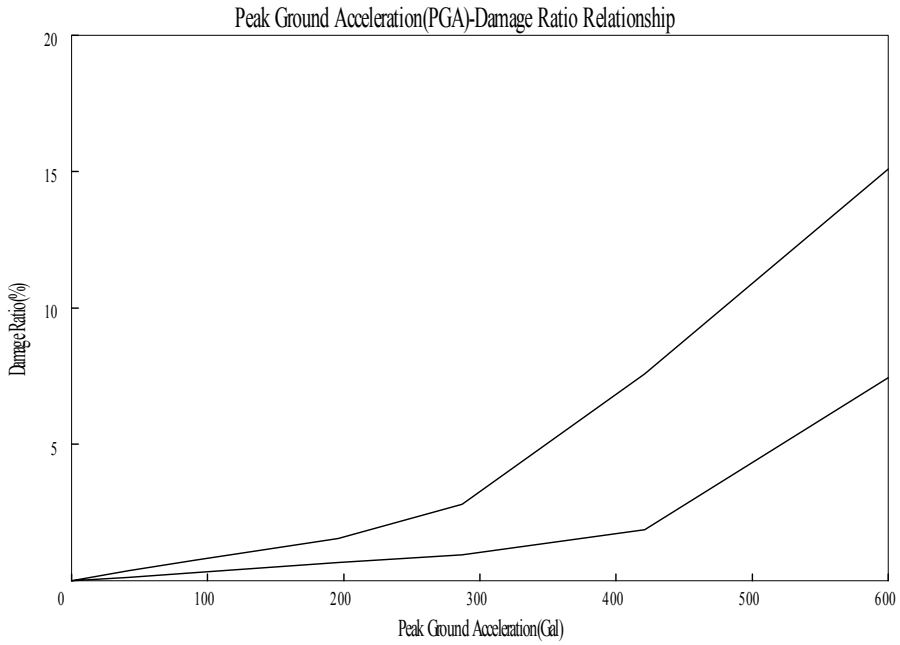

Figure 6-37. Vulnerability functions of Building #3

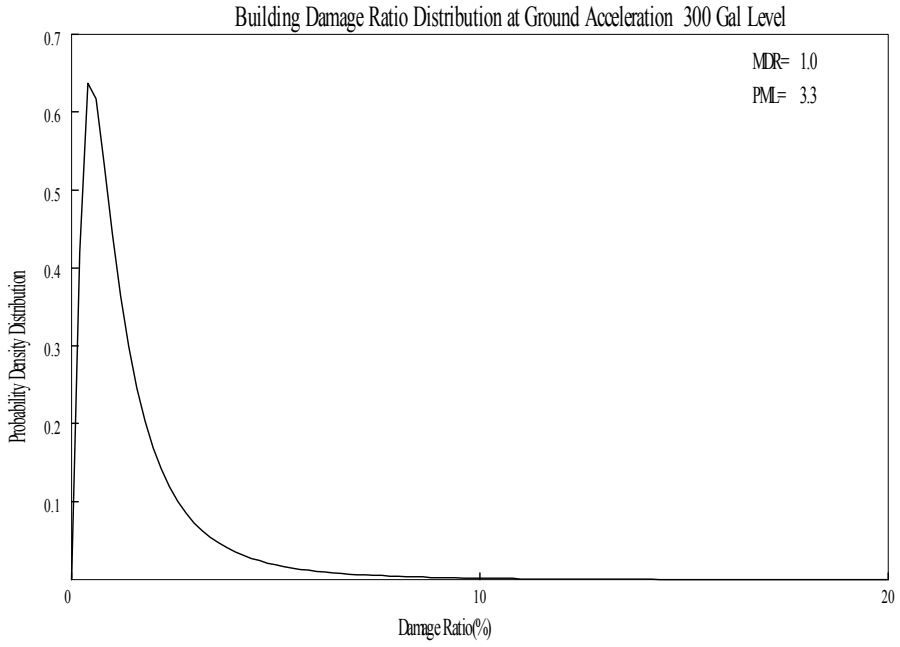

Figure 6-38. Damage distribution function of Building #3

6.4.3 Building vulnerabilities

Although two different methodologies were used for the assessment, building specific vulnerability curves were developed by introducing building characteristics associated with estimated dynamic behavior and component vulnerabilities. A summary of the vulnerability curves for the demonstration buildings is shown in Figure 6-39, Figure 6-40, and Figure 6-41.

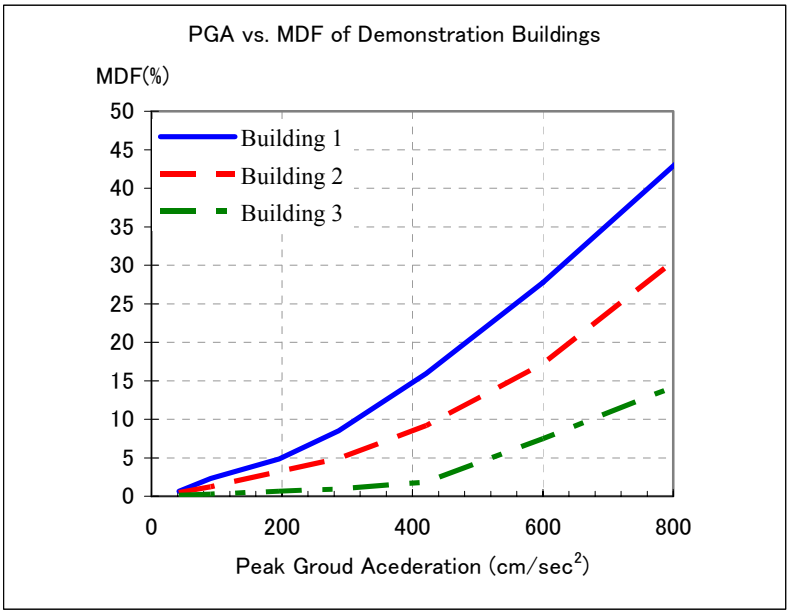

Figure 6-39. MDF vs. PGA for the demonstration buildings

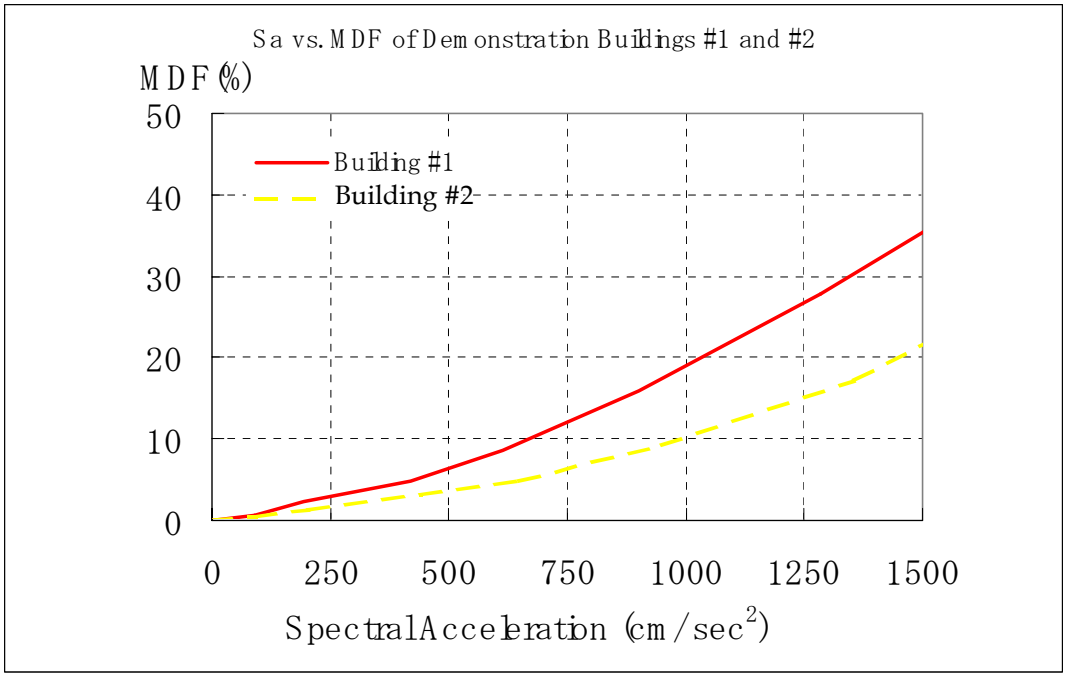

Figure 6-40. MDF vs. S_a for demonstration Buildings #1 and #2

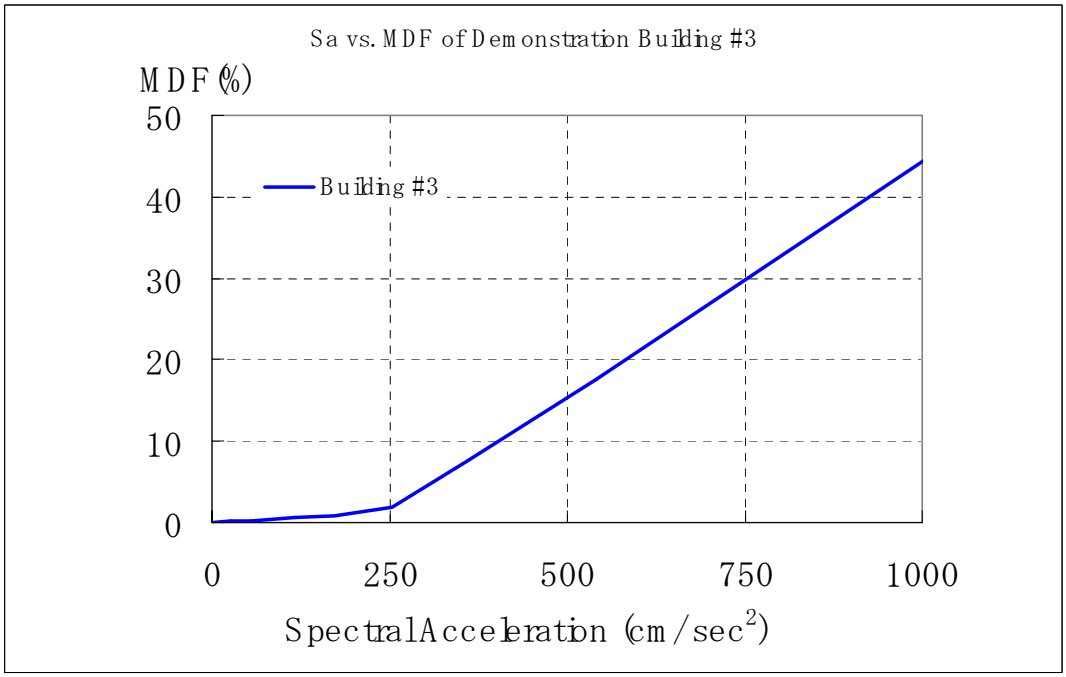

Figure 6-41. MDF vs. S_a for demonstration Building #3

6.5 RISK PROFILE

Loss exceedence probability (likelihood of exceeding specific loss levels) can be determined by integrating building vulnerabilities in Figure 6-39 and the hazard curve in Figure 6-13 using Eq. 6-10, assuming the foundation soil amplification factor is approximately 2.0.

$$P(x) = \int_{t=0}^{\infty} \{\ p_{acc}(t) \times p(x \le X \mid Acc(t))\ \} dt \qquad (6\text{-}10)$$

P(x): Annual loss exceedence probability for *x.*

$p_{acc}(t)$*:* Annual probability for a given return period of earthquake.

Acc(t): Expected peak ground acceleration for a given return period.

$P(x \le X \mid Acc)$*:* Loss probability exceedence for a given ground intensity.

Results are shown Figure 6-42 and Table 6-12. The estimated ground-up losses for the demonstration buildings within the next 475-year period, one of the seismic risk indices commonly used by the property and casualty insurance community, are 14.7%, 8.4%, and 1.7%. The average annual losses are 1.14%, 0.69% and 0.15% for Buildings #1 , #2 and #3, respectively, and these values are used to determine the premiums for the earthquake insurance that are used in this study. The premiums are assumed to be given by multiplying the average annual losses by 1.3.

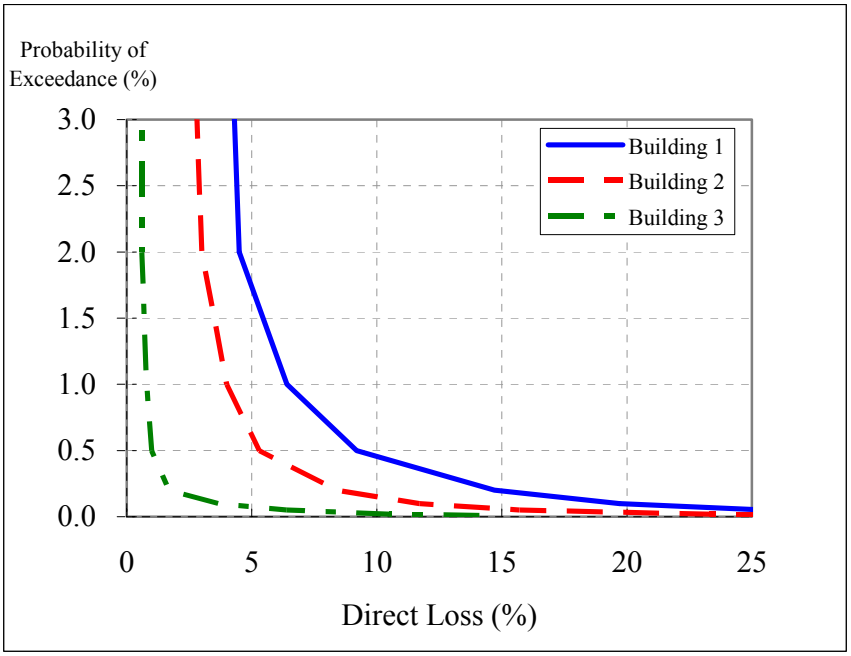

Figure 6-42. Risk profile of demonstration buildings

Table 6-12. Summary of risk profile of demonstration buildings

Annual Probability of Exceedence	Bldg. #1	Bldg. #2	Bldg. #3
2.0%	4.5	3.0	0.6
0.5%	9.7	5.3	1.0
0.2%	14.7	8.4	1.7
0.1%	19.7	11.7	3.7
Average Annual Loss	**1.14%**	**0.69%**	**0.15%**

6.6 MARKETABILITY ANALYSIS

When investors consider certain property investments, seismic risk is one of the important factors in Japan. This became especially important after the Great Hanshin (Kobe) earthquake in 1995. Foreign investors are especially concerned about this matter. Along with a seismic assessment, real estate investors, developers, and lenders make every effort to do a marketability analysis to estimate accurately and realistically the value of the investment opportunity.

There are many parameter values to be assumed. The major factors in initial investment, if it is development project, are land acquisition costs, construction costs, planning costs, design fees and marketing expenses. If it is an investment in an existing building, then purchasing price, renovation costs, retrofit costs and broker commission are the initial costs. In the operation phase, rents, occupancy rates, insurance and repair and maintenance costs need to be considered. The financial structure through out the project term has a great impact on project return. Tax issues are not only crucial during the initial and operation phases but also when selling.

6.6.1 Cash flow analysis using the Kajima-D program

6.6.1.1 Land prices in Japan

The official average land price announced by the Japanese government for 2001 fell 4.9% from 2000. For example, residential land dropped 4.2% and commercial land dropped 7.5%. In the greater Tokyo districts, land prices dropped by 5.8% in residential areas and 8.0% in commercial areas. On the other hand, it is recovering in the central business district. The fact that Japanese companies are restructuring their balance sheet and disposing real estate assets in the valuable CBD (central business district) is one of the backgrounds of this improvement. However, the average price is still dropping in suburban areas. It is expected that this bipolarization will continue for a while.

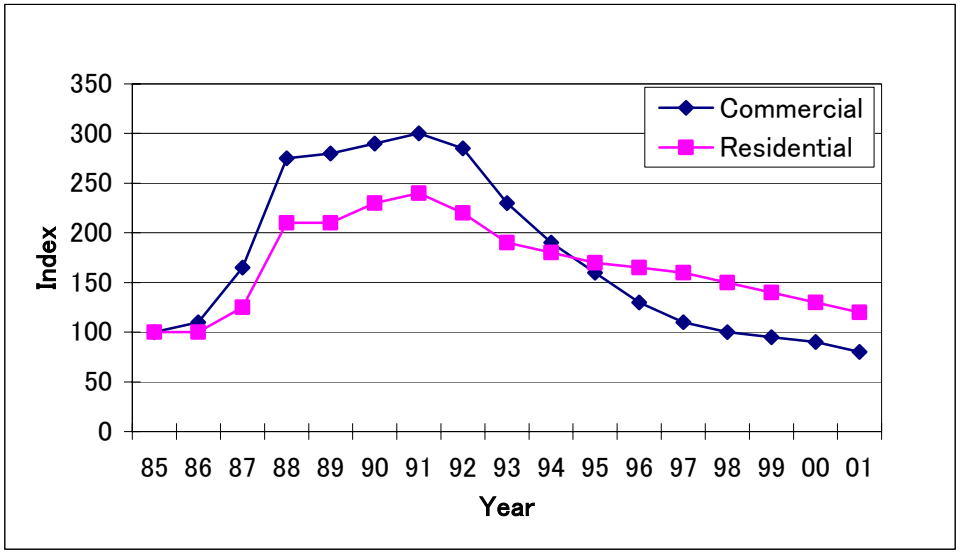

Figure 6-43. Official average land price in greater Tokyo districts

6.6.1.2 Tokyo office market

The vacancy rate for office space in Tokyo improved by 3% in 2000 from the previous year. This recovery is supported by information technology industries and the demand from foreign companies. However, the bearish tendency of average rent is under 20,000yen/tsubo/month (i.e., $55/sf/year), as of this writing where $1 ≈ ¥123. There is a strong demand for large-scale new premier class building that enhances the rent and occupancy rate of this sector. On the other hand, buildings that are not in demand because of their location, size or specification need to discount their rents in order to improve occupancy. The Tokyo CBD is going to have major large-scale office building supply in 2003. It is expected that the demand from tenants for buildings with state of the art systems will be stronger than before.

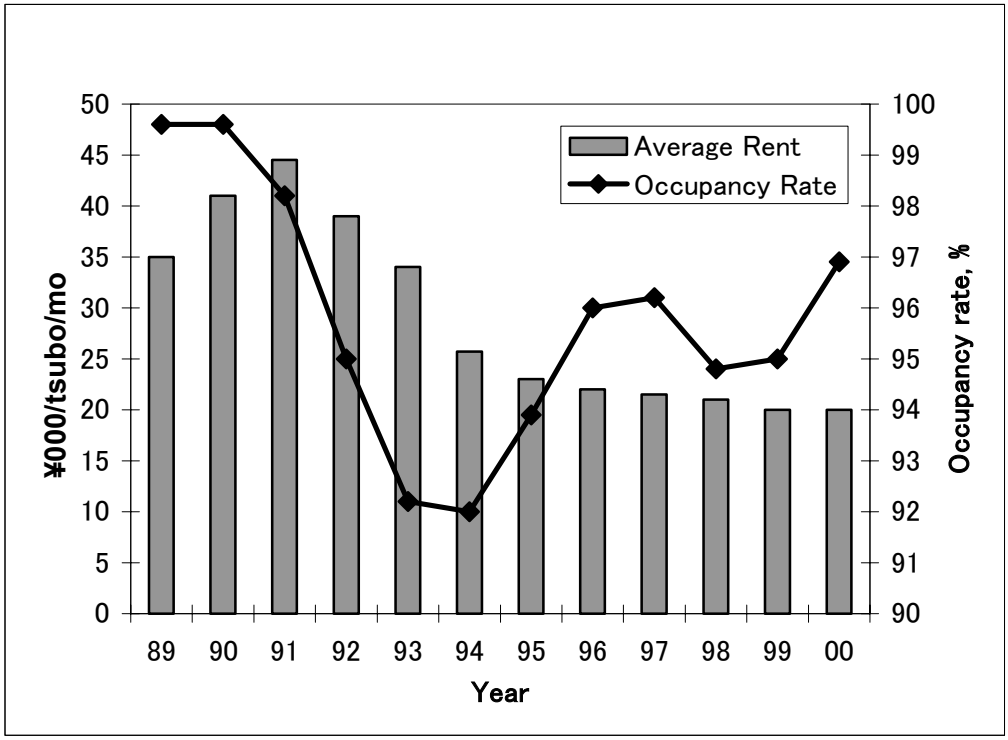

Figure 6-44. Tokyo office market rent and occupancy rates

6.6.1.3 Kajima-D program

The Kajima Development Group developed the Kajima-D program. It is a relatively sophisticated program that is quite simple to use to analyze and forecast cash flows for office, retail, and residential projects. Kajima's staff often uses this program at property screening, due diligence, negotiation, financial structuring, or during strategic planning processes. The program assists in understanding the risks and returns that are inherent in each real estate assignment, opportunity, or endeavor.

BUILDING 2		SCHEDULE OF PROSPECTIVE CASH FLOW (Acquisition ～15th)			
			2001	2002	2003
CASH FLOW		Pre-acquisit	1st	2nd	3rd
	Rents		21,262,376	21,262,376	21,262,376
Total Revenues			21,262,376	21,262,376	21,262,376
	Repairs & Replacement		2,920,000	2,920,000	2,920,000
	Insurance		73,000	73,000	73,000
	Seismic Insurance		38,421	38,421	38,421
	Maintenance		2,328,000	2,328,000	2,328,000
	Mgnt. Fee		637,871	637,871	637,871
	Marketing		755	755	755
	Tax	0	3,461,744	3,461,744	3,461,744
Total Expense		0	9,459,791	9,459,791	9,459,791
CASH FLOW (Before Interest & Tax)		0	11,802,585	11,802,585	11,802,585
	Residual Value		0	0	0
	Net Cash Flow	0	11,802,585	11,802,585	11,802,585
	ROA (C.F./Total Project Cost)		5.9%	5.9%	5.9%
	Present Value		11,490,817	10,891,770	10,323,952
Debt Service			5,594,379	5,594,379	5,594,379
Deposit (Refund)			0	0	0
Deposit (Receipt)			210,185	222,359	234,689
Cash Flow after Debt Service & Deposit			6,418,391	6,430,565	6,442,895
DSCR			2.11	2.11	2.11
P/L		Pre-acquisit	1st	2nd	3rd
Revenues	Rents	0	21,262,376	21,262,376	21,262,376
Expenses	C.F.Total Expense	0	9,459,791	9,459,791	9,459,791
	Depreciation	0	3,919,845	3,919,845	3,919,845
Operating Profit/Loss		0	7,882,740	7,882,740	7,882,740
Non-Operating Income	Interest earned		210,185	222,359	234,689
	Property Disposition		0	0	0
Non-Operating Expens	Interest expense	0	2,797,035	2,741,088	2,684,022
	Other Expense		0	0	0
Net Profit/Loss		0	5,295,890	5,364,011	5,433,407
Corporate Tax		0	2,252,423	2,281,396	2,310,911
Net Profit/Loss after Tax		0	3,043,467	3,082,615	3,122,496
(Cumulative)		0	3,043,467	6,126,082	9,248,578
		Pre-acquisit	1st	2nd	3rd
	C.F. after Debt Service		6,418,391	6,430,565	6,442,895
	Corporate Taxes		2,252,423	2,281,396	2,310,911
	Dividend-Equity1 (Included retirement)		982,860	972,041	960,995
	Dividend-Equity2 (Included retirement)		1,965,721	1,944,082	1,921,990
Cash Reserve			1,217,387	1,233,046	1,248,998
Accumulated Cash Reserve			1,217,387	2,450,433	3,699,431
B/S		Pre-acquisit	1st	2nd	3rd
ASSETS	Cash	21,018,476	22,235,863	23,468,909	24,717,908
	Real Estate	199,788,208	195,868,363	191,948,519	188,028,674
	Deferred Assets	0	0	0	0
Asset-total		220,806,684	218,104,226	215,417,428	212,746,581
LIABILITIES	Debt 1	99,894,104	97,896,001	95,857,936	93,779,110
	Debt 2	39,957,642	39,158,400	38,343,175	37,511,644
	Security Deposit	21,018,476	21,018,476	21,018,476	21,018,476
Liabilities-total		160,870,222	158,072,878	155,219,587	152,309,231

Figure 6-45. Portion of Kajima-D program screen

The assumptions for the Kajima-D program are simple. The major assumptions are as follows:

Property Outline

Fundamental parameter values for the cash flow analysis are the land and building size, PML (probable maximum loss) information and market value information. These numbers are the basis for transaction costs as well as operation in- and out-flows.

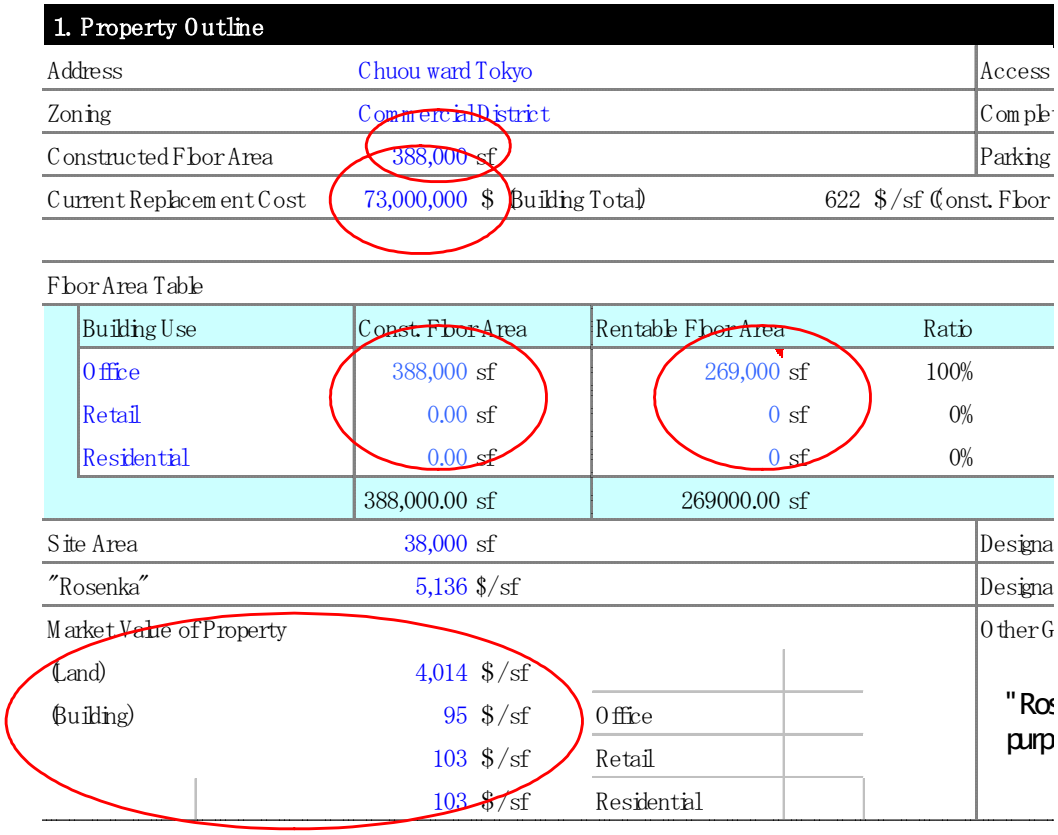

1. Property Outline

Address	Chuou ward Tokyo		Access
Zoning	Commercial District		Comple
Constructed Floor Area	388,000 sf		Parking
Current Replacement Cost	73,000,000 $ (Building Total)	622 $/sf (Const. Floor	

Floor Area Table

Building Use	Const. Floor Area	Rentable Floor Area	Ratio
Office	388,000 sf	269,000 sf	100%
Retail	0.00 sf	0 sf	0%
Residential	0.00 sf	0 sf	0%
	388,000.00 sf	269000.00 sf	

Site Area	38,000 sf		Designa
"Rosenka"	5,136 $/sf		Designa
Market Value of Property			Other G
(Land)	4,014 $/sf		
(Building)	95 $/sf	Office	"Ros purp
	103 $/sf	Retail	
	103 $/sf	Residential	

Figure 6-46. Kajima-D property outline

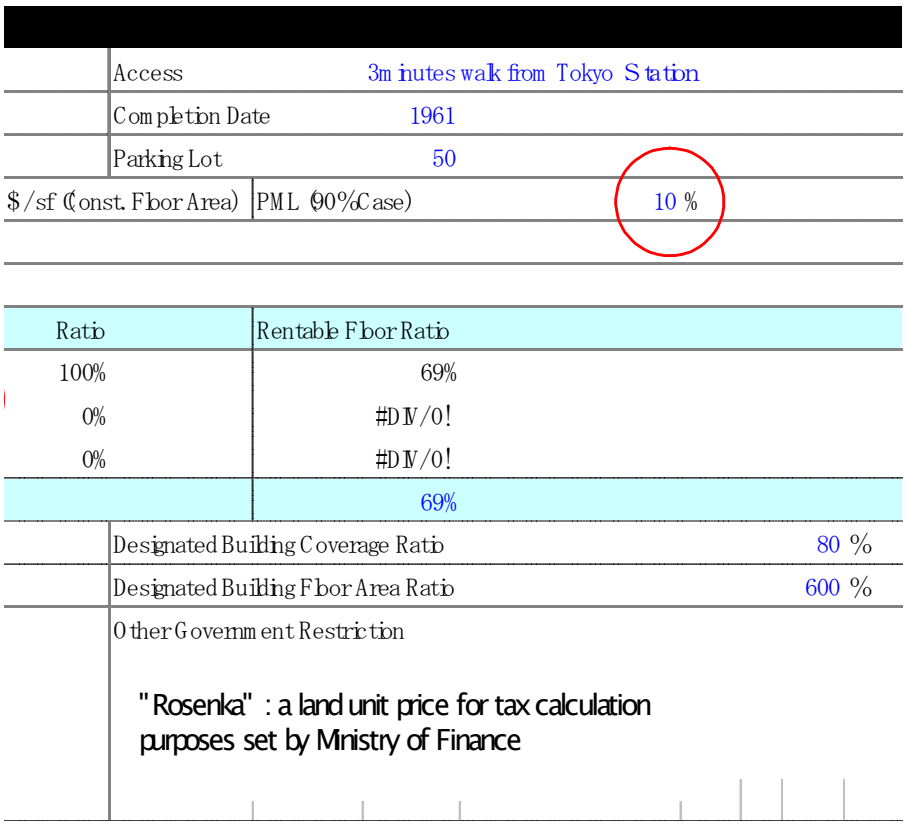

	Access	3minutes walk from Tokyo Station
	Completion Date	1961
	Parking Lot	50
$/sf (Const. Floor Area)	PML (90%Case)	10 %

Ratio	Rentable Floor Ratio
100%	69%
0%	#DIV/0!
0%	#DIV/0!
	69%

	Designated Building Coverage Ratio	80 %
	Designated Building Floor Area Ratio	600 %
	Other Government Restriction	

"Rosenka" : a land unit price for tax calculation purposes set by Ministry of Finance

Figure 6-47. Property outline, cont.

Leasing Assumptions

Leasing assumptions are for operating income projection. The parameter values for monthly rent and for inflation rate may be altered. Usually, the occupancy rate is not stable during the initial 3 years and so these rates can be changed for the initial 4 years.

Figure 6-48. Kajima-D leasing assumptions

Other Assumptions

For the operating expenses, the program allows repair and replacement costs to be input, as well as various insurance premiums including seismic insurance, building management fees, property management fees, and marketing expenses. For accounting purposes, depreciation data can be changed. Tax information is for acquisition and operation.

3. Other Assumptions						
Revenue	Interest Income	1.0 %				
Expense	Repairs Replacements	0.25 %	(Total estimated Replacement cost)	5 every year	100 %UP	
	Insurance	0.1 %	(Total estimated Replacement cost)	3 every year	3 %UP	
	Seismic Insurance	500 %	(Year expected Loss)	3 every year	3 %UP	
	Building Mgmt.	0.5 $/sf	(Const. Floor Area)	3 every year	3 %UP	
	Property Mgmt.	3.0 %	(Rent)			
	Marketing	755 $/year		3 every year	3 %UP	
Depreciation	Body/Dep.	65 %				
	Body	50 year	(FRM=0, SLM=1		1)	
	Equipments	15 year	(FRM=0, SLM=2		1)	
	Other Structure	10 year	(FRM=0, SLM=3		1)	
Deferred Asset Depreciation		6 year	Public Obligation Charge			
	Retained Earnings	40 %	(Net Profit/Loss)			

Schedule	Completion	Acquisition
	1961	2001

Tax					
Land	Property & Urban Planning Tax	1.7 %		3 every year	3 %UP
	Land Value Tax	0.0 %		3 every year	3 %UP
Building	Tax Base	70 %	(Total estimated Replacement cost)		
	Property and Urban Planning Tax	1.7 %			
Real Property Acquisition Ta		4.0 %			
Registration & License Tax		5.0 %	(Transfer)		
Registration & License Tax		0.6 %	(preservation)		
Profit Tax					
	Corporation Tax	30.0 %	(Deferred Loss=0, Neglect:	0)	
	Municipal Inhabitants Tax	20.7 %			
	Enterprise Tax	11.0 %	(Total Profit Tax #### %)		

Exit
2006

Figure 6-49. Kajima-D other assumptions

Project Costs

Initial project costs at acquisition are property price, tax, brokerage commission, and renovation and retrofit costs. The program can calculate these detailed transaction expenses.

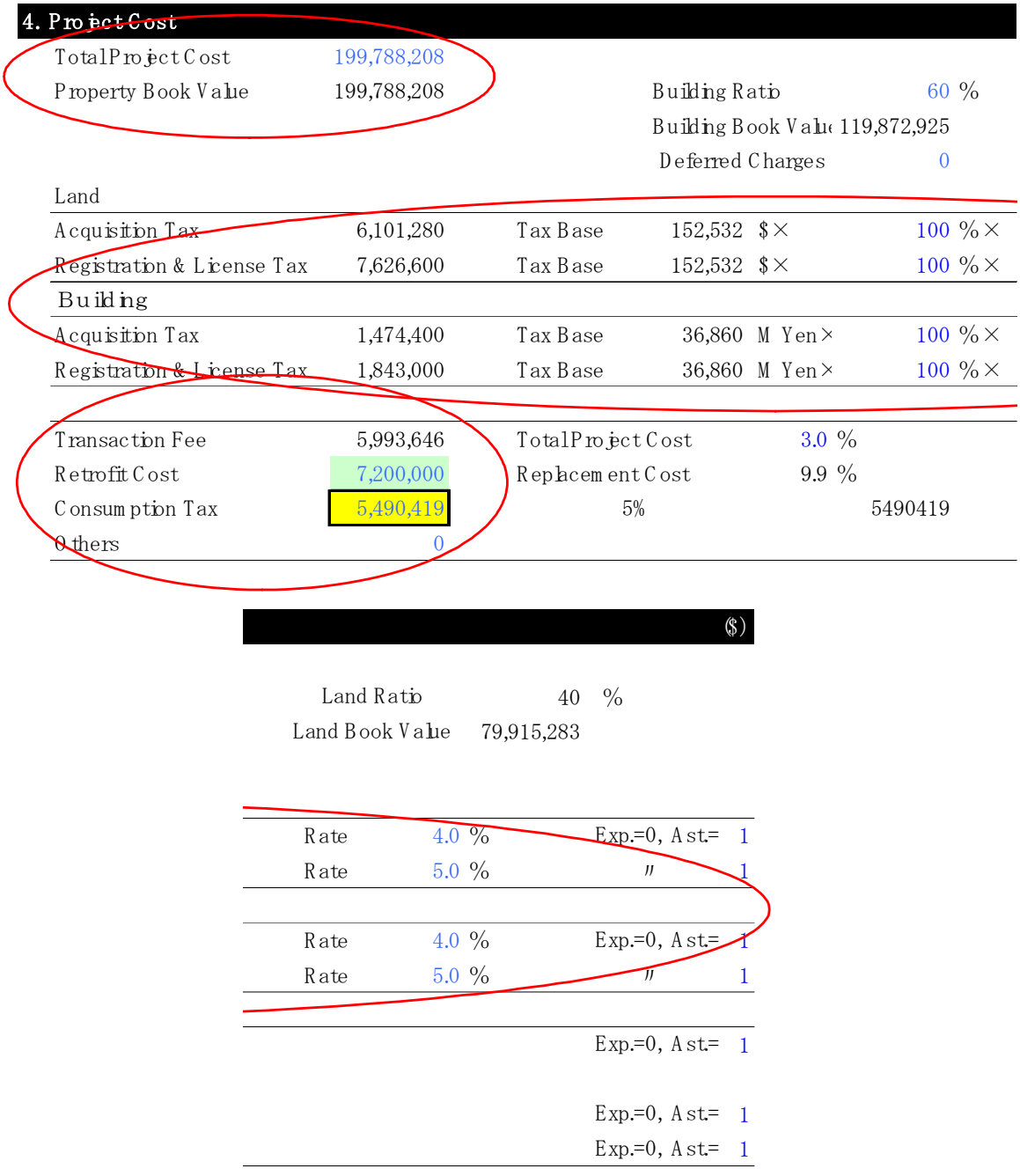

4. Project Cost					
Total Project Cost	199,788,208				
Property Book Value	199,788,208		Building Ratio		60 %
			Building Book Value		119,872,925
			Deferred Charges		0
Land					
Acquisition Tax	6,101,280	Tax Base	152,532 $×		100 %×
Registration & License Tax	7,626,600	Tax Base	152,532 $×		100 %×
Building					
Acquisition Tax	1,474,400	Tax Base	36,860 M Yen×		100 %×
Registration & License Tax	1,843,000	Tax Base	36,860 M Yen×		100 %×
Transaction Fee	5,993,646	Total Project Cost		3.0 %	
Retrofit Cost	7,200,000	Replacement Cost		9.9 %	
Consumption Tax	5,490,419	5%			5490419
Others	0				

($)

Land Ratio	40 %		
Land Book Value	79,915,283		
Rate	4.0 %	Exp.=0, Ast.=	1
Rate	5.0 %	〃	1
Rate	4.0 %	Exp.=0, Ast.=	1
Rate	5.0 %	〃	1
		Exp.=0, Ast.=	1
		Exp.=0, Ast.=	1
		Exp.=0, Ast.=	1

Figure 6-50. Kajima-D project cost data

Finance

Financial structure is becoming complex these days. It is possible to divide equity and debt finance into two different tranches.

5. Finance		Ratio						($)
Equity①	19,978,821	10.0%		33%				
Equity② (preferred)	39,957,642	20.0%		67%				
Debt①	99,894,104	50.0%	Interest	2.00 %	0 yr defere	35 yr Return	'& I=0, Principal=1	0
Debt②	39,957,642	20.0%	Interest	2.00 %	0 yr defere	35 yr Return	'& I=0, Principal=1	0
	199,788,208	100%	LTV	70%	DSCR	2.11	(first year)	

Figure 6-51. Kajima-D finance data

Present Value

The result of the analysis is the present value, which is the total present value of each year's cash flow, including residual value. The internal rate of return (IRR) is also calculated. In this case, the initial purchase value is based on the stabilized year's projected cash flow, divided by the expected initial capitalization rate. If there is need for structural upgrade, then the retrofit cost can be deducted from the present value.

6. Significant Results					
(1) Indexes for DCF Study					
	Holding Period		5	years	
	Discounted Rate	5.5%			
	Residual Cap Rate	6.0%	Commission	3%	
	PV	199,788,208	$		
	PV-Retrofit Cost	192,588,208	$		
(2) Stabilized Rents		21,262,376	$		
	1st year Expenses	9,459,791	$		
	Stabilized prospected NOI	11,802,585	$		
	Going-in Cap Rate	6	%		
	Purchase Price	196,709,751	$		

Figure 6-52. Kajima-D results

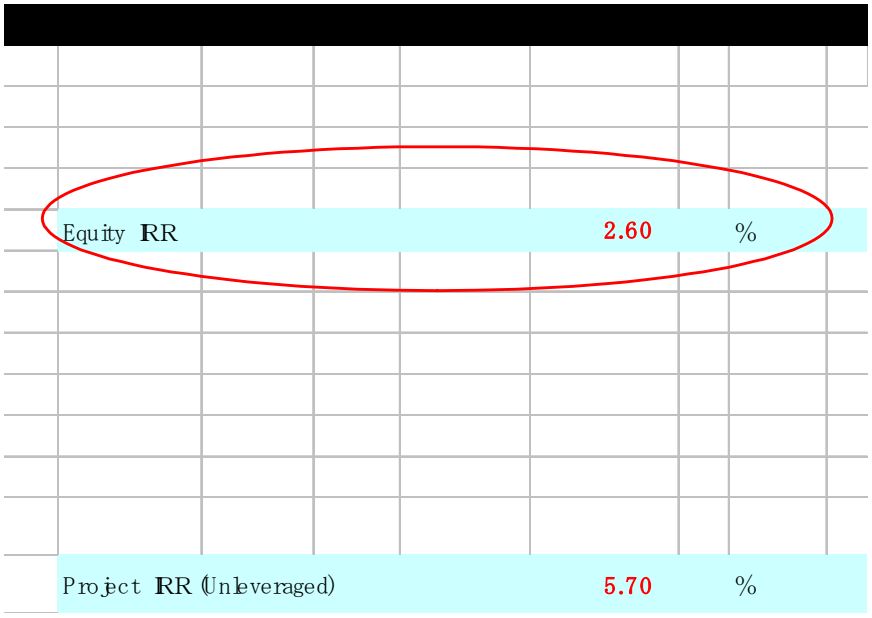

Figure 6-53. Kajima-D results, cont.

6.6.2 Cash flow analysis for the Kajima demonstration buildings

The Kajima team did a cash flow analysis for each of the three demonstration buildings. The fundamental idea is that these three different types of buildings are located at the same site in the Yaesu area of Tokyo. However, the building size and specifications are different. A summary of these buildings and the major assumptions are as follows:

Building #1 is an old building that was completed in 1961. There was a major renovation in the past. However, there was no structural upgrade after the new building code was issued in 1981.

Table 6-13. Characteristics of Building #1

Class:	B
Upgrade:	None
Building use:	Office
Completion Year:	1961
Total Floor Area:	388,000sf
Total Rentable Area:	269,000sf
Parking Space:	50
Site Area:	38,000sf
Story:	9F/B3/P2
Structure:	SRC
Replacement Cost:	US$73.0M
PML (90% case):	20%

Table 6-14. Base assumptions for Building #1

Rent	$6.90/sf/month
Occupancy rate	80%

Building #2 is the same building as Building #1, but with retrofit work done after 1989. From our experience, the occupancy rate improves after retrofit construction and this is taken into account in the cash flow analysis.

Table 6-15. Characteristics of Building #2

Class:	A
Upgrade:	Structural
Building use:	Office
Completion Year:	1961
Total Floor Area:	388,000sf
Total Rentable Area:	269,000sf
Parking Space:	50
Site Area:	38,000sf
Story:	9F/B3/P2
Structure:	SRC
Replacement Cost:	US$73.0M
Retrofit Costs:	US$7.2M
PML (90% case):	10%

Table 6-16. Base assumptions for Building #2

Rent	$6.90/sf/month
Occupancy rate	95%

Building #3 is a new high-rise building with state-of-the-art systems. This type of building could achieve the highest rental rates in the area.

Table 6-17. Characteristics of Building #3

Class:	Premier
Building use:	Office
Completion Year:	1999
Total Floor Area:	958,000sf
Total Retable Area:	667,000sf
Parking Space:	150
Site Area:	81,000sf
Story:	31F/B4/P2
Structure:	Steel
Replacement Cost:	US$254.0M
PML (90% case) :	5%

Table 6-18. Base assumptions for Building #3

Rent	$9.10/sf/month
Occupancy rate	95%

The Kajima-D program was used to perform a cash flow analysis to get the present value for each of the three buildings. Basic assumptions are as shown above. The rents were changed from a 20% decrease to a 20% increase and the occupancy rate was changed from 70% to 100% through out the specified project period of 10 years. The results for the calculations of the present value are as follows:

Building #1

Base Rent = $6.9/sf Month US $

	Rent −20%	Rent −10%	Base Rent	Rent +10%	Rent +20%
Occupancy Rate 100%	143,838,334	180,698,320	217,558,305	254,418,291	291,278,276
Occupancy Rate 95%	129,094,340	164,111,326	199,128,312	234,145,299	269,162,285
Occupancy Rate 90%	114,350,346	147,524,333	180,698,320	213,872,307	247,046,294
Occupancy Rate 85%	99,606,351	130,937,339	162,268,327	193,599,315	224,930,302
Occupancy Rate 80%	84,862,357	114,350,346	★ 143,838,334	173,326,323	202,814,311
Occupancy Rate 75%	70,118,363	97,763,352	125,408,341	153,053,330	180,698,320
Occupancy Rate 70%	55,374,369	81,176,359	106,978,348	132,780,338	158,582,328
				★	Base Case

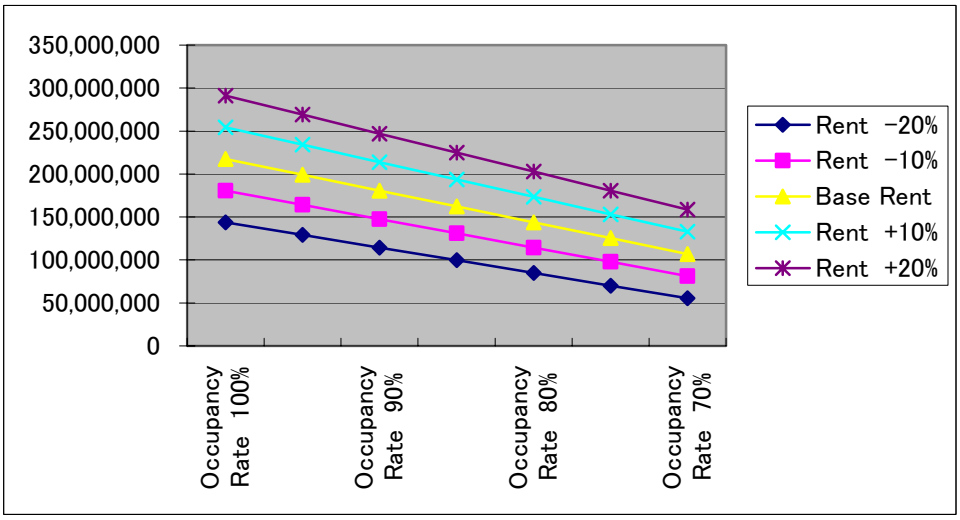

Figure 6-54. Present value of Building #1

Building #2

Base Rent = $6.9/sf Month US $

	Rent −20%	Rent −10%	Base Rent	Rent +10%	Rent +20%
Occupancy Rate 100%	137,298,229	174,158,215	211,018,201	247,878,186	284,738,172
Occupancy Rate 95%	122,554,235	157,571,221	★ 192,588,208	227,605,194	262,622,180
Occupancy Rate 90%	107,810,241	140,984,228	174,158,215	207,332,202	240,506,189
Occupancy Rate 85%	93,066,247	124,397,234	155,728,222	187,059,210	218,390,198
Occupancy Rate 80%	78,322,252	107,810,241	137,298,229	166,786,218	196,274,206
Occupancy Rate 75%	63,578,258	91,223,247	118,868,237	146,513,226	174,158,215
Occupancy Rate 70%	48,834,264	74,636,254	100,438,244	126,240,234	152,042,224
				★	Base Case

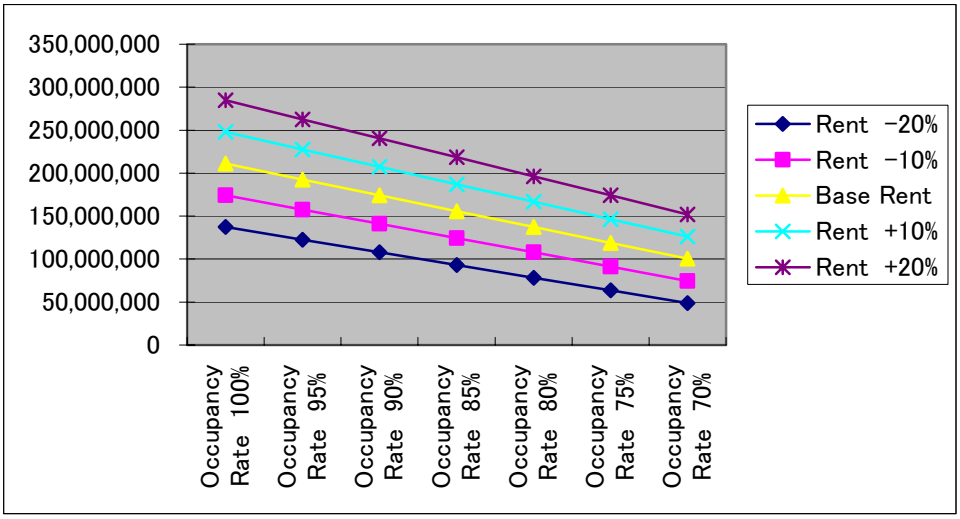

Figure 6-55. Present value of Building #2

Building #3

Base Rent = $9.1/sf Month US $

	Rent -20%	Rent -10%	Base Rent	Rent +10%	Rent +20%
Occupancy Rate 100%	709,646,214	831,512,421	953,378,627	1,075,244,834	1,197,111,040
Occupancy Rate 95%	660,899,732	776,672,628	892,445,524	1,008,218,420	1,123,991,316
Occupancy Rate 90%	612,153,249	721,832,835	831,512,421	941,192,006	1,050,871,592
Occupancy Rate 85%	563,406,766	666,993,042	770,579,317	874,165,593	977,751,868
Occupancy Rate 80%	514,660,284	612,153,249	709,646,214	807,139,179	904,632,145
Occupancy Rate 75%	465,913,801	557,313,456	648,713,111	740,112,766	831,512,421
Occupancy Rate 70%	417,167,319	502,473,663	587,780,008	673,083,352	758,392,697

★ Base Case

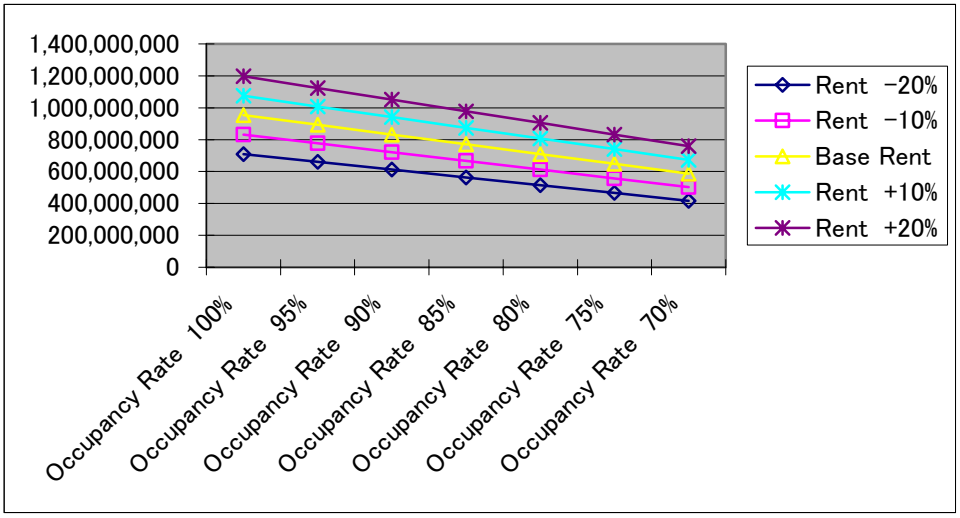

Figure 6-56. Present value of Building #3

6.7 LIFETIME PROPERTY VALUE AND RISK-RETURN PROFILE

6.7.1 Formulation of risk-return profile

The decision-maker's preference in investment choices can be evaluated by expected utility, which is a quantitative expression for ordering the decision-maker's subjective valuation of two decisions. The expected utility for net asset value V can be determined by the following equation.

$$E[u(V)] = \int_{-\infty}^{\infty} u(v) f_V(v) dv \tag{6-11}$$

in which $u(v)$ is the utility function and $f_V(v)$ is probability density function of net asset value denoted by v. The utility function $u(v)$ is modeled by an exponential function with the risk tolerance denoted by ρ, which is the parameter mathematically representing the decision-maker's attitude toward risks;

$$u(v) = 1 - \exp(-v/\rho) \tag{6-12}$$

While the probability density function $f_V(v)$ is evaluated considering market risk X and seismic risk Y, so that $V = X + Y$. Thus, $f_V(v)$ is expressed by,

$$f_V(v) = \int_{-\infty}^{\infty} f_{X,Y}(v-y, y)dy \tag{6-13}$$

If market risk and seismic risk can be formulated as stochastically independent, then

$$f_V(v) = \int_{-\infty}^{\infty} f_X(v-y) f_Y(y)dy \tag{6-14}$$

The expected utility of Eq. 6-11 can be calculated by

$$E[u(V)] = \int_{-\infty}^{\infty} (1 - e^{-v/\rho}) \left[\int_{-\infty}^{\infty} f_X(v-y) f_Y(y)dy \right] dv \tag{6-15}$$

In the previous section, the seismic risk of the demonstration buildings was evaluated by the exceedance probability of earthquake losses, $P_Y(y)$. Therefore, substituting $f_Y(y) = -dP_Y(y)/dy$ into Eq. 6-15, the expected utility is given by the following equation;

$$E[u(V)] = \int_{-\infty}^{\infty} (1 - e^{-v/\rho}) \left[\int_{-\infty}^{\infty} \frac{d}{dy} f_X(v-y) \cdot P_Y(y)dy \right] dv \tag{6-16}$$

6.7.2 Simplified model for expected utility

For illustrating the concept of expected utility, a simplified model for the probability density function of the net asset value is examined. The following Gaussian distribution function with average M and standard deviation σ is utilized for the uncertain net asset value according to market risk and seismic risk:

$$f_V(v) = \frac{1}{\sqrt{2\pi}\sigma} \exp\left\{ -\frac{(v-M)^2}{2o^2} \right\} \tag{6-17}$$

Substituting equations (6-17) and (6-12) into (6-11), the expected utility for the Gaussian-distributed net asset value is then obtained as follows:

$$E[u(V)] = 1 - \exp\left\{ -\frac{M}{\rho}\left(1 - \frac{M\delta^2}{2\rho}\right) \right\} \tag{6-18}$$

where δ is the coefficient of variance ($\delta = \sigma/M$).

In Eq. 6-18, the average M and risk tolerance ρ are included in the normalized form, such as M/ρ. Thus, these parameters can be considered as non-dimensional though both have a monetary scale, such as \$or ¥.

Figure 6-57 through Figure 6-59 show the examples of expected utility variation with respect to risk tolerance ρ. The average M indicates expected return from the property, while the coefficient of variance δ can be considered as uncertainty or risk in the investment. Figure 6-57 shows the effect of risk on the expected utility. It is reasonable that the expected utility, that is, preference for the risk-return profile, decreases according to risk. This result indicates that any decision-maker must avoid the risk. Figure 6-58 shows the result of a low-risk case and a high-risk case. In the case of low risk, a high-return profile is preferable for any ρ-person. On the other hand, the result of high-risk case indicates that risk-averse (lower-ρ) person prefers a conservative investment with a lower-return profile.

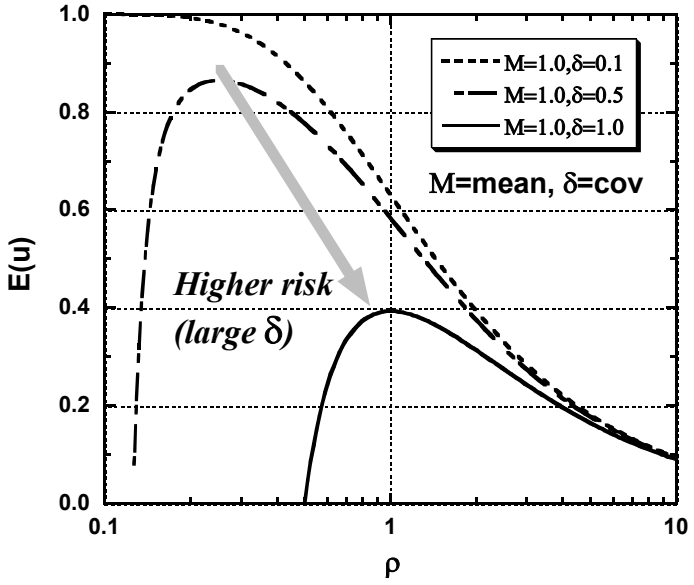

Figure 6-57. Expected utility; effect of risk

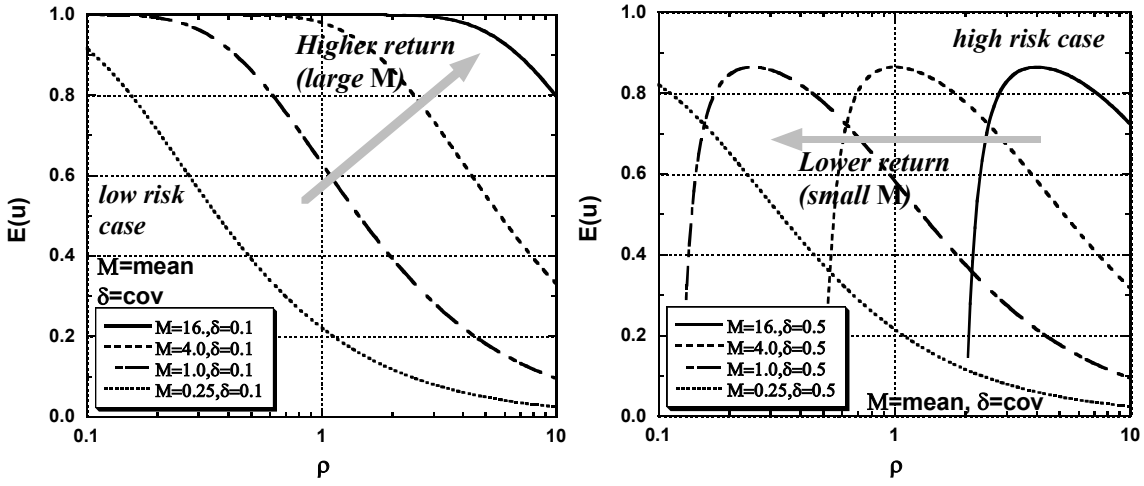

Figure 6-58. Example low-risk case (left), high-risk case (right)

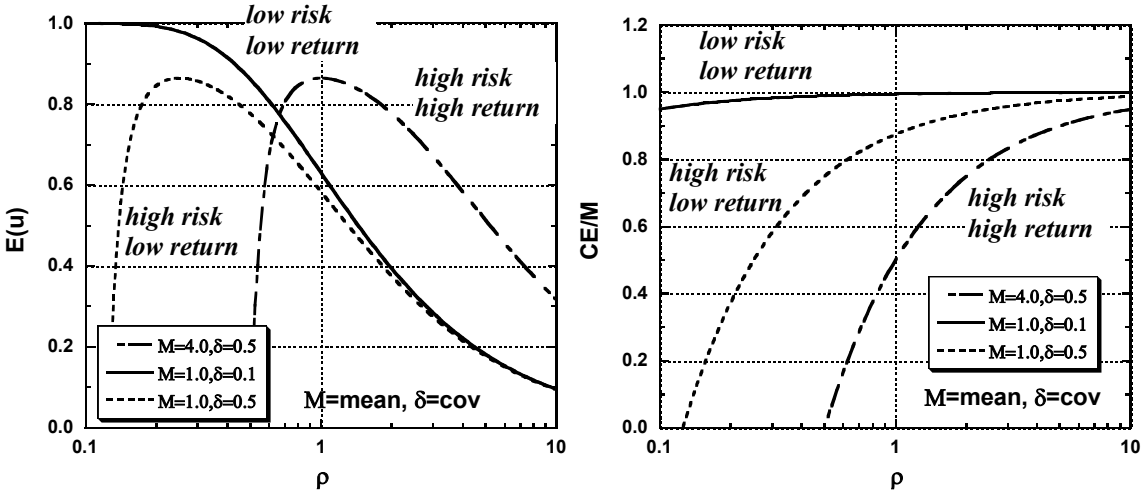

Figure 6-59. Example of expected utility (left) and of certainty equivalent normalized by mean value

The left-hand side of Figure 6-59 shows the expected utility with three cases of risk-return profile. It can be seen that the preference in risk-return profile is different according to the decision-maker's risk attitude expressed by ρ, but also that the high-risk and low-return profile is always avoided. The right-hand side of Figure 6-59 shows the certainty equivalent normalized by mean value for the same cases. From Eq. 6-18, the certainty equivalent can be obtained as follows:

$$u(CE) = 1 - \exp(-CE/\rho) = E[u(V)]$$
$$\therefore CE = -\rho \ln\{1 - E[u(V)]\} = M(1 - \frac{M\delta^2}{2\rho}) \tag{6-19}$$

The equation above indicates the certainty equivalent calculated for this model must be less than expected return value. As shown in Figure 6-59, the certainty equivalent in the case of conservative investment with low-risk and low-return profile takes the closest value to the expected return.

6.7.3 Discrete expression for calculation of expected utility

Generally, the analytical formulation for calculation of the expected utility cannot be derived because of the integral in Eq. 6-16. This section introduces a discrete expression of the integration based on several assumptions of the probability functions.

The normal distribution function with average μ_X and standard deviation σ_X is assumed to express the present value of net income stream denoted by X.

$$f_X(x) = \frac{1}{\sqrt{2\pi}\sigma_X} \exp\left[-\frac{(x-\mu_X)^2}{2\sigma_X{}^2} \right] \tag{6-20}$$

Thus, $f_X(v\text{-}y)$ in Eq. 6-16 is given by

$$\begin{aligned} f_X(v-y) &= \frac{1}{\sqrt{2\pi}\sigma_X} \exp\left[-\frac{(v-y-\mu_X)^2}{2\sigma_X{}^2} \right] \\ &= \frac{1}{\sqrt{2\pi}\sigma_X} \exp\left[-\frac{(y-v^*)^2}{2\sigma_X{}^2} \right] \end{aligned} \tag{6-21}$$

The probability density function of net asset value is then given by

$$\begin{aligned} f_V(v) &= -\int_{-\infty}^{\infty} f_X(v-y) \cdot \frac{dP_Y(y)}{dy} dy \\ &= -f_X(v-y) \cdot P_Y(y)\Big|_{-\infty}^{\infty} + \int_{-\infty}^{\infty} \frac{d}{dy} f_X(v-y) \cdot P_Y(y) dy \\ &= \int_{-\infty}^{\infty} \frac{d}{dy} f_X(v-y) \cdot P_Y(y) dy \end{aligned} \tag{6-22}$$

where $P_Y(y)$ is exceedance probability of earthquake losses, determined by

$$f_Y(y) = -\frac{d}{dy} P_y(y) \tag{6-23}$$

In Eq. 6-22, the first term in the integral can be calculated as follows.

$$\frac{d}{dy} f_X(v-y) = -\frac{y-v^*}{\sqrt{2\pi}\sigma_X{}^3} \exp\left[-\frac{(y-v^*)^2}{2\sigma_X{}^2}\right] \tag{6-24}$$

For the calculation of the integral equation, the exceedance probability of earthquake losses is assumed to be a set of linear functions:

$$P_Y(y) = a_i y + b_i, \ \ (y_i \le y < y_{i+1}) \tag{6-25}$$

Substituting Eq. 6-24 and Eq. 6-25 into Eq. 6-22, the probability density function for net asset value can be given as following discrete expression.

$$\begin{aligned} f_V(v) &= -\sum_i \int_{y_i}^{y_{i+1}} \frac{y-v^*}{\sqrt{2\pi}\sigma_X{}^3} \exp\left[-\frac{(y-v^*)^2}{2\sigma_X{}^2}\right] \cdot (a_i y + b_i) dy \\ &= -\sum_i \int_{y_i}^{y_{i+1}} \frac{a_i y^2 + (b_i - a_i v^*) y - b_i v^*}{\sqrt{2\pi}\sigma_X{}^3} \exp\left[-\frac{(y-v^*)^2}{2\sigma_X{}^2}\right] dy \end{aligned} \tag{6-26}$$

Utilizing variable transformation

$$t = \frac{y-v^*}{\sigma_X}, \ \ y = \sigma_X t + v^*, \ \ dy = \sigma_X dt \tag{6-27}$$

Then, Eq. 6-26 is expressed as follows.

$$\begin{aligned} f_V(v) &= -\sum_i \int_{t_i}^{t_{i+1}} \frac{a_i(\sigma_X t + v^*)^2 + (b_i - a_i v^*)(\sigma_X t + v^*) - b_i v^*}{\sqrt{2\pi}\sigma_X{}^2} e^{-\frac{t^2}{2}} dt \\ &= -\sum_i \int_{t_i}^{t_{i+1}} \frac{a_i}{\sqrt{2\pi}} t^2 e^{-\frac{t^2}{2}} dt - \sum_i \int_{t_i}^{t_{i+1}} \frac{a_i v^* + b_i}{\sqrt{2\pi}\sigma_X} t e^{-\frac{t^2}{2}} dt \end{aligned} \tag{6-28}$$

From the deviation of exponential function as

$$\frac{d}{dt}e^{-\frac{t^2}{2}} = -te^{-\frac{t^2}{2}},\ \frac{d}{dt}(te^{-\frac{t^2}{2}}) = e^{-\frac{t^2}{2}} - t^2 e^{-\frac{t^2}{2}} \tag{6-29}$$

The integrals in Eq. 6-29 can be analytically expressed.

$$\begin{aligned}
&\int_{t_i}^{t_{i+1}} t^2 e^{-\frac{t^2}{2}} dt = \int_{t_i}^{t_{i+1}} e^{-\frac{t^2}{2}} dt - te^{-\frac{t^2}{2}}\Big|_{t_i}^{t_{i+1}} = [\sqrt{2\pi}\Phi(t) - te^{-\frac{t^2}{2}}]\Big|_{t_i}^{t_{i+1}} \\
&\int_{t_i}^{t_{i+1}} te^{-\frac{t^2}{2}} dt = -e^{-\frac{t^2}{2}}\Big|_{t_i}^{t_{i+1}}
\end{aligned} \tag{6-30}$$

where $\Phi(t)$ is the standard Gaussian cumulative distribution function. Substituting Eq. 6-30 into Eq. 6-28, the probability density function $f_V(v)$ is given as follows.

$$\begin{aligned}
f_V(v) &= -\sum_i \frac{a_i}{\sqrt{2\pi}}[\sqrt{2\pi}\Phi(t) - te^{-\frac{t^2}{2}}]\Big|_{t_i}^{t_{i+1}} + \sum_i \frac{a_i v^* + b_i}{\sqrt{2\pi}\sigma_X} e^{-\frac{t^2}{2}}\Big|_{t_i}^{t_{i+1}} \\
&= -\sum_i a_i \Phi(t)\Big|_{t_i}^{t_{i+1}} + \sum_i \frac{a_i(\sigma_X t + v^*) + b_i}{\sqrt{2\pi}\sigma_X} e^{-\frac{t^2}{2}}\Big|_{t_i}^{t_{i+1}} \\
&= -\sum_i a_i \Phi(\frac{y - v^*}{\sigma_X})\Big|_{y_i}^{y_{i+1}} + \sum_i \frac{a_i y + b_i}{\sqrt{2\pi}\sigma_X} \exp\left[-\frac{(y - v^*)^2}{2\sigma_X{}^2}\right]\Big|_{y_i}^{y_{i+1}}
\end{aligned} \tag{6-31}$$

Finally, discrete form of the expected utility can be derived as follows:

$$\begin{aligned}
E[u(V)] &= \int_{-\infty}^{\infty} [1 - \exp(-v/\rho)] \cdot f_V(v) dv \\
&= -\int_{-\infty}^{\infty} \exp(-v/\rho) \cdot f_V(v) dv \\
&= \int_{-\infty}^{\infty} \exp(-v/\rho) \cdot \sum_i \left[a_i \Phi(\frac{y - v^*}{\sigma_X}) - \frac{a_i y + b_i}{\sqrt{2\pi}\sigma_X} \exp\left[-\frac{(y - v^*)^2}{2\sigma_X{}^2}\right]\right]\Big|_{y_i}^{y_{i+1}} dv
\end{aligned} \tag{6-32}$$

Chapter 7. Investment Case Studies

7.1 SUMMARY OF US REAL ESTATE INVESTMENT INDUSTRY

It is worthwhile to examine the business context in which the investment decision-making procedure presented here would be used. Toward that end, several investors were contacted and interviewed to understand their current investment procedures, post-investment risk-management practice, and risk attitude. First, it is desirable to understand the number, size, and segmentation of real estate investment companies in the U.S. and Japan, in order to determine to what extent the investors are characteristic of the larger population.

In 1997, there were approximately 91,000 US business establishments specializing in residential and nonresidential real-estate investment (US Census Bureau, 2000b). Of this total, California had approximately 12,500 establishments, employing 57,000 people, with an annual payroll of $1.2 billion and annual revenues of $11.8 billion. The California industry is second only to New York State, where 1997 annual revenues totaled approximately $17.0 billion. Statistics for the United States, New York, California, and other significantly seismically active states are shown in Figure 7-1.

Table 7-1. Real estate investment in the US, 1997

Geography	Number of establishments	Number of employees	Annual payroll ($1,000)	Receipts ($1,000)
United States	91,215	413,101	8,502,291	77,726,341
New York	14,923	61,194	1,623,679	17,037,894
California	12,459	56,990	1,178,769	11,834,572
Illinois	3,197	17,248	387,799	3,172,660
Massachusetts	1,591	9,294	233,420	1,877,763
Washington	2,646	11,462	202,072	1,870,291
Missouri	1,726	7,575	145,285	1,217,685
Tennessee	1,390	6,681	123,002	926,386
South Carolina	678	2,504	44,855	374,820
Utah	477	2,280	38,124	298,209
Arkansas	643	2,240	33,351	288,188
Alaska	209	1,152	27,963	193,855

Real estate investment journals such as Commercial Property News (Commercial Property News Network, 2000) provide insight into common market segmentation. One way the industry segments itself is by property type: multifamily, industrial, office, retail, distribution/warehouse, health care, and hotel. Another is by the size or nature of the investment firm. Large institutional investors, for example, include banks, real estate investment trusts (REITs), pension funds, endowments, and life-insurance companies, who purchase relatively large properties with relatively low leverage, and look for stable earnings from leasing income. Smaller, entrepreneurial investors tend to use more leverage and expect their income to derive from market appreciation. Most California real estate firms are small. As shown in Figure 7-1, approximately 60% have four or fewer employees, and 95% of firms have fewer than 20 employees (US Census Bureau, 2000b). A third natural means of segmentation is by geographic region. While large investment companies can have hundreds or thousands of properties worldwide, smaller firms tend to specialize locally.

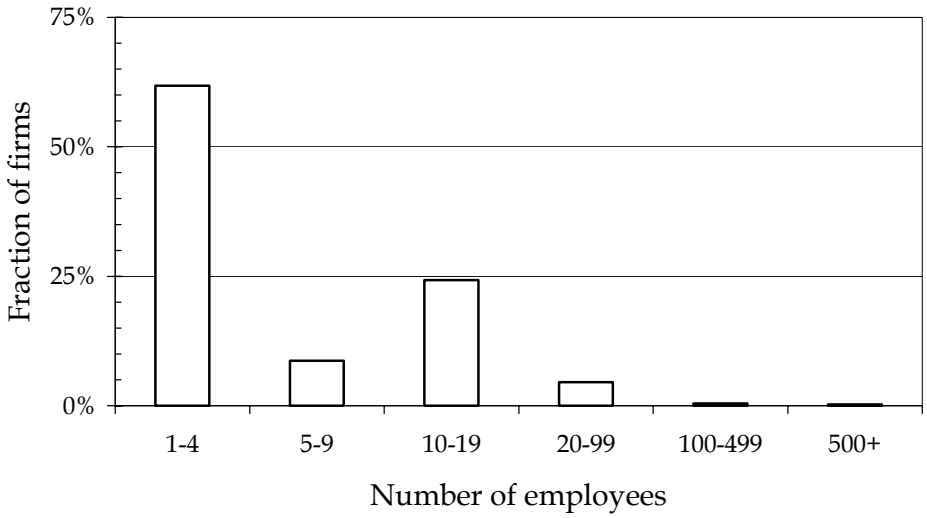

Figure 7-1. Size of California real estate firms

Several lessons can be drawn from these facts regarding implementation, dissemination, and marketing of the research results.

- Given the predominance of small firms, it is likely that most firms do not have dedicated risk managers who would already be familiar with technical concepts of risk. Consequently, any implementation of the decision-making procedures

presented and illustrated in the foregoing chapters must be simple, easy for investors to use in practice, and introduce the minimum amount of novelty into their current decision-making procedures.

- Since the methodologies presented here require estimation of annualized earthquake losses, rather than PML, it will be necessary to disseminate the concepts involved in calculating annualized losses, including the hazard curve and vulnerability function.

- Because of the large number of these small firms, widespread dissemination of the results of this study would require the methodology be communicated broadly such as via investment trade journals rather than one-on-one presentations.

- Geographic and property-type segmentation of the investor market suggests that dissemination in the U.S. should focus on California investors and California properties, and be written for the investor in commercial properties.

7.2 US INVESTOR CASE STUDY

7.2.1 Investor collaboration

The Caltech team arranged collaboration with two investment firms. For purposes of ensuring these companies' anonymity, the investment firms are referred to here as A and B.

Company A is a small real estate investment group with four employees, specializing in class-A commercial properties in the range of $10-$100 million value in the San Francisco Bay area. Company B is a publicly traded real estate investment trust (REIT). It specializes in developing, investing in, and managing large commercial properties in California, including office, retail, and mixed-use buildings. It owns and manages a total inventory in the range of 10 to 50 million sf. A typical property might be 50,000 sf to 500,000 sf in area, class-A, lowrise, midrise, or highrise.

The investors were introduced to the project as follows: "The objective of the research is to develop a methodology that helps real estate investors to account for

seismic risk in investment decisions. The methodology goes beyond PML studies to assess the probabilistic effect of seismic risk on investment return. It combines decision analysis with a new procedure to assess building-specific seismic risk."

The investor was asked to participate in two conversations, whose objectives are, first, to assess subjective risk attitude; second, to summarize the current practice of investment decision-making, and third, to assess the reasonableness of the methodology resulting from the research. Results of these interviews are now summarized.

7.2.2 Investment decision procedures

Companies A and B follow generally the same procedures to identify and assess investment opportunities. Typically, a real-estate broker approaches the investor with a package of information about an investment opportunity. The package typically contains a physical description of the property, area measures (occupied and total by type of use), information about the rent roll, including income and lease term for each tenant, expected operational and capital expenses, and all other details necessary to perform a financial analysis of the property. The information is often provided in both paper and electronic format.

Investors follow a two-stage analysis approach: in the first stage, the investor decides whether and how much to bid on the project. The analysis of the property during this stage is limited to a few labor hours. The property is screened to ensure that it is in the investor's market segment, and of appropriate size and quality. The pro-forma financial assumptions presented by the broker are assessed using in-house expertise for reasonableness. These assumptions include lease marketability, future vacancy, condition, and cost of management. A deterministic financial analysis is then performed to determine the yield on investment, with an analysis period of five to ten years. Limited studies are performed to determine the sensitivity of the yield to key uncertainties such as future vacancy rate and property rent inflation.

This first stage lasts two to four weeks, after which the first bidding round begins. A top executive at the level of President typically decides whether and how much to bid, based on the results of these preliminary analyses. Company A's

investment decision typically uses yield as the investment criteria; if the property will yield more than approximately 10%, the company will bid.

Within four to six weeks of the first bidding round, a winning bidder is selected. The winning bidder is not yet committed to the purchase, which is typically contingent on the results of a detailed due-diligence assessment of the property. The due-diligence stage can last 30 to 45 days.

The due-diligence assessment is more extensive than the preliminary assessment. In this latter stage, attorneys confirm the leasing conditions with the current tenants, and engineers review all aspects of the property, including structural, architectural, mechanical, electrical, and plumbing components. The purpose of these engineering analyses is to determine the need for maintenance and improvement expenses. The cost of these analyses for a recent $75 million investment by Company A was $50,000. Company B recently spent $100,000 on a due-diligence study of a $150 million property, and $30,000 for a study of a $25 million property.

The due-diligence assessment includes a study to evaluate earthquake risk, typically quantified as probable maximum loss (PML). The PML figure is used to determine whether earthquake insurance will be required. If the PML exceeds 20% to 25%, lenders typically require the purchase of insurance to cover the lender's equity. Neither Company A nor B purchases earthquake insurance to cover their own potential future earthquake losses, nor do they consider those uncertain costs in evaluating the investment yield. (This is in keeping with standard financial practice not to consider any uncertain event in the income stream.) Thus, these investors can be exposed to substantial earthquake risk, but ignore it in their financial analysis.

If the property passes the due-diligence assessment, the investor then has 30 to 60 days to arrange the purchase financing, after which the investor is committed to the purchase and the transaction is completed.

7.2.3 Post-investment practice

Neither Company A nor B perform any seismic risk-management after purchasing a property, other than the preparation of evacuation plans, and the

implementation of upgrades required by the lender. From that point until the liquidation decision, no further risk-management is performed.

Regarding liquidation of properties, Company A's president makes his decisions based on intuition, considering the company's current financial situation, and a desire to take profits at prudent intervals. His typical holding time is 18 months to 4 years.

Company B has so far liquidated very few properties, and has no formulated corporate policies on the liquidation decision. However, the decision-maker from Company B was able to summarize the decision process used to date. His past decisions to liquidate have been driven first by balance-sheet considerations, rather than considerations of the changing value of its properties. If the company's financial officers decide that cash is needed, they determine how much, and the liquidation decision is framed in terms of which property or properties should be sold to produce the desired income. Once this decision is made, the most important factors in the decision of which properties to sell include the following:

- The market: if the value of the property is down and not likely to rise soon, or if it is at the peak and likely to drop, the property is desirable to sell.
- Physical characteristics: older age and upcoming repair costs (deferred maintenance) make a property desirable to liquidate.
- Stabilization: Company B prefers to liquidate a property if all rents have been brought to market level.
- Portfolio consistency: is the property efficient, that is, within Company B's specialty, close to other properties and thus inexpensive to manage? If not, it is a good choice for liquidation.

7.2.4 Investor risk attitude

The procedures described in Appendix A were employed to determine the risk attitude of the investment decision-maker from Company A and Company B. Both interviews were successful. These data were compiled with previously derived data of

risk tolerance and company size for some decision-makers involved in real-estate development and other business not directly involved in real estate. The accumulated data are shown in Figure 7-2, which appears to indicate that risk tolerance is strongly related to company size, as measured in terms of annual revenue or department budget. The regression line shown in Figure 7-2 could be used to predict the behavior of competing bidders, or as a guideline for use with investors who are either unavailable for interviewing or who object to the form of the questions presented in Appendix A. The fit to the six data points quite good over an annual revenue range from $200,000 to $2 billion, as reflected in the high value (close to the maximum of 1.0) of R^2.

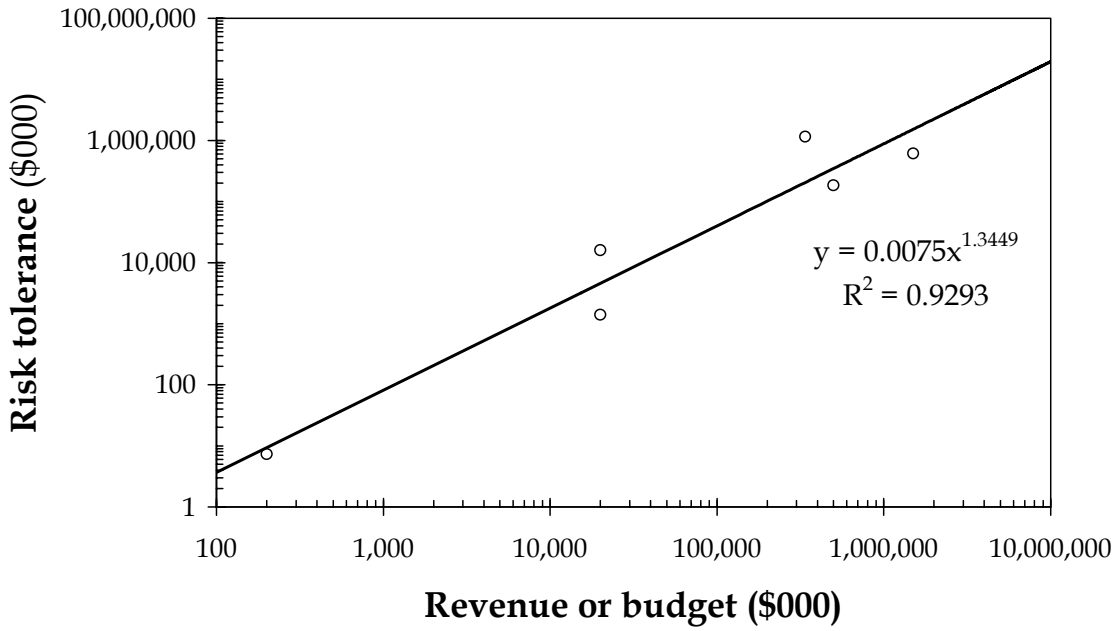

Figure 7-2. Relationship between risk tolerance and company size

It is also of interest to relate a decision-maker's risk tolerance to the size of investments in which he or she is commonly involved. Figure 7-3 illustrates an apparent relationship between the size of deals in which the decision-makers commonly invests, and the decision-makers' risk tolerance. The "deal size" measures the initial investment amount required for deals in which the decision-maker is typically involved. The decision-makers whose data are shown in the figure were asked what investment amount represented a typical small deal in which they would be involved, and a typical

large deal. They were allowed to define for themselves what a small deal and a large deal were.

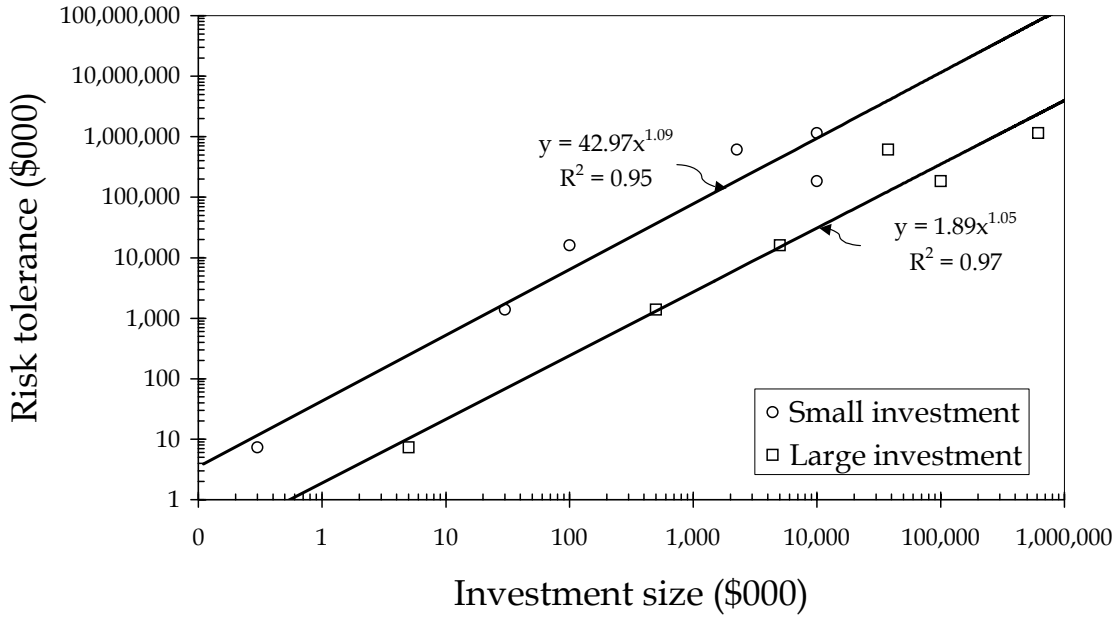

Figure 7-3. Relationship between risk tolerance and investment sizes

7.2.5 Feedback on proposed procedures

The results of this research were presented in summary form to the decision-maker of Company A. The methodology for calculating annualized loss was presented, and the results for the CUREE demonstration building were discussed. The decision-maker was asked whether the level of earthquake risk calculated for the CUREE demonstration building would be significant in an investment decision. He was also asked which aspects of the proposed decision-making procedures appear to be most practical, and therefore most likely to be adopted by investors.

The decision-maker feels that the level of risk in the CUREE demonstration building is on a borderline: the as-is building represents a significant risk whose annualized losses he would want to include in his financial analysis, and the risk to the retrofitted building is too small to consider. (The reader will recall from Chapter 5 that the as-is building has annualized loss on the order of 1% of the replacement cost of the

building, whereas the retrofitted building has an annualized loss on the order of 0.1% of replacement cost. These losses are before tax.)

The decision-maker was more receptive to the use of annualized loss. He feels that the expense for PML studies is mostly wasted, but that he would get real value from the annualized loss, particularly if it were easy to calculate and include in his financial analysis. He was less receptive to the decision-analysis aspects of the study. He believes that his current approach to handling market risk—via an increased discount rate—gives satisfactory results and adequately addresses his risk attitude and uncertainty on future income. This approach to handling market risk and risk attitude is fairly universal, and has a great deal of momentum that would be difficult to overcome among practitioners. The annualized loss aspects of the research, in contrast, do not compete with existing methods, and would encounter less resistance among investors.

7.2.6 Conclusions from investor collaboration

It is clear from the investor interviews that earthquake risk is a marginal consideration in their current practice. PML is the only earthquake risk parameter they consider, and they do not use PML in their financial analysis of an investment opportunity. Rather, a PML study is commissioned primarily to satisfy lenders, and the value of such a study is on the order of 0.02% of the purchase price (i.e., 20% of the cost of the overall due-diligence study). Therefore, to extend such an earthquake risk study to include economic parameters that are of value to the investor rather than the lender might be worth an additional 0.02% of the purchase price. That is, investors might be willing to spend a total of 0.04% or so to account for seismic risk in their financial analysis.

7.3 SUMMARY OF JAPANESE REAL ESTATE INVESTMENT INDUSTRY

7.3.1 Real estate investment trends in Japan

Real-estate investment trends in Japan have been changing, since international business standards came into Japan starting in 1997, causing a merger of real estate and financial business sectors as in the U.S. Nowadays, the role of the developers who are producing projects and investors who are taking a financial position is differentiating. Operating expertise, such as property management, facility management, and asset management become quite important for maximizing operating profits.

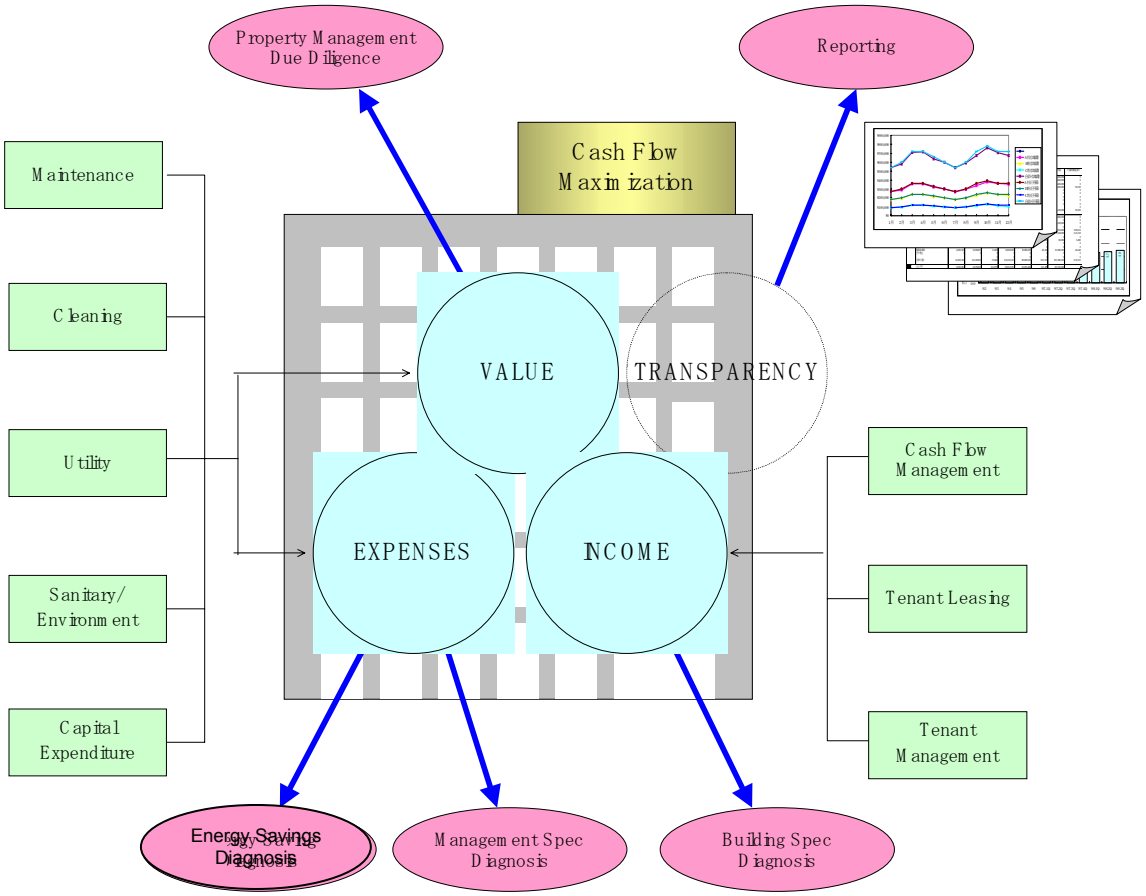

Figure 7-4. Property management to maximize operating income

The Japanese government adopted international accounting standards starting in 2000. In this circumstance, consolidated balance sheet and fair market value evaluation become crucial for corporate administration strategies. One of the solutions for corporate real estate strategy is leasing rather than ownership. Selling the head-office building

and leasing it back, non-recourse project finance, and securitization have become popular approaches to addressing these issues. The objective of corporate strategy is to minimize the company balance sheet and to maximize profit to enhance company credit.

Asset-backed securities. In 1999, publicly subscribed asset-backed securities (ABS) from real-estate projects totaled approximately 103 billion yen (US$940 million), which is 16.9% of the total ABS from that year.

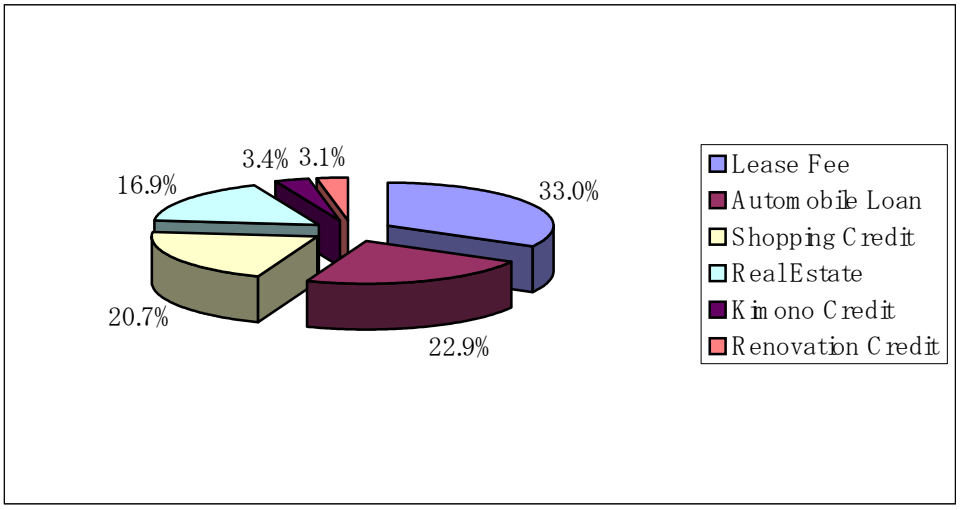

Figure 7-5. Asset-backed securities, per IBJS Credit Commentary (April 2000).

Investment. Investors are seeking income-producing property, mainly office and residential properties, and investments in new construction projects are not active in Japan at this moment. Investors are evaluating properties by the income-capitalization method. This method is quite different from the sales-comparison method that includes an expectation of capital gain, which was popular during the bubble era of the late 1980s. Investors are requiring developers to ensure that project parameters such as floor plans, operation, and value, will be suitable for investment after completion. Developers need expertise for these requirements. An example of the type of discounted cash-flow analysis that investors use is depicted in Figure 7-6.

Cash Flow of Office Building "X" at suburban city of Tokyo District

(US$)

		Year1	Year2	Year3	Year4	Year5	Year6	Year7	Year8	Year9	Year10	Year11
Revenue												
Rental Revenue		7,336,925	6,892,243	6,546,642	6,301,698	6,296,008	6,328,064	6,360,120	6,392,176	6,424,233	6,456,289	6,488,375
Common Area Charge Revenue		1,493,590	1,641,167	1,788,745	1,936,323	1,936,323	1,936,323	1,936,323	1,936,323	1,936,323	1,936,323	1,936,323
Parking Revenue		321,907	324,307	326,310	327,811	327,764	329,402	331,051	332,710	334,370	336,041	337,723
Other Revenue		64,885	66,040	67,179	68,334	68,334	68,470	68,607	68,745	68,882	69,020	69,158
Total Potential Gross Revenue		9,217,307	8,923,757	8,728,876	8,634,166	8,628,429	8,662,259	8,696,102	8,729,955	8,763,808	8,797,673	8,831,579
General Vacancy		2,269,619	1,829,544	1,387,512	942,045	939,189	943,982	948,777	953,573	958,369	963,166	967,965
Collection Loss		0	0	0	0	0	0	0	0	0	0	0
Effective Gross Revenue:①		6,947,688	7,094,213	7,341,364	7,692,121	7,689,240	7,718,277	7,747,324	7,776,382	7,805,439	7,834,507	7,863,614
Expense												
Maintenance Expense		1,330,000	1,330,000	1,330,000	1,330,000	1,330,000	1,332,660	1,335,325	1,337,996	1,340,672	1,343,353	1,346,040
Property Taxes		879,861	879,861	879,861	879,861	879,861	881,621	883,384	885,151	886,921	888,695	890,472
Insurance		46,400	46,400	46,400	46,400	46,400	46,493	46,586	46,679	46,773	46,866	46,960
Capital Reserve		284,281	284,281	284,281	284,281	284,281	284,281	284,281	284,281	284,281	284,281	284,281
Other Expense		513,444	563,423	612,677	662,656	662,656	663,981	665,309	666,640	667,973	669,309	670,648
Total Expense:②		3,053,986	3,103,965	3,153,219	3,203,198	3,203,198	3,209,036	3,214,885	3,220,747	3,226,620	3,232,504	3,238,401
Effective net retune③=①-②		3,893,702	3,990,248	4,188,144	4,488,922	4,486,042	4,509,241	4,532,439	4,555,635	4,578,819	4,602,003	4,625,213
Deposit												
Deposit Balance		4,127,835	4,161,684	4,280,225	4,484,121	4,484,121	4,506,939	4,529,761	4,552,585	4,575,409	4,598,236	4,621,079
Deposit Interest		82,557	83,234	85,604	89,682	89,682	90,139	90,595	91,052	91,508	91,965	92,422
Cash Flow After Deposit		3,976,259	4,073,482	4,273,749	4,578,605	4,575,724	4,599,380	4,623,034	4,646,687	4,670,328	4,693,967	4,717,635
PV		3,716,132	3,557,942	3,488,661	3,493,018	3,262,446	3,064,751	2,878,995	2,704,418	2,540,331	2,386,178	

Total Present Value		31,092,872	
Residual Value Terminal Cap Rate=	6.9%	68,371,516	
Net Residual Value		66,320,371	:Residual Value-Transaction expense
Present Net Residual Value Discount Rate=	7.0%	33,713,961	
Value		***64,806,832***	

Figure 7-6. Discounted cash-flow analysis

In Figure 7-6, total present value for *n* years is given by

$$PV_n = CF_1 / (1+DR) + CF_2 / (1+DR)^2 + \cdots\cdots + CF_n / (1+DR)^n \qquad (7\text{-}1)$$

Internal rate of return (IRR) is calculated by finding the value of IRR such that

$$-CF_o = CF_1/(1+IRR) + CF_2/(1+IRR)^2 + \cdots\cdots + CF_n/(1+IRR)^n \qquad (7\text{-}2)$$

where

CF_n = cash flow in year *n*

DR = discount rate

Fee Business. Compensation for real-estate expertise is in the form of a consultation fee. Fee-based business without any initial investment is a business opportunity for developers. Due diligence, seismic risk analysis, environment assessment, asset management, property management, fee development, and construction management are examples of these types of services. Kajima's real-estate investment advisory services can be outlined as shown Figure 7-7. These services seek to answer the following types of client questions:

- What is the advantage of owning properties?
- What is the fair market value?
- How much is the seismic risk for the property?
- Is it possible to take cash out of the property by project finance or securitization?
- What is the balance between risk and return for ownership of the property?
- How should the operating income be maximized?
- What is the best organization for operation?

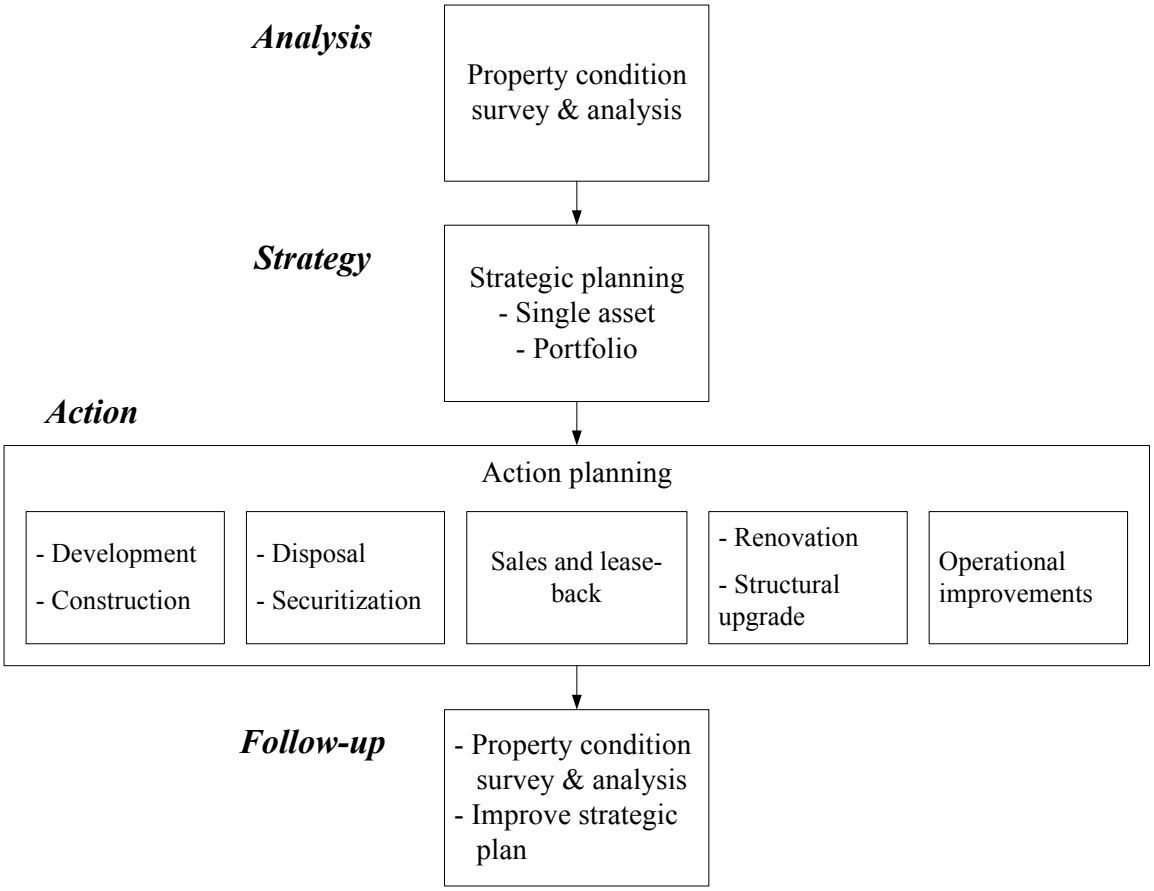

Figure 7-7. Kajima real-estate investment advisory services

Business opportunity. As mentioned in Chapter 6, average land prices announced by the Japanese government in 2001 fell. However, prices are recovering in the Tokyo central business district (CBD). This shows that the peak of corporate restructuring is over and an appropriate land price is being established. Securitization and international accounting standards underlie this trend. In addition, the current major supply of apartments, major supply of office space in 2003, new fixed-term lease contract law, and new J-REIT laws are supporting this change. It can be said that this is a revolution of the Japanese real estate business. Entities that cannot adjust to this change may not survive in this new economic world.

7.3.2 Risk management practice in real estate

When equity holders or lenders study real estate assignment or opportunity, they usually consider the following issues.

- Marketability analysis
- Due diligence
  (Property condition assessment and environment risk assessment)
- Property ownership & boundary line
- Tenant credit
- Governmental restrictions
- Neighborhood issues

Marketability analysis. Marketability analysis is of crucial importance before an investment. The goal of this analysis is to estimate the property value. There are three methods to establish property value: the cost approach, the sales-comparison approach, and the income-capitalization approach.

The cost approach works by adding the estimated value of land to the current cost of constructing a reproduction or replacement of improvements (such as structures) and deducting the amount of depreciation. The sales-comparison approach estimates value by comparing the subject property to recent sales prices of similar properties. The income-capitalization approach converts anticipated economic benefits of property ownership into a value estimate through a capitalization approach.

Between the end of World War II and the collapse of the Japanese bubble economy, land values never dropped. Consequently, most often Japanese properties were evaluated by the sales-comparison approach. Because land values have recently dropped, current assessment practice is shifting toward the income-capitalization approach. Because one cannot count on land-value appreciation, the project financing or securitization scheme must provide for the payment of interest to lenders and provision of profit to investors. Most Japanese real estate finance was corporate-based finance prior to four years ago.

The income-capitalization value is calculated by projection of cash flows. All annual income such as rents, parking fees, and even vending-machine income is included, as well as expenses such as property tax, management fees, insurance, and

reserves for repair and replacement. Due-diligence analysis is quite important for verifying assumptions of income and expenses.

During the strategic-planning process, several cases are considered, usually by changing rent, occupancy rate, or expected return rates. Optimistic, pessimistic, and most-likely cases are considered.

Property condition assessment. The purpose of property-condition assessment is to investigate current and future operating expenses. These expenses are input to a cash-flow projection. Major items are as follows:

- Immediate and short-term cost estimate to remedy deficiencies
- Long-term replacement reserve analysis
- Seismic risk analysis such as PML studies as a basis for evaluating seismic insurance premiums or for retrofit construction
- Building replacement cost estimate as a basis for evaluating replacement reserve and insurance

In addition to this analysis, ADA compliance, building code violation issues, and other problems are also investigated.

Environment risk assessment. Environmental risk was not a principal focus in Japan in the past. However, in the last four years, international business standards have come to Japan, and investors have become sensitive about this issue. The impact of environmental risk appears as litigation costs with tenants or buyers, soil improvement costs, and other improvement costs. At the preliminary stage of an environmental-risk study, investors investigate the following issues**:**

- Code compliance
- Potential source of geological contamination
- Hydrogeology
- PCB contamination
- Asbestos

- Underground and aboveground storage tanks

Property ownership and boundary-line determination. Property ownership is quite complicated and property law is favorable for tenants in Japan. Traditional leasehold and tenant lease law strongly protects tenants. Once they occupy a certain space, it is difficult to ask them to leave. However, the tenants can vacate the space after appropriate prior notice to the owner. This law was established soon after the Second World War, when there was shortage of housing. The situation is changing these days. Fixed-term leaseholds were established in 1993 and a fixed-term lease law was also established in 2000. This law allows the owner to control the leases as well as making it easier to predict future cash flow. During due diligence, investors also investigate the land registration record. Sometimes the boundary line between neighboring properties is not fixed. It is important to fix the boundary before purchase to avoid future trouble.

Tenant credit. To ensure stability of cash flow, the credit-worthiness of tenants is important. This is relevant not only because of the occupancy issue but also because if the problem tenant exists, the value of the property may go down.

Governmental restrictions. Governmental restrictions may have an impact on a property. For example, if a planned road ("Urban Planning Road") exists, it may affect the property site and future redevelopment. It is important to understand and investigate where local governments are currently planning roads.

7.4 JAPANESE INVESTOR CASE STUDY

7.4.1 Investor collaboration

As described in the previous section, real-estate investment practice in Japan has been transformed from being one of permanent property ownership through development and construction to being one of many investment choices sources in a general financial market. It can be also said that the Japanese real estate business is now required to engage in similar activities as US firms. From such a background trend, it is becoming increasingly important to estimate rationally the amount of uncertainty and risk involved in real-estate property values throughout the property lifetime. It is then of interest to compare the typical risk attitude of decision-makers in the US and Japan. When making financial decisions on various risk-return alternatives, the differences and similarities in subjective preference of decision-makers should directly affect their investment choices.

To investigate decision situations for investors and decision-makers in Japan, interviews were planned and performed along the concept of those done by the CUREE team. Figure 7-4 shows the interview process and potential applications of interview results. The interview script created by the CUREE team (see Appendix A) was translated into Japanese, including the conversion of monetary parameters into yen, as presented in Appendix B. The interview results were arranged in an Excel spreadsheet that was also prepared by the CUREE team. The utility functions obtained from these interviews for measuring Japanese risk attitude were evaluated in yen. The risk tolerances were re-converted to US dollars for comparing between US and Japanese investors. The results from US and Japanese interviews are applicable for making decisions on real estate investment in both countries.

As shown in Table 7-2, the interviews in Japan were performed with six persons concerned with decision-making for investment choices or financial planning. Decision makers 1, 4, and 5 are staff members at a financial department in a general company. DM#2 is a bank employee, and DM#3 and DM#6 are decision-makers in investment firms. All the interviewees are financial experts who understood the purpose of the interview and provided a great deal of valuable collaboration.

Their planning periods for investment have a range from three years to six years, regardless of their employment. The discount rates used varied widely, one percent to eighteen percent. The reason of this difference is not properly understood. The deal size for investment, especially the large investment, seems to correlate well with the annual revenue of the projects in which these decision-makers participate, as also found in the interviews with US decision-makers, performed by the CUREE team.

The interview results were analyzed to obtain the utility functions that account for the risk attitude of the Japanese decision-makers. The risk-tolerance parameter that determines the utility function can be calculated by minimizing the sum of squared errors from the expected utilities, as shown in the following section. The risk tolerances for the interviewees are summarized also in Table 7-2. The values for DM#3 and DM#6 could not be obtained because of the rejection of most of the hypothetical deals in the interview, and the subsequent divergence of the calculations. The results for DM#3 gave no minimum point with respect to the risk tolerance. DM#6 only provided two probabilities for small deals (x_S=\$50M) with a loss less than the initial investment, which were 50% for the deal of \$83M gain and \$17M loss, and 70% for the deal of \$33M gain and \$17M loss. These answers gave ρ=\$26.4M and \$15.9M respectively. The risk attitude of DM#6 may be more risk-averse than this evaluation suggests.

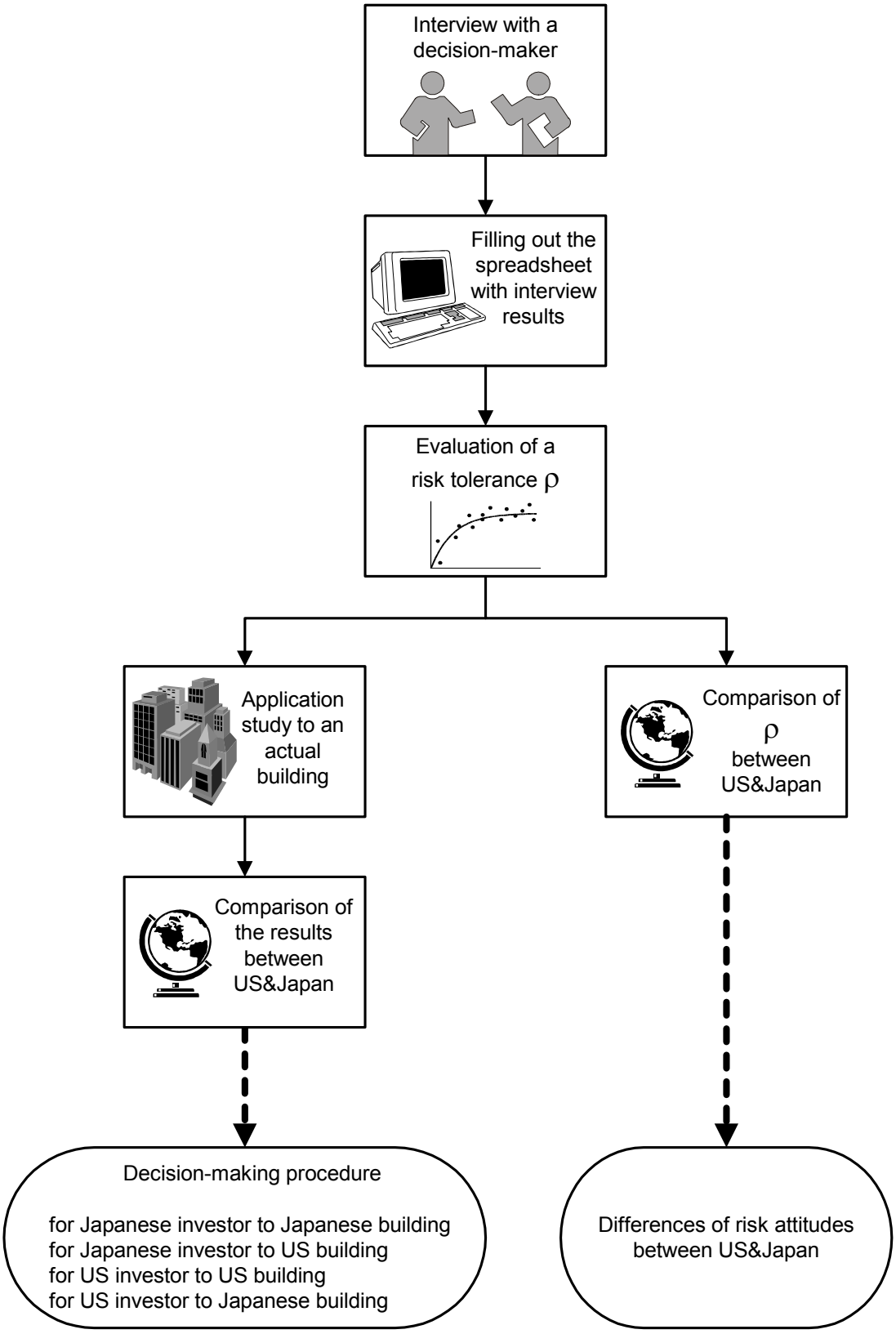

Figure 7-8. Risk attitude interview and applicability of interview results

Table 7-2. Summary of interviews in Japan

DM	Employ-ment (*1)	Date of interview	Planning period (year)	Discount rate (%)	Annual revenue ($M)	Small investment ($M)	Large investment ($M)	Risk tolerance ($M)
#1	C	10/23/00	3	8	800	30	300	311.72
#2	B	12/3/00	5	1	1000	100	1000	2124.63
#3	A	12/5/00	3	10	1000	5	500	
#4	C	12/14/00	6	18	6	5	25	33.18
#5	C	12/14/00	5	5	16	10	80	99.43
#6	A	3/19/01	3	15	20	50	200	

(*1) A : Investment firm
B : Bank
C : Financial dept. in general company

7.4.2 Investor risk attitude

The utility function $u(x)$ is described by an exponential with risk tolerance ρ:

$$u(x) = 1 - \exp(-x/\rho) \tag{7-1}$$

Let p_i be interviewee's indifference probability for the i^{th} deal. Considering ithe utility of zero to be zero, the expected utility of a single deal is given by

$$\begin{aligned} E[u(0)] = 0 &= E[u_i] \\ &= p_i\{1-\exp(-g_i/\rho)\} + (1-p_i)\{1-\exp(l_i/\rho)\} \end{aligned} \tag{7-2}$$

where g_i and l_i are the net gain and the net loss from the i^{th} deal. The value of the risk tolerance can be calculated by an iteration procedure such as the Newton-Raphson method for each hypothetical deal in the interview.

The risk tolerance representing the interviewee's risk attitude to all of the deals is then determined by minimizing the following sum of the squared errors, $e(\rho)$,

$$e(\rho) = \sum_{i=1}^{N} \left(E[u_i] \right)^2 \tag{7-3}$$

Figure 7-9 and Figure 7-10 show the risk tolerances calculated for each deal and the sum of the squared errors. The value of each interviewee's risk tolerance is identified as the value of ρ giving minimum error in the right-hand figures and are depicted as "ρ-average calculated" in the left-hand figures. As mentioned before, the sum of the squared errors for DM#3 has no minimum point. Figure 7-11 shows the risk tolerances compared with the results in the US. The solid line indicates the regression line of the US risk tolerances obtained by the CUREE team. These results can be summarized as follows:

- The utility functions accounting for decision-maker's risk attitude were evaluated for four of the six interviewees.
- The risk tolerance ρ shows correlation with the net gain and the net loss of the deal, especially loss values.
- Comparing with the US results, Japanese decision-makers in a relatively small project show greater risk tolerance. However, both DM#4 and DM#5 are financial experts in a big company dealing with general business. Decision-makers in small investment firms may have a more risk-averse attitude.
- Considering the above, risk attitudes of Japanese decision-makers show similar tendencies as US decision-makers with respect to project revenue or budget.
- The risk tolerances obtained from the interviews range from \$1M to \$2,000M. These results are applicable to a feasibility study in actual real estate business.

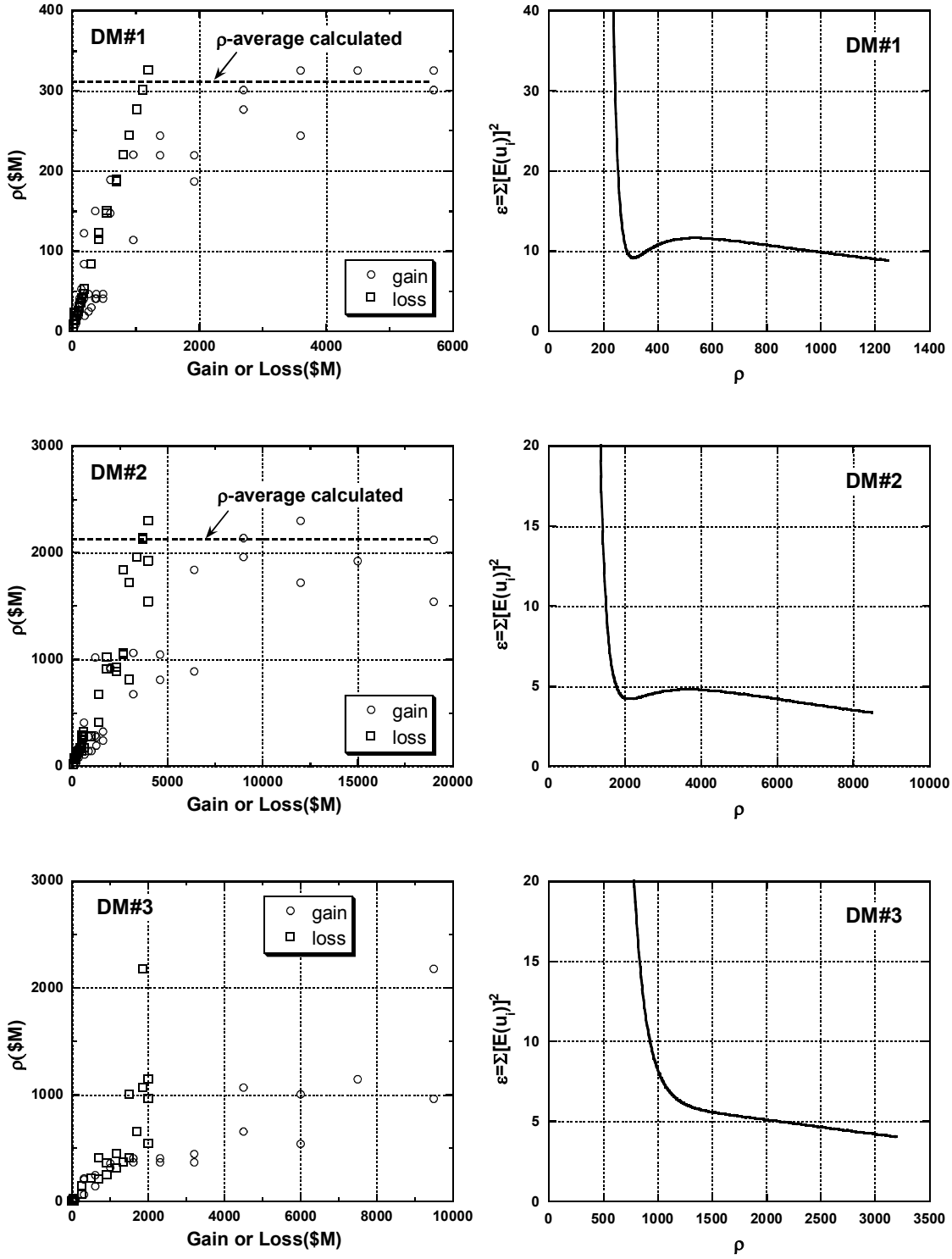

Figure 7-9. Interview results: risk tolerance ρ calculated for each deal (left) and errors vs. ρ (right)

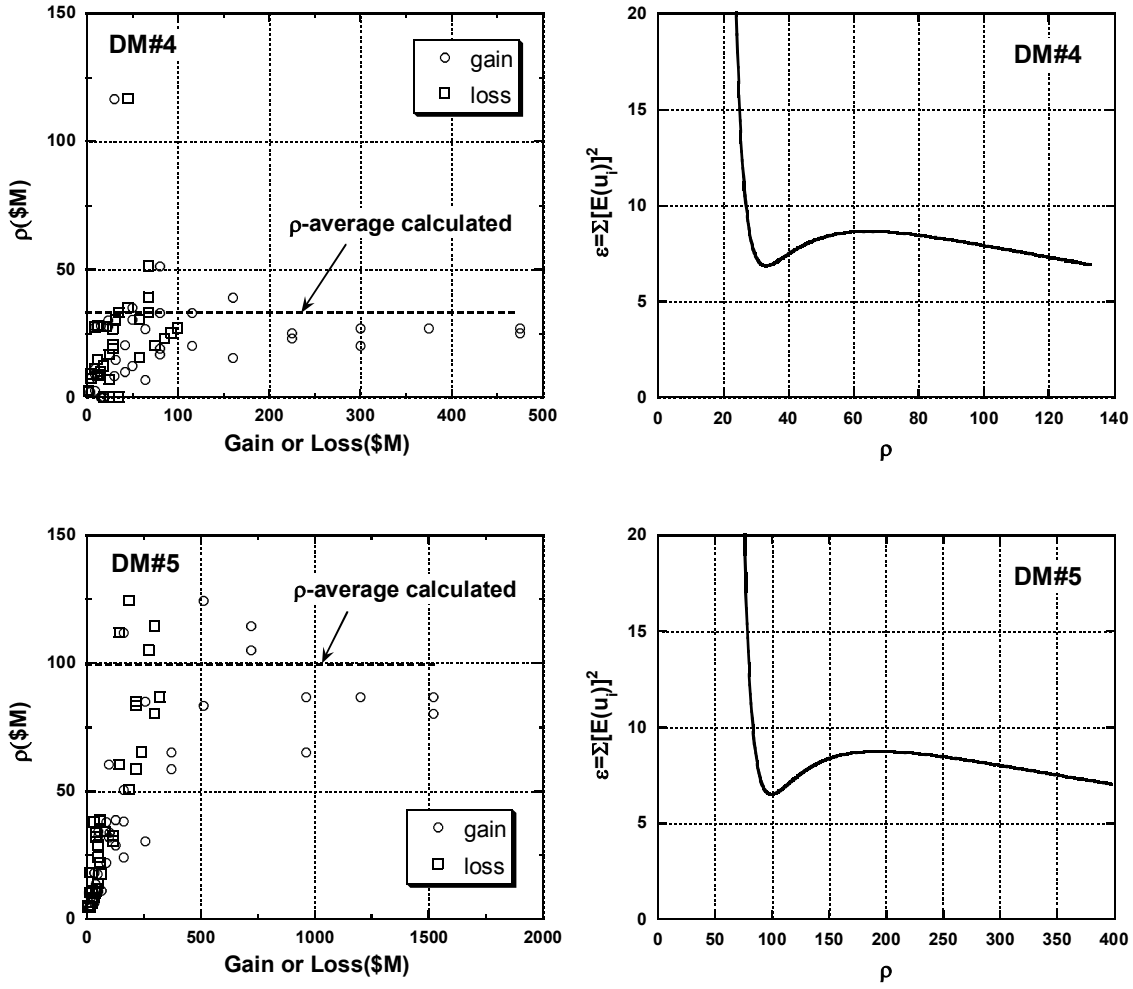

Figure 7-10. Interview results: risk tolerance ρ calculated for each deal (left) and errors vs. ρ (right) (continued)

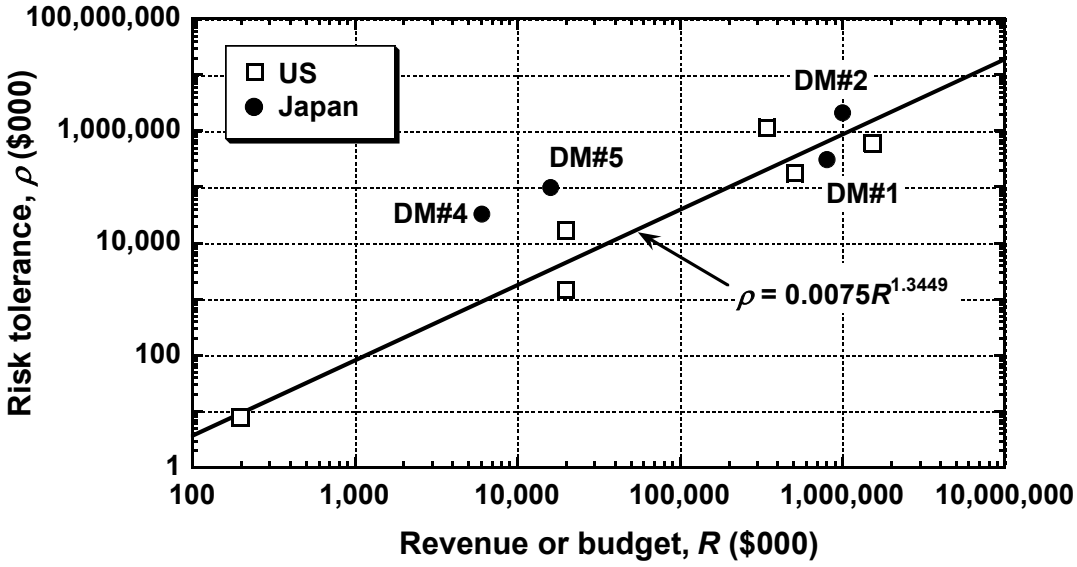

Figure 7-11. Comparison of risk tolerance ρ between US and Japan

Chapter 8. Conclusions and Future Work

8.1 CONCLUSIONS

Chapter 3 developed a methodology for calculating net asset value considering uncertain future net income, uncertain future earthquake repair losses, and initial equity. Future earthquake losses are modeled using a seismic vulnerability function, the site seismic hazard function, and an assumption that strong shaking at a site follows a Poisson process. The resulting formulae for mean and variance of net asset value are fairly simple.

Chapter 4 presented a methodology for making real estate investment decisions using the principles of decision analysis. It proposes that the investor choose among competing investment alternatives on the basis of the certainty equivalent (*CE*) of a deal, a parameter that gives the certain amount of money that the investor should consider equivalent to the uncertain investment. That is, the investor should be indifferent between accepting the *CE* immediately, or buying the property whose future net income (including future earthquake losses) is uncertain.

Figure 8-1 illustrates the decision-making methodology. In this figure, the present value of future net income is denoted by *I*, the decision-maker's risk-tolerance parameter is denoted by ρ, and the present value of future earthquake losses is denoted by *L*. The certainty equivalent is given by Equation 8-1, in which C_0 represents the investor's initial equity:

$$CE = E[I] - C_0 - E[L] - \frac{1}{2\rho}\left(\mathrm{Var}[I] + \mathrm{Var}[L]\right) + R \qquad (8\text{-}1)$$

Note that CE equals the expected net asset value (i.e., mean value net of the initial investment and expected lifetime earthquake losses), reduced by a quantity proportional to the total variance on net asset value, plus a negligible remainder term *R*. The constant of proportionality is 1/2ρ, which shows that as the decision-maker's risk tolerance ρ increases, the certainty equivalent increases to approach the expected net asset value, i.e., the decision approaches risk neutrality. (Chapter 5 showed that for the

CUREE demonstration building, Var[L] is small compared with Var[I], and can be neglected in Equation 8-1.)

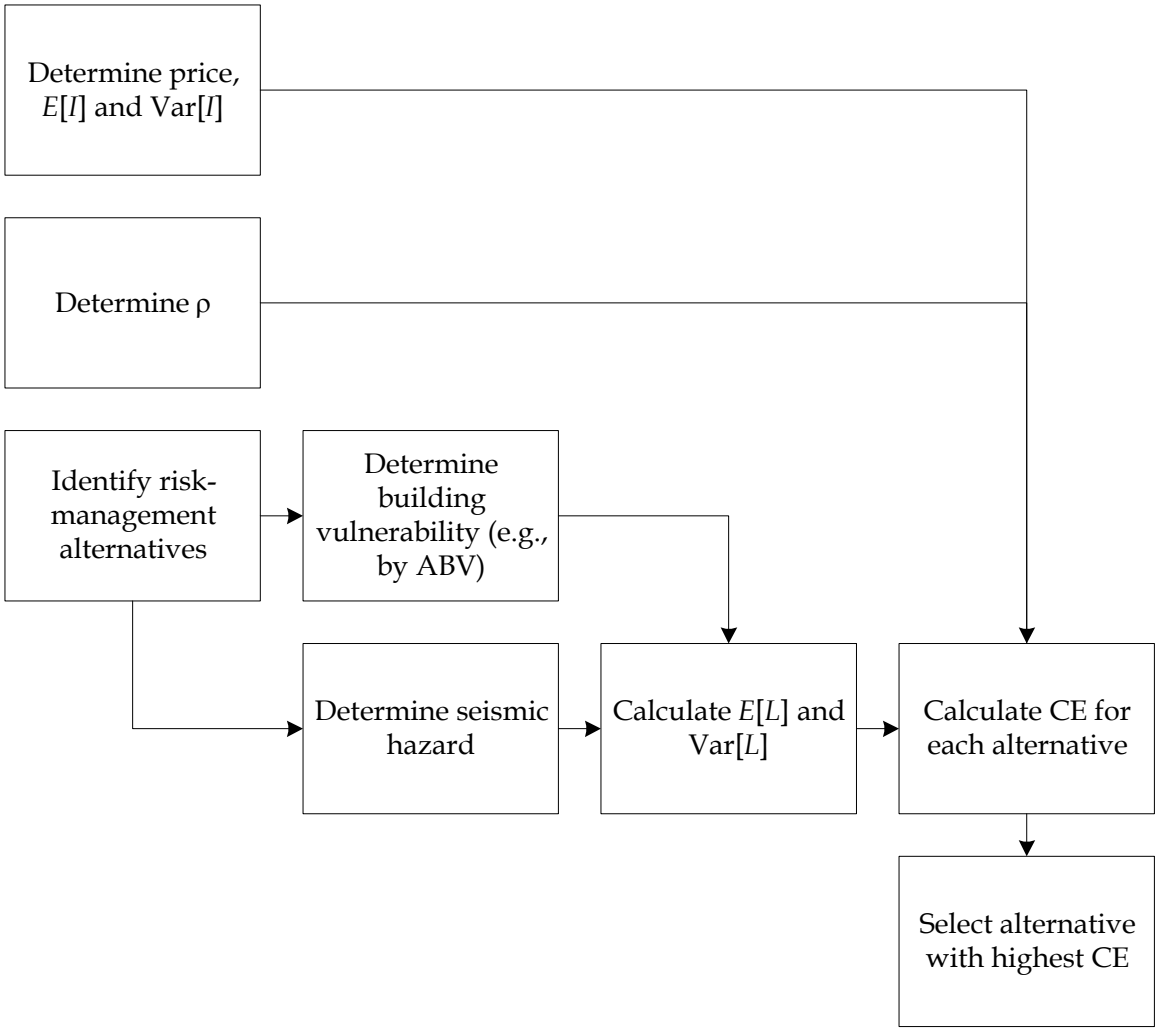

Figure 8-1. Proposed investment decision procedure

Chapter 5 illustrated the principles of Chapters 3 and 4 using a demonstration building located in Southern California. The investment opportunity was framed as a choice among four competing alternatives: do not buy; buy and leave the building as-is; buy and seismically retrofit; or buy the building and purchase earthquake insurance. The investment analysis relied on assembly-based vulnerability (ABV), a method of evaluating seismic vulnerability on a building-specific basis that was developed during Phase III of the Joint CUREE-Kajima Research Program.

In the process of creating the seismic vulnerability model of the CUREE demonstration building, the present study enhanced the library of fragility functions usable in future ABV analyses with several new assembly fragility functions for reinforced concrete moment frames. It also reflected for the first time uncertainty in the mass, viscous damping, and force-deformation behavior of the structural elements of the building under study.

Chapter 5 showed that for the CUREE demonstration building on the sample site, annualized earthquake losses are significant, and the differences between the annualized earthquake losses for the three purchase alternatives are significant: $43,000 for the retrofit alternative, $33,000 for the insurance alternative, and $55,000 for the as-is alternative (these are before-tax figures). The chapter also compared the present value of future earthquake losses with the present value of future income. It showed that earthquake loss $E[L]$ is a significant fraction (4%) of the expected present value of income, $E[I]$. This is equivalent to a reduction in the capitalization rate from the nominal level of 13% to an earthquake-risk-adjusted value of 12.5%. Thus, earthquake risk modestly affects the true capitalization rate.

The decision analysis for the CUREE demonstration building showed that for likely ranges of the variables chosen by the decision-maker—the risk-free discount rate, market risk, and decision-maker's risk tolerance—the best alternative is to purchase the building and leave it as-is. The *CE* of the as-is alternative slightly exceeds that of buying and retrofitting the building, because the cost of retrofit slightly exceeds the expected reduction in future earthquake losses. Note that the value of human life was ignored in the present analysis. Had it been included, the difference between as-is and retrofit would have been less, or retrofit might have been preferred to as-is. The illustration also showed that both of these alternatives are preferable to purchasing insurance, and that all three are preferable to not buying.

The decision analysis showed that two of the parameters selected by the decision-maker, namely the risk tolerance and market risk (variability of income), materially affect the decision. That is, taking different reasonable values for them can lead to a different preferred decision. The risk-free discount rate is immaterial to the

decision for a reasonable range of possible values of the parameter. In the presence of low to moderate uncertainty on income, and for moderate to high investor risk tolerance, the best decision is to buy and leave the building as-is. In the presence of a high uncertainty on net income or low investor risk tolerance, the best decision is the do-not-buy alternative. (It may be that for short planning periods, the buy and insure alternative would be preferable, but this possibility was not investigated.)

Chapter 5 also showed that the bulk of future economic losses for the CUREE demonstration building were attributable to low to moderate shaking levels ($S_a \leq 0.2$g), whose return periods are on the order of 50 years or less (i.e., whose exceedance probability is 10% or greater in 5 years). This is as opposed to events associated with the probable maximum loss (PML), whose return period is typically on the order of 500 years (10% probability of exceedance in 50 years). This indicates that the PML-level performance, while it remains a reasonable worst-case loss, is largely irrelevant to the likely economic cost of owning this property.

Chapter 6 presents three additional methods of evaluating seismic vulnerability, using techniques developed by the Kajima Corporation. They offer low-level, moderate-level and high-level alternatives for seismic evaluation on a building-specific basis. Based on these methods and seismic hazard estimation at a site, the seismic vulnerability analysis was performed using three demonstration buildings. These buildings have different levels of seismic performance, i.e., low-level, low-level but retrofitted and very high-level performances. The expected earthquake losses over the next 475 years were estimated as 14.7%, 8.4%, and 1.7% of replacement cost, respectively. The marketability analysis using "Kajima D Program" also demonstrated the cash flows of the buildings. Rental rate and occupancy rent were considered as the parameters to be varied. The analysis results showed that the seismic retrofit is efficient for increasing the cashflow. Moreover, a simple model for probability function of net asset value was examined to illustrate the relationship between the expected utility and the risk tolerance.

Chapter 7 summarizes the real-estate investment industry and standard investment practice in the United States and Japan. It shows that in the United States, small investment firms predominate. Because of the small size of firms, it is concluded

that any implementation of the decision-making procedures developed here must be simple, easy to use, and introduce a minimum amount of novelty into current decision-making procedures. Because of the large number of small firms, widespread dissemination of the results of this study would require the methodology to be communicated broadly, such as via investment trade journals, rather than through one-on-one presentations. In addition, the geographic and property-type segmentation of the real estate investment market suggests that dissemination in the U.S. should focus on California investors and California properties, and be written for the investor in commercial properties. Real-estate trends and the risk management practices in Japan are also summarized.

From the investor interviews, it is found that investors are unaware of concepts of annualized losses, seismic hazard and seismic vulnerability; successful dissemination of the results of this study must introduce these concepts. The investors interviewed all but ignore seismic risk in real estate investment decision-making, using PML solely to secure loans. PML studies are performed during the due-diligence phase of an investment, and cost on the order of 0.02% of the purchase price of the building. It can be concluded that investors would be receptive to the decision procedures developed here only if they could be implemented with a similar level of effort.

The investor interviews performed for this study and in earlier studies show useful relationships between the decision-maker's risk-tolerance parameter and his or her revenue or budget, and between the risk-tolerance parameter and the size of deals in which he or she typically engages. These relationships can be used as guidelines or as a sanity check of risk tolerance in implementing the decision procedure for other investors. These relationships are duplicated in Figure 8-2, Figure 8-3, and Figure 8-4. The interviews in Japan suggested that there is little difference between the risk tolerance of US and Japanese decision-makers, as shown in Figure 8-4.

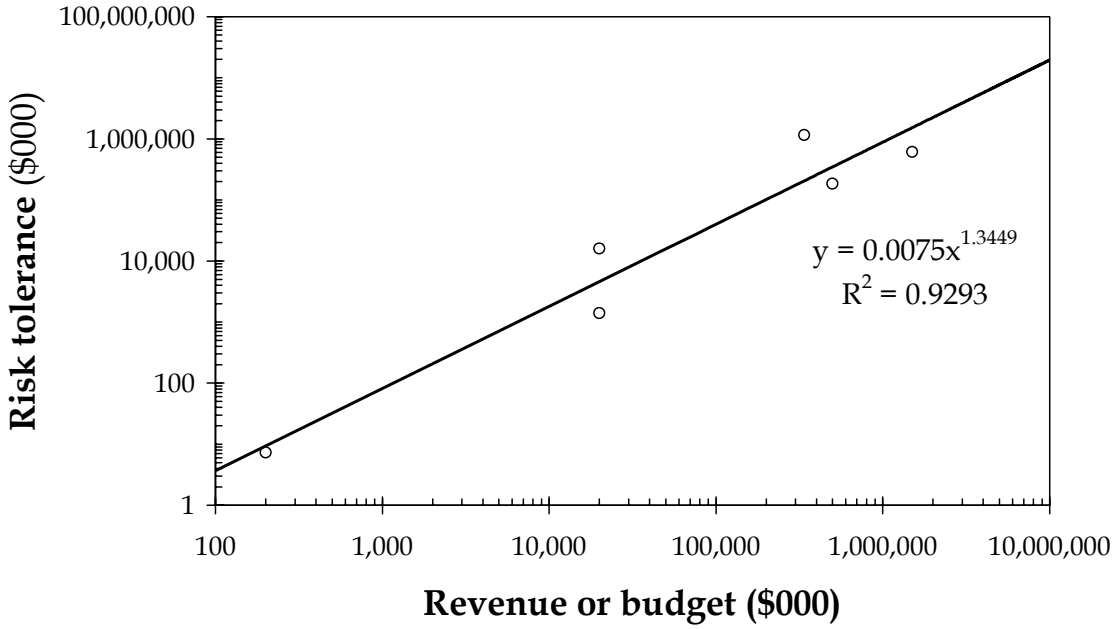

Figure 8-2. Relationship between risk tolerance and company size

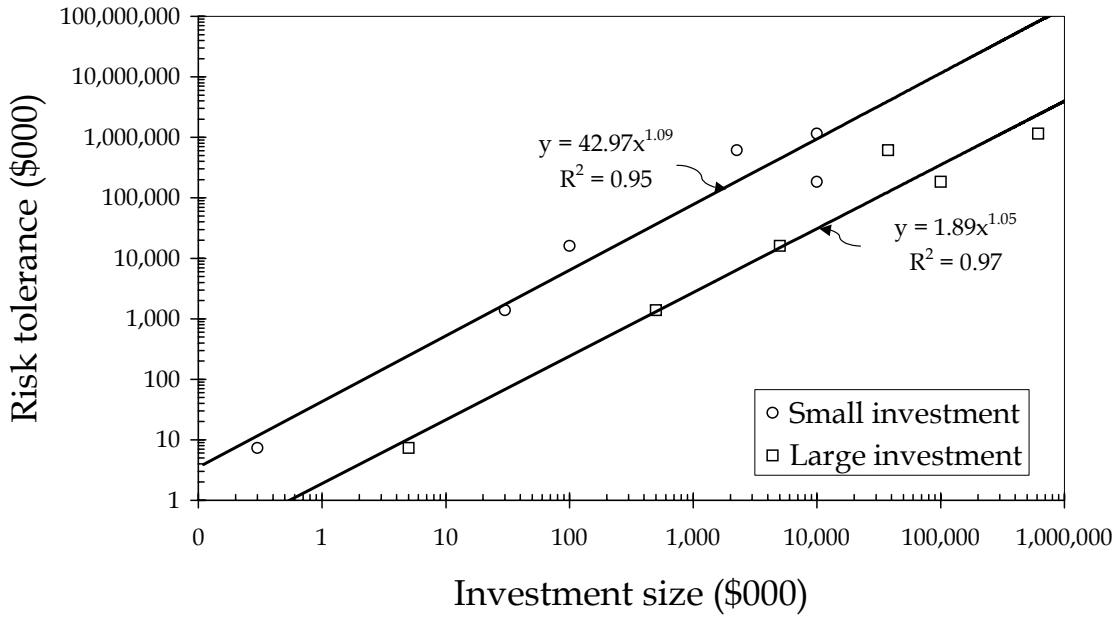

Figure 8-3. Relationship between risk tolerance and investment sizes

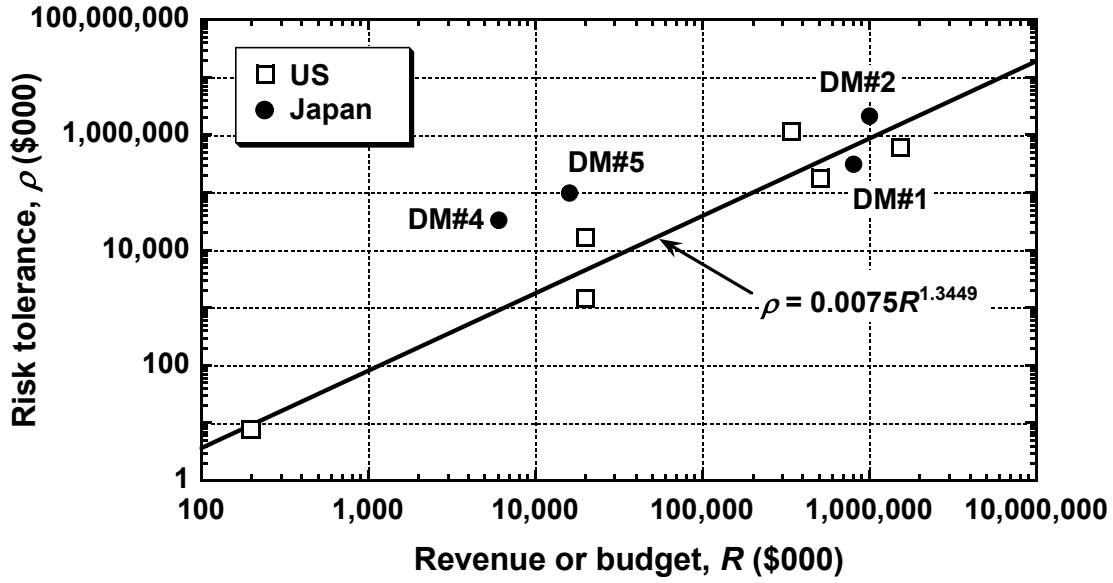

Figure 8-4. Comparison of risk tolerance ρ between US and Japan

8.2 FUTURE WORK

Improve the market-risk stochastic model. It is found that market risk represents the vast majority of uncertainty on asset value, and therefore accounts for the bulk of the effect of investor risk aversion on the decision process. However, a random-walk model of future income that was studied here produces questionable results, perhaps because it inadequately accounts for investor knowledge. It would therefore be valuable to improve the market-risk stochastic model and validate it using a statistically significant number of investment case studies, where actual long-term income is compared with initial income projections.

Improve the risk-attitude interview. It is found that some investors objected to some of the questions of the risk-tolerance interview, indicating that the situations these questions posited (namely, large financial losses) would never occur in practice. It would therefore be desirable to improve the risk-attitude interview to reflect only common investment situations.

Account for uncertainties in repair method and in loss conditioned on repair cost. The ABV procedure for evaluating seismic vulnerability is implemented here to account for

uncertainties in ground motion, mass, damping, force-deformation behavior, assembly fragility, assembly repair cost, and contractor overhead and profit. However, some uncertainties are neglected, which could be included in later studies. First, the present study identified situations where a particular assembly damage state could be repaired by a choice from several competing methods, so that the repair method that would be chosen for future damage is uncertain. Second, loss as a function of repair cost could be uncertain, for example because of variable insurance-adjustment techniques. It would be interesting to expand the analysis to evaluate the effects of these uncertainties on the overall loss uncertainty.

Couple damage state with force-deformation relationship. Another interesting issue is that, as implemented here, ABV decouples structural load-deformation behavior from structural assembly damage. That is, structural response is conditioned on ground motion, member configuration, mass, damping, and the force-deformation behavior of structural members, but structural assembly damage is conditioned only on the structural response to which it is subjected. For example, the beam damage state is taken as a random function of maximum beam curvature. It would be interesting to associate the damage state of each structural assembly more closely with the point reached on its force-deformation curve during the structural analysis in each simulation. For example, the yield and ultimate points on the moment-curvature relationship for a reinforced concrete beam could be conditioned on uncertain concrete cylinder strength. If the beam exceeds the (uncertain) yield point but not the (uncertain) ultimate point, it would be taken as being in the yield damage state.

Examine simpler dynamic analysis as a means to estimate vulnerability. Since the variance on the lifetime earthquake loss was shown to have a negligible effect on the investment decision, it would also be interesting to determine whether simpler dynamic analysis can produce the same mean vulnerability function as the relatively computationally intensive ABV method examined here. For example, would the simpler Kajima methods or other approaches produce a similar vulnerability function for the CUREE demonstration building? Would ABV produce the same vulnerability function

as the Kajima methods for the Kajima demonstration buildings? These are questions worthy of additional study.

Examine the relationship between simplified engineering demand parameters and performance. Performance-based design standards being developed specify peak interstory drift ratios associated with operability, immediate occupancy, life safety, and collapse prevention. Since the ABV method models building performance at a very detailed level, it would be valuable to check the drift-to-performance relationships posited in these developing codes.

Create category-based vulnerability functions. It would be interesting to develop category-based seismic vulnerability functions that employ detailed ABV analyses of individual buildings. Current category-based methods rely extensively on expert opinion. While such an approach has been historically necessary, it is shown in the present study that expert opinion can underestimate uncertainty in loss. In general, reliance on expert opinion can reduce the apparent information value of a loss estimate, compared with one based on detailed engineering analyses, providing decision-makers with an excuse not to act. It would therefore be valuable to compile a large number of building-specific vulnerability functions that do not rely heavily on expert opinion, and use them to create category-based vulnerability functions to check or enhance those based on expert opinion. Additional automation of the ABV methodology could make such research practical.

Collaborate with lenders and real-estate industry analysts on risk-management standards. The REIT decision-maker interviewed for this study was unreceptive to the notion of accounting for seismic risk in his financial analysis, because to do so would decrease the apparent value of the REIT's properties to shareholders and independent analysts. The decision-maker would include seismic risk in his analysis only if lenders, insurers or analysts required him to do so, or if it were the industry's standard practice to do so. It would be valuable to discuss seismic risk assessment with lenders and industry analysts to determine the conditions under which they believe seismic risk should be evaluated and reflected in investors' financial analysis.

Chapter 9. References

Aboutaha, R. S., Engelhardt, M.D., Jirsa, J.O., and Kreger, M.E., 1993, "Seismic Strengthening of R/C Columns Using Steel Jackets," ***American Society of Civil Engineering Structures Congress***, Irvine CA.

Abramowitz, M., and Stegun, I.A., 1964, ***Handbook of Mathematical Functions,*** Washington, DC: U.S. Government Printing Office

Aguilar, J., Juarez, H., Ortega, R., and Iglesias, J., 1989, "The Mexico Earthquake of September 19, 1985 -- Statistics of Damage and Retrofitting Techniques in Reinforced Concrete Buildings Affected by the 1985 Earthquake", ***Earthquake Spectra, Vol. 5, No. 1***, Oakland, CA: Earthquake Engineering Research Institute, pp. 145-151.

Altin, S., Ersoy, U., and Tankut, T., 1992, "Hysteretic Response of Reinforced Concrete Infilled Frames", ***Journal of Structural Engineering, Vol. 118, No 8.***

American Concrete Institute (ACI), 1996a, ***ACI 224.1R-96, Causes, Evaluation, and Repair of Cracks in Concrete Structures***

American Concrete Institute (ACI), 1996b, ***ACI 546R-96, Concrete Repair Guide***

American Institute of Steel Constructions (AISC), Inc., 1997, ***Seismic Provisions for Structural Steel Buildings,*** Chicago, IL.

American Society for Testing and Materials (ASTM), 1999, ***E 2026-99 Standard Guide for the Estimation of Building Damageability in Earthquakes,*** West Conshohocken, PA, 24 pp.

Ang, A.H.S., and Tang, W.H., 1975, ***Probability Concepts in Engineering Planning and Design, Vol. 1., Basic Principles,*** John Wiley and Sons, New York, 409 pp.

Ang, A.H.S., Der Kiureghian, A., Fillippou, F., Pires, J., and Polak, E., 1996, ***Reliability-Based Optimal Aseismic Design of Reinforced Concrete Buildings,*** Richmond, CA: Consortium of Universities for Research in Earthquake Engineering

Aoyama, H., Kato, D., Katsumata, H., and Hosokawa, Y., 1984, "Strength and Behavior of Postcast Shear Walls for Strengthening of Existing Reinforced Concrete

Buildings", ***Eighth World Conference on Earthquake Engineering, San Francisco CA, Vol. 1.***

Applied Technology Council, 1985, ***ATC-13: Earthquake Damage Evaluation Data for California,*** Redwood City, CA, 492 pp.

Au, S.K. and Beck, J.L., 2000, ***On the Solution of First-Excursion Failure Problem for Linear Systems by Efficient Simulation***, Division of Engineering and Applied Science, California Institute of Technology, Pasadena, CA, 46 pp.

Banon, H., Biggs, J.M., and Irvine, H.M., 1981, "Seismic Damage in Reinforced Concrete Frames", ***Journal of Structural Engineering, Vol. 107***, pp. 429-444.

Beck, J., Kiremidjian, A., Wilkie, S., Mason, A., Salmon, T., Goltz, J., Olson, R., Workman, J., Irfanoglu, A., and Porter, K., 1999, ***Decision Support Tools for Earthquake Recovery of Businesses,*** Richmond, CA: Consortium of Universities for Research in Earthquake Engineering

Bonacci, J.F., and Maalej, M., 2000, "Externally Bonded FPR for Service-Life Extension of RC Infrastructure", ***Journal of Infrastructure Systems, Vol. 6, No. 1,*** pp. 41-51.

Boore, D.M., Joyner, W.B., and Fumal, T.E., 1997, "Equations for Estimating Horizontal Response Spectra and Peak Accelerations from Western North American Earthquakes: a Summary of Recent Work," in ***Seismological Research Letters, Vol. 68, No. 1, January/February1997,*** El Cerrito, CA: Seismological Society of America, pp. 128-153

Bush, T.D., Talton, C.R., and Jirsa, J.O., 1976, "Behavior of Structure Strengthened Using Reinforced Concrete Piers", ***ACI Structural Journal***.

Byrne, P., and Cadman, D., 1984, ***Risk, Uncertainty, and Decision-making in Property Development,*** Cambridge, Great Britain: University Press, 182 pp.

Capen, E.C., 1976, "The Difficulty of Assessing Uncertainty," ***Journal of Petroleum Technology,*** August 1976, Society of Petroleum Engineers, 843-850

Carr, A.J., 2001, ***Ruaumoko,*** Christchurch, New Zealand: University of Canterbury

Case, F.E., 1988, ***Investing in Real Estate, 2nd Edition,*** Des Moines, IA: Prentice Hall Books, 288 pp.

Chai, Y.H., Romstad, K.M., and Bird, S.M., 1995, "Energy-Based Linear Model for High-Intensity Seismic Loading", ***Journal of Structural Engineering, Vol. 121***, pp. 857-864

Commercial Property News (CPN) Network, 2000, series, ***Commercial Property News***, San Francisco, CA: Miller Freeman, Inc.

Corazao, M., and Durrandi, A.J., 1989, ***Repair and Strengthening of Beam-to-Column Connections Subjected to Earthquake Loading, Technical Report NCEER-89-0013,*** Buffalo, NY: National Center for Earthquake Engineering Research, State University of New York

Earthquake Engineering Research Institute (EERI), 1994, ***Expected Seismic Performance of Buildings***, ***Publication SP-10***, Oakland, CA.

Earthquake Engineering Research Institute (EERI), 1994b, ***Northridge Earthquake January 17, 1994, Preliminary Reconnaissance Report, Publication 94-01***, Oakland, CA, 96 pp.

Earthquake Engineering Research Institute (EERI), 1997, ***Earthquake Spectra, Vol. 13, No. 4,*** Oakland, CA, 114 pp.

Eberhard, M.O., Mookerjee, A., Parrish, M., 2001, ***Uncertainties in Performance Estimates for RC Columns,*** Pacific Earthquake Engineering Research Center, Richmond, CA, http://ce.washington.edu/~peera1

Ellingwood, B., Galambos, T.V., MacGregor, J.G., and Cornell, C.A., 1980, ***Development of a Probability Based Criterion for American National Standard A58, Special Publication 577,*** Washington, DC: National Bureau of Standards, 222 pp.

Ersoy, U., 1992, "Repair and Strengthening of R/C Structures – Research at METU", ***International Symposium on Earthquake Disaster Prevention, Vol. 2***

Ersoy, U., Tankut, A.T., and Suleiman, R., 1993, "Behavior of Jacketed Columns", ***ACI Structural Journal, Vol. 90, No 3.***

Federal Emergency Management Agency (FEMA), 1997, ***FEMA-273: NEHRP Guidelines for the Seismic Rehabilitation of Buildings,*** Washington, DC, 386 pp.

Federal Emergency Management Agency (FEMA), 2000, ***FEMA-356: Prestandard And Commentary for the Seismic Rehabilitation of Buildings,*** Washington, DC, 517 pp.

Flynn, G., 1998, personal communication.

Frankel, A., Mueller, C., Barnhard, T., Perkins, D., Leyendecker, E. V., Dickman, N., Hanson, S., and Hopper, M., 1996, ***Seismic Hazard Maps for the Coterminous United States, USGS Open File Report 96-532.*** Menlo Park: US Geological Survey.

Frankel, A., and Leyendecker, E. V.,2001, ***Seismic Hazard Curves and Uniform Hazard Response Spectra for the United States, User Guide, Software Version 3.10,*** Denver, CO: US Geological Survey.

Fujiwara T., 1996, "Damage on Reinforced Concrete Buildings", The Hanshin-Awaji Great Disaster, -Measure for disaster prevention research-, ***Disaster Prevention Research Institute, Kyoto University***, pp.424-442. (in Japanese)

Goel, S.C., and Lee, H.S., 1990, "Seismic Strengthening of R/C structures by Ductile Steel Bracing System", ***Proceedings of Fourth U.S. National Conference on Earthquake Engineering, Palm Springs CA, Vol. 3***.

Hipley, P., 1997, "Bridge Retrofit Construction Techniques", ***Second National Seismic Conference on Bridges and Highways, Sacramento, California, July 8-11, 1997.***

Holland, A.S., Ott, S.H., and Riddiough, T.J., 2000, "The Role of Uncertainty in Investment: An Examination of Competing Investment Models Using Commercial Real Estate Data", ***Real Estate Economics, Vol. 28,*** pp. 33-64

Howard, R.A., 1970, "Risk Preference," ***Readings on The Principles and Applications of Decision Analysis, vol. 2: Professional Collection,*** R.A. Howard and J. E. Matheson, eds., Menlo Park, CA: Strategic Decisions Group, pp. 627-663

Howard, R.A., and Matheson, J.E., 1989, ***Readings on The Principles and Applications of Decision Analysis,*** Menlo Park, CA: Strategic Decisions Group

International Code Council, 2000, ***International Building Code,*** Whittier, CA: International Conference of Building Officials, 756 pp.

International Conference of Building Officials (ICBO), 1991, ***Uniform Code for Building Conservation,*** Whittier, CA

International Conference of Building Officials (ICBO), 1997, ***Uniform Building Code,*** Whittier, CA

Irfanoglu, A., 2000, ***Structural Design Under Seismic Risk Using Multiple Performance Objectives, EERL Report No. 2000-02,*** Pasadena, CA: California Institute of Technology

Islam, M.S., 1996a, "Analysis of the Response of an Instrumented 7-story Nonductile Concrete Frame Building Damaged During the Northridge Earthquake," ***Proceedings of the 1996 Annual Meeting of the Los Angeles Tall Buildings Structural Council, May 10, 1996, Los Angeles, CA.***

Islam, M.S., 1996b, "Holiday Inn," ***1994 Northridge Earthquake Buildings Case Study Project Proposition 122: Product 3.2,*** Sacramento CA: Seismic Safety Commission, 189-233.

Islam, M.S., Gupta, M., and Kunnath, B., 1998, "Critical Review of The State-Of-The-Art Analytical Tools and Acceptance Criterion in Light of Observed Response of an Instrumented Nonductile Concrete Frame Building," ***Proceedings, Sixth US National Conference on Earthquake Engineering, Seattle, Washington, May 31-June 4, 1998,*** Oakland CA: Earthquake Engineering Research Institute, 11 pp.

Jennings, P.C., 1971, ***Engineering Features of the San Fernando Earthquake of February 9, 1971, Report EERL 71 – 02,*** Pasadena, CA: California Institute of Technology

Jeong, G.D., and Iwan, W.D., 1988, "Effects of Earthquake Duration on the Damage of Structures", ***Earthquake Engineering and Structural Dynamics, Vol. 16,*** pp. 1201-1211.

Karter, M.J., 1999, ***Fire Loss in the United States During 1998,*** Quincy, MA: National Fire Protection Association, 42 pp.

Kunnath, S.K., Reinhorn ,A.M., and Lobo, R.F., 1992, ***IDARC Version 3.0: A Program for the Inelastic Damage Analysis of RC Structures, Technical Report NCEER-92-0022,*** Buffalo, NY: National Center for Earthquake Engineering Research, State University of New York

Kustu, O., 1986, "Earthquake Damage Prediction for Buildings Using Component Test Data," ***Proc. Third U.S. National Conference on Earthquake Engineering, Aug 24-28, 1986, Charleston, SC,*** El Cerrito, CA: Earthquake Engineering Research Institute, pp. 1493-1504

Kustu, O., Miller, D.D., and Brokken, S.T., 1982, ***Development of Damage Functions for Highrise Building Components,*** San Francisco: URS/John A Blume & Associates for the US Department of Energy

Li, Y.R., and Jirsa, J.O., 1998, "Nonlinear Analyses of an Instrumented Structure Damaged in the 1994 Northridge Earthquake," ***Earthquake Spectra, 14 (2),*** Oakland, CA: Earthquake Engineering Research Institute, 245-264.

MacGregor, J.G., 1988, ***Reinforced Concrete. Mechanics and Design***, Englewood Cliffs, New Jersey: Prentice Hall

Machin, J., 2001 (Professional Cost Estimator), personal communication.

Maffei, J., 2000, "The Corporate Sector," ***Financial Management of Earthquake Risk,*** Oakland CA: Earthquake Engineering Research Institute, 43-48.

Moehle, J.P., Nicoletti, J.P., and Lehman, D.E., 1994, ***Review of Seismic Research Results on Existing Buildings, Report No. SSC 94-03,*** Sacramento, CA: California Seismic Safety Commission

Mosallam, A.S., 2000, "Strength and Ductility of Reinforced Concrete Moment Frame Connections Strengthened with Quasi-isotropic Laminates" ***Composites Part B – Engineering***, ***Vol. 31***, pp. 481-497.

Nakano Y. and Okada T., 1989, "Reliability Analysis on Seismic Capacity of Existing Reinforced Concrete Buildings in Japan", ***Journal of Structural and Construction Engineering, Transactions of AIJ, No.406***, pp.37-43. (in Japanese)

National Institute of Building Sciences (NIBS), 1995, ***Development of a Standardized Earthquake Loss Estimation Methodology,*** Washington, DC: Federal Emergency Management Agency, 500 pp.

Ozaka, Y., and Suzuki, M., ND, "Study on Shear Failure and Repair Method of Reinforced Concrete Beam", ***Japanese Society of Civil Engineers, Concrete Library International, No 9.***

Pacific Earthquake Engineering Research Center, 2001, ***PEER Testbeds Home Page,*** http://www.peertestbeds.net

Papaulis, A., 1991, ***Probability, Random Variables, and Stochastic Processes,*** New York, NY: McGraw-Hill.

Park, Y.J., and Ang, A.H.S., 1985, "Mechanistic Seismic Damage Model for Reinforced Concrete", ***Journal of Structural Engineering, Vol. 111,*** pp. 722-739.

Pincheira, J.A., Dotiwala, F.S., and D'Souza, J.T., 1999, "Seismic Analysis of Older Reinforced Concrete Columns," ***Earthquake Spectra, Vol. 15, No. 2,*** Oakland, CA: Earthquake Engineering Research Institute, pp. 245-272.

Porter, K.A., 2000, ***Assembly-Based Vulnerability and Its Uses in Seismic Performance Evaluation and Risk-Management Decision-Making, A Doctoral Dissertation,*** Stanford, CA: Stanford University, 195 pp.

Porter, K.A., Kiremidjian, A.S., and LeGrue, J.S., 2001, "Assembly-Based Vulnerability of Buildings and Its Use in Performance Evaluation," ***Earthquake Spectra, Vol. 17, No. 2***, Oakland, CA: Earthquake Engineering Research Institute, pp. 291-312

Porter, K.A., Beck, J.L., Scawthorn, C.R., Seligson, H.A., Tobin, L.T., and Boyd, T., 2002a, ***Improving Loss Estimation for Woodframe Buildings, Vol. 1, Report,*** Berkeley, CA: Consortium of Universities for Research in Earthquake Engineering, 136 pp.

Porter, K.A., Beck, J.L., and Shaikhutdinov, R.V., 2002b, ***Investigation of Sensitivity of Building Loss Estimates to Major Uncertain Variables for the Van Nuys Testbed,*** Pacific Earthquake Engineering Research Center, Richmond, CA

Priestley, M.J.N., Seible, F., and Calvi, G.M., 1996, ***Seismic Design and Retrofit of Bridges***, New York, NY: John Wiley & Sons, Inc.

Public Works Research Institute (PWRI), 1986, ***Manual For Repair Methods of Civil Engineering Structures Damaged by Earthquakes***, (Japanese version, 1986) The Public Works Research Institute, Ministry of Construction, Vol. 45, (English version, 1988) Buffalo, NY: National Center for Earthquake Engineering Research, State University of New York

Ratcliff, R.U., and Schwab, B., 1970, "Contemporary Decision Theory and Real Estate Investment," in ***Appraisal Journal, April 1970***, reprinted in Cooper, J.R., 1974, ***Real Estate Investment Analysis,*** Toronto, Canada: D.C. Heath and Company, pp. 25-47

Reiter, L., 1990, ***Earthquake Hazard Analysis: Issues and Insights***, New York, NY: Columbia University Press

Rissman and Rissman Associates, 1965, ***Holiday Inn Van Nuys Structural Drawings,*** Pacific Palisades, CA

Rocha, C., 2002 (structural engineer involved in retrofit of CUREE demonstration building), personal communication.

Rodriguez, M., and Park, R., 1992, "Lateral Load Response of Reinforced Concrete Columns Strengthened by Jacketing", ***International Symposium on Earthquake Disaster Prevention, Vol. 2.***

Roufaiel, M.S.L., and Meyer, C., 1987, "Analytical Modeling of Hysteretic Behavior of R/C Frames", ***Journal of Structural Engineering, Vol. 113,*** pp. 429-444.

RS Means Co., Inc., 2001, ***Means Assemblies Cost Data 2001,*** Kingston, MA.

Rubin, H.W., 1991, ***Dictionary of Insurance Terms,*** New York, NY: Barron's Educational Services Inc., 465 pp.

Saadatmanesh, H., and Malek, A.M., 1998, "Design guidelines for Flexural Strengthening of RC Beams with FRP Plates", ***Journal of Composites for Construction, Vol. 2, No 4,*** pp. 158-164.

SAC Steel Project, 1999, ***The SAC Steel Project, Welcome,*** Richmond, CA, http://www.sacsteel.org/

Saiidi, M., and Sozen, M.A., 1979, ***Simple and Complex Models for Nonlinear Seismic Response of Reinforced Concrete Structures, Report UILU-ENG-79-2031,*** Urbana, IL: Department of Civil Engineering, University of Illinois

Scholl, R.E., 1981, ***Seismic Damage Assessment for Highrise Buildings, Annual Technical Report, Open-file Report 81-381,*** Menlo Park, CA: US Geological Survey, 143 pp.

Scholl, R.E., and Kustu, O., 1984, "Procedures and Data Bases for Earthquake Damage Preduction and Risk Assessment," ***Primer on Improving the State of Earthquake Hazards Mitigation and Preparedness, Open File Report 84-0772,*** Gori, P., ed., Reston VA: US Geological Survey, pp. 162-213

Scholl, R.E., Kustu, O., Perry, C.L., and Zanetti, J.M., 1982, ***Seismic Damage Assessment for High-Rise Buildings, URS/JAB 8020,*** San Francisco, CA: URS/John A. Blume & Associates, Engineers, 321 pp.

Sharpe, R.D., 1974, ***The Nonlinear Response of Inelastic Structures., Ph.D. Thesis,*** Christchurch, New Zealand: Department of Civil Engineering, University of Canterbury.

Somerville, P., Smith, N., Punyamurthula, S., and Sun, S., 1997, ***Development of Ground Motion Time Histories for Phase 2 of the FEMA/SAC Steel Project***, SAC Joint Venture, Background Document Report No. SAC/BD-97/04.

Spetzler, C.S., 1968, "The Development of a Corporate Risk Policy for Capital Investment Decisions," ***IEEE Transactions on Systems Science and Cybernetics, vol. SSC-4, no. 3.,*** September 1968, Institute of Electronics and Electrical Engineers, pp. 279-300, reprinted in 1989 ***Readings on The Principles and Applications of Decision Analysis, vol. 2: Professional Collection,*** R.A. Howard and J. E. Matheson, eds., Menlo Park, CA: Strategic Decisions Group, pp. 667-688

Stephens, J.E., and Yao, J.T.P., 1987, "Damage Assessment Using Response Measurements", ***Journal of Structural Engineering, Vol. 113,*** pp. 787-801.

Stone, W.C., and Taylor, A.W., 1993, ***Seismic Performance of Circular Bridge Columns Designed in Accordance With AASHTO/CALTRANS Standards, NIST Building Science Series 170,*** Gaithersburg, MD: National Institute of Standards and Technology

Stoppenhagen, D.R., Jirsa, J.O., and Wyllie, L.A., 1995, "Seismic Repair and Strengthening of a Severely Damaged Concrete Frame", ***ACI Structural Journal, Vol. 92, No 2.***

Structural Engineers Association of California, 1999, ***Recommended Lateral Force Requirements and Commentary, 7th Edition,*** Sacramento, CA, 440 pp.

Takahashi K., Takemura, M., Tohdo, M., Watanabe T. and Noda, S., 1998, "Empirical Response Spectral Attenuations on the Rocks with Vs=0.5 to 3.0km/s, in Japan", ***Proceedings of the 10th Japan Earthquake Engineering Symposium, Vol.1***, pp.547-552. (in Japanese)

Tinsley, J.C., and Fumal, T.E., 1985, "Mapping Quaternary Sedimentary Deposits for Areal Variations in Shaking Response," ***Evaluating Earthquake Hazards in the Los***

Angeles Region—An Earth-Science Perspective, U.S. Geological Survey Professional Paper 1360, Washington DC: U.S. Government Printing Office, pp. 101-126

Trifunac, M.D., and Brady, A.G., 1975, "On the Correlation of Seismic Intensity with Peaks of Recorded Strong Ground Motion," ***Bulletin of the Seismological Society of America, Vol. 65,*** pp. 139-162

Trifunac, M.D., S.S. Ivanovic, and M.I. Todorovska, 1999, ***Instrumented 7-Storey Reinforced Concrete Building in Van Nuys, California: Description of the Damage from the 1994 Northridge Earthquake and Strong Motion Data, Report CE 99-02,*** University of Southern California Department of Civil Engineering, Los Angeles, CA

Tversky, A., and Kahneman, D., 1974, "Judgment under Uncertainty: Heuristics and Biases," ***Science, Vol. 185,*** September 27, 1974, pp. 1124-1131

US Census Bureau, 1999, ***American Housing Survey for the United States: 1997,*** Washington, DC: US Census Bureau.

US Census Bureau, 2000a, ***ST-99-3 State Population Estimates: Annual Time Series, July 1, 1990 to July 1, 1999,*** Washington, DC: US Census Bureau.

US Census Bureau, 2000b, ***1997 Economic Census***, Washington, DC: US Census Bureau.

US Geological Survey, 2001, ***Probabilistic Hazard Lookup By Latitude and Longitude,*** http://eqint.cr.usgs.gov/eq/html/lookup.shtml

Von Neumann, J., and Morgenstern, O., 1944, ***Theory of Games and Economic Behavior,*** Princeton, NJ: Princeton University Press, 625 pp.

Waerden, B.L., 1969, ***Mathematical Statistics***, New York, NY: Springer-Verlag

Wang, M.L., and Shah, S.P., 1987, "Reinforced Concrete Hysteresis Model Based on the Damage Concept", ***Earthquake Engineering and Structural Dynamics, Vol.15, No 8,*** pp. 993-1003.

Williams, M.S., and Sexsmith, R.G., 1997, "Seismic assessment of concrete bridges using inelastic damage analysis", ***Engineering Structures, Vol.19, No 3,*** pp.208-216.

Williams, M.S., Villemure, I., and Sexsmith, R.G., 1997, "Evaluation of Seismic Damage Indices for Concrete Elements Loaded in Combined Shear and Flexure", ***ACI Structural Journal, Vol. 94, No. 3***, pp. 315-322.

Working Group for Southern California Earthquake Probabilities, 1995, "Seismic Hazards in Southern California, Probable Earthquakes, 1994 to 2024," ***Bulletin of the Seismological Society of America, Vol.* 85, *No. 2***, pp. 379-439

Zadeh, M.M., 2000, "Understanding Risk Management," ***Financial Management of Earthquake Risk,*** Oakland CA: Earthquake Engineering Research Institute, pp. 1-14

ZEvent, 2000, ***UCFyber Version 2.4.1,*** Berkeley, CA

Appendix A. Risk-Attitude Interview

A.1 THE MEANING OF RISK TOLERANCE

Before discussing a methodology to elicit a decision-maker's (DM's) risk attitude, it is useful to illustrate in somewhat greater detail the meaning of risk tolerance, ρ, discussed in Chapter 2, and repeated for convenience here:

$$u(x) = a + b \exp(-x/\rho) \tag{A-1}$$

When decisions have financial outcomes whose absolute values are significantly below ρ, perhaps half an order of magnitude or more, the DM acts relatively risk-neutrally. That is, the alternative with the greatest expected value of financial outcome is the most desirable one. When outcomes reach or exceed the order of magnitude of ρ, however, the DM acts with greater and greater caution, demanding expected values of financial outcome significantly above what a risk-neutral attitude would dictate as reasonable. Alternatively, the DM requires higher and higher probability of success before accepting deals that involve the possibility of large loss.

For example, consider a double-or-nothing bet, where the stakes are to gain or lose a value x with probability p. When the stakes are small with respect to risk tolerance ρ, one accepts the deal if the probability of winning is as low as $p = 0.5$. At this probability or higher, the expected value of the financial outcome is nonnegative. When the stakes grow higher, however, the probability of winning must be closer and closer to 1.0 to make the DM willing to take the bet. The probability at which the DM is just indifferent between taking the bet and rejecting it, called the *indifference probability*, is readily shown to be

$$p = 1/(1 + \exp(-x/\rho)) \tag{A-2}$$

and is plotted as a function of x/ρ, in Figure A-1. (An event-tree depiction of the double-or-nothing bet is shown as an inset of Figure A-1.) The indifference probability is used in the present study to elicit a DM's risk attitude, and to infer the DM's risk tolerance ρ.

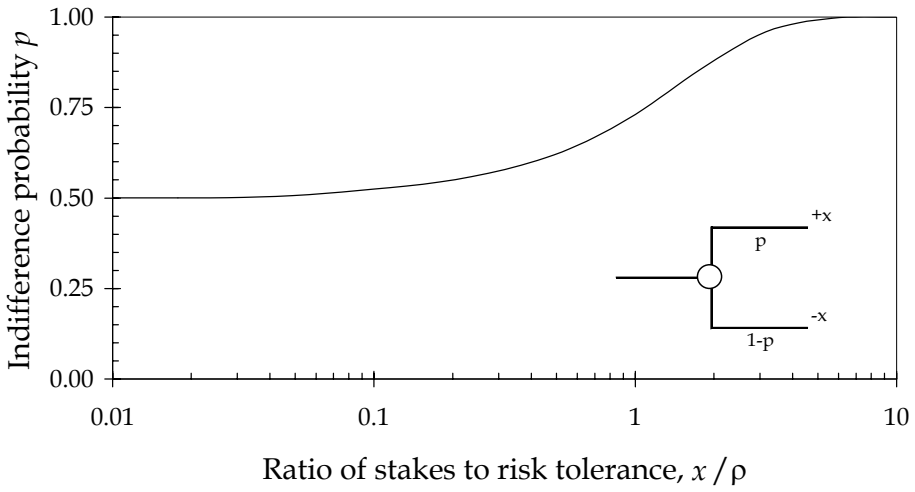

Figure A-1. Risk tolerance ρ illustrated in terms of a double-or-nothing bet.

Equation A-2 can be demonstrated as follows. At indifference, the expected value of the utility of the deal is zero. One can assign a and b arbitrarily, as long as utility increases with increasing x, i.e., as long as $b < 0$. It is convenient to make u(0) = 0, which makes $a = -b$, and one can arbitrarily assign $a = 1$. Thus, at indifference,

$$\begin{aligned} \mathrm{E}[u] &= pu(x) + (1-p)u(-x) \\ 0 &= p(1-\exp(-x/\rho)) + (1-p)(1-\exp(x/\rho)) \\ &= p - p\exp(-x/\rho)) + 1 - \exp(x/\rho) - p + p\exp(x/\rho)) \\ &= -p\exp(-x/\rho)) + 1 - \exp(x/\rho) + p\exp(x/\rho)) \\ &= -p\exp(-x/\rho)) + 1 + (p-1)\exp(x/\rho) \end{aligned}$$

Multiplying both sides by $\exp(x/\rho)$, and substituting $c = \exp(x/\rho)$,

$$\begin{aligned} 0 &= -p + c + (p-1)c^2 \\ &= -p + c + pc^2 - c^2 \\ c^2 - c &= p(c^2 - 1) \\ p &= (c^2 - c)/(c^2 - 1) \\ &= c(c-1)/(c-1)(c+1) \\ &= c/(c+1) \\ &= \exp(x/\rho)/(\exp(x/\rho) + 1) \\ &= 1/(1 + \exp(-x/\rho)) \qquad \text{QED} \end{aligned}$$

A.2 AN INTERVIEW TO INFER DECISION-MAKER'S RISK TOLERANCE

To determine the DM's utility function, an interview process similar to that of Spetzler (1968) is performed. This reference, though old, provides the best-documented, most-systematic procedure found. The procedure employs a series of N hypothetical deals of the form shown in the event tree of Figure A-2. Each deal has two possible outcomes of fixed value: success, which involves a net gain of g, or failure, which involves a net loss of l. The probability of success in each deal is a variable. The interview process determines the DM's indifference probability p for each deal. When the DM is just indifferent between accepting the deal and rejecting it, the utility of the deal is identically equal to the utility of zero change in wealth state.

If the arbitrary parameters a and b of Equation A-1 are set to 1 and –1, respectively, the utility of a zero change in wealth is zero ($u(x=0) = 0$), regardless of the value of ρ. Thus, for the deal shown in Figure A-2, when p = the indifference probability, the utility of the deal is zero. Then, if the DM's utility function is well described by the exponential form shown in Equation A-1, the sum of the utilities of all the hypothetical deals should also be zero, and the sum of the squares of these utilities is also zero. This fact allows one to infer ρ by least-squares based on a series of N hypothetical deals.

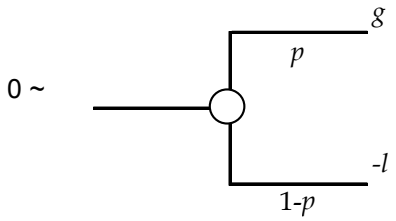

Figure A-2. Two-outcome financial decision situation used in interview.

Let g_i refer to net gain from deal i, l_i refers to net loss from deal i, and p_i refers to indifference probability from deal i. The expected utility of a single hypothetical deal i is:

$$E[u_i] = p_i(1 - \exp(-g_i/\rho)) + (1 - p_i)(1 - \exp(l_i/\rho)) \qquad \text{(A-3)}$$

Risk tolerance ρ is then determined by minimizing the sum of the squared errors, $e(\rho)$:

$$e(\rho) = \sum_{i=1}^{N} \left(E\left[u_i \right] \right)^2 \qquad \text{(A-4)}$$

A.3 IMPLEMENTING THE INTERVIEW

The Spetzler (1968) procedure is used to gather the data employed in Equations A-3 and A-4, with some modifications. Before detailing the interview process, these differences and the reasons for them are summarized. First, the utility function is assumed to be exponential rather than logarithmic, which permits the application of the delta property. (The delta property allows one to consider costs and savings without reference to the DM's total wealth state. Use of a logarithmic utility function, which does not satisfy the delta property, requires that all decisions be made with reference to total wealth state under the various outcomes.)

A second difference is in the introduction to the interview. In the introduction, the interviewee is informed of the basic nature of a utility curve, illustrating the notion of risk aversion with example of a coin toss for ever-larger sums of money. Further, the nature of the upcoming financial questions is summarized. This introduction appears useful in preparing the DM to answer the questions more consistently than if he or she must learn the pattern during the first few deals.

A third difference is that the magnitude of financial decisions commonly made by the DM is considered as an explicit parameter of the interview process. This addition to the Spetzler (1968) procedure makes the new procedure more generally applicable to other DMs. Finally, whereas Spetzler (1968) assumes a planning period, denoted by T, and discount rate, denoted by i, and applies these to the questions, in the present study the DM's own T and i are applied to the hypothetical deals.

The interview therefore proceeds as follows. First, the introduction is given as noted above. The DM is asked for his or her planning period T; discount rate i; a typical investment amount (denoted by x_S) for a small deal in which he or she might engage; and that of a large deal (denoted by x_L). The DM is free to define *small* and *large* in this context. The DM is also asked for the annual revenue, or in the case of a nonprofit

institution the annual budget, denoted by R, of his or her company or institution. Annual revenue appears to be relevant to risk attitude.

Individual deal outcomes g_i and l_i are scaled by x_S and x_L as shown:

$$g_i = d_i^* x_i \tag{A-5}$$

$$l_i = c_i^* x_i \tag{A-6}$$

In these equations, c_i and d_i are predefined constants tabulated in advance (see Table A-1), and x_i is either x_S or x_L, depending on deal i. As shown in the table, loss outcomes l range from $0.33x$ to $6.33x$ whereas gains g range from $0.6x$ to $19.0x$.

For each deal i, the DM is posed the hypothetical deal, and asked if he or she would accept it if the probability of success were 95%. If the answer is yes, the question is posed for a probability of success of 90%. The process repeats until the DM is either indifferent between accepting and rejecting the deal, or until the DM switches from a yes answer to no. In the former case, p_i is the last probability stated. In the latter, p_i is the mean of the last two probabilities stated.

A probability wheel is used to assist the DM to visualize the probabilities being stated. A probability wheel is a small plastic or pasteboard device with a two-segment, green-and-red pie chart approximately 6 inches in diameter on its face. The fraction shown by green can represent success; red, failure. There are no numbers on the face, but the fraction shown by green can be adjusted and read from the back, the side facing the interviewer.

The indifference probability is recorded for each deal. The interview is concluded when all the probabilities are recorded. The analyst can then determine ρ by minimizing the objective function in Equation A-4. Care must be taken when minimizing $e(\rho)$, as $\rho = \infty$ represents a minimal but trivial solution.

Table A-1. Hypothetical deals.

Question	Investment x	Loss multiple c	Gain multiple d
1	x_S	1.00	0.67
2	x_L	2.70	6.40
3	x_L	4.00	12.00
4	x_S	1.00	3.00
5	x_L	1.80	1.20
6	x_S	3.00	8.33
7	x_S	3.67	3.00
8	x_S	5.00	3.67
9	x_L	2.70	3.20
10	x_L	0.50	1.20
11	x_L	3.40	9.00
12	x_S	4.33	4.67
13	x_S	0.33	1.67
14	x_L	1.40	0.60
15	x_L	2.30	2.00
16	x_L	3.00	12.00
17	x_L	3.70	9.00
18	x_L	1.80	2.00
19	x_S	3.00	1.67
20	x_S	5.67	8.33
21	x_L	3.70	19.00
22	x_S	5.67	16.00
23	x_S	1.67	1.67
24	x_L	1.00	0.60
25	x_L	4.00	19.00
26	x_S	6.33	4.67
27	x_S	0.33	0.67
28	x_S	3.67	10.00
29	x_L	0.50	0.60
30	x_S	5.67	12.67
31	x_S	5.00	16.00
32	x_L	2.70	4.60
33	x_S	2.33	3.00
34	x_L	4.00	15.00
35	x_S	2.33	6.33
36	x_L	1.40	3.20
37	x_L	2.30	6.40
38	x_S	1.67	1.67
39	x_S	5.00	12.67
40	x_L	3.00	4.60

A.4 INTERVIEW SCRIPT

The following script can be used to perform the interview, but it need not be followed verbatim, as long as the interviewee is prepared by understanding the purpose of the interview and the nature of the questions. The exposition on decision theory is intended as a courtesy to explain the use to which the results can be put.

"The purpose of this interview is to elicit your attitude toward risk. It can take up to 30 minutes or so. It starts with an introduction of about 5 to 10 minutes, and then I ask you a series of questions that help determine your risk attitude. Using an economic theory called *decision theory* or *decision analysis*, one can quantify risk attitude using an abstract measure called *utility* that measures how much a person likes or dislike some condition.

"One can measure utility for a variety of conditions: a person's wealth after a financial decision, his or her health after a medical procedure, or even whether an outdoor party is spoiled by rain. Decision analysis can help to make all sorts of risky, high-value decisions in a rational, mathematically rigorous fashion that is consistent with the decision-maker's personal preference for risk, and accounts for all the uncertainties involved in the outcome. Most often, decision analysis is used to make risky financial decisions.

"Some pharmaceutical companies such as Eli Lilly use decision analysis to allocate resources among research and development projects. Oil and gas companies such as Texaco use it to decide on pursuing costly exploration projects. Before they can use decision analysis though, they have to determine their risk attitude, which means creating one of these utility functions. The procedure we are going to follow in this interview is a rigorous method for creating your utility function.

"First, let's clarify the notion of utility. Consider a simple financial decision: a bet on a coin toss. Most decision-makers would be comfortable flipping a coin double-or-nothing for $0.25, $1.00, perhaps $10, because the utility of winning $1.00 for most people is about the same as the disutility of losing $1.00; they like the one about as much as they dislike the other, so 50-50 odds means they can expect on average to break even

in financial terms and also in terms of preference. As the stakes rise, however, a decision-maker tends to require better-than-even odds (a chance of winning greater than 50%) before risking $100, $1,000, or $10,000 (assuming there were no entertainment value as in casino gambling). They wouldn't toss a coin for $10,000, even though the expected value of the bet is the same as a coin toss for $1.00. Does that behavior agree with your experience?

"The reason in mathematical terms is that for most people the disutility of losing $10,000 is much more than the utility of winning $10,000. So even though the expected value of a $10,000 double-or-nothing bet is zero, the expected utility of the large double-or-nothing bet is negative, less than the utility of passing on the deal entirely. A rational decision-maker chooses the alternative with the greater utility, which in this case is to pass.

"By finding out what probability of winning a person requires before taking various bets, we can determine that person's risk attitude. That is what we'll do now for you, as a decision-maker for your company. Before we begin, tell me please what is your financial planning period in years. For example, how long do you plan to hold a typical investment?" [The answer is recorded as T] "And what discount rate do you use?" [The answer is recorded as i.] "When you make financial decisions for your company, what up-front cost represents a large deal for you?" [Record the value as x_L.] "What is a small deal for you?" [Record x_S.] "Finally, considering the group for which you make financial decisions, what is the annual revenue? Bear in mind that neither you nor your company will be identified by name anywhere in our study." [Record the value R.]

"I am going to pose a series of 40 investment situations that you may either take or not take, depending on whether you believe your company should invest in it. I don't mean whether your company probably *would* invest in such a situation, but whether you believe it *should,* and would recommend that it did so. In each case there will be an initial investment amount that your company must put up.

"For each situation there will be only two possible outcomes: success or failure occurring within your planning period of *T* years. Each outcome will be associated with a net gain or loss in dollars, which I will tell you. These are present-value dollars, discounted at your cost of capital, which you have told me is *i*%." [Use the *T* and *i* just provided.] "When I say 'net', I mean net of your initial investment. So in the case of success, you get back the amount of your initial investment plus the net gain. If failure, you may have to pay an additional amount, if the net loss is greater than your initial investment."

"I will tell you that according to your judgment, the chance of success is some percentage such as 95%, or 90%, or whatever, and ask you if the company should invest under those conditions. Then I would like you to answer yes or no – accept or reject the deal. If you accept, I will reduce the probability of success and ask if you should take the deal now, with the same outcomes but a lower chance of success. The process repeats until you reject the deal, and then we move on to the next investment situation."

"For example, suppose you have the opportunity to invest $5,000 today, with only two possible outcomes: success or failure within *T* years. Success means a net gain of $32,000; failure, a net loss of $13,500. Both the net gain and net loss are in present-value dollars, that is, dollars discounted at the rate of your discount rate. Again, these amounts are net of your investment. Should your company invest if you believed the probability of success were 95%?"

[Show the probability wheel with 95% showing.] "In other words, if this were a dartboard and we spun it and threw a dart at it, and the dart landed on the green, that would be success; if it landed on the red, that would be failure. If you say yes, I'll ask again for the same deal, but with a lower chance of success, and you tell me whether or not you should take the deal if you believed the chance of success were about 90%, as shown now, and then 85%, as shown now, and so on. Do you understand the deal?" [If not, explain until the interviewee clearly understands the procedure and what is meant by the terms of each deal.]

"Remember, these are your own beliefs about probability, not those of some consultant or outside expert. Also remember that there are no right or wrong answers, because the answers reflect your risk attitude, and risk attitude is subjective. By the way, I can also pose the same questions in terms of breakeven chance or equivalent annual payment if you think better in those terms. Would you prefer one of these two forms, or the one I just outlined?

"Then let's begin. In the first deal, your up-front investment is [x_1]. If the venture is successful, it results in a net gain of [d_1x_1], that is, net of you initial investment. If the venture fails, it results in a net loss of [c_1x_1]. Should you take the deal if you believed the probability of success were 95%?" [State the values of x_1, d_1x_1, and so on, rather than the names of the variables. Show 95% on the probability wheel. If the answer is yes, ask:] "What if it were 90%?" [Show 90%. Proceed until the decision changes from yes to no. Record the lowest probability where the answer is yes. Move on to the next question. If the interviewee begins to lose interest and shows signs of not taking the questions seriously anymore, stop the interview and use the data collected so far. They are randomized so there is no more significance to the last question as the first.]

Appendix B. Interview Script in Japanese

The following script has the same content as documented in Appendix A.4, which was translated into Japanese, including the conversion of monetary parameters into yen. The interviews with Japanese decision makers were performed using this interview script.

このインタビューは，あなたの投資リスクに対する考え方をお聞きするために行います。30 分前後で終わります。最初の 5 分から 10 分でインタビュー内容の紹介をしてから，あなたの投資リスクの判断傾向を調べるために一連の質問をします。経済学の分野で意思決定理論（decision theory）または意思決定分析（decision analysis）と呼ばれる理論があります。この理論を用いると，投資リスクに対する投資家の姿勢，つまりハイリスク―ハイリターン型かローリスクーローリターン型かというような投資条件の好みは，ユーティリティ関数と呼ばれる物差しで計ることができます。

このユーティリティ関数は，色々な条件に対して調べることができます。仕事上の重要な意思決定はもちろん，何かの病気の時に医学的な処置を受けるかどうかという判断，あるいは雨に会う可能性のある屋外のパーティーを開催するかどうかという決断に対してさえも使えます。リスクを伴う重要な判断に対して，決断を下す人の考え方や様々な不確定要因を加味しながら最適な答えを見つけることが，意思決定分析の役割です。リスクが見込まれる財務上の決断では，ユーティリティ関数が良く用いられています。

例えば Eli Lilly というアメリカの製薬会社では，研究開発のプロジェクトへの投資計画に意思決定理論を用いています。また，Texaco などの石油会社は，高額な資源探査プロジェクトの決断に用いています。意思決定理論を用いる時は，その前にどの程度のリスクを許容するかということを決めておかなければなりません。それはユーティリティ関数を設定しておくということです。このインタビューの結果から，あなたのユーティリティ関数が設定できます。

インタビューを始める前に，ユーティリティ関数という概念をはっきりさせましょう。投資の簡単な例題として，コインの裏表による賭けを考えてみます。ほとんどの人は，コインの賭けに 25 円か 100 円，多分 1000 円位までなら気軽に応じるでしょう。それは，100 円が儲かる得と 100 円を失う損を，それほど無理なく天秤にかけられるからです。つまり，コインの賭けのような勝ち負け半々の賭けは，数学的には期待値ゼロですが，賭け金があまり高くない場合に限れば，人間の主観的な価値判断から言っても平均的に損得なしということが信じられる訳です。ところが，賭け金が 1 万円，10 万円，あるいは 100 万円と高くなるにつれて，私達は五分五分以上のオッズ，つまり 50%以上の勝つチャンスを欲しがります。たとえ勝つチャンスが同じでも，私達はコインの裏表に 100 円を賭けても 100 万円は賭けないでしょう。あなたの経験に照らし合せて，いかがでしょうか。

その理由は，ほとんどの人間にとって 100 万円を失う不利益は 100 万円が儲かる利益よりも大事だからです。従って，たとえ勝つ確率と負ける確率が同じであっても，損得半々の賭けに大きな金額を賭けるユーティリティは，賭けをしないユーティリティよりも小さいことになります。色々な金額の賭けに対して，ある人がどの程度勝つ確率を要求するのかを見つけだすことで，その人のリスクに対する判断を判定できます。これが，意思決定者としてのあなたに対して，今から行おうとしている質問の意味合いです。

先ず最初に，あなたが会社のプロジェクトで何かの投資を計画することを想定してください。あなたやあなたの会社の名前は一切公表しません。プロジェクトの期間，例えば投資期間として何年位が適当なのかを教えてください。［答えを T に記入。］次に，ディスカウントレートとして何%を設定しますか。［i に記入。］そのプロジェクトにとって，大きな取り引きと思われる投資額はいくらですか。［x_L に記入。］小さな取り引きはいくらですか。［x_S に記入。］プロジェクトの年間の総売上げはいくらですか。［R に記入。］

今から 40 ケースの投資を持ちかけますので，あなたの会社が投資すべきかどうかを判断してください。あなたの会社が投資するのかどうかではありません。投資すべきとあなたが思うかどうか，投資するように会社に勧めるかどうかです。それぞれのケースで，あなたの会社が払うべき初期投資額を示します。

投資の結果はふたつしかありません。投資期間［T］年間に成功するか失敗するかです。その結果は純利益または純損失として金額で示します。金額は，あなたの［T］と［i］%で現在価値で表わしたものと考えてください。“純”という意味は，初期投資に対するネットの金額ということです。従って，投資に成功した場合には投資額と純利益を足した額が戻ってきます。もし失敗して，純損失が投資額よりも多い場合，あなたには追加の支払いが必要になります。

投資が成功する確率を 95%，90%というようにパーセンテージで示して，その条件で会社が投資すべきかどうかを尋ねます。あなたはその商談に応じるか否かを yes／no で答えてください。yes の場合，成功の確率を下げて，より低い成功のチャンスでも同じ投資をするかどうかを尋ねます。同じ質問をあなたが no と言うまで繰り返してから，次の投資の商談に移ります。

例をあげますと，あなたに今日，［T］年間に成功か失敗かというふたつの結果をもたらす 50 万円の投資の機会があるとします。成功は 320 万円の純利益，失敗は 135 万円の純損失です。両方とも現在価値の金額で，あなたの設定したディスカウントレートで割り引かれた金額です。繰り返しますが，これらの金額は純利益，純損失を意味しています。成功の確率が 95%と予想される時，あなたの会社は投資すべきですか。

［95%の確率ホイールを示す。］他の表現をすれば，これがダーツの的で，これをくるくる回してダーツを投げることを考えます。緑のところに当たれば成功，赤のところでは失敗という訳です。もしあなたの答えが yes ならば，成功のチャンスを下げて同じ商談を繰り返します。成功のチャンスがこのように 90%の場合，このように 85%の場合といった時に，投資の決断を下すべきかどうかを答えてください。この質問が理解できましたか。［もし理解されない場合，相手が質問の方法や内容をはっきりと理解するまで説明する。］

もうひとつ大切なことは，これはあなた自身が信じる確率であって，コンサルタントや外部の専門家の予想ではないということです。また，質問の答えに正解・不正解はありません。その理由は，質問の答えはあなたのリスク判断を反映したものであり，リスク判断は主観的なものだからです。質問を通じて，損得なしとなる成功の確率（breakeven chance）や，ディスカウントレートで換算した投資期間の毎年の受け取り額あるいは支払い額を示すこともできますが，質問の参考にしますか。それとも必要ありませんか。

それでは始めましょう。最初の商談は，初期投資額が［x_1］です。もしこの投機が成功すれば，［d_1x_1］の純利益をもたらします。これはあなたの初期投資に対する純益です。もし投機が失敗すれば，純損失は［c_1x_1］となります。成功の確率が 95%と予想される時，この商談に応じますか。［確率ホイールで 95%を示す。もし答えが yes ならば，次の質問をする。］90%ではどうですか。［90%を示す。答えが，yes から no に変わるまで同様の質問を続ける。答えが yes の最小の確率を記録し，次の質問に移る。インタビュー相手が興味を失い始めて，これ以上の質問が苦痛の様子に見えた場合，インタビューを中止してそれまで集めたデータを用いる。これらの質問はランダムに並べられており，最後の質問が最初より重要ということはない。］

Appendix C. Fragility and Repair of Reinforced Concrete Flexural Elements for Seismic Damage and Loss Analyses

C.1 LITERATURE REVIEW FOR BEAM-COLUMN FRAGILITY

The assembly-based vulnerability (ABV) methodology (Porter, 2000) requires that every damageable building assembly be associated with clearly defined damage states, and that each damage state is defined in terms of particular repair tasks. Since the ABV methodology is applied to a 1960s-era reinforced-concrete moment-frame building, fragility functions must be developed for a variety of components, most notably nonductile reinforced-concrete beams and columns. A number of researchers have examined both the fragility of these members and the construction efforts required to repair damage to them.

The seismic response of a building can be characterized in many ways: maximum acceleration, maximum displacement, interstory drift and so on. The resulting damage for every assembly is found to depend primarily on only a small subset of these parameters. In other words, if we consider a damage state of some particular assembly, we will find that the onset of this damage state is most highly correlated with only one or a few parameters of the response. This fact raises the issue of choosing the parameter that best characterizes a damage state of a given assembly. In particular, the interest for this study is damage suffered by reinforced-concrete moment-frame members. Over the past two decades, a number of appropriate response parameters have been proposed, which are generally referred to as damage indices.

Williams *et al.* (1997) conducted a study of appropriate damage indices. They introduced five damage states, shown in Table C-1. Damage states are defined in terms of visible and measurable damage, which is convenient for relating damage to repair efforts. The third column of the table shows the repair efforts that might be undertaken to repair the damage. These repair methods are described in EERI (1994), and Williams *et al.* (1997) relate them to particular damage states, although they do not offer substantial justification for these relationships.

Williams *et al.* (1997) performed a series of laboratory tests of reinforced-concrete beam-columns. The test program included six specimens that were loaded by combined cyclic shear-flexure loads to the point of failure. During each test, four damage states were identified and corresponding damage indices were measured. The data give uniform and consistent grounds for comparing damage indices. Based on these tests, the authors performed a statistical calibration of seven damage indices including ductility, cumulative ductility (Banon *et al.* 1981), modified stiffness ratio (Roufaiel *et al.* 1987), modified Park-Ang damage index (Kunnath *et al.* 1992), and damage indices proposed by Stephens *et al.* (1987), Wang *et al.* (1987), Jeong *et al.* (1988). Given the experimental data, the authors conclude that ductility, modified stiffness ratio and the Park-Ang damage index provide the most reliable indication of the various damage states. However, no consistent measure of accuracy of these damage indices was used. In order to make further distinction between these three indices, there is a need for a quantitative measure of damage-index quality.

Table C-1. Williams *et al.* (1997) damage states and consequences for concrete columns.

Damage state	**Visible damage**	**Likely Consequences**
None	None or small number of light cracks, either flexural (90^0) or shear (45^0)	No loss of use or structural repair needed.
Light	Widespread light cracking; or a few cracks >1 mm wide; or light shear cracks tending to flatten towards 30^0	Only minimal loss of use, possible some minor repair needed to restore structure to its design strength.
Moderate	Significant cracking, e.g. 90^0 cracks >2 mm; 45^0 cracks >2 mm; 30^0 cracks >1 mm.	Structure closed for several weeks for major repairs
Severe	Very large flexure or shear cracks, usually accompanied by limited spalling of cover concrete.	Structure damaged beyond repair and must be demolished
Collapse	Very severe cracking and spalling of concrete; buckling, kinking or fracture of rebar.	Structure has completely or partially collapsed.

To be defensible, the choice is limited to those indices that have an array of experimental data that is large enough for empirically establishing fragility functions. The best statistics available at the time of this study, both in terms of clear definition of damage states and number of tests, are those for the modified Park-Ang damage index (PADI) defined by (Kunnath et al., 1992):

$$PADI = \frac{\Phi_m - \Phi_r}{\Phi_u - \Phi_r} + \beta\left(\frac{A_t}{\Phi_u M_y}\right) \qquad \text{(C-1)}$$

where

Φ_m = maximum curvature attained during seismic loading

Φ_u = nominal ultimate curvature capacity of the section

Φ_r = recoverable curvature at unloading

M_y = yield moment of section

A_t = total area contained in M-Φ loops

β = strength deterioration parameter.

Note that when $\beta = 0$, PADI reduces to a ductility measure.

Stone and Taylor (1993) examined the seismic performance of 81 circular reinforced-concrete bridge columns, and related PADI to three limit states of interest: yielding, ultimate loading and a limit state called "failure", associated with the likely collapse of a column. These limit states define the boundaries between the damage states as shown in Table C-2. Values of the energy (second term) and displacement (first term) parts of PADI are given separately in Stone and Taylor (1993). For the present study, these data are reviewed to create probabilistic capacity distributions on reinforced-concrete sections. The recommendations of Stone and Taylor (1993) for defining damage states together with the likely consequences will also be considered for application to the present study.

Table C-2. Stone and Taylor (1993) damage states for concrete columns.

Limit state	Damage state	Likely consequences
	No damage: no yielding of longitudinal reinforcement.	Light cracking may have occurred without compromising serviceability.
Yield: actual yielding of longitudinal steel.	*Repairable*: yielded, not yet reached ultimate	The element has yielded. Extensive spalling may have occurred but inherent stiffness remains and economics will likely dictate that the structure should be repaired rather than replaced.
Ultimate: maximum moment capacity is reached.	*Demolish*: between ultimate and failure limit state.	The element has been loaded beyond ultimate load and must be replaced.
Failure: moment capacity reduced to 80% of maximum	*Collapse*: exceeded failure limit state	The element has completely failed. (Implies additional collapse in structural system.)

As described earlier, Williams *et al.* (1997) performed six tests on reinforced-concrete flexural members, measuring PADI at the four damage states shown in Table C-1. For the present study, the results are used for comparative analysis of several proposed damage indices, and as a source of experimental data for the "light" damage state.

Williams and Sexsmith (1997) examined the load-displacement behavior of concrete bridge bents, with PADI used as a measure of response. Their work gives two more data points for the "collapse" damage state, which are used for extending the database of experimental results for the damage state.

C.2 DEVELOPMENT OF BEAM-COLUMN FRAGILITY FUNCTIONS

The choice among damage indices for reinforced-concrete flexural elements is limited by availability of experimental data. Sample sizes must be large enough for confident estimation of the corresponding distributions. Appropriate data have been collected for the modified Park-Ang damage index (PADI), as described in the previous section. Although PADI has been commonly used by researches, there is no consensus

about the energy term participation in this index. Different authors proposed different values of β in Equation C-1, usually ranging from 0.05 to 0.4 (see Chai *et al.* 1995, Kunnath *et al.* 1992).

Analysis of the experimental data reported by Stone and Taylor (1993) reveals that the parameter β might even have negative values. Let *DDI* refer to the displacement part of Equation C-1, and let *EDI* refer to the energy part.

$$DDI = \frac{\Phi_m - \Phi_r}{\Phi_u - \Phi_r}$$

$$EDI = \left(\frac{A_t}{\Phi_u M_y} \right) \tag{C-2}$$

where all terms are as defined for Equation C-1. Figure C-1 shows a scatter plot of Stone and Taylor (1993) data for the collapse damage state and a fitted linear regression model relating EDI and DDI. The model implies a value for β of -1/1.66 = -0.6, indicating negative participation of the dissipated energy to PADI.

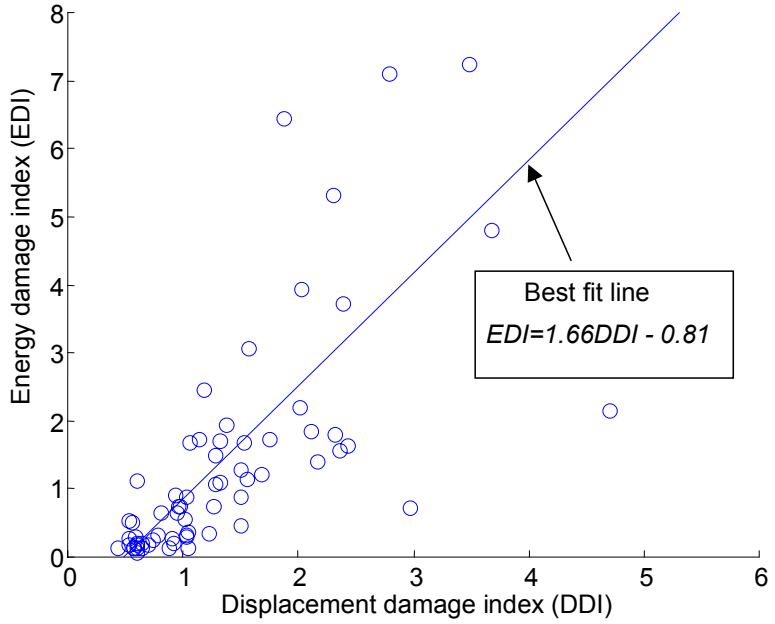

Figure C-1. Displacement term versus energy term from Stone and Taylor (1993) data.

Controversial and inconsistent test data together with a lack of consensus about the dissipated energy participation in failure show that researchers have so far failed to capture the whole complexity of the phenomenon, including some of its essential features. For the present study, the value of β is therefore taken to be zero, and fragility functions are developed in terms of the displacement damage index (*DDI*) given by Equation C-2. Williams *et al.* (1997) support this choice of damage index. They conclude that a simple, predominantly deformation-based measure such as ductility provides a more reliable indication of the various damage levels than many of the apparently more-sophisticated indices.

Given that the response parameter of interest is the DDI, we now turn to the question of relating DDI to physical damage. This relationship is established by a fragility function. Generically, a fragility function gives the probability of a system exceeding some undesirable limit state, given an input excitation. The fragility function can also be seen as the probability distribution of a variable representing the system's uncertain capacity to resist the undesirable state, in terms of the excitation that is assumed to govern whether the system enters the undesirable state.

A structural engineer might think of capacity in terms of the ultimate strength of a member: if the member is subjected to a static force less than the strength, the member does not collapse. If the force exceeds the strength, the member collapses. If the strength is uncertain, then the force associated with collapse is uncertain, and could be expressed via a probability distribution. The probability that the strength is less than any particular value is equivalent to the probability that, if subjected to that level of static loading, the member will collapse.

Thus, the probability distribution of capacity is equivalent to the member's fragility function. One can therefore create fragility functions using the distribution of member capacity observed in laboratory tests. The dataset provided by Stone and Taylor (1993) can be used to establish fragility functions for circular reinforced-concrete columns. The central jagged lines of Figure C-2 through Figure C-4 present the fragility functions from the data for the yield, ultimate, and failure damage states recorded by Stone and Taylor (1993). That is, they are cumulative frequency histograms as a function

of DDI. The figures also show smooth curves are that approximate these observed distributions, along with 95% confidence intervals.

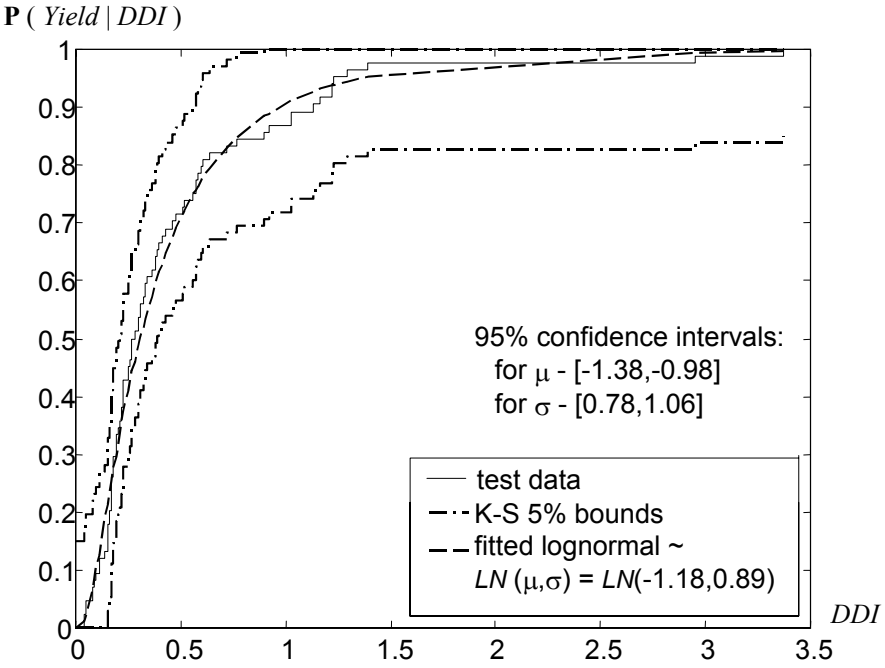

Figure C-2. DDI probability distribution for "yield" Stone-Taylor damage state.

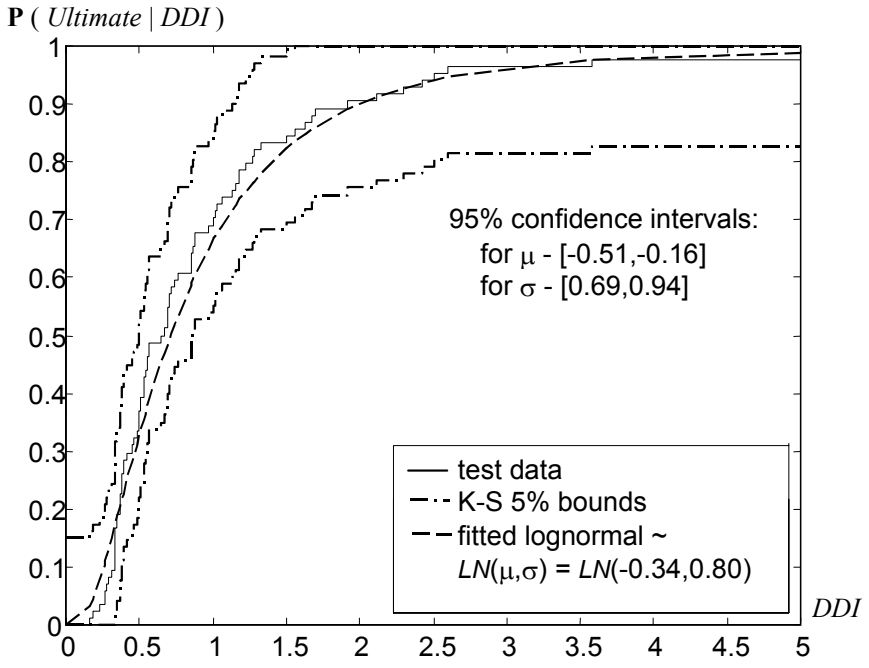

Figure C-3. DDI distribution for "ultimate" Stone-Taylor damage state.

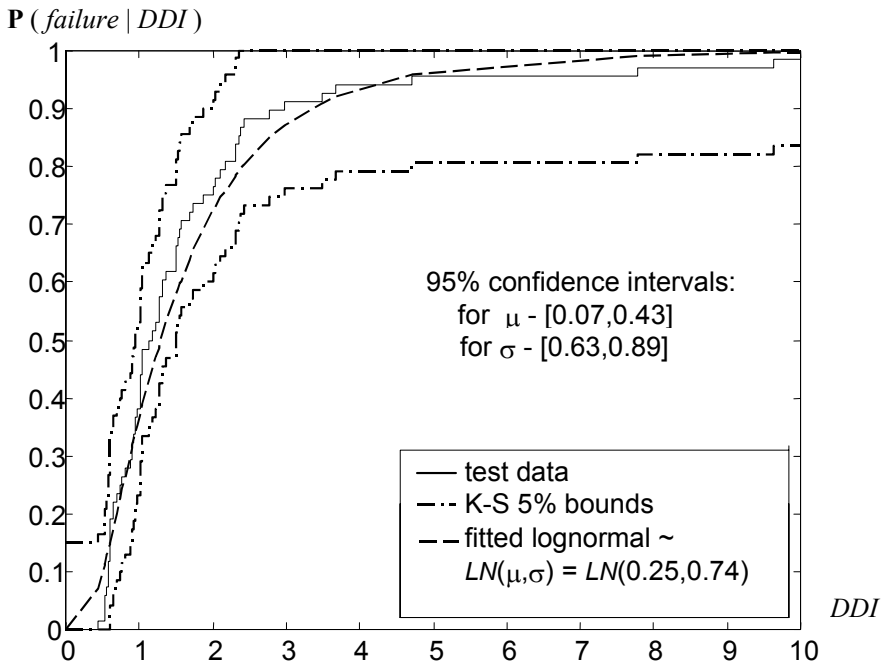

Figure C-4. DDI probability distribution for "failure" Stone-Taylor damage state.

The smooth curves are cumulative lognormal distributions. This approximation of the observed capacity by a lognormal distribution is supported by Park *et al.* (1984), who show that a lognormal distribution gives a good fit between PADI and the failure limit state. Furthermore, MacGregor (1988) shows that the distribution of the yield strength of steel reinforcement in reinforced concrete is well approximated by a lognormal.

To find the parameters of the proposed lognormal distribution functions, the natural logarithm of sample data points is taken. That is, we evaluated $Y = \ln(X)$, where $X = \{x_1, x_2, \ldots, x_n\}$ is a vector of sample data, i.e., the values of the damage index corresponding to the specified damage state for n test specimens. The sample mean ($\tilde{\mu}$) and sample standard deviation ($\tilde{\sigma}$) of the sample of Y are the best estimators of the mean and standard deviation for the corresponding Gaussian distribution of $Y \sim N(\mu, \sigma)$ and for the corresponding parameters of lognormal $X \sim LN(\mu,\sigma)$. These parameters of the lognormal distribution are related to the mean and variance of capacity X as:

$$E[X] = e^{\mu+\frac{1}{2}\sigma^2}, V[X] = e^{2(\mu+\sigma^2)} - e^{2\mu+\sigma^2} \qquad \text{(C-3)}$$

The 95% confidence intervals for estimators $\tilde{\mu}$ and $\tilde{\sigma}$ are given by Abramowitz *et al.* (1964):

$$\mu_l = \tilde{\mu} + \frac{Tinv(\alpha/2)\tilde{\sigma}^2}{\sqrt{n}} \qquad \mu_h = \tilde{\mu} + \frac{Tinv(1-\alpha/2)\tilde{\sigma}^2}{\sqrt{n}}$$
$$\sigma_l = \frac{\tilde{\sigma}^2\sqrt{n-1}}{\chi^2 inv(\alpha/2)} \qquad \sigma_h = \frac{\tilde{\sigma}^2\sqrt{n-1}}{\chi^2 inv(1-\alpha/2)} \tag{C-4}$$

where

α = probability that the parameter is not in the interval (5% in this case),

μ_l, σ_l = lower bounds of the confidence intervals for μ and σ respectively,

μ_h, σ_h = upper bounds of the confidence intervals for μ and σ respectively,

Tinv = inverse of Student's T distribution function with n-1 degrees of freedom,

$\chi^2 inv$ = inverse of χ^2 distribution function.

A Kolmogorov-Smirnov goodness-of-fit test (Ang and Tang, 1975) is used to check that the lognormal distribution reasonably matches the observed data. The dash-dot lines of Figure C-2 through Figure C-4 show that the lognormal falls within the 5% bounds for each damage state.

Stone and Taylor (1993) do not examine pre-yield damage. Williams *et al.* (1997) do provide limited data (the sample consists of five data points) on a damage state that they label as light, defined in Table C-1. For the reasons described before, the distribution for the light damage state is assumed to be lognormal. The parameters of this distribution are estimated as before. Results are given in Figure C-5. Confidence intervals are much wider because of the small data sample, but the fitted curve agrees well with test data and passes both Kolmogorov-Smirnov and one-sided delta test (Waerden, 1969).

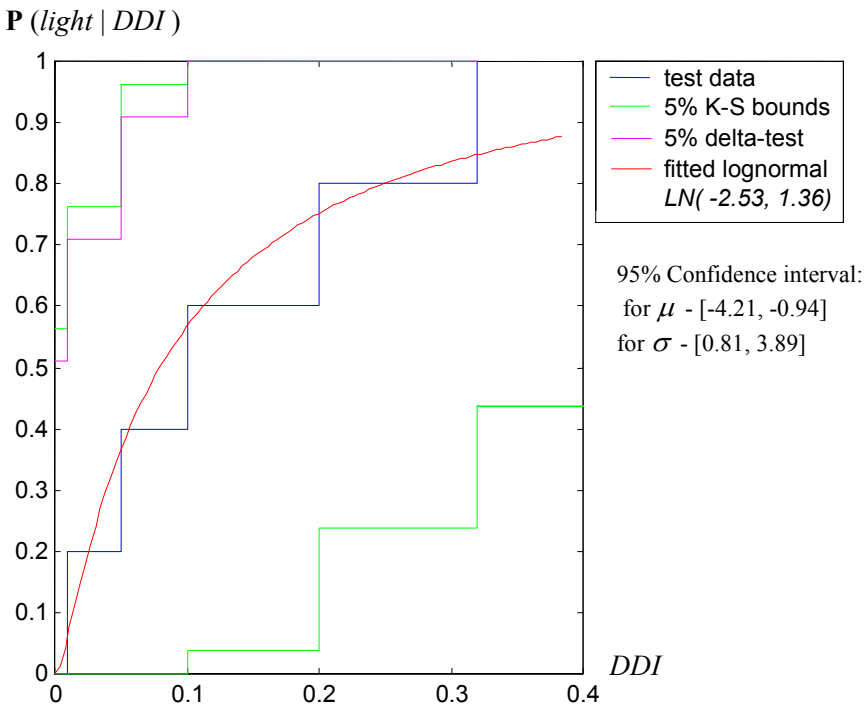

Figure C-5. Fragility function for light damage, from Williams *et al.* (1997) data.

It is desirable to reconcile the Williams *et al.* (1997) and Stone and Taylor (1993) fragility information. A statistical analysis, illustrated in Figure C-6, reveals close similarity between the yield damage state as defined by Stone and Taylor (1993) and the moderate damage state as defined by Williams *et al.* (1997). A Wilcoxon rank-sum test (Waerden, 1969) examines the null hypothesis that two sets of data are consistent with the same probability model. Here, the data sets are the PADI (with $\beta = 0.1$) at which the specimens tested by Williams *et al.* (1997) entered the moderate damage state, at which the Stone and Taylor (1993) specimens entered the yield damage state. The Wilcoxon test does not reject the null hypothesis at a 5% significance level. Given that the null-hypothesis is true, the test gives 97% probability that two newly generated samples from the same distribution would differ more than the present ones do. This result implies that the samples can be viewed as identically distributed.

It is difficult to distinguish clearly between the severe and collapse damage states. While identifying failure, researchers usually note decreased load capacity, without specifying the exact amount of the reduction. In terms of repair efforts, the distinction between these two damage states seems to be of minor importance, since

both states are usually classified as irreparable, implying the need for replacement in both cases. However, many of reviewed studies demonstrated effective repair of the failed reinforced-concrete members, implying a nonzero probability that such damage would be repaired.

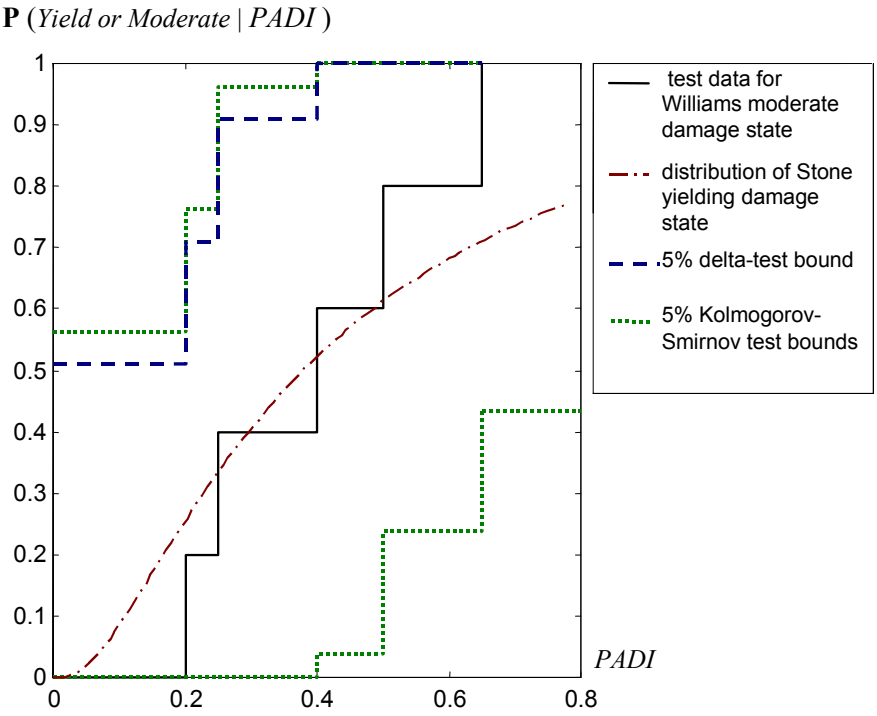

Figure C-6. Comparing Stone and Taylor (1993) yield with Williams *et al.* (1997) moderate damage.

A summary of the final fragility functions to be used in the present study is presented in Figure C-7. Table C-3 gives the final damage state descriptions and capacity parameters. The damage state names correspond to those used by Williams *et al.* (1997). Descriptions are based both on Stone and Taylor (1993) and Williams *et al.* (1997). The light damage state is defined according to Williams *et al.* (1997). The moderate damage corresponds to yield, per Stone and Taylor (1993), and moderate, per Williams *et al.* (1997). The severe and collapse damage states coincide with ultimate and failure, as defined by Stone and Taylor (1993). The parameters x_m and β refer to the median and logarithmic standard deviation of the fitted lognormal distributions of capacity, in terms of the displacement damage index, *DDI*.

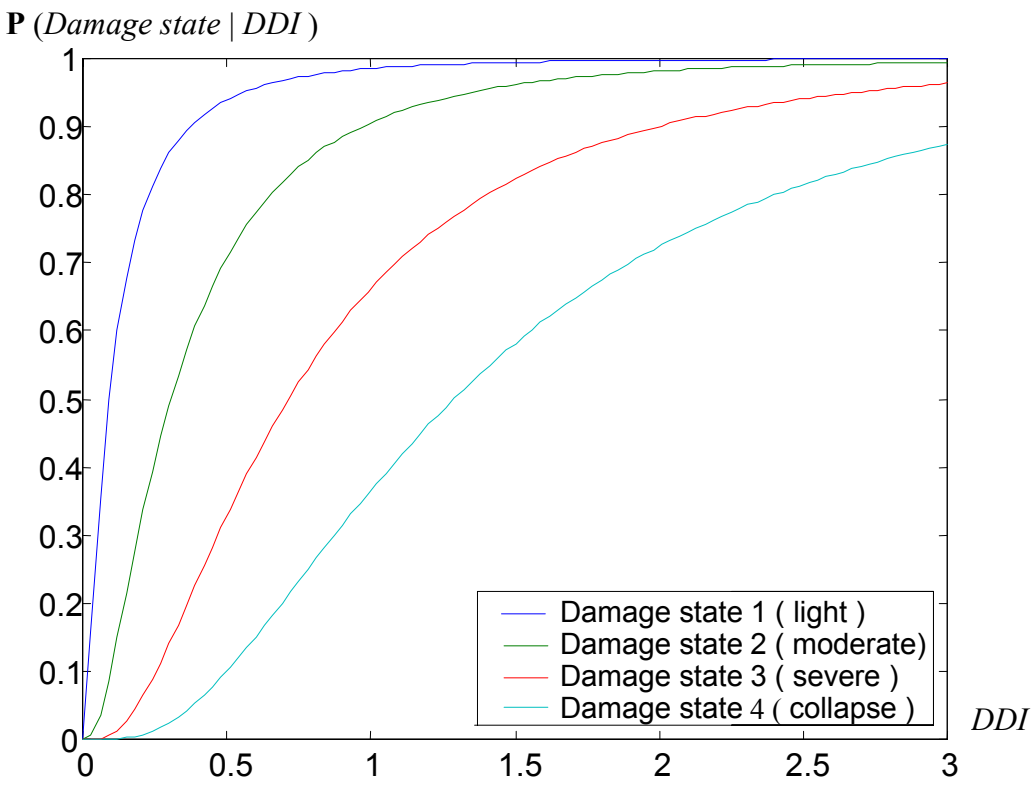

Figure C-7. Fragility functions for reinforced-concrete moment-frame members.

Table C-3. Damage-state descriptions and capacity parameters.

Damage state	**Description**	x_m	β
Light	Widespread light cracking; or a few cracks >1 mm, ≤ 2 mm wide; or light shear cracks tending to flatten towards 30^0	0.080	1.36
Moderate	Significant cracking, e.g. 90^0 cracks >2 mm; 45^0 cracks >2 mm; 30^0 cracks >1 mm. or yielded, not yet reached ultimate, where ultimate – maximum moment capacity.	0.31	0.89
Severe	Exceeded ultimate moment capacity but not yet decreased to 80% of maximum	0.71	0.80
Collapse	Moment capacity decreased below 80% of maximum	1.28	0.74

Note that we extrapolate from the Stone and Taylor (1993) and Williams *et al.* (1997) tests to all the reinforced concrete flexural members of the CUREE demonstration building, regardless of shape, dimension, reinforcing details, etc. This extrapolation is made because of the limited availability of test data. It would be valuable to revisit this analysis as additional data become available.

C.3 AVAILABLE REPAIR METHODS

To employ the capacities developed here in loss analyses, each damage state must be associated with loss consequences in terms of necessary repair efforts or implications for life safety or functionality. Let us first consider what repair methods are available. We will then turn to their apparent frequency of use. A variety of repair methods are available and have been used to restore damaged reinforced concrete elements. These include:

1. *Epoxy injection*. This requires filling the cracks with epoxy grout under pressure. According to ACI 546R-96 Section 22.6.6.3, this procedure can prevent all movement at an opening and restore the full strength of a cracked concrete member. Ozaka *et al.* (ND) support this statement by an experimental study of specimens repaired with epoxy injection of specimens with shear cracks less than 1 mm. The method is simple and widely used. Jennings (1971) gives examples of its application for buildings that were lightly damaged after 1971 San Fernando earthquake. However, some researchers report that the method is not always effective. Corazio and Durrandi (1989) repaired beam-to-column connections with cracks less than 1/8 in wide, and found that epoxy injection by itself might not be adequate for restoring strength and stiffness. In particular, restoring the bond and anchorage of bars can be difficult and unreliable. This is likely to restrict the method to light damage states where deterioration of bonds is negligible. Otherwise, the method is difficult to implement and its effectiveness depends greatly on the quality of the work.

   The Japanese Ministry of Construction Manual (PWRI, 1986) gives a good description of damaged concrete members that can be repaired by this method. This description agrees well with the light damage state given by Williams *et al.* (1997). Recommendations and requirements for epoxy material choice, surface preparation,

application techniques and equipment are also given in American Concrete Institute (1996a and 1996b).

2. *Replacement of damaged concrete.* This usually involves shoring of the structure, removal of the damaged concrete and replacement with new concrete. The bond between the old and the new concrete is ensured by applying an epoxy-based bonding agent to the old concrete surface. Corazio and Durrandi (1989) study the performance of two beam-to-column joints repaired with this technique. Damage was characterized by concrete spalling, penetrating cracks, deterioration of bond between longitudinal reinforcement and the concrete, and intact reinforcement. This type of damage can be recognized as the "yield" Stone-Taylor damage state. The technique is shown to be effective for restoring strength, stiffness and energy dissipation characteristics of the subassembly. Guidelines for removal of concrete, surface preparation and choosing epoxy bondage is given by the American Concrete Institute (1996b).

3. *Interior reinforcing.* A common method of providing additional reinforcement across cracked surfaces is to install new dowels in holes drilled perpendicular to the crack surfaces. The entire length of the dowel is fixed to the concrete by the use of a bonding matrix. Epoxy injection is commonly used to fill all cracks after installation of the dowels and their adhesive. The methodology and examples are described by the American Concrete Institute (1996b). The procedure is simple and uses commonly available equipment, but its applicability for seismic repair is doubtful. First, for severe damage states, the cracks penetrate in various directions and develop in large number, so there is no perpendicular direction for all of them. Second, for light damage, space constraints from the outside of the member may not permit drilling holes transverse to the crack. This situation would be typical for buildings. Third, the seismic performance of members repaired with this technique is not confirmed experimentally.

4. *Exterior reinforcing by reinforced-concrete jacketing.* This involves encasement with a reinforced concrete jacket together with additional reinforcement. Stoppenhagen *et al.* (1987) investigate the behavior of upgraded columns acting in moment-resisting

frame. Their results show that the method effectively prevents shear failure. Corazio and Durrandi (1989) demonstrate that strength, stiffness and energy dissipation capabilities can be effectively restored by jacketing the columns along with the beam segments adjacent to the columns, even in case of very severe damage. In particular, one test involved a column damaged to the point that its contribution to lateral load resistance was considerably reduced. Stoppenhagen *et al.* (1995) also show the effectiveness of this repair technique. Heavily damaged columns with shear failure, extensive spalling, bent longitudinal bars, and ½-in cracks, were encased with new columns containing longitudinal and shear reinforcement. The lateral capacity of the repaired frame increased by a factor of five, preserving the original stiffness. Ersoy *et al.* (1993) obtained similar results. They tested specimens in two damage states: one in which initial signs of concrete crushing were observed, and the other where considerable crushing and rebar buckling occurred. After repair, the columns had strength about 10% less than the corresponding monolithic column but with considerably less deformation capacity. The authors also emphasize that members repaired without unloading performed significantly worse. Rodriguez *et al.* (1992) repaired and tested specimens that were damaged beyond the failure damage state as classified by Stone and Taylor (1993). The repaired unit demonstrated an increase in strength and stiffness about three times those of the original specimen.

5. *Exterior reinforcing by steel jacketing*. This involves encasement of a member in steel plates, with epoxy resin used to bond the plates to the concrete. Ersoy (1992) points out that merely bonding plates to the concrete provides inadequate improvement, but that strengthened beams behaved well when the end of the plate was either welded to the main bar or was both clamped and epoxied to the beam. The technique is less laborious than concrete jacketing and is commonly used. Aboutaha *et al.* (1993) demonstrated that the method is effective for increasing shear strength of short columns. They tested original intact columns that were strengthened with steel jackets. They performed no tests involving damaged specimens. Tests with lightly damaged specimens were performed by Corazio and Durrandi (1989), who conclude that the method can be quite effective in restoring and improving the structural

performance of beam-column connections provided that design details properly address the transfer of forces through the joint.

6. *Exterior reinforcing by steel bracing*. This involves supplementing an exiting reinforced concrete frame with a steel frame. Goel *et al.* (1990) studied a repaired reinforced concrete frame that was damaged to the point close to ultimate loading capacity (2% drift). They find that response of the repaired frame was stable with increased stiffness, strength and energy dissipation.

7. *Combined methods*. Corazio and Durrandi (1989) report a combination of several techniques for repairing heavily damaged beams. The damage was in the form of severe flexural and diagonal cracks accompanied by the spalling of the cover concrete and buckling of the longitudinal reinforcement steel. Repair efforts included injection of resin, splicing the buckled portion of the reinforcement with new bars, and replacement of damaged concrete with epoxy mortar. The repaired specimens exhibited increased strength, ductility and energy dissipation capabilities along with reduced stiffness. Overall performance proved quite satisfactory, and specimens suffered much less damage after the repairs were performed.

   Ozaka and Suzuki (ND) repaired six specimens with epoxy injection accompanied by steel plates attached to the beam webs. Damage before repair was characterized by shear cracks 2 mm wide. The yield load after repair was 15% higher. The authors conclude that the steel plates increase the shear strength and member deformability.

8. *FRP jacketing.* This involves encasing in fiber-reinforced polymers (FRP), an innovative technique that has only recently been an object of experimental studies. Mosallam (2000) used specimens damaged to the point beyond yielding and then repaired them with epoxy injection, carbon-epoxy and E-glass-epoxy quasi-isotropic laminates. The ductility and strength of the repaired specimens were increased up to 42% and 53% respectively, as compared to the control specimens.

9. *Infill walls and wing walls*. Quite a number of researchers studied the performance of this type of reinforcement e.g., Bush *et al.* (1976), Altin *et al.* (1992), Aoyama *et al.* (1984). For a more complete list, see Moehle *et al.* (1994). Although these methods are

widely accepted within the industry and were generally reported as satisfactory for retrofitting existing buildings, no tests with previously damaged frames have been conducted, which poses a question about the adequacy of this technique for repair.

C.4 STATISTICS OF APPLICATION OF REPAIR TECHNIQUES

Given the variety of repair methods available, the next question to be addressed is how frequently each is used. Aguilar *et al.* (1989) studied 114 buildings that were damaged during 1985 Mexico City earthquake. They created a database containing descriptions of the buildings, types of damage and the repair techniques used. The level of damage for all buildings is described as severe. For the present study, the point of particular interest is the frequency of usage of different repair techniques for reinforced concrete moment frames. The relevant statistics are given in Table C-4.

Table C-4. Frequency of usage of different repair techniques for reinforced concrete frames after 1985 Mexico City earthquake.

Repair and strengthening technique	Number of times used
Epoxy resin	3
RC jacketing	35
Steel jacketing	9
Infill walls, wing walls	22
Steel bracing	7
Replacement	12

Bonacci *et al.* (2000) present a comparative study of the usage of steel jacketing and fiber reinforced polymer (FRP) jacketing. Their paper summarizes the results of a comprehensive survey of field applications of both steel plates and FRP composites as external reinforcement for the life extension of deteriorating RC flexural members. The authors demonstrate a trend toward using FRP jacketing rather than steel jacketing. This trend should be accounted for when evaluating the likelihood of using these methods in the future.

C.5 RELATING DAMAGE STATES TO REPAIR EFFORTS

There are no universally accepted standards for choosing repair methods for damaged reinforced-concrete flexural members. Even if a damage state is clear, there are several techniques that can be used, and it is difficult to predict the repair procedure an unknown engineer will specify in any future application. The engineer's depends not only on the damage itself but on a number of uncertain circumstances such as availability of materials, equipment, personnel, and company expertise. Table C-5 relates common repair techniques to damage.

Because more than one possible repair technique is associated with each damage state, a qualitative probabilistic relationship is proposed in Table C-6. The table gives the approximate likelihood that a particular damage state would be repaired in a particular way. The estimates are based on statistics of application and modern trends in the industry together with considerations addressed by Table C-5: the apparent acceptance by the engineering and construction industry, the availability of standards, the labor required to perform the repair, and any design difficulties. Methods employed to address the collapse damage state are assumed to be applicable to the severe damage state as well. The difference between the severe and collapse damage states is reduced to increasing likelihood of replacement for collapse damage state. Qualitative probabilities given in the table can form the basis for assigning a set of quantitative probabilities to repair events.

There is another factor that could affect the choice of repair techniques: overall repair objectives. If the owner's final goal is not merely to restore the structure but to improve its strength above its pre-earthquake condition, then methods that are unable to provide additional strength can be ruled out, reducing the available choices and altering the probabilities for remaining repair techniques.

Table C-5. Characteristics of repair techniques.

Technique	Damage states	Performance	Other remarks
Epoxy injection	Light to moderate	Good results for light damage. For heavier damage it is difficult to insure proper filling of every crack.	Commonly used (PWRI, 1986). Standards available (ACI 546R-96, ACI 224.1R-93). Easily implemented for light damage states. No design requirements. Requires care and high quality of the work for moderate damage.
Replacement of damaged concrete	Moderate	Provides full restoration of all member loading characteristics (strength, stiffness, energy dissipation). Does not provide strengthening. Requires full unloading of the member.	Every step (removing of damaged concrete, surface preparation, replacing with new concrete) is well documented by ACI standards (ACI 546R-96). No design requirements. Laborious. No data on acceptance of the method as a whole within the industry
R/C jacketing	Moderate to collapse	Provides full restoration or increasing of strength, stiffness and energy dissipation up to five times of original level, depending on repair details. May require unloading of the structure. Applied to the whole column, starting from the first floor.	Standards available (ACI 546R-96, building codes). Requires design. Very laborious. Accepted within the industry (Corazio and Durrandi, 1989).
Steel jacketing	Light to moderate	Effective for restoring and strengthening R/C structures providing proper design. Usually accompanied by epoxy injection.	Standards available (Hipley, 1997). Requires design. Less laborious than R/C jacketing. Well accepted within the industry (Bonacci *et al.* 2000).

Table B-5 (continued). Characteristics of repair techniques.

Technique	Damage states	Performance	Other remarks
Steel bracing	Moderate	Could effectively restore and strengthen the whole structure providing proper design. Applied to the whole frame.	Standards available (Seismic provisions 1997). Qualified designer required. Laborious. Accepted within the industry.
Epoxy injection and bar splicing and replacement of damaged concrete with epoxy mortar	Severe or collapse (plastic hinges)	Very effective for repair of isolated plastic hinges of beams far from beam-column joint, possible in specially designed joints.	Standards on each procedure are readily available (ACI 546R-96). No design requirements. Moderately laborious. No data on acceptance with the industry.
FRP jacketing	Moderate	Reported to be effective for recovery and increasing load capacity.	Standards and guidelines are available (Hipley, 1997, Saadatmanesh *et al.,* 1998). Easy to implement. Composite-materials designer is required. Method is finding increasing popularity in the industry. It is usually used as an alternative to steel jacketing (Bonacci *et al.,* 2000).
Infill walls and wing walls	No data	Shown to be effective as strengthening- retrofitting technique. Is applied to the whole column (wing walls) or to several bays (infill walls)	Some standards and guidelines for design are available from Caltrans (Hipley, 1997). Requires design. Laborious. Well accepted within the industry.

Table C-6. Proposed relation between damage states and repair techniques.

Damage state	Possible repair methods	Probability of usage*
Light	Epoxy injection	High
	FRP jacketing	Low
Moderate	Infill walls or wing walls	Low
	Steel bracing	Low
	R/C jacketing	Average
	FRP jacketing	Average
	Steel jacketing	Below average
Severe	Replacement	Above average
	R/C jacketing	Average
	Infill walls or wing walls	Average
Collapse	Replacement	High
	R/C jacketing	Below average
	Infill walls or wing walls	Below average

* Scale: low – below average – average – above average – high; applied independently to each damage state.

C.6 REINFORCED CONCRETE REPAIR COSTS

For the purposes of this project, repair costs were calculated by professional construction-cost estimators at Young & Associates of Palm Desert, California. The cost of three distinct repair efforts were estimated: epoxy injection of lightly damaged columns; reinforced concrete jacketing of moderately damage columns; and replacement of columns with severe or collapse damage. For each repair effort, two cases were considered: one where a partition abuts the column (and would be affected by the repair); and the other where there is no partition abutting the column. The cost estimates are shown in several tables. Table C-7 and Table C-8 show the cost of epoxy injection, at columns with and without an abutting partition. Table C-9 and Table C-10 show the cost of reinforced-concrete jacketing of a reinforced-concrete column. Table C-11 and Table C-12 give the cost to demolish and replace a reinforced-concrete column.

Some modification of these estimates was required for use in the analysis. First, on the advice of a shoring contractor, the cost estimator assumes that to replace a column would require shoring of the column from the ground floor to the roof,

regardless of the story level of the column being replaced. In the present loss estimate, this assumption is replaced by one that column replacement requires shoring from the ground up to and including the floor of the damaged column. A uniform distribution was assumed for the story level of a column requiring repair.

Second, the cost estimator assumes that for any repair of a column, scaffolding is required from the ground level to the roof. This assumption is similarly modified. In the case of epoxy injection, scaffolding is probably not required, as a window-washing rig could be used instead. In the case of column jacketing and column replacement, it is assumed that scaffolding is required only up to the floor level of the repair. Finally, painting costs are removed from the cost estimates, and are considered instead under line-of-site costs.

Third, contractor overhead and profit are excluded, and are included instead as a fraction of the total repair cost.

Table C-7. Unit cost of epoxy injection at column not abutted by partition.

SPEC	DESCRIPTION	QTY	unit	LABOR Unit Cost	Labor	MATERIAL Unit Cost	Mat'l	SUBCONTR. Unit Cost	Subcontr	TOTAL
(2)	**SITEWORK** Subtotal for Division: **$ 11,547**									
	Demolition:									
	Remove vinyl base, carpet & pad, window & frame at ea side of column	5	hrs	33.00	165		0.00		0.00	165
	Scaffolding:									
	Scaffolding for one column extends the length of ea unit at ea side of column, from ground to roof, approx. 24 ft wide	1	ls		0.00		0.00	11,100.00	11,100	11,100
	Temporary protection:									
	The unit is protected with visqueen screen walls for the demolition and the cleaning of the column	4	hrs	33.00	132	37.50	150		0.00	282
(3)	**CONCRETE** Subtotal for Division: **$ 1,505**									
	Concrete column repair:									
	Epoxy injection of all cracks incl scraping and cleaning of column after injection process - lineal footage allowance	80	lf		0.00		0.00	16.00	1,280	1,280
	Sacking, patching and grinding	4	hrs	45.00	180	3.75	15	7.50	30	225
(8)	**DOORS, WINDOWS, & GLASS** Subtotal for Division: **$ 2,592**									
	Metal windows:									
	Reset the existing aluminum windows at each side of the damaged column	144	sf		0.00		0.00	18.00	2,592	2,592
(9)	**FINISHES** Subtotal for Division: **$ 1,216**									
	Drywall:									
	Respray the acoustic ceiling at the bedroom areas of each affected unit including masking and cleanup	250	sf		0.00		0.00	1.85	463	463
	Painting:									
	Repaint the repaired column and the connecting beams	172	sf		0.00		0.00	1.45	249	249
	Flooring:									
	Replace carpet pad and re-install carpet	56	sy	4.50	252	4.50	252		0.00	504
(15)	**MECHANICAL** Subtotal for Division: **$ 98**									
	HVAC:									
	Reset window-mounted AC unit, 2 units	1	ea	97.50	98		0.00		0.00	98
		Subtotal			827		417		15,714	16,957
								General conds	5%	847.87
								TOTAL	Subtotal	$17,805

Table C-8. Unit cost of epoxy injection at column abutted by partition.

SPEC	DESCRIPTION	QTY	unit	LABOR Unit Cost	LABOR Labor	MATERIAL Unit Cost	MATERIAL Mat'l	SUBCONTR. Unit Cost	SUBCONTR. Subcont.	TOTAL
(2)	**SITEWORK**									
	Subtotal for Division:									
	$ 12,024									
	Demolition:									
	Remove vinyl base, carpet, pad, drywall, & metal studs at demising wall, window & frame ea side of column (X2), 9 mh/unit	18	hrs	33.00	594		0.00		0.00	594
	Remove wallpaper ea side of demising wall	600	sf		0.00		0.00	0.55	330	330
	Scaffolding:									
	Scaffolding extends length of unit ea side of col., ground to roof, ~24 ft. wide	1	ls		0.00		0.00	11,100	11,100	11,100
(3)	**CONCRETE**									
	Subtotal for Division:									
	$ 1,505									
	Concrete column repair:									
	Epoxy injection incl. scraping & cleaning of column after injection	80	lf		0.00		0.00	16.00	1,280	1,280
	Sack, patch and grind	4	hrs	45.00	180	3.75	15	7.50	30	225
(8)	**DOORS, WINDOWS, & GLASS**									
	Subtotal for Division:									
	$ 1,728									
	Metal windows:									
	Reset windows ea side of col	288	sf		0.00		0.00	6.00	1,728	1,728
(9)	**FINISHES**									
	Subtotal for Division:									
	$ 5,025									
	Drywall:									
	Metal studs and 5/8" drywall both sides	5	lf	108.00	540	15.00	75		0.00	615
	Respray acoustic ceiling at bedroom areas of ea unit incl. masking & cleanup	500	sf		0.00		0.00	1.85	925	925
	Painting:									
	Prime the walls of the bedroom area	600	sf		0.00		0.00	0.65	390	390
	Repaint column and connecting beams	172	sf		0.00		0.00	1.45	249	249
	Flooring:									
	Replace carpet pad, reinstall carpet	56	sy	4.50	252	4.50	252		0.00	504
	Vinyl base at 2 affected units	142	lf		0.00		0.00	1.70	241	241
	Wallpaper:									
	Install new wallpaper at affected units	1,200	sf		0.00		0.00	1.75	2,100	2,100
(10)	**SPECIALTIES**									
	Subtotal for Division:									
	$ 135									
	Shelving:									
	Reset closet shelving at 2 affected units	2	ea	67.50	135		0.00		0.00	135
(15)	**MECHANICAL**									
	Subtotal for Division:									
	$ 195									
	HVAC:									
	Reset AC unit at the two units	2	ea	97.50	195		0.00		0.00	195
		Subtotal			1,896		342		18,374	20,612
							General conds		5%	1,030.59
									TOTAL	$21,642

Table C-9. Unit cost of concrete jacketing, column not abutted by partition.

SPEC	DESCRIPTION	QTY	unit	LABOR Unit Cost	LABOR	MATERIAL Unit Cost	MATERIAL Mat'l	SUBCONTR. Unit Cost	SUBCONTR. Subcontr.	TOTAL
(2)	**SITEWORK**									
	Subtotal for Division:									
	$ 11,547									
	Demolition:									
	Remove vinyl base, carpet, pad, window & frame at ea side of column	5	hrs	33.00	165		0.00		0.00	165
	Scaffolding:									
	Scaffolding extends length of unit ea side of column, from ground to roof, ~24 ft wide	1	ls		0.00		0.00	11,100	11,100	11,100
	Temporary protection:									
	Unit is protected with visqueen screen walls for demolition and chipping of col.	4	hrs	33.00	132	37.50	150		0.00	282
(3)	**CONCRETE**									
	Subtotal for Division:									
	$ 5,056									
	Concrete column repair:									
	Chip cover concrete ~3-4", expose rebar, transport debris to ground-level container	24	hrs	33.00	792		0.00		0.00	792
	New vertical #5 @ 8" o.c. epoxy dowels into existing beams T&B, #3 @ 4" o.c. horizontal	1	ls	720	720	250.00	250		0.00	970
	Rebar #5 dowels epoxied into beams above and below to tie in new vert. steel	20	ea		0.00		0.00	45.00	900	900
	Column forms and braces, plyform, chamfer strips, 2X4 walls & diag braces	24	hrs	45	1,080	12.50	300		0.00	1,380
	Concrete pump rental - 52 meter pump	2	hrs		0.00		0.00	185.00	370	370
	Concrete 5000 psi pump mix	0.75	cy	180.00	135	125.00	94		0.00	229
	Strip forms, drypack void at the top of the column, sacking, patching and grinding	8	hrs	45.00	360	3.13	25	3.75	30	415
(8)	**DOORS, WINDOWS, & GLASS**									
	Subtotal for Division:									
	$ 2,592									
	Metal windows:									
	Reset E windows at ea side of column	144	sf		0.00		0.00	18.00	2,592	2,592
(9)	**FINISHES**									
	Subtotal for Division:									
	$ 1,216									
	Drywall:									
	Respray ceiling, incl. masking and cleanup	250	sf		0.00		0.00	1.85	463	463
	Painting:									
	Repaint column & connecting beams	172	sf		0.00		0.00	1.45	249	249
	Flooring:									
	Replace carpet pad, reinstall carpet	56	sy	4.50	252	4.50	252		0.00	504
(15)	**MECHANICAL**									
	Subtotal for Division:									
	$ 98									
	HVAC:									
	Reset E AC units	1	ea	97.50	98		0.00		0.00	98
		Subtotal			3,734		1,071		15,704	20,508
							General conds		5%	1,025.41
									TOTAL	$21,534

Table C-10. Unit cost of concrete jacketing, column abutted by partition.

SPEC	DESCRIPTION	QTY	unit	LABOR Unit Cost	LABOR Labor	MATERIAL Unit Cost	MATERIAL Mat'l	SUBCONTR. Unit Cost	SUBCONTR. Subcont.	TOTAL
	SITEWORK									
	Subtotal for Division: **$12,024**									
	Demolition:									
	Remove vinyl base, carpet, pad, drywall & metal studs, window & frame ea side of col.	18	hrs	33.00	594		0.00		0.00	594
	Remove wallpaper ea side of demising wall	600	sf		0.00		0.00	0.55	330	330
	Scaffolding:									
	Scaffolding extends length of unit each side of column, from ground to roof and ~24 ft wide	1	ls		0.00		0.00	11,100	11,100	11,100
(3)	**CONCRETE**									
	Subtotal for Division: **$5,056**									
	Concrete column repair:									
	Chip cover concrete ~3-4", expose rebar, transport debris to ground-level container	24	hrs	33.00	792		0.00		0.00	792
	New vertical #5 @ 8" o.c. epoxy dowels into existing beams T&B, #3 @ 4" o.c. horizontal	1	ls	720	720	250	250		0.00	970
	Rebar #5 dowels epoxied into beams above and below to tie in the new vert. steel	20	ea		0.00		0.00	45.00	900	900
	Column forms and braces, plyform, chamfer strips, 2X4 walls and diagonal braces	24	hrs	45	1,080	12.50	300		0.00	1,380
	Concrete pump rental - 52 meter pump	2	hrs		0.00		0.00	185.00	370	370
	Concrete 5000 psi pump mix	0.75	cy	180.00	135	125	94		0.00	229
	Strip forms, drypack void at the top of the column, sacking, patching and grinding	8	hrs	45.00	360	3.13	25	3.75	30	415
(8)	**DOORS, WINDOWS, & GLASS**									
	Subtotal for Division: **$5,184**									
	Metal windows:									
	Replace damaged Al windows ea side of col.	288	sf		0.00		0.00	18.00	5,184	5,184
(9)	**FINISHES**									
	Subtotal for Division **$5,025**:									
	Drywall:									
	Metal studs & 5/8" drywall	5	lf	108.00	540	15.00	75		0.00	615
	Respray ceiling incl. masking & cleanup	500	sf		0.00		0.00	1.85	925	925
	Painting:									
	Prime the walls of the bedroom area	600	sf		0.00		0.00	0.65	390	390
	Repaint column and connecting beams	172	sf		0.00		0.00	1.45	249	249
	Flooring:									
	Replace carpet pad, re-install carpet	56	sy	4.50	252	4.50	252		0.00	504
	Vinyl base at the two affected units	142	lf		0.00		0.00	1.70	241	241
	Wallpaper:									
	Install new wallpaper at the two affected units	1,200	sf		0.00		0.00	1.75	2,100	2,100
(10)	**SPECIALTIES**									
	Subtotal for Division: **$135**									
	Shelving: Reset the closet shelving	2	ea	67.50	135		0.00		0.00	135
(15)	**MECHANICAL**									
	Subtotal for Division: **$195**									
	HVAC:									
	Reset E AC unit at the two units	2	ea	97.50	195		0.00		0.00	195
		Subtotal			4,803		996		21,820	27,619
							General conditions		5%	1,380.93
									TOTAL	$28,999

Table C-11. Unit cost of column replacement, column not abutted by partition.

SPEC	DESCRIPTION	QTY	unit	LABOR Unit Cost	LABOR	MATERIAL Unit Cost	MATERIAL Mat'l	SUBCONTR. Unit Cost	SUBCONTR. Subcontr.	TOTAL
(2)	**SITEWORK**									
	Subtotal for Division: **$24,981**									
	Demolition:									
	Remove vinyl base, carpet, pad, window & frame ea side of col.	5	hrs	33.00	165		0.00		0.00	165
	Scaffolding:									
	Scaffold length of unit ea side of col., ground to roof, ~24ft wide	1	ls		0.00		0.00	11,100	11,100	11,100
	Shoring:									
	Temp shoring 7 floors incl. drawings, engineering and labor	140	hrs	33.00	4,620	51.79	7,250		0.00	11,870
	Temporary protection:									
	Protect units with carpet mask & visqueen screen walls for demolition and shoring	42	hrs	33.00	1,386	10.95	460		0.00	1,846
(3)	**CONCRETE**									
	Subtotal for Division: **$4,942**									
	Concrete column repair:									
	Demolish column & rebar incl transporting debris to ground-level container	32	hrs	33.00	1,056		0.00		0.00	1,056
	Rebar replacement - column C10 with six #9 bars and #3 ties at 4" o.c.	1	ls	720	720	250.00	250		0.00	970
	Column forms & braces, plyform, chamfer strips, 2X4 walls and diagonal braces	24	hrs	45	1,080	12.50	300		0.00	1,380
	Concrete pump rental - 52 meter pump	4	hrs		0.00		0.00	185.00	740	740
	Concrete 5000 psi pump mix	1.25	cy	180.00	225	125.00	156		0.00	381
	Strip forms, drypack void at the top of the column, sacking, patching and grinding	8	hrs	45.00	360	3.13	25	3.75	30	415
(8)	**DOORS, WINDOWS, & GLASS**									
	Subtotal for Division: **$2,592**									
	Metal windows:									
	Replace the damaged aluminum windows at each side of the damaged column	144	sf		0.00		0.00	18.00	2,592	2,592
(9)	**FINISHES**									
	Subtotal for Division: **$4,847**									
	Drywall:									
	Metal studs and 5/8" drywall both sides to fill the opening in the demising wall	5	lf	108.00	540	15.00	75		0.00	615
	Respray ceiling incl. masking & cleanup	1,750	sf		0.00		0.00	1.85	3,238	3,238
	Painting:									
	Repaint column and connecting beams	172	sf		0.00		0.00	1.45	249	249
	Flooring:									
	Replace carpet pad, re-install carpet	56	sy	4.50	252	4.50	252		0.00	504
	Vinyl base at the two affected units	142	lf		0.00		0.00	1.70	241	241
(15)	**MECHANICAL**									
	Subtotal for Division: **$98**									
	HVAC:									
	Reset E AC units	1	ea	97.50	98		0.00		0.00	98
		Subtotal			10,502		8,768		18,190	37,460
							General conditions		5%	1,873.00
									Total	$39,333

Table C-12. Unit cost of column replacement, column abutted by partition.

SPEC	DESCRIPTION	QTY	unit	LABOR Unit Cost	LABOR Labor	MATERIAL Unit Cost	MATERIAL Mat'l	SUBCONTR. Unit Cost	SUBCONTR. Subcontr.	TOTAL
(2)	**SITEWORK**									
	Subtotal for Division: **$25,740**									
	Demolition:									
	Remove vinyl base, carpet, pad, window & frame ea side of col.	18	hrs	33.00	594		0.00		0.00	594
	Remove wallpaper	600	sf		0.00		0.00	0.55	330	330
	Scaffolding:									
	Scaffold ground to roof, 24ft wide	1	ea		0.00		0.00	11,100	11,100	11,100
	Shoring:									
	Shore 7 floors incl. drawings, eng., & labor	140	hrs	33.00	4,620	51.79	7,250		0.00	11,870
	Temporary protection:									
	Protect units w/carpet mask & visqueen screen walls for demolition and shoring	42	hrs	33.00	1,386	10.95	460		0.00	1,846
(3)	**CONCRETE**									
	Subtotal for Division: **$4,942**									
	Concrete column repair:									
	Demolish column & rebar incl transporting debris to ground-level container	32	hrs	33.00	1,056		0.00		0.00	1,056
	Rebar replacement - column C10 with six #9 bars and #3 ties at 4" o.c.	1	ls	720	720	250.00	250		0.00	970
	Column forms & braces, plyform, chamfer strips, 2X4 walls and diagonal braces	24	hrs	45	1,080	12.50	300		0.00	1,380
	Concrete pump rental - 52 meter pump	4	hrs		0.00		0.00	185.00	740	740
	Concrete 5000 psi pump mix	1.25	cy	180.00	225	125.00	156		0.00	381
	Strip forms, drypack void at the top of the column, sacking, patching and grinding	8	hrs	45.00	360	3.13	25	3.75	30	415
(8)	**DOORS, WINDOWS, & GLASS**									
	Subtotal for Division: **$5,184**									
	Metal windows:									
	Replace damaged windows ea side of col.	288	sf		0.00		0.00	18.00	5,184	5,184
(9)	**FINISHES**									
	Subtotal for Division: **$11,485**									
	Drywall:									
	Metal studs and 5/8" drywall	5	lf	108.00	540	15.00	75		0.00	615
	Respray ceiling incl. masking & cleanup	3,500	sf		0.00		0.00	1.85	6,475	6,475
	Painting:									
	Prime the walls of the bedroom area	2,000	sf		0.00		0.00	0.65	1,300	1,300
	Repaint column & connecting beams	172	sf		0.00		0.00	1.45	249	249
	Flooring:									
	Replace carpet pad, re-install carpet	56	sy	4.50	252	4.50	252		0.00	504
	Vinyl base at the two affected units	142	lf		0.00		0.00	1.70	241	241
	Wallpaper: Install new wallpaper	1,200	sf		0.00		0.00	1.75	2,100	2,100
(10)	**SPECIALTIES**									
	Subtotal for Division: **$135**									
	Shelving: Reset closet shelving	2	ea	67.50	135		0.00		0.00	135
(15)	**MECHANICAL**									
	Subtotal for Division: **$195**									
	HVAC: Reset E AC units	2	ea	97.50	195		0.00		0.00	195
		Subtotal			11,163		8,768		27,750	47,681
							General conditions		5%	2,384.05
									TOTAL	$50,065

Appendix D. Discrete-Time Market Risk Analysis

GIVEN:

r = (known) decision-maker's risk-free discount rate per term, above inflation

c = (known) initial investment amount at time 0, i.e., initial equity

V = (uncertain) net present value of property (neglecting earthquake risk), for ownership period n

X_i = (uncertain) return on equity c in term i, i = 0, 1, 2, …

Y_i = (uncertain) income in term i, i = 0, 1, 2, … paid at beginning of term

$\sigma = (E[(X_i - X_{i-1})^2])^{0.5}$, i = 0, 1, … i.e., volatility of annual return (known constant value)

REQUIRED:

δ_V, i.e., the coefficient of variation on V

where

$$V = Y_0 + Y_1\exp(-r) + Y_2\exp(-2r) + \ldots$$
$$= Y_0 + \Sigma_{i=1\ldots\infty} Y_i\exp(-ir) \quad \text{(D-1)}$$

From the given information,

$$Y_i = cX_i, \; i = 0, 1, 2, \ldots \quad \text{(D-2)}$$

From (D-1) & (D-2), and observing that X_0 is known at the time of investment,

$$V = c(x_0 + \Sigma_{i=1..\infty} X_i\exp(-ir)) \quad \text{(D-3)}$$

Let F_i be independent and identically distributed standard Gaussian variates, i.e., $F_i \sim N(\mu = 0, \sigma = 1)$, i = 1, 2, …

$$X_i = X_{i-1} + \sigma F_i$$
$$= X_{i-2} + \sigma F_{i-1} + \sigma F_i$$
$$\ldots$$

$$= x_0 + \sigma(F_1 + F_2 + \dots F_i)$$

$$= x_0 + \sigma i^{0.5} G_i \qquad \text{(D-4)}$$

where $G_I = i^{(-0.5)} \Sigma_{j=1..i} F_j$

Substituting (D-4) in (D-3),

$$V = c(x_0 + \Sigma_{i=1..\infty}\{x_0 + \sigma i^{0.5} G_i\}\exp(-ir))$$

$$= c(x_0 + \Sigma_{i=1..\infty}\{x_0 \exp(-ir)\} + \Sigma_{i=1..\infty}\{\sigma i^{0.5} G_i \exp(-ir)\})$$

$$= cx_0 \Sigma_{i=0..\infty}\{\exp(-ir)\} + c\sigma\Sigma_{i=1..\infty}\{i^{0.5} G_i \exp(-ir)\}$$

$$= cx_0/r + c\sigma\Sigma_{i=1..\infty}\{i^{0.5} G_i \exp(-ir)\} \qquad \text{(D-5)}$$

$$E[V] = E[cx_0/r] + E[c\sigma\Sigma_{i=1..\infty}\{i^{0.5} G_i \exp(-ir)\}]$$

$$= cx_0/r \qquad \text{(D-6)}$$

$$\text{Var}[V] = \text{Var}[c\sigma\Sigma_{i=1..\infty}\{i^{0.5} G_i \exp(-ir)\}]$$

$$= (c\sigma)^2 \text{Var}[\Sigma_{i=1..\infty}\{i^{0.5} G_i \exp(-ir)\}]$$

$$= (c\sigma)^2 E[(\Sigma_{i=1..\infty}\{i^{0.5} G_i \exp(-ir)\})^2]$$

$$= (c\sigma)^2 E[\Sigma_{i=1..\infty}\Sigma_{j=1..\infty}(ij)^{0.5} G_i G_j \exp(-(i+j)r)]$$

$$= (c\sigma)^2 \{\Sigma_{i=1..\infty}\Sigma_{j=1..\infty}(ij)^{0.5} E[G_i G_j]\exp(-(i+j)r)\} \qquad \text{(D-7)}$$

$$E[G_i G_j] = ij^{(-0.5)} E[\Sigma_{k=1..i}\Sigma_{l=1..j} F_k F_l]$$

$$= ij^{(-0.5)} \Sigma_{k=1..min(i,j)} E[(F_k)^2] \qquad \text{N.B. } E[F_k F_l]=0 \text{ for } k \neq l$$

$$= ij^{(-0.5)} min(i,j) \qquad \text{(D-8)}$$

Substituting (D-8) into (D-7),

$$\text{Var}[V] = (c\sigma)^2 \{\Sigma_{i=1..\infty}\Sigma_{j=1..\infty} min(i,j)\exp(-(i+j)r)\}$$

$$= (c\sigma)^2 \{\Sigma_{i=1..\infty} i\exp(-ir)\, \Sigma_{j=i..\infty} \exp(jr) + \Sigma_{i=2..\infty} \exp(-ir)\, \Sigma_{j=1..i-1} j\exp(jr)\}$$

$$= (c\sigma)^2 \left\{ \frac{\exp(-2r)}{[1-\exp(-r)][1-\exp(-2r)]} + \frac{\exp(-3r)}{[1-\exp(-r)]^3} - \frac{2\exp(-4r) - \exp(-5r) - \exp(-6r)}{[1-\exp(-r)]^2 [1-\exp(-2r)]^2} \right\}$$

$$= (c\sigma)^2 \frac{\exp(-2r)}{[1-\exp(-2r)][1-\exp(-r)]^2} \qquad \text{(D-9)}$$

first order approximation for Var(V):

$$\mathrm{Var}[V] \approx (c\sigma)^2/(2r^3) \tag{D-10}$$

For typical values of r (0.01..0.2), expression (D-10) provides relative error less than 1% as compared to (D-9)

$$\begin{aligned}\delta_V &= (\mathrm{Var}[V])^{0.5}/\mathrm{E}[V] \\ &= (c\sigma/(2r^3)^{0.5})/(cx_0/r) \\ &= \sigma/((2r)^{0.5}x_0)\end{aligned} \tag{D-11}$$

Thus, the market risk is a simple factor $(1/(2r)^{0.5})$ of the ratio of volatility on return (σ) to initial return (x_0). More volatility relative to initial return on equity means more uncertainty on value, as one would expect.

Appendix E. A Stochastic Model of Net Income

E.1 INTRODUCTION

In this appendix, a probability model is derived for $I(t_L)$, the present value of the net income stream over the specified lifetime t_L for the income property. This model is based on a stochastic-process model for the after-tax net income stream.

Let $r_e(t)$ be the after-tax income yield at time t. Then if P is the purchase price for the property, $Pr_e(t)$ is the after-tax income rate at time t. Therefore,

$$I(t_L) = P\int_0^{t_L} e^{-rt} r_e(t)\, dt \tag{E-1}$$

where e^{-rt} is the continuous-time discount factor and r is the specified discount rate. It is noted that r should be selected as the appropriate risk-free interest rate less the inflation rate. The risk-free interest rate can be taken as the government bond rate with a maturity date at time t_L into the future. The inflation rate over time t_L will be very uncertain and so it, and hence r, should be treated as random variables. It is common, however, to take a constant estimated inflation. Consider, for example, the present value of a repair cost one year hence if it costs \$100 today. If the expected inflation rate in this cost is 3% over the year, then the repair will cost \$103 when done. If the risk-free interest rate is currently 5% per annum, then \$98 must be invested today to have the \$103 for the repair one year later. This is equivalent to saying that the \$100 cost must be discounted at the real interest rate of 2% (= 5% – 3%) to get its present value of \$98.

E.2 MEAN DISCOUNTED NET INCOME

A reasonable model for the mean after-tax yield at time t is:

$$\mathbf{E}[r_e(t)] = \mathbf{E}[r_e(0)]e^{gt} \tag{E-2}$$

where g is the real growth rate in after-tax yield (i.e., actual growth rate less the inflation rate). From Equations E-1 and E-2, the mean discounted net over time period t_L is given by:

$$\begin{aligned}\mathbf{E}[I(t_L)] &= P\mathbf{E}[r_e(0)]\int_0^{t_L} e^{(g-r)t}\,dt \\ &= P\mathbf{E}[r_e(0)]\left(e^{(g-r)t_L}-1\right)/(g-r), \qquad if\ g \neq r \\ &= P\mathbf{E}[r_e(0)]t_L, \qquad if\ g = r\end{aligned} \tag{E-3}$$

Note that $g - r$ = actual growth rate less the risk-free discount rate and so, unlike g and r, it is independent of the inflation rate.

E.3 VARIANCE OF DISCOUNTED NET INCOME

Define $\delta r_e(t) = r_e(t) - \mathbf{E}[r_e(t)]$. Then the variance of the discounted net income over time period t_L is given by:

$$\begin{aligned}\mathbf{Var}[I(t_L)] &= \mathbf{E}[\{I(t_L) - \mathbf{E}[I(t_L)]\}^2] \\ &= \mathbf{E}\left[\left\{P\int_0^{t_L} e^{-rt}\delta r_e(t)\,dt\right\}^2\right] \\ &= P^2\int_0^{t_L}\int_0^{t_L} e^{-r(s+t)}\mathbf{E}[\delta r_e(s)\delta r_e(t)]\,ds\,dt\end{aligned} \tag{E-4}$$

The variance therefore depends on the autocovariance of the after-tax income stream, $\mathbf{E}[\delta r_e(s)\delta r_e(t)]$, which describes the correlation between times s and t.

A reasonable model for this autocovariance is one corresponding to a continuous-time random walk for $r_e(t)$ with drift $\mathbf{E}[r_e(t)]$, also known as a Wiener process (Papoulis, 1991), which gives:

$$\mathbf{E}[\delta r_e(s)\delta r_e(t)] = \mathbf{Var}[r_e(0)] + \lambda^2 \min(s,t) \tag{E-5}$$

This gives a variance for $r_e(t)$ that increases linearly in time:

$$\mathbf{Var}[r_e(t)] = \mathbf{E}[\delta r_e(t)^2] = \mathbf{Var}[r_e(0)] + \lambda^2 t \tag{E-6}$$

Substituting Equation E-6 into E-4 and carrying out the necessary integrations:

$$\begin{aligned}\mathbf{Var}[I(t_L)] = &\frac{P^2}{r^2}\mathbf{Var}[r_e(0)](1-e^{-rt_L})^2 \\ &+\frac{\lambda^2 P^2}{2r^3}(1-4e^{-rt_L}+3e^{-2rt_L}+2rt_L e^{-2rt_L})\end{aligned} \tag{E-7}$$

E.4 DISTRIBUTION FOR DISCOUNTED NET INCOME

Suppose the after-tax yield, $r_e(t)$, is modeled as a Gaussian process with mean and autocovariance given by Equations E-2 and E-5 respectively. Since the integration in Equation E-1 is a linear operation, the result is also Gaussian, implying that $I(t_L)$ is normally distributed with mean and variance given by Equations E-3 and E-7, respectively.

Appendix F. Moments of the Lifetime Loss

F.1 INTRODUCTION

In this appendix, we derive the expression for the moment generating function of the present value of the total earthquake loss, L(t):

$$L(t) = \sum_{k=1}^{N(t)} C_k e^{-rT_k} \tag{F-1}$$

where $r \geq 0$ is the discount rate and there are $N(t)$ earthquakes occurring at successive times $T_1,\ldots,T_{N(t)}$ in the region around the site of a structure of interest, which lead to losses $C_1,\ldots,C_{N(t)}$, respectively, for the structure. The derivation is based on the three assumptions:

1. The number of earthquake events of interest during the lifetime t, $N(t)$, is modeled by a Poisson process with mean occurrence rate v.

2. The earthquake losses $\{C_1, C_2, \ldots\}$ are assumed to be independent and identically distributed (i.i.d.) with probability density function $f_C(c)$.

3. These losses are also assumed to be independent of the time of occurrence of earthquakes, that is, the arrival times $\{T_1, T_2, \ldots\}$.

Note that the distribution of the earthquake arrival times is implied by the probability model for $N(t)$. Obviously, each T_k $\left(k \leq N(t)\right)$ assumes values between 0 and t. From the theory of Poisson processes, they are dependent (e.g., $T_1 < \cdots < T_{N(t)}$), and each T_k follows a gamma distribution with parameters k and v. The dependent nature of the arrival times $\{T_1, T_2, \ldots\}$ unfortunately renders $L(t)$ difficult to analyze.

The approach used here to obtain the statistical properties of $L(t)$ is based on the following simple but important observation (to be proved shortly): *the order in which the arrival times enter the expression for* $L(t)$ *does not affect the distribution of* $L(t)$. Specifically, let

$\{U_k : k = 1,2,\ldots\}$ be i.i.d. uniform random variables on (0,1), which are also independent of $N(t)$. For every $t \geq 0$, define a random variable

$$R_U(t) = \sum_{k=1}^{N(t)} C_k e^{-rtU_k} \tag{F-2}$$

Then, as we will show, $L(t)$ and $R_U(t)$ are identically distributed for every t. The expression for $R_U(t)$ is the same as that for $L(t)$ except that the arrival times $\{T_1,\ldots,T_{N(t)}\}$ in the latter are replaced by $\{U_1,\ldots,U_{N(t)}\}$ in the former. The important feature of $R_U(t)$ is that it only involves random variables that are mutually independent, which makes $R_U(t)$ substantially easier to analyze than $L(t)$ and consequently allows its statistical moments to be obtained in manageable forms. The statistical properties for $R_U(t)$ can then be used as those for $L(t)$, since they are identically distributed for every t.

In the remainder of this appendix, the statistical equivalence of $L(t)$ and $R_U(t)$ is established. The moment generating function of $L(t)$ is then derived, which provides a means for evaluating the expected value of utility functions that are an exponential function of $L(t)$. It also provides a means for obtaining the statistical moments of $L(t)$, from which the expectation of any function of $L(t)$ can be evaluated using a Taylor-series representation of the function.

F.2 STATISTICAL EQUIVALENCE OF $L(T)$ AND $R_u(T)$

In this section, the statistical equivalence of $L(t)$ and $R_U(t)$ is established in a series of propositions. For convenience in notation, we use braced quantities to denote the set of quantities inside the brace generated by running the subscripted index (or indexes) of the brace from 1 to the superscripted index (or indexes). For example, $\{\sigma_n(k)\}_k^n = \{\sigma_n(1),\ldots,\sigma_n(n)\}$. We start with the following proposition, which says that the distribution of the sum $\sum_{k=1}^n y_k X_k$ is unaltered by shuffling the i.i.d. X_k's.

Proposition 1. Let $\{X_k\}_k^n$ be i.i.d. random variables, $\{y_k\}_k^n \in \mathbf{R}, n \in \mathbf{Z}^+$, and $\{\sigma_n(k)\}_k^n$ be any given permutation of {1,…,*n*}. Then for any $c \in \mathbf{R}$,

$$\mathbf{P}\left(\sum_{k=1}^{n} y_k X_k \le c\right) = \mathbf{P}\left(\sum_{k=1}^{n} y_k X_{\sigma_n(k)} \le c\right) \tag{F-3}$$

Proof: Let $\mathbf{I}_A$ be the indicator function of a set A, $F_{\{x_k\}}$ be the joint distribution function of $\{X_k\}_k^n$ and F_X be the marginal distribution function of X_k. Then

$$\begin{aligned}\mathbf{P}\left(\sum_{k=1}^{n} y_k X_k \le c\right) &= \int \mathbf{I}_{\left\{\sum_{k=1}^{n} y_k x_k \le c\right\}} dF_{\{X_k\}}(x_1,\ldots,x_n) \\ &= \int \mathbf{I}_{\left\{\sum_{k=1}^{n} y_k x_k \le c\right\}} dF_X(x_1)\cdots dF_X(x_n), \quad \text{since } \{X_k\}_k^n \text{ are i.i.d.}\end{aligned} \tag{F-4}$$

Since $(x_1,\ldots,x_n)$ are just dummy integration variables, we can replace them by $\left\{x_{\sigma_n(1)},\ldots,x_{\sigma_n(n)}\right\}$, while keeping the domain of integration the same. The right-hand side of Equation F-4 then becomes:

$$\begin{aligned}\mathbf{P}\left(\sum_{k=1}^{n} y_k X_k \le c\right) &= \int \mathbf{I}_{\left\{\sum_{k=1}^{n} y_k x_{\sigma_n(k)} \le c\right\}} dF_X\left(x_{\sigma_n(1)}\right)\cdots dF_X\left(x_{\sigma_n(n)}\right) \\ &= \mathbf{P}\left(\sum_{k=1}^{n} y_k X_{\sigma_n(k)} \le c\right)\end{aligned}$$

The next proposition says that Proposition 1 is also true when the coefficients are random as long as they are independent of the X_k's.

Proposition 2. Let $\{X_k\}_k^n$ be i.i.d. random variables, $\{Y_k\}_k^n$ be random variables independent of $\{X_k\}_k^n$ and $\{\sigma_n(k)\}_k^n$ be any given permutation of {1,…,*n*). Then for any $c \in \mathbf{R}$,

$$\mathbf{P}\left(\sum_{k=1}^{n} X_k Y_k \le c\right) = \mathbf{P}\left(\sum_{k=1}^{n} X_{\sigma_n(k)} Y_k \le c\right) \tag{F-5}$$

Proof:

$$\mathbf{P}\left(\sum_{k=1}^{n} X_k Y_k \le c\right)$$

$$= \int \mathbf{P}\left(\sum_{k=1}^{n} X_k y_k \le c \,\middle|\, \{Y_k\} = \{y_k\}\right) dF_{\{Y_k\}}(y_1,\ldots,y_n)$$

$$= \int \mathbf{P}\left(\sum_{k=1}^{n} X_k y_k \le c\right) dF_{\{Y_k\}}(y_1,\ldots,y_n), \quad \text{since } \{X_k\}_k^n \text{ and } \{Y_k\}_k^n \text{ are independent}$$

$$= \int \mathbf{P}\left(\sum_{k=1}^{n} X_{\sigma_n(k)} y_k \le c\right) dF_{\{Y_k\}}(y_1,\ldots,y_n), \quad \text{by Equation D3}$$

$$= \int \mathbf{P}\left(\sum_{k=1}^{n} X_{\sigma_n(k)} y_k \le c \,\middle|\, \{Y_k\} = \{y_k\}\right) dF_{\{Y_k\}}(y_1,\ldots,y_n)$$

$$= \mathbf{P}\left(\sum_{k=1}^{n} X_{\sigma_n(k)} Y_k \le c\right)$$

Corollary 1. Proposition 2 holds for any random permutation $\{\sigma_n(k)\}_k^n$ of {1,…,*n*} that is independent of X_k's and Y_k's.

The next proposition shows that the invariance in the distribution of the sum $\sum_{k=1}^{n} X_k Y_k$ to any shuffling in the X_k's implies invariance to any shuffling in the Y_k's as well.

Proposition 3. Let $\{X_k\}_k^n$ be i.i.d. random variables, $\{Y_k\}_k^n$ be random variables independent of $\{X_k\}_k^n$ and $\{\sigma_n(k)\}_k^n$ be any given permutation of {1,…,*n*}. Then for any $c \in \mathbf{R}$,

$$\mathbf{P}\left(\sum_{k=1}^{n} X_k Y_k \le c\right) = \mathbf{P}\left(\sum_{k=1}^{n} X_k Y_{\sigma_n(k)} \le c\right) \tag{F-6}$$

Proof: For a given permutation σ_n, since there is a $1-1$ correspondence between {1,…,*n*} and $\{\sigma_n(1),\ldots,\sigma_n(n)\}$, the inverse σ_n^{-1} of σ_n exists, which is also a permutation of {1,…,*n*}. By Proposition 2,

$$\mathbf{P}\left(\sum_{k=1}^{n} X_k Y_k \le c\right) = \mathbf{P}\left(\sum_{k=1}^{n} X_{\sigma_n^{-1}(k)} Y_k \le c\right) \tag{F-7}$$

For each k = 1,…,n, let $j_k = \sigma_n^{-1}(k)$, so that $k = \sigma_n(j_k)$. Substituting $j_k = \sigma_n^{-1}(k)$ and $k = \sigma_n(j_k)$ into Equation F-7, and changing the index of summation from k to j_k gives the required result in Equation F-6.

Corollary 2. Proposition 3 holds for any random permutation $\{\sigma_n(k)\}$ of $\{1,\ldots,n\}$ that is independent of X_k's and Y_k's.

In summary, when $\{X_k\}_k^n$ are i.i.d. and independent of $\{Y_k\}_k^n$, the distribution of the sum $\sum_{k=1}^n X_k Y_k$ is invariant to any random shuffling of the X_k's or Y_k's, no matter how the Y_k's are distributed; Y_k's need not be independent or identically distributed for this statement to hold. The next proposition goes to the heart of our problem by applying this observation.

Proposition 4. For every t > 0, conditional on $N(t) = n$, $n \in \mathbf{Z}^+$, $L(t)$ and $R_U(t)$ are identically distributed.

Proof: Let $\{\sigma_n(k)\}_k^n$ be a random permutation of $\{1,\ldots,n\}$ which is independent of everything else. Using Corollary 2 with $X_k = C_k$ and $Y_k = e^{-rT_k}$, k = 1,…,n, we have for any $c \in \mathbf{R}$,

$$\mathbf{P}\left(R(t) \le c \middle| N(t) = n\right) = \mathbf{P}\left(\sum_{k=1}^{n} C_k e^{-rT_{\sigma_n(k)}} \le c \middle| N(t) = n\right) \tag{F-8}$$

From the theory of Poisson processes, given that $N(t) = n$, the unordered statistics, that is, a random permutation, of the arrival times $\{T_k\}_k^n$ are independent and identically distributed as the independent and uniformly distributed random variables $\{tU_k\}_k^n$. This means $\{T_{\sigma_n(k)}\}_k^n$ are identically distributed as $\{tU_k\}_k^n$, which are also independent of $\{C_k\}_k^n$. Thus, we can replace $\{T_{\sigma_n(k)}\}_k^n$ in Equation D8 by $\{tU_k\}_k^n$ without altering the resulting probability:

$$\begin{aligned}\mathbf{P}\left(L(t)\le c\,\middle|\,N(t)=n\right)&=\mathbf{P}\left(\sum_{k=1}^{n}C_k e^{-rtU_k}\le c\,\middle|\,N(t)=n\right)\\&=\mathbf{P}\left(R_U(t)\le c\,\middle|\,N(t)=n\right)\end{aligned}\tag{F-9}$$

which completes the proof.

Proposition 5. For every $t > 0$, $L(t)$ and $R_U(t)$ are identically distributed.

Proof:

$$\begin{aligned}\mathbf{P}\left(L(t)\le c\right)&=\sum_{n=0}^{\infty}\mathbf{P}\left(L(t)\le c\,\middle|\,N(t)=n\right)\mathbf{P}\left(N(t)=n\right)\\&=\sum_{n=0}^{\infty}\mathbf{P}\left(R_U(t)\le c\,\middle|\,N(t)=n\right)\mathbf{P}\left(N(t)=n\right),\quad\text{by Proposition 4}\\&=\mathbf{P}\left(R_U(t)\le c\right)\end{aligned}$$

F.3 MOMENT GENERATING FUNCTION OF $L(T)$

The fact that $L(t)$ and $R_U(t)$ are identically distributed for every $t \ge 0$ allows us to derive the statistical properties of $L(t)$ for every t by studying $R_U(t)$, which is a more feasible task since the random variables involved are mutually independent. In this section, we derive the moment generating function of $L(t)$.

Proposition 6. The moment generating function of $L(t)$ is defined by:

$$M_{L(t)}(\xi)=\mathsf{E}\left[e^{\xi L(t)}\right]=e^{\upsilon t(Q_t(\xi)-1)}\tag{F-10}$$

where $Q_t(\xi)$ is the moment generating function of Ce^{-rtU} when C and U are independently distributed as C_k and U_k, respectively.

Proof: Since $L(t)$ and $R_U(t)$ are identically distributed for every $t \ge 0$,

$$\begin{aligned}M_{L(t)}(\xi)&=\mathsf{E}\left[e^{\xi L(t)}\right]=\mathsf{E}\left[e^{\xi R_U(t)}\right]\\&=P\left(N(t)=0\right)+\sum_{n=1}^{\infty}\mathsf{E}\left[e^{\xi\sum_{k=1}^{n}C_k e^{-rtU_k}}\right]P\left(N(t)=n\right)\end{aligned}\tag{F-11}$$

For n = 1,2,…, since the sequence of random variable $\{C_k e^{-rtU_k}\}_k^n$ are i.i.d.,

$$\mathsf{E}\left[e^{\xi \sum_{k=1}^{n} C_k e^{-rtU_k}} \right] = Q_t(\xi)^n \tag{F-12}$$

where

$$Q_t(\xi)^n = \mathsf{E}\left[e^{\xi C e^{-rtU}} \right]$$

is the moment generating function of Ce^{-rtU} when C and U are independently distributed as C_k and U_k, respectively. Substituting Equation F-12 into Equation F-11, and using $P(N(t)=n) = e^{-vt}(vt)^n / n!$ since $N(t)$ is a Poisson process with rate v,

$$\begin{aligned} M_{L(t)}(\xi) &= e^{-vt} + \sum_{n=1}^{\infty} e^{-vt} \frac{(vt)^n}{n!} Q_t(\xi)^n \\ &= e^{-vt} \sum_{n=0}^{\infty} \frac{(vt)^n}{n!} Q_t(\xi)^n \\ &= e^{vt(Q_t(\xi)-1)} \end{aligned} \tag{F-13}$$

Proposition 7. The moment generating function

$$Q_t(\xi) = \mathsf{E}\left[e^{\xi C e^{-rtU}} \right] \tag{F-14}$$

of Ce^{-rtU} when C and U are independently distributed as C_k and U_k, respectively, can be expressed:

(a) either as an integral:

$$Q_t(\xi) = \frac{1}{rt}\mathsf{E}[E_i(\xi C) - E_i(\xi C e^{-rt})] = \frac{1}{rt}\int_0^{\infty} [E_i(\xi c) - E_i(\xi c e^{-rt})] f_C(c)\, dc \tag{F-15}$$

where, for $x \neq 0$, the exponential integral function is defined by

$$E_i(x) = \int_{-\infty}^{x} \frac{e^z}{z} dz \tag{F-16}$$

(b) or as a series:

$$Q_t(\xi) = 1 + \frac{1}{rt} \sum_{n=1}^{\infty} \frac{\xi^n}{n!n} \mathbf{E}[C^n](1 - e^{-nrt}) \tag{F-17}$$

Proof: (a) Note that from Equation F-14:

$$Q_t(\xi) = \int \mathbf{E}\left[e^{\xi c e^{-rtU}} \right] f_C(c) dc \tag{F-18}$$

and for every $c \in (0, \infty)$,

$$\begin{aligned} \mathbf{E}\left[e^{\xi c e^{-rtU}} \right] &= \int_0^1 e^{\xi c e^{-rtu}} du \\ &= \frac{1}{rt} \int_{\xi c e^{-rt}}^{\xi c} \frac{e^z}{z} dz, \quad \text{by a change of variable } z = \xi c e^{-rtu} \\ &= \frac{1}{rt} \left[E_i(\xi c) - E_i\left(\xi c e^{-rt}\right) \right] \end{aligned} \tag{F-19}$$

where $E_i(\cdot)$ is the exponential integral function given by Equation F-16. Substituting Equation F-18 into Equation F-17 yields Equation F-15.

(b) In Equation F-18, a series representation can be used for

$$\mathbf{E}\left[e^{\xi c e^{-rtU}} \right] = 1 + \sum_{n=1}^{\infty} \frac{\xi^n c^n}{n!} \mathbf{E}\left[e^{-nrtU} \right] \tag{F-20}$$

where

$$\mathbf{E}[e^{-nrtU}] = \int_0^1 e^{-nrtu} du = \frac{1}{nrt}(1 - e^{-nrt}) \tag{F-21}$$

Equation F-17 is obtained by substituting Equation F-21 into Equation F-20 and then substituting the resulting equation into Equation F-18.

Proposition 8. The moment generating function of $L(t)$ is given by:

$$\ln M_{L(t)}(\xi) = \frac{\nu}{r} \sum_{n=1}^{\infty} \frac{\xi^n}{n!n} \mathbf{E}[C^n](1 - e^{-nrt}) \tag{F-22}$$

Proof: Substitute Equation F-17 into the logarithm of Equation F-10.

F.4 STATISTICAL MOMENTS OF $L(t)$

The statistical moments of $L(t)$ can be obtained from its moment generating function. Let $\mu_m(t)$ be the m^{th} moment of $L(t)$, then, as a well-known fact in probability theory (e.g., Papoulis, 1991), $\mu_m(t)$ is equal to the m^{th} derivative of the moment generating function of $L(t)$ evaluated at $\xi = 0$, that is,

$$\mu_m(t) = \mathbf{E}\left[L(t)^m \right] = M_{L(t)}^{(m)}(0) \tag{F-23}$$

where the superscripted index in parenthesis denotes the m^{th} order derivative with respect to ξ. The following proposition offers a way to compute all the moments $\{\mu_m(t) : m = 1,2,...\}$ in a recursive manner:

Proposition 9. For m = 1,2,…,

$$\mu_m(t) = \frac{v}{r} \sum_{k=0}^{m-1} \binom{m-1}{k} \mathbf{E}\left[C^{k+1} \right] \frac{1 - e^{-(k+1)rt}}{k+1} \mu_{m-k-1}(t) \tag{F-24}$$

where $\binom{m}{k} = m!/k!(m-k)!$.

Proof: Differentiating Equation F-10 with respect to ξ,

$$M_{L(t)}^{(1)}(\xi) = vtQ_t^{(1)}(\xi) e^{vt(Q_t(\xi)-1)} = vtQ_t^{(1)}(\xi) M_{L(t)}(\xi) \tag{F-25}$$

Thus, for m = 1, we get the mean of $L(t)$:

$$\mu_1(t) = M_{L(t)}^{(1)}(0) = vtQ_t^{(1)}(0) M_{L(t)}(0) = \mathbf{E}[C] \frac{v}{r} (1 - e^{-rt}) \tag{F-26}$$

since $M_{L(t)}(0) = 1$ and $Q_t^{(1)}(0) = \mathbf{E}\left[Ce^{-rtU} \right] = \mathbf{E}[C]\mathbf{E}\left[e^{-rtU} \right] = \mathbf{E}[C](1 - e^{-rt})/rt$. Equation F-26 shows that Equation F-24 holds for m = 1.

For m = 2,3,…, differentiating Equation F-25 with respect to ξ for (m – 1) times gives

$$M_{L(t)}^{(m)}(\xi = vt\sum_{k=0}^{m-1}\binom{m-1}{k}Q_t^{(k+1)}(\xi)M_{L(t)}^{(m-1-k)}(\xi) \tag{F-27}$$

and hence, evaluating the above equation at $\xi = 0$ and using Equation F-23,

$$\mu_m(t) = vt\sum_{k=0}^{m-1}\binom{m-1}{k}Q_t^{(k+1)}(0)\mu_{m-k-1}(t) \tag{F-28}$$

But,

$$\begin{aligned} Q_t^{k+1}(0) &= \mathbf{E}\left[\left(Ce^{-rtU}\right)^{k+1}\right] \\ &= \mathbf{E}\left[C^{k+1}\right]\mathbf{E}\left[e^{-(k+1)rtU}\right] \\ &= \mathbf{E}\left[C^{k+1}\right]\int_0^1 e^{-(k+1)rtu}du \\ &= \mathbf{E}\left[C^{k+1}\right]\frac{1-e^{-(k+1)rt}}{(k+1)rt} \end{aligned} \tag{F-29}$$

Substituting Equation F-29 into Equation F-28 gives the required relationship in Equation F-24. It can be shown, by using a similar procedure as above, that the m^{th} moment of the de-meaned variable $L(t)-\mu_m(t)$ follows the same recursive relationship for m = 2,3, ...

Substituting m = 2 in Equation F-24 gives the second moment of $L(t)$, from which the variance of $L(t)$ can be computed:

$$\mathbf{Var}[L(t)] = \mu_2(t) - \mu_1(t) = \frac{v}{2r}\mathbf{E}[C^2](1-e^{-2rt}) \tag{F-30}$$

It is interesting to note that $\mathbf{Var}[L(t)]$ depends on $\mathbf{E}[C^2]$ rather than on $\mathbf{Var}[C]$. This means that even in the case where the C_k are fixed to a common value ($\mathbf{Var}[C_k]=0$), there will still be variability in $L(t)$. Such variability comes from the variability in the arrival times of the events.

Note that by substituting Equations F-26 and F-30 into Equation F-22, we can write:

$$\ln M_{L(t)}(\xi) = \mathbf{E}\left[L(t)\right]\xi + \tfrac{1}{2}\mathbf{Var}\left[L(t)\right]\xi^2 + R(\xi) \tag{F-31}$$

where R(ξ) corresponds to the remaining terms for n>2 in Equation F-22:

$$R(\xi) = \frac{\nu}{r}\sum_{n=3}^{\infty}\frac{\xi^n}{n!n}\mathbf{E}[C^n](1-e^{-nrt}) \tag{F-32}$$

An upper bound can be derived for R(ξ) as follows. Note that:

$$\mathbf{E}[C^n] = \mathbf{E}[C\,C^{n-1}] \le \mathbf{E}[C]P^{n-1} \tag{F-33}$$

since the earthquake loss, C, given that an earthquake has occurred in the region, will not exceed the replacement cost, P, for the structure. Equations F-32 and F-33 lead to:

$$\begin{aligned} \left|R(\xi)\right| &\le \frac{\nu}{r}\mathbf{E}[C]\sum_{n=3}^{\infty}\frac{\xi^n P^{n-1}}{n!n} \\ &= \mathbf{E}[L(\infty)]\xi\sum_{n=3}^{\infty}\frac{(\xi P)^{n-1}}{(n-1)!n^2} \\ &\le \mathbf{E}[L(\infty)]\xi\tfrac{1}{9}\sum_{n=3}^{\infty}\frac{(\xi P)^{n-1}}{(n-1)!} \\ &= \mathbf{E}[L(\infty)]\xi(e^{\xi P}-1-\xi P)/9 \end{aligned} \tag{F-34}$$

where Equation F-26 has been used. This gives the desired upper bound expression for the remainder term $R(\xi)$ in Equation F-31.

Appendix G. Structural Model of CUREE Demonstration Building

During the 1994 Northridge Earthquake, the south frame of the demonstration building suffered severe damage. For the present study, this frame was chosen for performing a 2-dimensional inelastic dynamic analysis using a finite-element model. The structural elements in the model are described in this appendix. The inelastic dynamic analysis program Ruaumoko (Carr, 2001) was used for performing the structural analyses.

The model uses two generic types of element: nonlinear flexural members and nonlinear shear springs. The flexural behavior of the beams and columns is represented by one-component Giberson beam with plastic hinges at the ends (Sharpe, 1974). Shear deformation for the beams is assumed to be elastic and is incorporated by the flexural elements. Shear deformation of the columns is modeled using nonlinear springs attached to the ends of the flexural elements. Figure G-1 shows a fragment of the structural model. In the figure, beams and columns are marked according to the original structural drawings: 1C-1 refers to column number 1, first floor; 1C-2 refers to column number 2, first floor; and 2FSB-8 refers to spandrel beam 8 on the second floor.

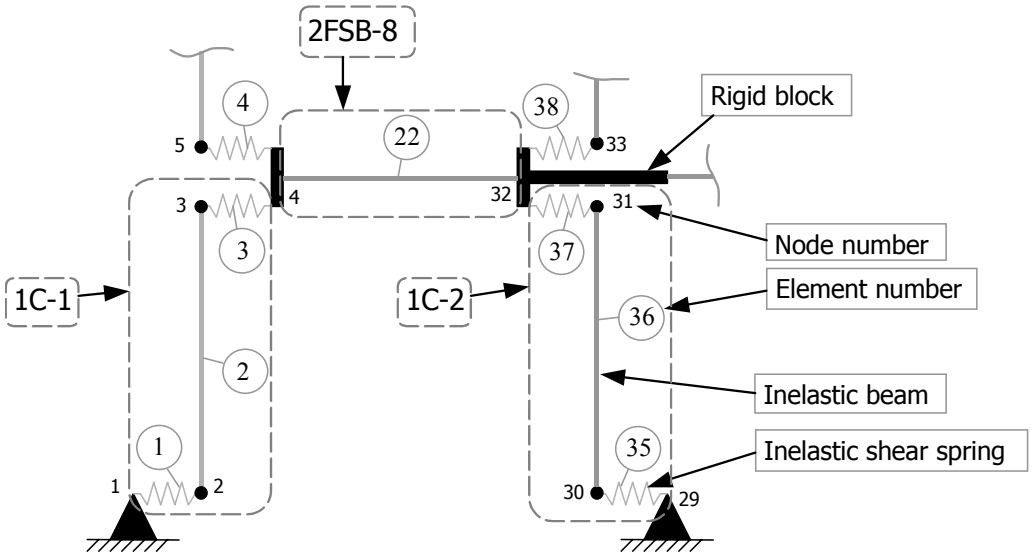

Figure G-1. Fragment of the finite element model.

Two types of hysteretic rules are used to model the reinforced-concrete members' behavior: the SINA tri-linear hysteresis rule (Saiidi, 1979) is used to model stiffness degradation of reinforced concrete members in flexure. The Q-HYST bi-linear hysteresis (Saiidi, 1979) is used to model the stiffness degradation of reinforced concrete members in shear. A strength-degradation pattern introduced by Pincheira *et al.* (1999), is applied to both hysteretic rules. The models are depicted in Figure G-2 and Figure G-3.

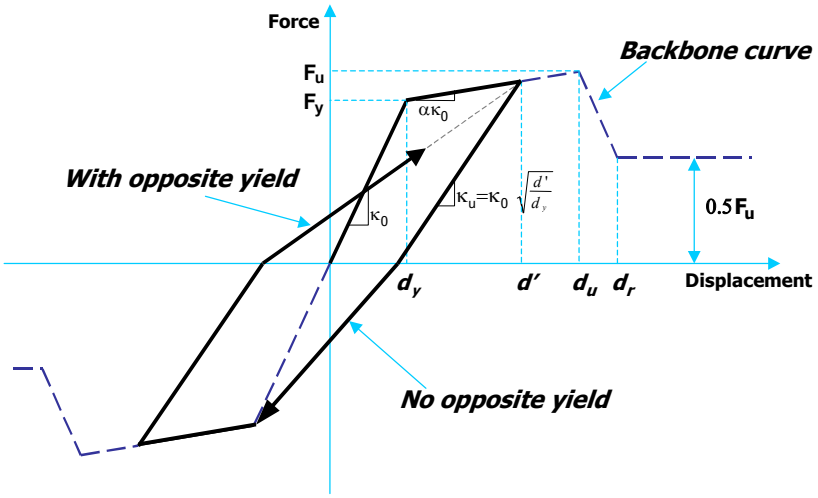

Figure G-2. Shear spring hysteresis rule: Q-HYST with strength degradation.

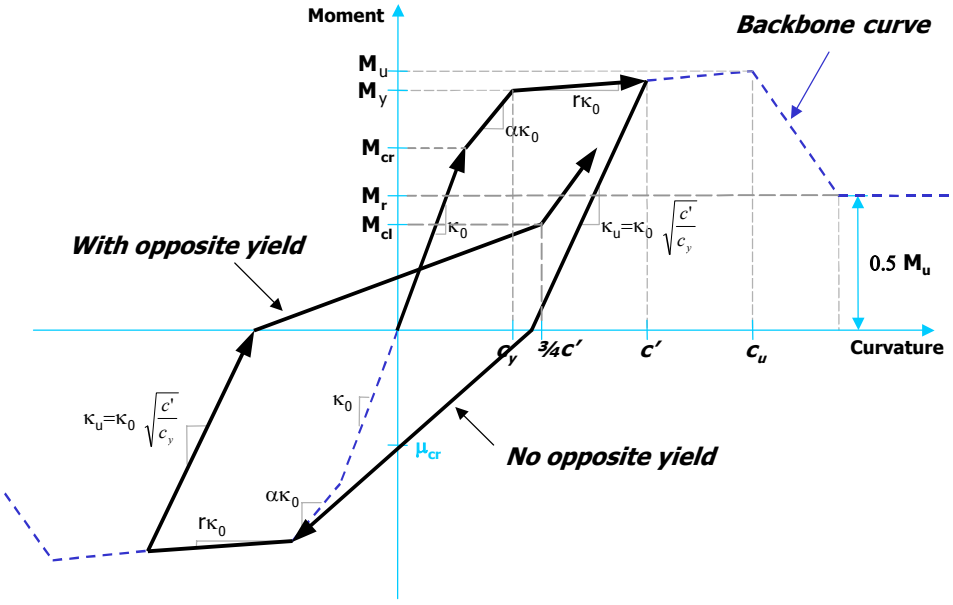

Figure G-3. Flexure hysteresis rule: SINA with strength degradation.

Parameters of the hysteresis models are calculated from the original structural drawings (Rissman and Rissman Associates, 1965). The software program UCFyber (ZEvent, 2000) is used to calculate parameters of the backbone of the force-deformation curves for each flexural member. Figure G-4 illustrates the cross section for an example member, 1C-1 in the CUREE demonstration building. Similar reports were created for all beams and columns in the structure. Figure G-5 shows the results of the analysis performed by UCFyber for the cross section of the member 1C-1, loaded by a bending moment in the y-direction.

Section Details:

X Centroid:	-9.235E-6 in
Y Centroid:	-18.07E-6 in
Section Area:	280.0 in^2
Reinforcing Bar Area:	7.994 in^2
Percent Longitudinal Steel:	2.855 %
Overall Width:	14.00 in
Overall Height:	20.00 in
Number of Fibers:	590
Number of Bars:	8 #9
Number of Materials:	3

Material Types and Names:

Unconfined Concrete:	Unconfined5ksi
Strain Hardening Steel:	Steel60ksi
Confined Concrete:	Confined5ksi-1-t5

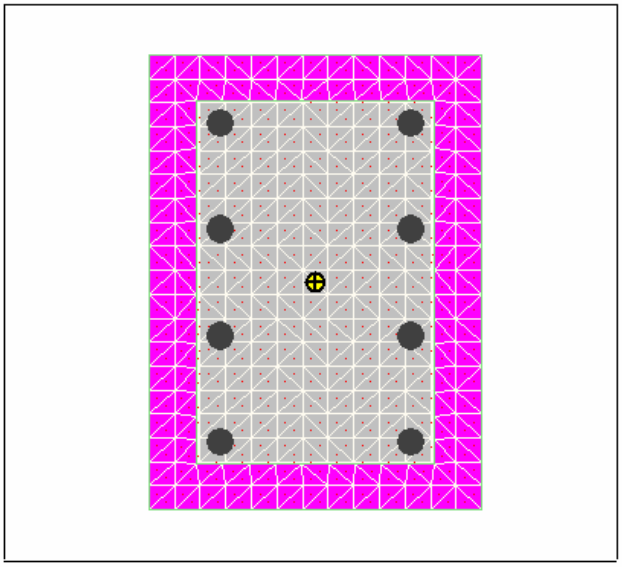

Figure G-4. Section report for 1C-1 column.

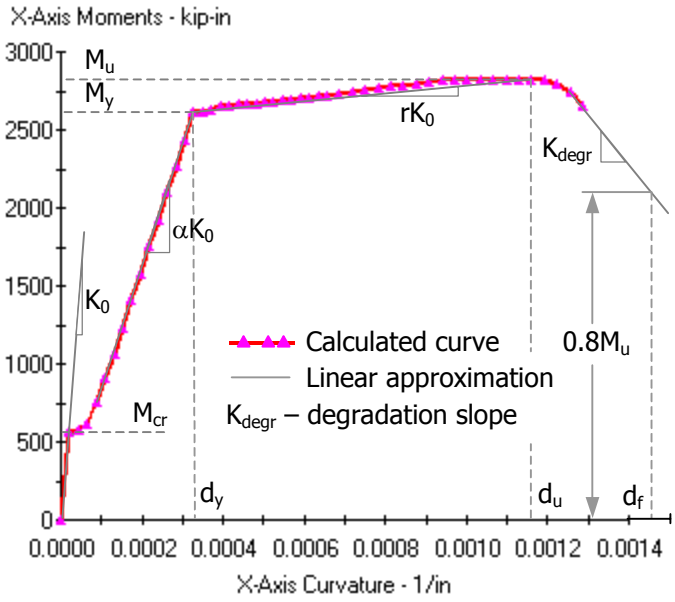

Figure G-5. Moment-curvature diagram for column 1C-1.

Yield surfaces in the moment-axial-force space are also calculated using UCFyber (ZEvent, 2000). Figure G-6 gives the yield surface for member 1C-1. In this figure, PYC refers to compressive yield strength; PYT to tensile yield strength; point B (MB, PB) defines the linear section AB; points B (MB, PB), B1 (2/3PB, M1B), B2 (1/3PB, M2B), and O (0, M0) define cubic approximation to the nonlinear section of the surface; and segment CO is approximated by a line. A sample calculation for the flexural behavior of 1C-1 is presented in . Units are kips and inches.

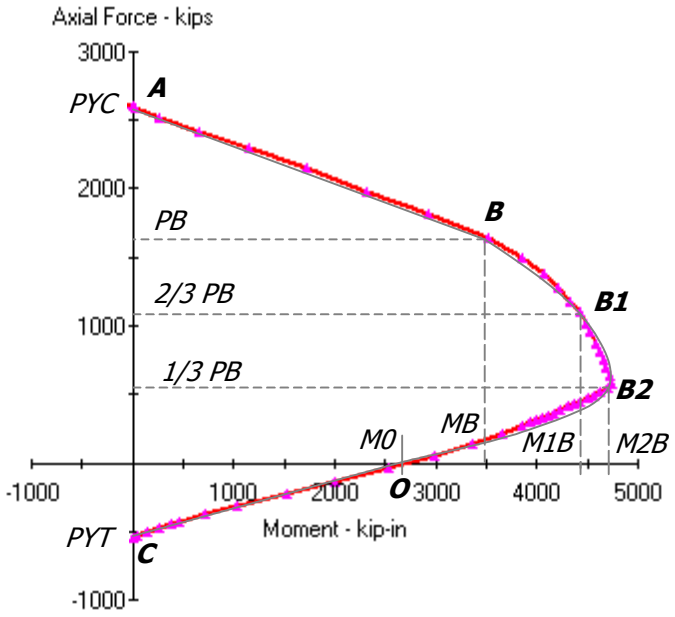

Figure G-6. Yield surface for column 1C-1.

Table G-1. Ruaumoko input data for element 2 (bending 1C-1 in y-direction).

Input variable	Value	Description	Remarks
ITYPE	2	Concrete BEAM-COLUMN element	Allows for flexure-axial force interaction
IPIN	0	Member built-in to joint	
ICOND	0	No initial load (prestress) applied	
IHYST	8	SINA hysteresis rule	
ILOS	1	Strength reduction based on ductility	
IDAMG	0	No damage indices computed*	
ICOL	3	Column ductilities computed at each time step using current axial load	
E	4992	Concrete elastic modulus	Computed for concrete with nominal strength 5ksi [(2)]
G	1996.8	Concrete shear modulus	= 0.4E
A	280	Cross-sectional area	
AS	0	Effective shear area	Shear deformation is suppressed, since it is handled by spring members
I (in4)	5144.9	Moment of inertia of section	= K_0/E
WGT	25.07	Weight per unit length	
END1	0	Length of rigid block at End 1	Equals to ¼ of height of adjacent member
END2	7.5	Length of rigid block at End 2	
FJ1	0	Joint flexibility at End 1	Rigid joints are assumed
FJ2	0	Joint flexibility at End 2	
RA	0	Bi-linear factor (Axial)	
RF	0.0115	Bilinear factor (Flexure)	Equals ***r*** in
H1	14	Plastic hinge length at End 1	Equals to the member depth
H2	14	Plastic hinge length at End 2	
PYC (kips)	-2605	Axial compression yield force	See
PB (kips)	-1664	Axial compression force at B	See
MB (kip in)	3438	Yield moment at B	See
M1B (kip-in)	4500	Yield moment at P = (2/3)*PB	See
M2B (kip in)	4660	Yield moment at P = (1/3)*PB	See
M0 (kip-in)	2604	Yield moment at P=0.0	M0 – or M_y –

Table G-1 (cont.). Ruaumoko input data for element 2 (bending 1C-1 in *y*-direction).

Input variable	Value	Description	Remarks
PYT (kips)	544	Axial tension yield force	See
IEND	0	End 2 has the same yield surface	
DUCT1	3.252	Ductility at which degradation begins	d_u/d_y –
DUCT2	6.658	Ductility at which degradation stops	Found from K_{degr} () and M_r (Figure G-3)
RDUCT	0.3451	Residual strength as a fraction of the initial yield strength	
DUCT3	35.819	Ductility at 0.01 initial strength	
ALFA	0.304	Bi-linear factor (positive cracking)	Equals α in
BETA	0.304	Bi-linear factor (negative cracking)	Same as ALFA, since member is symmetrical
FCR1+	584.3	Cracking moment (positive) at End 1.	
FCR1-	-584.3	Cracking moment (negative) at End 1.	Magnitude is the same as FCR1+ due to symmetry
FCC1	584.3	Crack closing moment at End 1.	$= 0.5A_sf_{sy}(d\text{-}d')$ (3)
FCR2+	584.3	Cracking moment (positive) at End 2.	Same as at End 1
FCR2-	-584.3	Cracking moment (positive) at End 2.	Same as at End 1
FCC2	584.3	Crack closing moment at End 2.	Same as at End 1
MU1	4.387	Ultimate ductility at End 1	d_f/d_y –
MU2	4.387	Ultimate ductility at End. 2	Same as End 1

(1) Park-Ang damage indices are computed manually, using $\beta = 0$, d_y is taken from , d_u is equal to d_f from

(2) Expected actual strength is used, estimated by: $f_c = (f_c'+1.5s)*m$ (MacGregor, 1988) where:
f_c' = nominal concrete strength,
s = strength standard deviation: $0.15f'_c$ for $f_c' < 4$ksi
= 600psi for $f_c' > 4$ksi
m = 1.3, maturity factor for type I cement

(3) A_s = longitudinal reinforcement area (Saiidi et al. 1979)
f_{sy} = steel yield stress
d-d' = distance between the centroids of compressive and tensile reinforcement

Shear-spring parameters are estimated by conventional analytical models. The spring stiffness is found as:

$$K = \frac{GA_s}{L/2} \tag{G-1}$$

where G = concrete shear modulus; L = member length; A_s = effective shear area, computed as $A_s = k_i A_g / k_s$; A_g is the gross section area; k_s =1.2 is the shape coefficient for a rectangular cross section; and k_i reflects the increased shear deformation in a flexurally-cracked reinforced-concrete column. It is usually assumed that the reduction in shear stiffness is proportional to the reduction in flexural stiffness (Priestley *et al.*, 1996), leading to $k_i = I_e/I_g$, where I_e is the effective moment of inertia and I_g is the gross moment of inertia of the cross section for the uncracked member. Equivalently, k_i can be found as K_e/K_0, the ratio of the effective stiffness to the initial stiffness of the member. The effective stiffness is determined from the moment-curvature relation shown in Figure G-5, as αK_0 = stiffness demonstrated by the member within the range of pre-yield loads. This makes $k_i = \alpha$.

The yield force for shear springs is obtained from the ACI-recommended expression (MacGregor, 1998):

$$F_y = 2(1 + \frac{N_u}{2000 A_g})\sqrt{f_c'} b_w d \text{ , where} \tag{G-2}$$

where

N_u = axial compression,

A_g = gross cross sectional area,

f'_c = concrete compressive strength,

b_w = web width,

d = distance from the extreme compression fiber to centroid of longitudinal tension reinforcement.

Input data for shear springs representing column 1C-1 are given in Table G-2. The Ruaumoko spring element (Carr, 2001) allows for different stiffness for different

degrees of freedom; here, all unused degrees of freedom of the spring element are made rigid.

Table G-2. Ruaumoko input data for a sample column.

Input variable	Value	Ruaumoko description	Remarks
ITYPE	1	No interaction between deformation components	
IHYST	12	Q-HYST hysteresis rule	
ILOS	1	Strength reduction is based on ductility	
IDAMG	0	No damage indices computed	Damage is based on the indices computed for flexural members
KX	1748	Spring stiffness in local X-direction	Equation F-1
KY	1.00E+10	Spring stiffness in local Y-direction	Rigid
GJ	1.00E+10	Rotational stiffness	Rigid
WGT	0	Weight per unit length	
RF	0.03	Bi-linear factor for spring forces	Assumed 0.03 for all shear springs
RT	1	Bi-linear factor, rotation	Linear dependence
PSX	0	Pre-load force in X-direction	
PSY	0	Pre-load force in Y-direction	
PSZ	0	Pre-load moment about Z-axis	
THETA	0	Angle between global X-axis and local X-axis	Only for zero-length elements
FX+	1.00E+10	Positive yield force in X-direction	No yield
FX-	1.00E+10	Negative yield force in X-direction	No yield
FY+	47.2	Positive yield force in X-direction	Equation G-2
FY-	47.2	Negative yield force in X-direction	Same as FY+ due to symmetry
MZ+	1.00E+10	Positive torsional yield	No yield
MZ-	1.00E+10	Negative torsional yield	No yield
DUCT1	2	Ductility at which degradation begins	Assumed 2 for all spring elements
DUCT2	2.3	Ductility at which degradation stops	Chosen 2.3 to provide sudden drop of loading capacity for nonductile members
RDUCT	0.56	Residual strength as a fraction of the initial yield strength	
DUCT3	21.3	Ductility at 0.01 initial strength	
ALFA	0.5	Unloading stiffness parameter	

Appendix H. Retrofit Cost Estimate

This appendix contains an estimate of the cost to retrofit the CUREE demonstration building with seven new 108-in-wide shearwalls, as discussed in Chapter 5. It is based on the cost-estimator's calculations for column replacement with and without abutting partitions, with modification to account for the quantity of formwork, reinforcing, concrete, and painting required for the larger shearwalls. Overhead and profit are taken as 0.15 of the total direct costs, and design and permitting fees are assumed to be 10% of the total construction cost.

Table H-1. Retrofit cost.

SPEC	DESCRIPTION	QTY	Unit	LABOR Unit Cost	LABOR Labor	MATERIAL Unit Cost	MATERIAL Mat'l	SUBCONTR. Unit Cost	SUBCONTR. Subcontr.	TOTAL
(2)	**SITEWORK**									
	Subtotal for Division: **$296,515**									
	Demolition:									
	Remove vinyl base, carpet and pad, drywall and metal studs at the demising wall, window and frame, in the units at each side of the concrete column (X2), nine man hours per unit	882	hrs	33.00	29,106		0.00		0.00	29,106
	Remove wallpaper from the bedroom area of the unit at the units at each side of the demising wall to be removed	29,400	sf		0.00		0.00	0.55	16,170	16,170
	Scaffolding:									
	Scaffolding for one column extends the length of each unit at each side of the column, extent is from ground to roof and approx. twenty four feet wide	7	ea		0.00		0.00	11,100	77,700	77,700
	Shoring:									
	Temporary shoring of each floor from the first floor to the roof (seven floors) including shoring drawings, engineering and labor	980	hrs	33.00	32,340	51.79	50,750		0.00	83,090
	Temporary protection:									
	The units without column repairs require shoring but not the floor and wall demolition will be protected with carpet mask and visqueen screen walls for the demolition and the setting of the shoring	2,058	hrs	33.00	67,914	10.95	22,535		0.00	90,449
(3)	**CONCRETE**									
	Subtotal for Division: **$713,227**									
	Concrete column repair:									
	Demolish the concrete column and rebar including transporting the debris to the container at ground level	1,568	hrs	33.00	51,744		0.00		0.00	51,744
	Rebar replacement – 60-#9 with 2-#3 hoops at 4" o.c. at boundary elements (1 ls = 1 column, 1 floor)	49	ls	7,200	352,800	2,500	122,500		0.00	475,300
	Column forms and braces, plyform, chamfer strips, 2X4 walls and diagonal braces	1,176	hrs	45	52,920	12.50	14,700		0.00	67,620
	Concrete pump rental – 52 meter pump	40	hrs		0.00		0.00	185.00	7,400	7,400
	Concrete 5000 psi pump mix	171.50	cy	420.00	72,030	125.00	21,438		0.00	93,468
	Strip forms, drypack void at the top of the column, sacking, patching and grinding	392	hrs	45.00	17,640	0.06	25	0.08	30	17,695

Table H-1 (continued). Retrofit cost.

SPEC	DESCRIPTION	QTY	Unit	LABOR Unit Cost	LABOR Labor	MATERIAL Unit Cost	MATERIAL Mat'l	SUBCONTR. Unit Cost	SUBCONTR. Subcontr.	TOTAL
(8)	**DOORS, WINDOWS, & GLASS**									
	Subtotal for Division: **$254,016**									
	Metal windows:									
	Replace the damaged aluminum windows at each side of the damaged column	14,112	sf		0.00		0.00	18.00	254,016	254,016
(9)	**FINISHES**									
	Subtotal for Division: **$552,488**									
	Drywall:									
	Metal studs and 5/8" drywall both sides to fill the opening in the demising wall	123	lf	4.41	540	15.00	1,838		0.00	2,378
	Respray the acoustic ceiling at the bedroom areas of each affected unit including masking and cleanup	171,500	sf		0.00		0.00	1.85	317,275	317,275
	Painting:									
	Prime the walls of the bedroom area	98,000	sf		0.00		0.00	0.65	63,700	63,700
	Repaint the exterior	20,490	sf		0.00		0.00	1.45	29,711	29,711
	Flooring:									
	Replace carpet pad and re-install carpet at each unit	2,744	sy	4.50	12,348	4.50	12,348		0.00	24,696
	Vinyl base at the two affected units	6,958	lf		0.00		0.00	1.70	11,829	11,829
	Wallpaper:									
	Install new wallpaper at the two affected units	58,800	sf		0.00		0.00	1.75	102,900	102,900
(10)	**SPECIALTIES**									
	Subtotal for Division: **$6,615**									
	Shelving:									
	Reset the closet shelving at the two affected units for the wallpaper installation	98	ea	67.50	6,615		0.00		0.00	6,615
(15)	**MECHANICAL**									
	Subtotal for Division: **$9,555**									
	HVAC:									
	Reset the existing window mounted AC unit at the two units	98	ea	97.50	9,555		0.00		0.00	9,555
		Subtotal			705,552		246,133		880,730	1,832,415
							General conditions		5%	91,620.76
									Subtotal	$1,924,036
							OH & PROFIT		0.15	$288,605
									Subtotal	$2,212,641
							DESIGN & PERMITS		0.1	$221,264
							TOTAL			**$2,433,905**

Appendix I. Output of Kajima D Program for Cash-Flow Analysis

The following pages show the cash flows of Kajima demonstration buildings described in Chapter 6. The Kajima D program was used to estimate total present value of each year cash flow. This computer program is composed of Microsoft Excel spreadsheets, so it is very easy to revise any parameters. The detailed description for understanding these output data and the outline of the program are presented in Section 6.4.

Leasing Project Proforma	PROJECT NAME	BUILDING 1

1. Property Outline

Address	Chuou ward Tokyo		Access	3minutes walk from Tokyo Station	
Zoning	Commercial District		Completion Date	1961	
Constructed Floor Area	388,000 sf		Parking Lot	50	
Current Replacement Cost	73,000,000 $ (Building Total)	622 $/sf(Const. Floor Area	PML (90%Case)	20 %	

Floor Area Table

Building Use	Const. Floor Area	Rentable Floor Area	Ratio	Rentable Floor Ratio
Office	388,000 sf	269,000 sf	100%	69%
Retail	0.00 sf	0 sf	0%	#DIV/0!
Residential	0.00 sf	0 sf	0%	#DIV/0!
	388,000.00 sf	269000.00 sf		69%

Site Area	38,000 sf	Designated Building Coverage Ratio	80 %
"Rosenka"	5,136 $/sf	Designated Building Floor Area Ratio	600 %
Market Value of Property		Other Government Restriction	
(Land)	4,014 $/sf		
(Building)	95 $/sf Office	"Rosenka" : a land unit price for tax calculation purposes set by Ministry of Finance	
	103 $/sf Retail		
	103 $/sf Residential		

2. Leasing Assumptions

	Monthly Rent				Security Deposit	
Office	6.9 $/sf	3 every year	3 %UP		12	month
Retail	0.0 $/sf	3 every year	3 %UP		24	month
Residential	0.0 $/sf	3 every year	3 %UP		2	month

Occupancy	Initial Year	2nd Year	3rd Year	4th Year	After 5th Year
Office	80 %	80 %	80 %	80 %	80 %
Retail	0 %	0 %	0 %	0 %	0 %
Residential	0 %	0 %	0 %	0 %	0 %

Parking											
	Hourly Charge	0 lot	Charge	4.88 $/hour	Ave.hour	2 h	4 cycle/day	Occupancy	50 %		
	Monthly Charge	50 lot	Charge	406.5 $/month	Deposit	0 $/lot	3 every year	3 %UP			

3. Other Assumptions

Revenue	Interest Income	1.0 %			
Expense	Repairs Replacements	0.25 % (Total estimated Replacement cost)	5 every year	100 %UP	
	Insurance	0.1 % (Total estimated Replacement cost)	3 every year	3 %UP	
	Seismic Insurance	500 %(Year expected Loss)	3 every year	3 %UP	
	Building Mgmt.	0.5 $/sf (Const. Floor Area)	3 every year	3 %UP	
	Property Mgmt.	3.0 % (Rent)			
	Marketing	755 $/year	3 every year	3 %UP	
Depreciation	Body/Dep.	65 %			
	Body	50 year(FRM=0, SLM=1		1)	
	Equipments	15 year(FRM=0, SLM=2		1)	
	Other Structure	10 year(FRM=0, SLM=3		1)	
Deferred Asset Depreciation		6 year	Public Obligation Charge		
	Retained Earnings	40 %(Net Profit/Loss)			

Tax				
Land	Property & Urban Planning Tax	1.7 %	3 every year	3 %UP
	Land Value Tax	0.0 %	3 every year	3 %UP
Building	Tax Base	70 % (Total estimated Replacement cost)		
	Property and Urban Planning Tax	1.7 %		
Real Property Acquisition Tax		4.0 %		
Registration & License Tax		5.0 %	(Transfer)	
Registration & License Tax		0.6 %	(preservation)	
Profit Tax				
	Corporation Tax	30.0 %	(Deferred Loss=0, Neglect	0)
	Municipal Inhabitants Tax	20.7 %		
	Enterprise Tax	11.0 %	(Total Profit Tax #### %)	

Schedule	Completion	Acquisition	Exit
	1961	2001	2006

※1Based on Total estimated Replacement cost

4. Project Cost ($)

Total Project Cost	143,838,334									
Property Book Value	143,838,334		Building Ratio	60 %		Land Ratio	40 %			
			Building Book Value	86,303,000		Land Book Value	57,535,334			
			Deferred Charges	0						
Land										
Acquisition Tax	6,101,280	Tax Base	152,532	$ ×	100 % ×	Rate	4.0 %	Exp.=0, Ast.=	1	
Registration & License Tax	7,626,600	Tax Base	152,532	$ ×	100 % ×	Rate	5.0 %	〃	1	
Building										
Acquisition Tax	1,474,400	Tax Base	36,860	M Yen ×	100 % ×	Rate	4.0 %	Exp.=0, Ast.=	1	
Registration & License Tax	1,843,000	Tax Base	36,860	M Yen ×	100 % ×	Rate	5.0 %	〃	1	
Transaction Fee	4,315,150	Total Project Cost	3.0 %					Exp.=0, Ast.=	1	
Retrofit Cost	0	Replacement Cost	0.0 %							
Consumption Tax	4,315,150	5%		4315150				Exp.=0, Ast.=	1	
Others	0							Exp.=0, Ast.=	1	

5. Finance ($)

		Ratio							
Equity①	14,383,833	10.0%		33%					
Equity②(preferred)	28,767,667	20.0%		67%					
Debt①	71,919,167	50.0%	Interest	2.00 %	0 yr deferre	35 yr Return	ｲ&I=0, Principal=1	0	
Debt②	28,767,667	20.0%	Interest	2.00 %	0 yr deferre	35 yr Return	ｲ&I=0, Principal=1	0	
	143,838,334	100%	LTV	70%	DSCR	2.12 (First year)			

6. Significant Results

(1) Indexes for DCF Study

Holding Period	5 years			
Discounted Rate	5.5%			
Residual Cap Rate	6.0%	Commission	3%	
PV	**143,838,334**	$	Equity IRR	1.34 %
PV-Retrofit Cost	**143,838,334**	$		

(2) Stabilized Rents	17,943,670	$		
1st year Expenses	9,398,651	$		
Stabilized prospected NOI	8,545,018	$		
Going-in Cap Rate	6	%		
Purchase Price	142,416,973	$	Project IRR (Unleveraged)	5.57 %

BUILDING 1　　SCHEDULE OF PROSPECTIVE CASH FLOW (Acquisition ～15th)　　(sf ＄)

			2001	2002	2003	2004	2005	2006	2007	2008	2009	2010	2011	2012	2013	2014	2015
CASH FLOW	(Pre-acquisition)		1st	2nd	3rd	4th	5th	6th	7th	8th	9th	10th	11th	12th	13th	14th	15th
	Rents		17,943,670	17,943,670	17,943,670	18,481,980	18,481,980	18,481,980	19,036,439	19,036,439	19,036,439	19,607,532	19,607,532	19,607,532	20,195,758	20,195,758	20,195,758
Total Revenues			17,943,670	17,943,670	17,943,670	18,481,980	18,481,980	18,481,980	19,036,439	19,036,439	19,036,439	19,607,532	19,607,532	19,607,532	20,195,758	20,195,758	20,195,758
	Repairs & Replacement		2,920,000	2,920,000	2,920,000	2,920,000	2,920,000	3,285,000	3,285,000	3,285,000	3,285,000	3,285,000	3,650,000	3,650,000	3,650,000	3,650,000	3,650,000
	Insurance		73,000	73,000	73,000	75,190	75,190	75,190	77,446	77,446	77,446	79,769	79,769	79,769	82,162	82,162	82,162
	Seismic Insurance		76,842	76,842	76,842	79,147	79,147	79,147	81,522	81,522	81,522	83,967	83,967	83,967	86,486	86,486	86,486
	Maintenance		2,328,000	2,328,000	2,328,000	2,397,840	2,397,840	2,397,840	2,469,775	2,469,775	2,469,775	2,543,868	2,543,868	2,543,868	2,620,185	2,620,185	2,620,185
	Mgnt. Fee		538,310	538,310	538,310	554,459	554,459	554,459	571,093	571,093	571,093	588,226	588,226	588,226	605,873	605,873	605,873
	Marketing		755	755	755	778	778	778	801	801	801	825	825	825	850	850	850
	Tax	0	3,461,744	3,461,744	3,461,744	3,539,535	3,539,535	3,539,535	3,619,660	3,619,660	3,619,660	3,702,189	3,702,189	3,702,189	3,787,194	3,787,194	3,787,194
Total Expense		0	9,398,651	9,398,651	9,398,651	9,566,950	9,566,950	9,931,950	10,105,297	10,105,297	10,105,297	10,283,845	10,648,845	10,648,845	10,832,749	10,832,749	10,832,749
CASH FLOW (Before Interest & Tax)		0	8,545,018	8,545,018	8,545,018	8,915,030	8,915,030	8,550,030	8,931,142	8,931,142	8,931,142	9,323,687	8,958,687	8,958,687	9,363,009	9,363,009	9,363,009
	Residual Value		0	0	0	0	138,225,484	0	0	0	0	0	0	0	0	0	0
	Net Cash Flow	0	8,545,018	8,545,018	8,545,018	8,915,030	147,140,514	0	0	0	0	0	0	0	0	0	0
	ROA(C.F./Total Project Cost)		5.9%	5.9%	5.9%	6.2%	102.3%	0.0%	0.0%	0.0%	0.0%	0.0%	0.0%	0.0%	0.0%	0.0%	0.0%
	Presentnt Value		8,319,300	7,885,592	7,474,495	7,391,613	112,767,335	0	0	0	0	0	0	0	0	0	0
Debt Service			4,027,696	4,027,696	4,027,696	4,027,696	94,233,806	0	0	0	0	0	0	0	0	0	0
Deposit (Refund)			0	0	0	0	17,699,770	0	0	0	0	0	0	0	0	0	0
Deposit (Receipt)			176,998	185,931	194,977	204,139	214,269	0	0	0	0	0	0	0	0	0	0
Cash Flow after Debt Service & Deposit			4,694,320	4,703,254	4,712,300	5,091,473	35,421,208	0	0	0	0	0	0	0	0	0	0
DSCR			2.12	2.12	2.12	2.21	1.56	0.00	0.00	0.00	0.00	0.00	0.00	0.00	0.00	0.00	0.00

P/L		(Pre-acquisition)	1st	2nd	3rd	4th	5th	6th	7th	8th	9th	10th	11th	12th	13th	14th	15th
Revenues	Rents	0	17,943,670	17,943,670	17,943,670	18,481,980	18,481,980	0	0	0	0	0	0	0	0	0	0
Expenses	C.F.Total Expense	0	9,398,651	9,398,651	9,398,651	9,566,950	9,566,950	0	0	0	0	0	0	0	0	0	0
	Depreciation	0	2,822,108	2,822,108	2,822,108	2,822,108	2,822,108	0	0	0	0	0	0	0	0	0	0
Operating Profit/Loss		0	5,722,910	5,722,910	5,722,910	6,092,922	6,092,922	0	0	0	0	0	0	0	0	0	0
Non-Operating Income	Interest earned		176,998	185,931	194,977	204,139	214,269	0	0	0	0	0	0	0	0	0	0
	Property Disposition		0	0	0	0	138,225,484	0	0	0	0	0	0	0	0	0	0
Non-Operating Expens	Interest expense	0	2,013,737	1,973,457	1,932,373	1,890,466	1,847,722	0	0	0	0	0	0	0	0	0	0
	Other Expense		0	0	0	0	0	0	0	0	0	0	0	0	0	0	0
Net Profit/Loss		0	3,886,171	3,935,384	3,985,515	4,406,595	142,684,953	0	0	0	0	0	0	0	0	0	0
Corporate Tax		0	1,652,848	1,673,779	1,695,101	1,874,192	1,896,680	0	0	0	0	0	0	0	0	0	0
Net Profit/Loss after Tax		0	2,233,323	2,261,605	2,290,414	2,532,402	140,788,273	0	0	0	0	0	0	0	0	0	0
(Cumulative)		0	2,233,323	4,494,928	6,785,342	9,317,745	150,106,018	0	0	0	0	0	0	0	0	0	0

		(Pre-acquisition)	1st	2nd	3rd	4th	5th	6th	7th	8th	9th	10th	11th	12th	13th	14th	15th
	C.F. after Debt Service		4,694,320	4,703,254	4,712,300	5,091,473	35,421,208	0	0	0	0	0	0	0	0	0	0
	Corporate Taxes		1,652,848	1,673,779	1,695,101	1,874,192	1,896,680	0	0	0	0	0	0	0	0	0	0
	Dividend-Equity1	(Included retirement)	716,048	708,278	700,345	734,773	12,417,208	0	0	0	0	0	0	0	0	0	0
	Dividend-Equity2	(Included retirement)	1,432,095	1,416,555	1,400,689	1,469,547	24,834,417	0	0	0	0	0	0	0	0	0	0
Cash Reserve			893,329	904,642	916,166	1,012,961	0	0	0	0	0	0	0	0	0	0	0
Accumulated Cash Reserve			893,329	1,797,971	2,714,137	3,727,098	0	0	0	0	0	0	0	0	0	0	0

B/S		(Pre-acquisition)	1st	2nd	3rd	4th	5th	6th	7th	8th	9th	10th	11th	12th	13th	14th	15th
ASSETS	Cash	17,699,770	18,593,099	19,497,741	20,413,907	21,426,868	0	0	0	0	0	0	0	0	0	0	0
	Real Estate	143,838,334	141,016,226	138,194,118	135,372,010	132,549,902	0	0	0	0	0	0	0	0	0	0	0
	Deferred Assets	0	0	0	0	0	0	0	0	0	0	0	0	0	0	0	0
Asset-total		161,538,104	159,609,325	157,691,859	155,785,916	153,976,769	0	0	0	0	0	0	0	0	0	0	0
LIABILITIES	Debt 1	71,919,167	70,480,625	69,013,312	67,516,652	65,990,060	0	0	0	0	0	0	0	0	0	0	0
	Debt 2	28,767,667	28,192,250	27,605,325	27,006,661	26,396,024	0	0	0	0	0	0	0	0	0	0	0
	Security Deposit	17,699,770	17,699,770	17,699,770	17,699,770	17,699,770	0	0	0	0	0	0	0	0	0	0	0
Liabilities-total		118,386,603	116,372,644	114,318,406	112,223,083	110,085,853	0	0	0	0	0	0	0	0	0	0	0
EQUITY	Equity 1	14,383,833	14,383,833	14,383,833	14,383,833	14,383,833	0	0	0	0	0	0	0	0	0	0	0
	Equity 2	28,767,667	28,767,667	28,767,667	28,767,667	28,767,667	0	0	0	0	0	0	0	0	0	0	0
	Retained Earnings	0	85,180	221,952	411,333	739,415	0	0	0	0	0	0	0	0	0	0	0
Equity-total		43,151,500	43,236,680	43,373,453	43,562,833	43,890,916	0	0	0	0	0	0	0	0	0	0	0
L&E-total		161,538,104	159,609,325	157,691,859	155,785,916	153,976,769	0	0	0	0	0	0	0	0	0	0	0

Leasing Project Proforma	PROJECT NAME	BUILDING 2

1. Property Outline

Address	Chuou ward Tokyo		Access	3minutes walk from Tokyo Station	
Zoning	Commercial District		Completion Date	1961	
Constructed Floor Area	388,000 sf		Parking Lot	50	
Current Replacement Cost	73,000,000 $ (Building Total)	622 $/sf(Const. Floor Area)	PML (90%Case)	10 %	

Floor Area Table

Building Use	Const. Floor Area	Rentable Floor Area	Ratio	Rentable Floor Ratio
Office	388,000 sf	269,000 sf	100%	69%
Retail	0.00 sf	0 sf	0%	#DIV/0!
Residential	0.00 sf	0 sf	0%	#DIV/0!
	388,000.00 sf	269000.00 sf		69%

Site Area	38,000 sf	Designated Building Coverage Ratio	80 %
"Rosenka"	5,136 $/sf	Designated Building Floor Area Ratio	600 %
Market Value of Property		Other Government Restriction	
(Land)	4,014 $/sf	"Rosenka" : a land unit price for tax calculation purposes set by Ministry of Finance	
(Building)	95 $/sf Office		
	103 $/sf Retail		
	103 $/sf Residential		

2. Leasing Assumptions

	Monthly Rent			Security Deposit
Office	6.9 $/sf	3 every year	3 %UP	12 month
Retail	0.0 $/sf	3 every year	3 %UP	24 month
Residential	0.0 $/sf	3 every year	3 %UP	2 month

Occupancy	Initial Year	2nd Year	3rd Year	4th Year	After 5th Year
Office	95 %	95 %	95 %	95 %	95 %
Retail	0 %	0 %	0 %	0 %	0 %
Residential	0 %	0 %	0 %	0 %	0 %

Parking	Hourly Charge	0 lot	Charge	4.88 $/hour	Ave.hour	2 h	4 cycle/day	Occupancy	50 %	
	Monthly Charge	50 lot	Charge	406.5 $/month	Deposit	0 $/lot	3 every year	3 %UP		

3. Other Assumptions

Revenue	Interest Income	1.0 %			
Expense	Repairs Replacements	0.25 % (Total estimated Replacement cost)	5 every year	100 %UP	
	Insurance	0.1 % (Total estimated Replacement cost)	3 every year	3 %UP	
	Seismic Insurance	500 %(Year expected Loss)	3 every year	3 %UP	
	Building Mgmt.	0.5 $/sf (Const. Floor Area)	3 every year	3 %UP	
	Property Mgmt.	3.0 % (Rent)			
	Marketing	755 $/year	3 every year	3 %UP	
Depreciation	Body/Dep.	65 %			
	Body	50 year(FRM=0, SLM=1		1)	
	Equipments	15 year(FRM=0, SLM=2		1)	
	Other Structure	10 year(FRM=0, SLM=3		1)	
Deferred Asset Depreciation		6 year	Public Obligation Charge		
	Retained Earnings	40 %(Net Profit/Loss)			

Tax				
Land	Property & Urban Planning Tax	1.7 %	3 every year	3 %UP
	Land Value Tax	0.0 %	3 every year	3 %UP
Building Tax Base		70 % (Total estimated Replacement cost)		
	Property and Urban Planning Tax	1.7 %		
Real Property Acquisition Tax		4.0 %		
Registration & License Tax		5.0 %	(Transfer)	
Registration & License Tax		0.6 %	(preservation)	
Profit Tax				
	Corporation Tax	30.0 %	(Deferred Loss=0, Neglect:	0)
	Municipal Inhabitants Tax	20.7 %		
	Enterprise Tax	11.0 %	(Total Profit Tax 42.53 %)	

Schedule	Completion	Acquisition	Exit
	1961	2001	2006

※1Based on Total estimated Replacement cost

4. Project Cost ($)

Total Project Cost	199,788,208									
Property Book Value	199,788,208			Building Ratio		60 %		Land Ratio	40 %	
				Building Book Value		119,872,925		Land Book Value	79,915,283	
				Deferred Charges		0				
Land										
Acquisition Tax	6,101,280	Tax Base	152,532	$ ×	100 % ×		Rate	4.0 %	Exp.=0, Ast.=	1
Registration & License Tax	7,626,600	Tax Base	152,532	$ ×	100 % ×		Rate	5.0 %	〃	1
Building										
Acquisition Tax	1,474,400	Tax Base	36,860	M Yen ×	100 % ×		Rate	4.0 %	Exp.=0, Ast.=	1
Registration & License Tax	1,843,000	Tax Base	36,860	M Yen ×	100 % ×		Rate	5.0 %	〃	1
Transaction Fee	5,993,646	Total Project Cost		3.0 %					Exp.=0, Ast.=	1
Retrofit Cost	7,200,000	Replacement Cost		9.9 %						
Consumption Tax	5,490,419	5%			5490419				Exp.=0, Ast.=	1
Others	0								Exp.=0, Ast.=	1

5. Finance ($)

		Ratio							
Equity①	19,978,821	10.0%		33%					
Equity②(preferred)	39,957,642	20.0%		67%					
Debt①	99,894,104	50.0%	Interest	2.00 %	0 yr deferre	35 yr Return	P&I=0, Principal=1	0	
Debt②	39,957,642	20.0%	Interest	2.00 %	0 yr deferre	35 yr Return	P&I=0, Principal=1	0	
	199,788,208	100%	LTV	70%	DSCR	2.11 (First year)			

6. Significant Results

(1) Indexes for DCF Study

Holding Period	5 years		
Discounted Rate	5.5%		
Residual Cap Rate	6.0%	Commission	3%
PV	**199,788,208**	$	
PV-Retrofit Cost	**192,588,208**	$	

Equity IRR	2.60	%

(2) Stabilized Rents	21,262,376	$
1st year Expenses	9,459,791	$
Stabilized prospected NOI	11,802,585	$
Going-in Cap Rate	6	%
Purchase Price	196,709,751	$

Project IRR (Unleveraged)	5.70	%

BUILDING 2 SCHEDULE OF PROSPECTIVE CASH FLOW (Acquisition ～15th) (sf $)

			2001	2002	2003	2004	2005	2006	2007	2008	2009	2010	2011	2012	2013	2014	2015
CASH FLOW		(Pre-acquisition)	1st	2nd	3rd	4th	5th	6th	7th	8th	9th	10th	11th	12th	13th	14th	15th
	Rents		21,262,376	21,262,376	21,262,376	21,900,248	21,900,248	21,900,248	22,557,255	22,557,255	22,557,255	23,233,973	23,233,973	23,233,973	23,930,992	23,930,992	23,930,992
Total Revenues			21,262,376	21,262,376	21,262,376	21,900,248	21,900,248	21,900,248	22,557,255	22,557,255	22,557,255	23,233,973	23,233,973	23,233,973	23,930,992	23,930,992	23,930,992
	Repairs & Replacement		2,920,000	2,920,000	2,920,000	2,920,000	2,920,000	3,285,000	3,285,000	3,285,000	3,285,000	3,285,000	3,650,000	3,650,000	3,650,000	3,650,000	3,650,000
	Insurance		73,000	73,000	73,000	75,190	75,190	75,190	77,446	77,446	77,446	79,769	79,769	79,769	82,162	82,162	82,162
	Seismic Insurance		38,421	38,421	38,421	39,574	39,574	39,574	40,761	40,761	40,761	41,984	41,984	41,984	43,243	43,243	43,243
	Maintenance		2,328,000	2,328,000	2,328,000	2,397,840	2,397,840	2,397,840	2,469,775	2,469,775	2,469,775	2,543,868	2,543,868	2,543,868	2,620,185	2,620,185	2,620,185
	Mgnt. Fee		637,871	637,871	637,871	657,007	657,007	657,007	676,718	676,718	676,718	697,019	697,019	697,019	717,930	717,930	717,930
	Marketing		755	755	755	778	778	778	801	801	801	825	825	825	850	850	850
	Tax	0	3,461,744	3,461,744	3,461,744	3,539,535	3,539,535	3,539,535	3,619,660	3,619,660	3,619,660	3,702,189	3,702,189	3,702,189	3,787,194	3,787,194	3,787,194
Total Expense		0	9,459,791	9,459,791	9,459,791	9,629,924	9,629,924	9,994,924	10,170,161	10,170,161	10,170,161	10,350,655	10,715,655	10,715,655	10,901,563	10,901,563	10,901,563
CASH FLOW (Before Interest & Tax)		0	11,802,585	11,802,585	11,802,585	12,270,324	12,270,324	11,905,324	12,387,094	12,387,094	12,387,094	12,883,318	12,518,318	12,518,318	13,029,429	13,029,429	13,029,429
	Residual Value		0	0	0	0	192,469,398	0	0	0	0	0	0	0	0	0	0
	Net Cash Flow	0	11,802,585	11,802,585	11,802,585	12,270,324	204,739,722	0	0	0	0	0	0	0	0	0	0
	ROA(C.F./Total Project Cost)		5.9%	5.9%	5.9%	6.1%	102.5%	0.0%	0.0%	0.0%	0.0%	0.0%	0.0%	0.0%	0.0%	0.0%	0.0%
	Presentnt Value		11,490,817	10,891,770	10,323,952	10,173,547	156,908,121	0	0	0	0	0	0	0	0	0	0
Debt Service			5,594,379	5,594,379	5,594,379	5,594,379	130,888,634	0	0	0	0	0	0	0	0	0	0
Deposit (Refund)			0	0	0	0	21,018,476	0	0	0	0	0	0	0	0	0	0
Deposit (Receipt)			210,185	222,359	234,689	247,179	260,907	0	0	0	0	0	0	0	0	0	0
Cash Flow after Debt Service & Deposit			6,418,391	6,430,565	6,442,895	6,923,124	53,093,518	0	0	0	0	0	0	0	0	0	0
DSCR			2.11	2.11	2.11	2.19	1.56	0.00	0.00	0.00	0.00	0.00	0.00	0.00	0.00	0.00	0.00

P/L		(Pre-acquisition)	1st	2nd	3rd	4th	5th	6th	7th	8th	9th	10th	11th	12th	13th	14th	15th
Revenues	Rents	0	21,262,376	21,262,376	21,262,376	21,900,248	21,900,248	0	0	0	0	0	0	0	0	0	0
Expenses	C.F.Total Expense	0	9,459,791	9,459,791	9,459,791	9,629,924	9,629,924	0	0	0	0	0	0	0	0	0	0
	Depreciation	0	3,919,845	3,919,845	3,919,845	3,919,845	3,919,845	0	0	0	0	0	0	0	0	0	0
Operating Profit/Loss		0	7,882,740	7,882,740	7,882,740	8,350,479	8,350,479	0	0	0	0	0	0	0	0	0	0
Non-Operating Income	Interest earned		210,185	222,359	234,689	247,179	260,907	0	0	0	0	0	0	0	0	0	0
	Property Disposition		0	0	0	0	192,469,398	0	0	0	0	0	0	0	0	0	0
Non-Operating Expens	Interest expense	0	2,797,035	2,741,088	2,684,022	2,625,815	2,566,444	0	0	0	0	0	0	0	0	0	0
	Other Expense		0	0	0	0	0	0	0	0	0	0	0	0	0	0	0
Net Profit/Loss		0	5,295,890	5,364,011	5,433,407	5,971,843	198,514,340	0	0	0	0	0	0	0	0	0	0
Corporate Tax		0	2,252,423	2,281,396	2,310,911	2,539,916	2,571,006	0	0	0	0	0	0	0	0	0	0
Net Profit/Loss after Tax		0	3,043,467	3,082,615	3,122,496	3,431,927	195,943,334	0	0	0	0	0	0	0	0	0	0
(Cumulative)		0	3,043,467	6,126,082	9,248,578	12,680,505	208,623,839	0	0	0	0	0	0	0	0	0	0

		(Pre-acquisition)	1st	2nd	3rd	4th	5th	6th	7th	8th	9th	10th	11th	12th	13th	14th	15th
	C.F. after Debt Service		6,418,391	6,430,565	6,442,895	6,923,124	53,093,518	0	0	0	0	0	0	0	0	0	0
	Corporate Taxes		2,252,423	2,281,396	2,310,911	2,539,916	2,571,006	0	0	0	0	0	0	0	0	0	0
	Dividend-Equity1 (Included retirement)		982,860	972,041	960,995	1,003,479	18,531,571	0	0	0	0	0	0	0	0	0	0
	Dividend-Equity2 (Included retirement)		1,965,721	1,944,082	1,921,990	2,006,958	37,063,142	0	0	0	0	0	0	0	0	0	0
Cash Reserve			1,217,387	1,233,046	1,248,998	1,372,771	0	0	0	0	0	0	0	0	0	0	0
Accumulated Cash Reserve			1,217,387	2,450,433	3,699,431	5,072,202	0	0	0	0	0	0	0	0	0	0	0

B/S		(Pre-acquisition)	1st	2nd	3rd	4th	5th	6th	7th	8th	9th	10th	11th	12th	13th	14th	15th
ASSETS	Cash	21,018,476	22,235,863	23,468,909	24,717,908	26,090,678	0	0	0	0	0	0	0	0	0	0	0
	Real Estate	199,788,208	195,868,363	191,948,519	188,028,674	184,108,829	0	0	0	0	0	0	0	0	0	0	0
	Deferred Assets	0	0	0	0	0	0	0	0	0	0	0	0	0	0	0	0
Asset-total		220,806,684	218,104,226	215,417,428	212,746,581	210,199,508	0	0	0	0	0	0	0	0	0	0	0
LIABILITIES	Debt 1	99,894,104	97,896,001	95,857,936	93,779,110	91,658,708	0	0	0	0	0	0	0	0	0	0	0
	Debt 2	39,957,642	39,158,400	38,343,175	37,511,644	36,663,483	0	0	0	0	0	0	0	0	0	0	0
	Security Deposit	21,018,476	21,018,476	21,018,476	21,018,476	21,018,476	0	0	0	0	0	0	0	0	0	0	0
Liabilities-total		160,870,222	158,072,878	155,219,587	152,309,231	149,340,667	0	0	0	0	0	0	0	0	0	0	0
EQUITY	Equity 1	19,978,821	19,978,821	19,978,821	19,978,821	19,978,821	0	0	0	0	0	0	0	0	0	0	0
	Equity 2	39,957,642	39,957,642	39,957,642	39,957,642	39,957,642	0	0	0	0	0	0	0	0	0	0	0
	Retained Earnings	0	94,886	261,378	500,888	922,378	0	0	0	0	0	0	0	0	0	0	0
Equity-total		59,936,462	60,031,348	60,197,840	60,437,351	60,858,841	0	0	0	0	0	0	0	0	0	0	0
L&E-total		220,806,684	218,104,226	215,417,428	212,746,581	210,199,508	0	0	0	0	0	0	0	0	0	0	0

Leasing Project Proforma	PROJECT NAME	BUILDING 3

1. Property Outline

Address	Chuou ward Tokyo	Access	3minutes walk from Tokyo Station
Zoning	Commercial District	Completion Date	1999
Constructed Floor Area	958,000 sf	Parking Lot	150
Current Replacement Cost	254,000,000 $ (Building Total) 876 $/sf(Const. Floor Area)	PML (90%Case)	5 %

Floor Area Table

Building Use	Const. Floor Area	Rentable Floor Area	Ratio	Rentable Floor Ratio
Office	958,000 sf	667,000 sf	100%	70%
Retail	0.00 sf	0 sf	0%	#DIV/0!
Residential	0.00 sf	0 sf	0%	#DIV/0!
	958,000.00 sf	667000.00 sf		70%

Site Area	81,000 sf	Designated Building Coverage Ratio	80 %
"Rosenka"	5,136 $/sf	Designated Building Floor Area Ratio	600 %
Market Value of Property		Other Government Restriction	
(Land)	4,014 $/sf		
(Building)	95 $/sf Office	"Rosenka" : a land unit price for tax calculation purposes set by Ministry of Finance	
	103 $/sf Retail		
	103 $/sf Residential		

2. Leasing Assumptions

	Monthly Rent				Security Deposit
Office	9.1 $/sf	3 every year	3 %UP		12 month
Retail	0.0 $/sf	3 every year	3 %UP		24 month
Residential	0.0 $/sf	3 every year	3 %UP		2 month

Occupancy	Initial Year	2nd Year	3rd Year	4th Year	After 5th Year
Office	95 %	95 %	95 %	95 %	95 %
Retail	0 %	0 %	0 %	0 %	0 %
Residential	0 %	0 %	0 %	0 %	0 %

Parking	Hourly Charge	0 lot	Charge	4.88 $/hour	Ave.hour	2 h	4 cycle/day	Occupancy	50 %		
	Monthly Charge	50 lot	Charge	406.5 $/month	Deposit	0 $/lot	3 every year	3 %UP			

3. Other Assumptions

Revenue	Interest Income	1.0 %			
Expense	Repairs Replacements	0.25 % (Total estimated Replacement cost)	5 every year	100 %UP	
	Insurance	0.1 % (Total estimated Replacement cost)	3 every year	3 %UP	
	Seismic Insurance	500 %(Year expected Loss)	3 every year	3 %UP	
	Building Mgmt.	0.5 $/sf (Const. Floor Area)	3 every year	3 %UP	
	Property Mgmt.	3.0 % (Rent)			
	Marketing	755 $/year	3 every year	3 %UP	
Depreciation	Body/Dep.	65 %			
	Body	50 year(FRM=0, SLM=1		1)	
	Equipments	15 year(FRM=0, SLM=2		1)	
	Other Structure	10 year(FRM=0, SLM=3		1)	
Deferred Asset Depreciation		6 year	Public Obligation Charge		
	Retained Earnings	40 %(Net Profit/Loss)			

Tax				
Land	Property & Urban Planning Tax	1.7 %	3 every year	3 %UP
	Land Value Tax	0.0 %	3 every year	3 %UP
Building	Tax Base	70 % (Total estimated Replacement cost)		
	Property and Urban Planning Tax	1.7 %		
Real Property Acquisition Tax		4.0 %		
Registration & License Tax		5.0 %	(Transfer)	
Registration & License Tax		0.6 %	(preservation)	
Profit Tax				
	Corporation Tax	30.0 %	(Deferred Loss=0, Neglect:	0)
	Municipal Inhabitants Tax	20.7 %		
	Enterprise Tax	11.0 %	(Total Profit Tax 42.53 %)	

Schedule	Completion	Acquisition	Exit
	1999	2001	2006

※1Based on Total estimated Replacement cost

4. Project Cost ($)

Total Project Cost	892,445,524									
Property Book Value	892,445,524			Building Ratio	60 %		Land Ratio	40 %		
				Building Book Value	535,467,314		Land Book Value	356,978,210		
				Deferred Charges	0					
Land										
Acquisition Tax	13,005,360	Tax Base	325,134	$ ×	100 % ×		Rate	4.0 %	Exp.=0, Ast.=	1
Registration & License Tax	16,256,700	Tax Base	325,134	$ ×	100 % ×		Rate	5.0 %	〃	1
Building										
Acquisition Tax	3,640,400	Tax Base	91,010	M Yen ×	100 % ×		Rate	4.0 %	Exp.=0, Ast.=	1
Registration & License Tax	4,550,500	Tax Base	91,010	M Yen ×	100 % ×		Rate	5.0 %	〃	1
Transaction Fee	26,773,366	Total Project Cost		3.0 %					Exp.=0, Ast.=	1
Retrofit Cost	0	Replacement Cost		0.0 %						
Consumption Tax	26,773,366	5%			26773365.72				Exp.=0, Ast.=	1
Others	0								Exp.=0, Ast.=	1

5. Finance ($)

		Ratio								
Equity①	89,244,552	10.0%		33%						
Equity②(preferred)	178,489,105	20.0%		67%						
Debt①	446,222,762	50.0%	Interest	2.00 %		0 yr deferre	35 yr Return	(P&I=0, Principal=1	0	
Debt②	178,489,105	20.0%	Interest	2.00 %		0 yr deferre	35 yr Return	(P&I=0, Principal=1	0	
	892,445,524	100%	LTV	70%		DSCR	2.10 (First year)			

6. Significant Results

(1) Indexes for DCF Study

Holding Period	5 years		
Discounted Rate	5.5%		
Residual Cap Rate	6.0%	Commission	3%
PV	**892,445,524**	$	
PV-Retrofit Cost	**892,445,524**	$	

Equity IRR	4.43	%

(2) Stabilized Rents	69,735,028	$
1st year Expenses	17,346,526	$
Stabilized prospected NOI	52,388,502	$
Going-in Cap Rate	6	%
Purchase Price	873,141,704	$

Project IRR (Unleveraged)	5.85	%

BUILDING 3　　SCHEDULE OF PROSPECTIVE CASH FLOW (Acquisition ～15th)　　(sf $)

			2001	2002	2003	2004	2005	2006	2007	2008	2009	2010	2011	2012	2013	2014	2015
CASH FLOW		(Pre-acquisition)	1st	2nd	3rd	4th	5th	6th	7th	8th	9th	10th	11th	12th	13th	14th	15th
	Rents		69,735,028	69,735,028	69,735,028	71,827,079	71,827,079	71,827,079	73,981,891	73,981,891	73,981,891	76,201,348	76,201,348	76,201,348	78,487,389	78,487,389	78,487,389
Total Revenues			69,735,028	69,735,028	69,735,028	71,827,079	71,827,079	71,827,079	73,981,891	73,981,891	73,981,891	76,201,348	76,201,348	76,201,348	78,487,389	78,487,389	78,487,389
	Repairs & Replacement		635,000	635,000	635,000	1,270,000	1,270,000	1,270,000	1,270,000	1,270,000	2,540,000	2,540,000	2,540,000	2,540,000	2,540,000	3,810,000	3,810,000
	Insurance		254,000	254,000	254,000	261,620	261,620	261,620	269,469	269,469	269,469	277,553	277,553	277,553	285,879	285,879	285,879
	Seismic Insurance		66,842	66,842	66,842	68,847	68,847	68,847	70,913	70,913	70,913	73,040	73,040	73,040	75,231	75,231	75,231
	Maintenance		5,748,000	5,748,000	5,748,000	5,920,440	5,920,440	5,920,440	6,098,053	6,098,053	6,098,053	6,280,995	6,280,995	6,280,995	6,469,425	6,469,425	6,469,425
	Mgnt. Fee		2,092,051	2,092,051	2,092,051	2,154,812	2,154,812	2,154,812	2,219,457	2,219,457	2,219,457	2,286,040	2,286,040	2,286,040	2,354,622	2,354,622	2,354,622
	Marketing		755	755	755	778	778	778	801	801	801	825	825	825	850	850	850
	Tax	0	8,549,878	8,549,878	8,549,878	8,715,696	8,715,696	8,715,696	8,886,489	8,886,489	8,886,489	9,062,406	9,062,406	9,062,406	9,243,600	9,243,600	9,243,600
Total Expense		0	17,346,526	17,346,526	17,346,526	18,392,194	18,392,194	18,392,194	18,815,182	18,815,182	20,085,182	20,520,859	20,520,859	20,520,859	20,969,607	22,239,607	22,239,607
CASH FLOW (Before Interest & Tax)		0	52,388,502	52,388,502	52,388,502	53,434,885	53,434,885	53,434,885	55,166,710	55,166,710	53,896,710	55,680,489	55,680,489	55,680,489	57,517,782	56,247,782	56,247,782
	Residual Value		0	0	0	0	863,863,979	0	0	0	0	0	0	0	0	0	0
	Net Cash Flow	0	52,388,502	52,388,502	52,388,502	53,434,885	917,298,865	0	0	0	0	0	0	0	0	0	0
	ROA(C.F./Total Project Cost)		5.9%	5.9%	5.9%	6.0%	102.8%	0.0%	0.0%	0.0%	0.0%	0.0%	0.0%	0.0%	0.0%	0.0%	0.0%
	Presentnt Value		51,004,648	48,345,638	45,825,249	44,303,830	702,966,159	0	0	0	0	0	0	0	0	0	0
Debt Service			24,989,855	24,989,855	24,989,855	24,989,855	584,674,026	0	0	0	0	0	0	0	0	0	0
Deposit (Refund)			0	0	0	0	69,491,128	0	0	0	0	0	0	0	0	0	0
Deposit (Receipt)			694,911	747,965	801,715	856,174	913,762	0	0	0	0	0	0	0	0	0	0
Cash Flow after Debt Service & Deposit			28,093,559	28,146,612	28,200,362	29,301,205	264,047,472	0	0	0	0	0	0	0	0	0	0
DSCR			2.10	2.10	2.10	2.14	1.57	0.00	0.00	0.00	0.00	0.00	0.00	0.00	0.00	0.00	0.00

P/L		(Pre-acquisition)	1st	2nd	3rd	4th	5th	6th	7th	8th	9th	10th	11th	12th	13th	14th	15th
Revenues	Rents	0	69,735,028	69,735,028	69,735,028	71,827,079	71,827,079	0	0	0	0	0	0	0	0	0	0
Expenses	C.F.Total Expense	0	17,346,526	17,346,526	17,346,526	18,392,194	18,392,194	0	0	0	0	0	0	0	0	0	0
	Depreciation	0	17,509,781	17,509,781	17,509,781	17,509,781	17,509,781	0	0	0	0	0	0	0	0	0	0
Operating Profit/Loss		0	34,878,721	34,878,721	34,878,721	35,925,104	35,925,104	0	0	0	0	0	0	0	0	0	0
Non-Operating Income	Interest earned		694,911	747,965	801,715	856,174	913,762	0	0	0	0	0	0	0	0	0	0
	Property Disposition		0	0	0	0	863,863,979	0	0	0	0	0	0	0	0	0	0
Non-Operating Expens	Interest expense	0	12,494,237	12,244,325	11,989,414	11,729,406	11,464,197	0	0	0	0	0	0	0	0	0	0
	Other Expense		0	0	0	0	0	0	0	0	0	0	0	0	0	0	0
Net Profit/Loss		0	23,079,395	23,382,361	23,691,021	25,051,873	889,238,649	0	0	0	0	0	0	0	0	0	0
Corporate Tax		0	9,816,020	9,944,876	10,076,154	10,654,945	10,792,236	0	0	0	0	0	0	0	0	0	0
Net Profit/Loss after Tax		0	13,263,375	13,437,485	13,614,867	14,396,928	878,446,413	0	0	0	0	0	0	0	0	0	0
(Cumulative)		0	13,263,375	26,700,860	40,315,727	54,712,654	933,159,067	0	0	0	0	0	0	0	0	0	0

		(Pre-acquisition)	1st	2nd	3rd	4th	5th	6th	7th	8th	9th	10th	11th	12th	13th	14th	15th
	C.F. after Debt Service		28,093,559	28,146,612	28,200,362	29,301,205	264,047,472	0	0	0	0	0	0	0	0	0	0
	Corporate Taxes		9,816,020	9,944,876	10,076,154	10,654,945	10,792,236	0	0	0	0	0	0	0	0	0	0
	Dividend-Equity1 (Included retirement)		4,324,063	4,275,581	4,226,087	4,295,830	91,713,433	0	0	0	0	0	0	0	0	0	0
	Dividend-Equity2 (Included retirement)		8,648,126	8,551,161	8,452,174	8,591,659	183,426,865	0	0	0	0	0	0	0	0	0	0
Cash Reserve			5,305,350	5,374,994	5,445,947	5,758,771	0	0	0	0	0	0	0	0	0	0	0
Accumulated Cash Reserve			5,305,350	10,680,344	16,126,291	21,885,062	0	0	0	0	0	0	0	0	0	0	0

B/S		(Pre-acquisition)	1st	2nd	3rd	4th	5th	6th	7th	8th	9th	10th	11th	12th	13th	14th	15th
ASSETS	Cash	69,491,128	74,796,478	80,171,472	85,617,419	91,376,190	0	0	0	0	0	0	0	0	0	0	0
	Real Estate	892,445,524	874,935,743	857,425,962	839,916,180	822,406,399	0	0	0	0	0	0	0	0	0	0	0
	Deferred Assets	0	0	0	0	0	0	0	0	0	0	0	0	0	0	0	0
Asset-total		961,936,652	949,732,221	937,597,434	925,533,599	913,782,589	0	0	0	0	0	0	0	0	0	0	0
LIABILITIES	Debt 1	446,222,762	437,297,321	428,193,371	418,907,342	409,435,593	0	0	0	0	0	0	0	0	0	0	0
	Debt 2	178,489,105	174,918,928	171,277,348	167,562,937	163,774,237	0	0	0	0	0	0	0	0	0	0	0
	Security Deposit	69,491,128	69,491,128	69,491,128	69,491,128	69,491,128	0	0	0	0	0	0	0	0	0	0	0
Liabilities-total		694,202,995	681,707,377	668,961,848	655,961,407	642,700,958	0	0	0	0	0	0	0	0	0	0	0
EQUITY	Equity 1	89,244,552	89,244,552	89,244,552	89,244,552	89,244,552	0	0	0	0	0	0	0	0	0	0	0
	Equity 2	178,489,105	178,489,105	178,489,105	178,489,105	178,489,105	0	0	0	0	0	0	0	0	0	0	0
	Retained Earnings	0	291,186	901,929	1,838,535	3,347,974	0	0	0	0	0	0	0	0	0	0	0
Equity-total		267,733,657	268,024,843	268,635,586	269,572,192	271,081,631	0	0	0	0	0	0	0	0	0	0	0
L&E-total		961,936,652	949,732,221	937,597,434	925,533,599	913,782,589	0	0	0	0	0	0	0	0	0	0	0